



<https://theses.gla.ac.uk/>

Theses Digitisation:

<https://www.gla.ac.uk/myglasgow/research/enlighten/theses/digitisation/>

This is a digitised version of the original print thesis.

Copyright and moral rights for this work are retained by the author

A copy can be downloaded for personal non-commercial research or study, without prior permission or charge

This work cannot be reproduced or quoted extensively from without first obtaining permission in writing from the author

The content must not be changed in any way or sold commercially in any format or medium without the formal permission of the author

When referring to this work, full bibliographic details including the author, title, awarding institution and date of the thesis must be given

Enlighten: Theses

<https://theses.gla.ac.uk/>
research-enlighten@glasgow.ac.uk

Isolation and Characterization of Reaction Centre-Antenna
Conjugates from a Range of Bacteriochlorophyll a-
Containing Species of Purple Bacteria.

by

Deborah J. Dawkins

A thesis submitted for the degree of Doctor of Philosophy

University of Glasgow.
Department of Botany.
March 1988.

ProQuest Number: 10948186

All rights reserved

INFORMATION TO ALL USERS

The quality of this reproduction is dependent upon the quality of the copy submitted.

In the unlikely event that the author did not send a complete manuscript and there are missing pages, these will be noted. Also, if material had to be removed, a note will indicate the deletion.



ProQuest 10948186

Published by ProQuest LLC (2018). Copyright of the Dissertation is held by the Author.

All rights reserved.

This work is protected against unauthorized copying under Title 17, United States Code
Microform Edition © ProQuest LLC.

ProQuest LLC.
789 East Eisenhower Parkway
P.O. Box 1346
Ann Arbor, MI 48106 – 1346

Science appears as what in truth she is,
Not as our glory and our absolute boast,
But as a succedaneum, and a prop
To our infirmity.

[Wordsworth, W]

SUMMARY

The photosynthetic apparatus of purple bacteria is made up of two major components; a well-characterized reaction centre, and light-harvesting antenna complexes. The latter complexes are responsible for absorbing incident radiation and transferring it to the reaction centre where it is utilized in the primary processes of photosynthesis. The antenna complex consists typically of a small number of bacteriochlorophyll a (2-3) and carotenoid molecules (1 or 2) bound noncovalently to two low molecular weight (5-7kd) hydrophobic polypeptides [Thornber *et al*, 1983]. Two types of antenna complex, which are differentiated with respect to their NIR absorption maxima, were recognized in the early studies of Aagaard and Sistrom (1972). The first type designated the B875 (B880) antenna complex, appears to be intimately associated with the reaction centre [(Drews *et al*, 1983)(Feick and Drews, 1978)(Monger and Parson, 1977)(Ueda *et al*, 1985)(Varga and Staehelin, 1985)], whereas the second type, the B800-850 complex, having no apparent fixed relationship with the reaction centre, is present in variable amounts depending upon the prevailing environmental conditions [(Firsow and Drews, 1977)(Monger and Parson, 1977)(Niederman *et al*, 1976)(Schumacher and Drews, 1978)].

The relationship existing between the reaction centre and B875 (B880) complex is emphatically illustrated in the photosynthetic membranes of bacteriochlorophyll b-containing species of purple bacteria, in particular of *Rhodopseudomonas viridis* and *Ectothiorhodospira halochloris* [(Eimhjellen *et al*, 1967)(Miller, 1979, 1982)(Jay *et al*, 1984)(Stark *et al*, 1984)(Engelhardt *et al*, 1986)]. Examination of these membranes, using electron microscopy and image-processing techniques, shows the membranes to consist

of an array of well-defined, identical structures, consisting of a reaction centre surrounded by, and complexed with, the B875-type (or B1012 in *Rps. viridis*) of antenna complex.

To date, a number of studies on bacteriochlorophyll a-containing species, including developmental, structural, immunofractionation, solubilization and functional analyses, have provided positive evidence supporting the existence of a fixed stoichiometric relationship between the reaction centre and the B875 (B880) antenna complex [(Aagaard and Siström, 1972)(Glazer, 1983)(Hayashi *et al*, 1982a)(Nishi *et al*, 1979)(Takemoto *et al*, 1982)(Ueda *et al*, 1985)]. However, whether this reflects the existence of a fixed stoichiometric core structure, similar to that observed in BChl b-containing species, still remains to be seen.

The method described by Firsow and Drews (1977) for the fractionation of detergent solubilized membranes has been modified in this study for the isolation of spectrally-pure RC-B875 and B800-850 antenna complexes from a range of BChl a-containing species of purple photosynthetic bacteria. Solubilization conditions were optimized for each species examined. The ratio of bacteriochlorophyll a present per reaction centre in the isolated RC-B875 conjugates was then determined from their respective absorption and oxidation-reduction difference spectra. For each species the ratio of RC:BChl a was constant irrespective of the light intensity at which the cells were grown. In making comparisons between species a degree of variation was apparent. Subsequent examination of the effects of additional, or alternative, detergents on this ratio value however, suggests that the variation may be a consequence of the experimental procedures adopted rather than the result of true species variation.

The fluorescence induction kinetics of these isolated complexes were also examined in order to determine their functional state.

The successful detection of variable fluorescence which depends upon the redox state of the reaction centre, suggests that the light-harvesting complexes are still functionally connected to the reaction centre in the isolated complexes. The polypeptide composition was confirmed by SDS-polyacrylamide gel electrophoresis. Finally in a quest to determine the organizational structure of the RC-antenna conjugate crystallization attempts have been made.

It appears from our results that all purple bacteria contain a common antenna-reaction centre "core" structure that forms the basis of their photosynthetic unit.

ACKNOWLEDGEMENTS

I am greatly indebted to Dr. R. J. Cogdell for his supervision, encouragement and support during this study.

I should like to acknowledge Professor J. R. Hillman, Dr. A. M. M. Berrie, and Dr. R. J. Cogdell for the use of facilities in the Botany Department.

I wish to thank Mr. J. Ullrich of the Physics Institute, University of Stuttgart, for kindly carrying out a number of spectral analyses. I also wish to thank Dr. R. G. Lindsay for the use of his laboratory, and Mr. J. Neagle for his time and helpful advice.

I wish to convey special thanks to the following people in the Botany Department:

Mrs. Linda Ferguson for her excellent technical assistance and to whom I wish to dedicate Chapter 6.

Ms. Caroline Crow and Dr. P. Dominy for their assistance with the fluorescence apparatus and for helpful discussions.

Mr. N. Tait for photography.

Mr. E. Robertson for technical advice on microscopy and photography.

My fellow research students, Ms. Joan Malcolm, Ms. Anne Taylor, Mr. Andrew Madden and Ms. Elizabeth McDonnell for their sound grammatical judgement and encouragement. A special acknowledgement must also go to Pickles.

Appreciation is also extended to the Science and Engineering Research Council who provided the monetary support to make this project possible.

Finally I wish to thank my parents for their support throughout my academic career.

Abbreviations

Wherever possible, S.I. Units were used in this thesis: some of the other abbreviations used were:-

A	Absorbance
Å	Angstrom
BChl <u>a/b</u>	Bacteriochlorophyll <u>a/b</u>
Bpheo	Bacteriopheophytin
BH	Benzamidine hydrochloride.
CD	Circular dichroism
DDAO	Dimethyldecylamine N-oxide
EDTA	Ethylene diamine tetra acetate
ϵ	Extinction coefficient
HPT	1, 2, 3 Heptane-triol.
IR	Infrared
kb	Kilobases
kD	KiloDaltons
LHC/LHAC	Light-harvesting (antenna) complexe(s)
LM	Lauryl maltoside/ dodecyl β -D-maltoside
LMW	Low molecular weight
LDAO	Lauryl dimethylamine N-oxide
M_r	Molecular weight
NIR	Near infrared
OG	n-octy- β -D-glucopyranoside
PAGE/PAGGE	Polyacrylamide (gradient) gel electrophoresis
PEG	Polyethylene glycol
RC	Reaction Centre
SD	Sodium deoxycholate
SDS	Sodium dodecyl sulphate

TEMED	NNN'N'-tetra methylethylene diamine
Tris	Tris (hydroxymethyl) aminomethane
UV	Ultra-violet
vis	Visible
λ	Wavelength
ϕ_f	Yield of fluorescence

TABLE OF CONTENTS.

	<u>PAGE</u>
SUMMARY	i
ACKNOWLEDGEMENTS	iv
ABBREVIATIONS	v
TABLE OF CONTENTS	vii
 <u>CHAPTER 1</u> <u>A General Introduction to the Photosynthetic Bacteria</u>	
1.1 Classification of Purple Photosynthetic Bacteria.	1
1.2 The Light-Harvesting Apparatus:	4
The Light-Harvesting Antenna Complexes	4
The Reaction Centre.	10
 <u>CHAPTER 2</u> <u>Methodology</u>	
2.1 Spectral Characterization.	20
2.2 The Isolation of the Light-Harvesting and Reaction Centre Complexes from Membrane Preparations	23.
2.3 Characterization of the 'Core Complex'.	29
2.4 The Polypeptide Composition of the Isolated Reaction Centre-Antenna Conjugates.	33
2.5 Examining the Functional Integrity of the Isolated Reaction Centre-Antenna Conjugate.	37
2.6 Crystallizations - Conclusive Evidence for the Existence of a Well-Defined Core-Complex.	41

CHAPTER 3 Materials and Methods.

3.1	Cell Culture.	48
3.2	Harvesting the Cells.	49
3.3	Membrane Preparation.	50
3.4	Cell Counts.	51
3.5	Spectrophotometry.	51
3.6	Isolation of the Light-Harvesting and Reaction- Centre Complexes from Membrane Preparations.	52
3.7	Absorption and Fluorescence Spectroscopy.	55
3.8	Determination of the Reaction Centre (RC):Light- Harvesting Bacteriochlorophyll <u>a</u> Ratio.	56
3.9	Determination of the Extinction Coefficient at 880 nm for Total Bacteriochlorophyll <u>a</u> .	57
3.10	Concentrating the Isolated Complexes.	57
3.11	Analysis of the Polypeptide Composition of the Isolated Complexes.	58
3.12	Measuring the Fluorescence Properties of the Isolated RC-B875 Conjugate.	61
3.13	Crystallization of the Isolated Conjugate.	62

CHAPTER 4 Isolation of the Reaction Centre-B875 Antenna Conjugate using the Technique of Sucrose Density-Gradient Centrifugation.

4.1	Optimization of Solubilization Conditions.	65
4.2	The Parameters of the Sucrose Density-Gradient.	72
4.3	Spectral Analysis of RC-B875 and B800-850 Antenna Complexes.	76

<u>CHAPTER 5</u>	<u>Determination of the Ratio of Bacteriochlorophyll a.to Reaction Centre Molecules in the Isolated RC-B875 Antenna Conjugates.</u>	78
<u>CHAPTER 6</u>	<u>Examination of the Polypeptide Composition of Reaction Centre-B875 Antenna Conjugate.</u>	98
<u>CHAPTER 7</u>	<u>Examining the Functional Integrity of the RC-B875 Antenna Complex.</u>	103
7.1	The Effects of Ascorbate and Ferricyanide Addition on Fluorescence Induction Kinetics.	112
7.2	Looking at the Effects of Detergent Additions on Variable Fluorescence.	113
<u>CHAPTER 8</u>	<u>Crystallization of the RC-B875 Antenna Complex.</u>	116
<u>CHAPTER 9</u>	<u>Conclusions and Discussion.</u>	128
<u>APPENDIX 1</u>	<u>Media and Buffers.</u>	
1.1	Acidophila Medium.	134
1.2	C-Succinate Medium.	135
1.3	Chromatium Medium.	137
1.4	Agar Stabs and Agar Plates.	138
1.5	MES Solutions.	138
1.6	Salt Solutions.	138
1.7	Protein Assay.	139

<u>APPENDIX 2</u>	<u>SDS-Polyacrylamide Gel Electrophoresis.</u>	
2.1	Stock Solutions for SDS-PAGE.	140
2.2	Preparation of Protein Samples for SDS-PAGE.	141
2.3	Staining and Destaining.	142
<u>APPENDIX 3</u>	<u>The Photodynamic Effect.</u>	143
<u>APPENDIX 4</u>	<u>Buffer Systems Employed in Polyacrylamide Gel Electrophoresis.</u>	144
<u>APPENDIX 5</u>	<u>Statistical Analyses.</u>	146
<u>APPENDIX 6</u>	<u>Quenching Processes.</u>	150
REFERENCES.		152

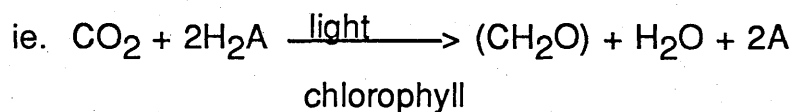
CHAPTER 1

A GENERAL INTRODUCTION TO THE PHOTOSYNTHETIC BACTERIA.

1.1 Classification of Purple Photosynthetic Bacteria:

"The phototrophic bacteria are a physiological group of different kinds of gram negative aquatic bacteria. They are considered to be evolutionary rather old and represent the first phototrophic organisms in our planet" [Stanier 1970].

Phototrophic purple bacteria carry out anoxygenic photosynthesis, that is to say, unlike in green plants and cyanobacteria (blue-green algae) there is no photochemical cleavage of water and hence no evolution of molecular oxygen. These organisms utilize reduced sulphur compounds, molecular hydrogen or simple organic compounds as their electron donor. Despite these differences, van Niel (1931, 1941) formulated a general equation of photosynthesis which summarizes the unanimity of photosynthesis in both plants and photosynthetic prokaryotes:



Where H_2A is representative of the electron donors mentioned above, CH_2O stored organic matter, and 2A the corresponding reduced products ie. molecular oxygen in plants; sulphur, sulphate, protons, organic compounds and carbon dioxide in purple photosynthetic bacteria [Pfennig, 1978].

Differences in the fine structure and pigments of their photosynthetic apparatus define the basis for the division of this family into two orders, namely the Rhodospirillales and Chlorobiales [Trüper and Pfennig, 1978]. The photosynthetic apparatus in the order Rhodospirillales is located in the cytoplasmic membrane and contains the photopigments BChl a or b. In Chlorobiales, however, the antenna BChl (c, d or e) is located on distinct organelles or chlorosomes which are attached to the innerside of the cytoplasmic membrane. The reaction centre (RC) BChl is located in the cytoplasmic membrane.

The order Rhodospirillales can be further differentiated on the basis of the ability/inability of the cells to use elemental sulphur as an electron donor for photosynthesis [Pfennig & Trüper, 1981] :

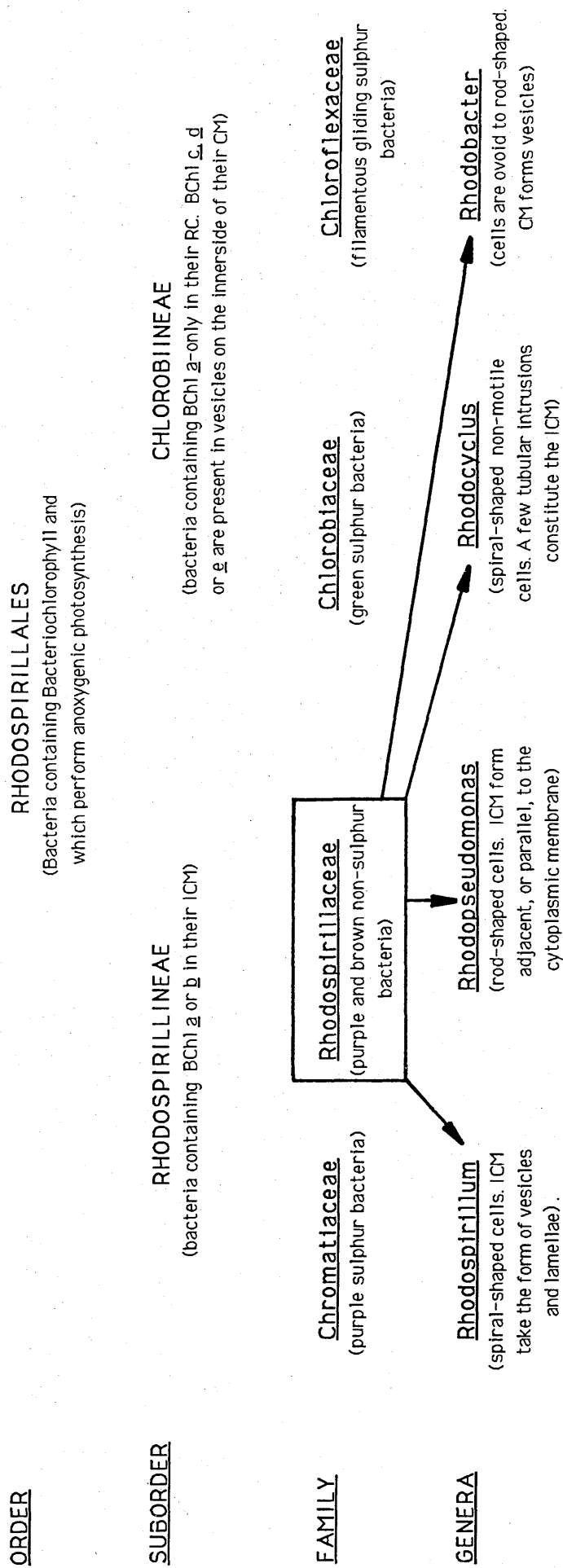
(1) Chromatiaceae or purple sulphur bacteria. As the name suggests, members of this family are capable of oxidizing sulphide to sulphate via elemental sulphur. These organisms are strictly anaerobic and are, therefore, obligately phototrophic. The presence of hydrogen sulphide and light dictate the occurrence of these organisms in nature, consequently they are often found in sulphide-rich aquatic areas from moist and muddy soils to estuaries, sulphur springs and salt lakes. An example of a purple sulphur bacterium is *Chromatium vinosum* [Pfennig and Trüper, 1981].

(2) The purple non-sulphur bacteria or Rhodospirillaceae. This group of bacteria, lacks the ability to oxidize elemental sulphur. These bacteria also show a characteristic preference for photoorganoheterotrophic growth but also have the capacity, with very little regulatory change, to undergo chemotrophic growth under aerobic conditions. Their physiological diversity has facilitated a wide distribution in nature, although their numbers are usually directly related to the amount of organic material present [Biebl and

Pfennig, 1981]. This group of bacteria is further differentiated amongst four genera, namely *Rhodobacter* [Imhoff *et al*, 1984], *Rhodopseudomonas* [Molisch, 1907], *Rhodospirillum* [Molisch, 1907] and *Rhodocyclus* [Pfennig, 1978]; differentiation has been made primarily on the basis of differences in their morphology and physiology [Imhoff *et al*, 1984]: Figure 1.1 shows the classification of the order Rhodospirillales into suborders and families.

In purple bacteria all components of the photosynthetic apparatus are incorporated into the intracytoplasmic membrane (ICM). The ICM originates from and remains contiguous with the cytoplasmic membrane, and assumes characteristic shapes which protrude into the lumen of the cell body [(Pfennig, 1978)(Drews, 1978)(Remson, 1978)(Varga and Staehelin, 1983)]. In *Chromatiaceae* most species have vesicular shaped ICM. In the *Rhodospirillaceae* which is representative of a structurally as well as physiologically diverse group, a number of different structural forms can be identified. Vesicular-shaped ICM characterize the members of the genus *Rhodobacter*, for example *Rhodobacter sphaeroides* (formerly *Rhodopseudomonas sphaeroides* [van Niel, 1944]). Tubular ICM are observed in *Rhodocyclus gelatinosus* (formerly *Rhodopseudomonas gelatinosus* [Molisch, 1907]) and membrane lamellar stacks or parallel layers can be seen in *Rhodopseudomonas palustris* and *Rhodopseudomonas acidophila* [Imhoff *et al*, 1984].

FIGURE 1.1 Illustrates the classification of the order Rhodospirillales into suborders and families. It also shows the four main genera of the family *Rhodospirillaceae*.



Differences in the fine structure and pigments of their photosynthetic apparatus define the basis for the division of this family into two orders, namely the Rhodospirillales and Chlorobiales [Trüper and Pfennig, 1978]. The photosynthetic apparatus in the order Rhodospirillales is located in the cytoplasmic membrane and contains the photopigments BChl a or b. In Chlorobiales, however, the antenna BChl (c, d or e) is located on distinct organelles or chlorosomes which are attached to the inside of the cytoplasmic membrane. The reaction centre (RC) BChl is located in the cytoplasmic membrane.

1.2 The Photosynthetic Apparatus:

Photosynthetic studies of purple bacteria are usually carried out on chromatophores, isolated fragments of membrane which have resealed into vesicles and share the same topology as the ICM [(Schachman *et al*, 1952)(Oelze and Drews, 1972)]. Detergent solubilization of these chromatophores has allowed the isolation of the various components of the photosynthetic apparatus [(Reed and Clayton, 1968)(Thornber, 1970)(Cogdell *et al*, 1983)]. These chromoproteins have been identified and fall into two functional classes: the photochemical reaction centre (RC), which is responsible for performing the primary electron transfer processes of photosynthesis, and the light-harvesting or antenna complexes (LHC) which absorb solar energy and transfer it to the RC.

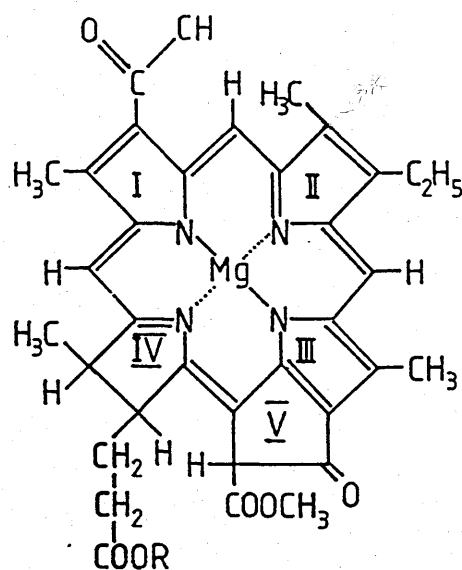
The light-harvesting antenna complexes:

The primary role of the LHC is the absorption of light energy. This process requires photopigments adapted for the absorption of light energy of wavelengths specific to the bacteria's natural habitat. Purple bacteria usually develop in aquatic environments beneath an often dense layer of cyanobacteria, algae and plants which effectively screens out certain absorption bands of solar energy. However, these organisms possess light-harvesting bacteriochlorophyll and carotenoid pigments which harness light energy of wavelengths well outside the range usable for oxygenic photosynthesis. Light-harvesting bacteriochlorophyll has strong absorption bands, *in vivo*, in the far-red and infrared regions of the spectrum, and carotenoids, which act as accessory light-harvesting pigments absorbing light energy in regions unharnessed by chlorophyllous pigments ie. in the 450-570 nm region [(Cohen-Bazire

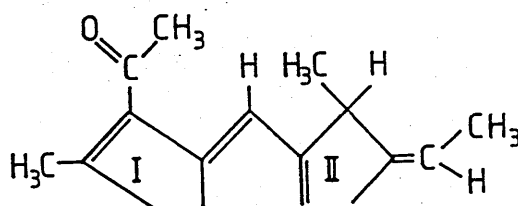
and Sistrom, 1966)]. In addition to their contributions as light-harvesting pigments, carotenoids play a major role in protecting the organism from harmful photo-oxidative reactions. These are believed to result from the transfer of energy from triplet state bacteriochlorophyll to molecular oxygen, thereby yielding the powerful oxidant, singlet oxygen: carotenoids function to prevent this photodynamic reaction (Appendix 3) [(Griffiths *et al*, 1955)(Cohen-Bazire and Stanier, 1958)(Cogdell, 1985)]. Most species of purple photosynthetic bacteria possess BChl a as their major light-absorbing pigment, although a few species for example *Rhodopseudomonas viridis* contain the related pigment BChl b (Figure 1.2 a) [Eimhejellen *et al*, 1963]. It should be noted at this point that the spectral properties of these pigments *in vivo* are largely, although not entirely, a consequence of their combined state in the photosynthetic apparatus [Stanier *et al*, 1981]. Table 1.1 illustrates the *in vivo* and *in vitro* absorption bands of these BChl.

Table 1.1 illustrates the *in vivo* and *in vitro* absorption bands of the major light absorbing pigment, bacteriochlorophyll a, which is common to most purple photosynthetic bacteria, and also of bacteriochlorophyll b which is natural to a few species. [Stanier *et al*, 1976].

	<u>WAVELENGTH OF MAXIMUM ABSORPTION</u>		
	<u>ETHER</u>	<u>WHOLE CELLS</u>	<u>RED SHIFT</u>
BChl <u>a</u>	775 nm	850 - 910 nm.	75 - 135 nm
BChl <u>b</u>	790 nm	1020 - 1035 nm	230 - 246 nm



BChl a



BChl b

FIGURE 1.2a Molecular Structures of Bacteriochlorophyll a (BChl a) and b. (BChl b).

In the figures shown above describing the molecular structures of BChl a and BChl b, the presence of a carbon atom is implied at each unlabelled junction of bonds. Comparing the two structures (only rings I and II of BChl b are shown in the figure, the rest of the structure is identical to that of BChl a), it can be seen that BChl b differs from BChl a only at ring II where it carries an exocyclic bond in conjugation to the bacteriochlorin π -system. The residue R is a long-chain hydrocarbon phytyl group, in *Rs.rubrum* this is known to be geranylgeranyl.

The bulk of photopigments, the nature and composition of which is dependent upon the species, are contained within the pigment-protein light-harvesting complexes (LHC) [Lascelles, 1968]. For example, in purple nonsulphur bacteria the antenna complex accounts for 80-90% of the total pigment content, the rest being contained within the RC [Shiozawa *et al*, 1982].

Detergents have played an important role in investigating the structure of the photosynthetic apparatus. Their utilization has allowed the isolation of different types of LHC. These can be differentiated with respect to the NIR-absorption maxima expressed by their BChl *a* molecules, and can thus also provide a basis for the classification of photosynthetic bacteria [Aagaard and Sistrom, 1972]. Three types of complex are recognized (these are illustrated in Figure 1.2b):

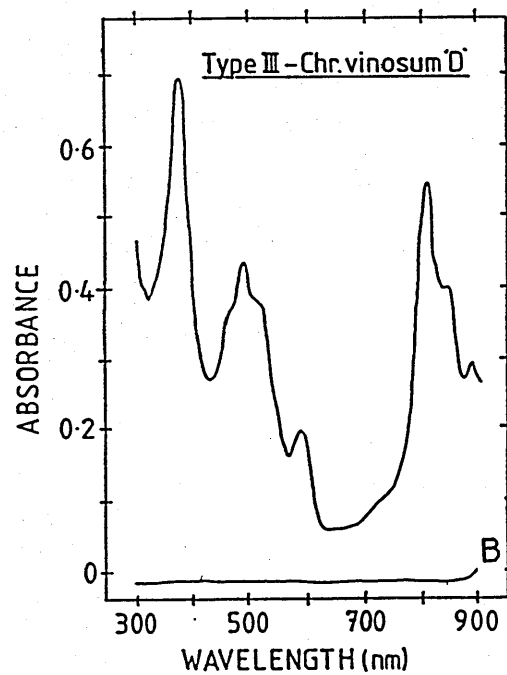
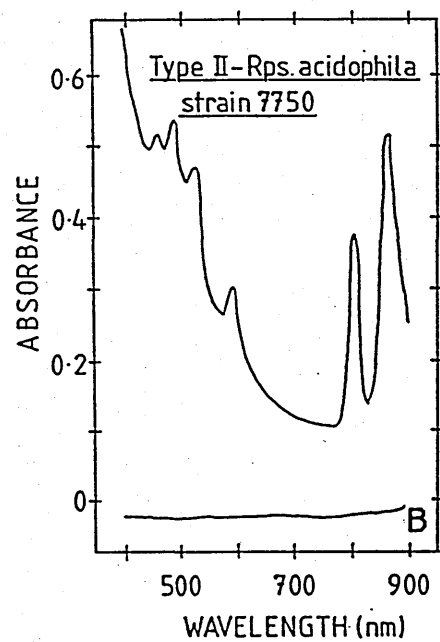
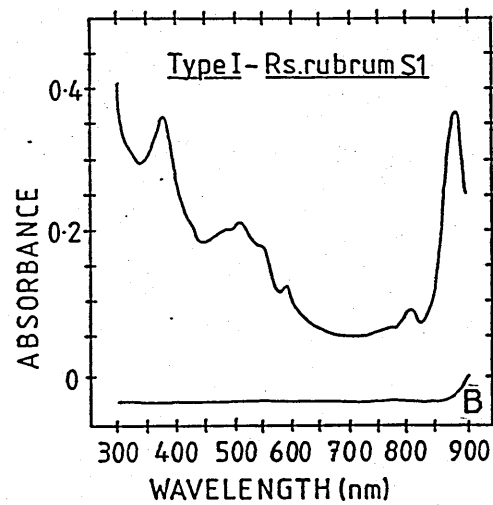
(1) the B890 (B870) complex - so called because the bulk of BChl absorbs at or around 890 (870) nm. All wild type bacteria possess this antenna complex. Type I bacteria however, for example *Rhodospirillum rubrum* strain S1 and carotenoidless mutant strains of *Rhodobacter sphaeroides* and *Rhodobacter capsulatus*, possess only this type of complex [(Cogdell and Thornber, 1979)(Picorel *et al*, 1983)(Sauer and Austin, 1978)].

(2) the B800-850 antenna complex exhibits NIR-absorption maxima at 800 nm and 850 nm. Type II species of purple bacteria possess both the B870 and B800-850 antenna complexes, for example *Rhodobacter sphaeroides* and *Rhodobacter capsulatus* [(Broglie *et al*, 1980)(Clayton and Clayton, 1972)(Cogdell and Thornber, 1979 and 1980)(Cogdell and Valentine, 1983)]. In most Type II species, the BChl *a* absorbs light in constant proportions at 800 nm and 850 nm such that peak height at 800 nm is less than, or equal to, that at 850 nm. Some species however, show increased absorption at 800 nm relative to that at 850 nm. This modification

FIGURE 1.2b Spectral Differentiation of Purple Photosynthetic Bacteria.

This figure presents room temperature absorption spectra of membranes isolated from the species *Rs.rubrum* S1, *Rps.acidophila* 7750 and *Chromatium vinosum* strain D. In the NIR regions of each spectrum, spectral properties typically characteristic of each species can be observed; *Rs.rubrum* S1 which possesses only one type of LHC, has peak absorbance at about 890 nm, and a second smaller peak at 800 nm. These peaks can be attributed to B890 antenna complex and RC absorption respectively. *Rps.acidophila* 7750, however, shows two absorption peaks in the NIR region of the spectrum; the two peaks, one at 800 nm and the other at approximately 860 nm, are the result of absorption by the LHC B800-850. The B875 antenna complex causes a shift in the position of the 850 nm peak towards longer wavelengths. RC absorption also contributes to the peak observed at 800 nm. The absorption spectrum of *Chromatium vinosum* strain D shows a prominent peak at 800 nm which shoulders at approximately 850 nm and at 890 nm. This pattern of absorption is a typical product of absorption by the three types of LHC recognized ie. the B800-850, B800-820 and B875 antenna complexes. These species of bacteria with their characteristic absorption properties are typically representative of the three types of purple bacteria recognized ie. Types I, II and III respectively.

The membranes were prepared as described in section 3.3, and resuspended in 20 mM Tris-HCl, pH 8.0. The absorption spectra were recorded using a SP8-500 UV/VIS spectrophotometer for wavelengths throughout the visible and NIR regions (Absorbance pathlength 1 cm)



B - baseline

of peak height ratio is usually accompanied by the addition of a third antenna complex ie. the B800-820 complex; this complex absorbs additionally at around 820-830 nm. Type III species, for example *Chromatium vinosum* strain D and *Rhodopseudomonas acidophila* strain 7050 (grown at low light intensities) and strain 7750 (grown at low temperatures) exhibit absorption maxima characteristic of all three antenna complexes [(Cogdell and Thornber, 1980)(Thornber, 1970)(Cogdell *et al*, 1983)(Angerhofer *et al*, 1986)(Schmidt *et al*, 1987)].

Since their initial identification, a number of studies have set out to examine both the structural and functional characteristics of these different antenna complexes [see Reviews (Amesz, 1985)(Zuber, 1985)]. The B800-850 complex, which has been most extensively studied, is constructed of pigment-protein complexes. Two specific low molecular weight (LMW) polypeptides, α and β [(Brunisholz *et al*, 1981)(Füglister *et al*, 1984)(Tadros *et al*, 1984 and 1985)(Theiler *et al*, 1984a&b)] provide an anchor for the noncovalent binding of the photosynthetic pigments. Some species, for example *Rhodobacter capsulatus* and *Rhodopseudomonas viridis* possess an additional colourless polypeptide, Y [Shiozawa *et al*, 1982]. The α and β polypeptides occur in *Rhodobacter sphaeroides* in a fixed 1:1 ratio [Cogdell and Thornber, 1980] and in *Rhodopseudomonas capsulata*, which has the additional Y polypeptide, the ratio is 1:1:1 [Shiozawa *et al*, 1982]. The primary structure of the α and β B800-850 light-harvesting polypeptides from *Rhodobacter sphaeroides*, and the B800-850 α [Tadros *et al*, 1983] and B800-850 β [Tadros *et al*, 1985] from *Rhodobacter capsulatus*, have been examined. All have been shown to exhibit a tripartite domain structure consisting of a polar N-terminus, a central hydrophobic region, and a polar C-terminus. A variety of experiments including labelling [Brunisholz *et al*, 1984b], protease

degradation techniques [Brunisholz *et al*, 1984 a, b] suggest that the N-terminus is positioned on the cytoplasmic side of the membrane whereas the C-terminus is positioned on the periplasmic side [(Brunisholz *et al*, 1986)(Tadros *et al*, 1987a, b)]. Results of IR, and UV-CD spectra [(Theiler *et al*, 1984b)(Breton and Navedryk, 1984a)] also suggest that the hydrophobic stretch assumes an α -helix conformation, which is thought to traverse the membrane [(Francis and Richards, 1980)(Cogdell and Scheer, 1985)]. Comparison of the primary structures of α and β antenna polypeptides from a range of purple bacteria (Figure 1.2c) reveals the conservation of a number of amino acids, in particular of a conserved AxxxHis sequence which is believed to be the bacteriochlorophyll a binding site [(Theiler and Zuber, 1984)(Youvan and Ismail, 1985)(Tadros *et al*, 1987c)]. Two such conserved sites are observed within the hydrophobic stretch of the β -polypeptides. Also noticeable are the conserved aromatic residues positioned at a definite distance from the putative bacteriochlorophyll binding sites. It is suggested that these probably interact with bacteriochlorophyll and carotenoids [Brunisholz *et al*, 1984a]. These polypeptides, therefore, are complexed with photopigments to form the B800-850 antenna complex. The cache of photopigments making up the basic unit of the B800-850 antenna complex consists of 2 BChl a 800 molecules together with 4 BChl a 850 and 3 carotenoid molecules, therefore assuming a 2:1 ratio of BChl 850 : BChl 800 [(Cogdell and Crofts, 1978)(Cogdell and Thornber, 1979)(Sauer and Austin, 1978)(van Grondelle *et al*, 1982)], and a 2:1 ratio of BChl a:carotenoid [(Kramer *et al*, 1984a)(Radcliffe *et al*, 1984)(Evans, unpublished)]. This basic, or minimal, unit structure is then aggregated into larger groups yielding a larger complex structure.

α -POLYPEPTIDES

	N-TERMINAL		CENTRAL		C-TERMINAL	
	POLAR, CHARGED DOMAIN.		HYDROPHOBIC DOMAIN		POLAR, CHARGED DOMAIN.	
<u>Rs.rubrum</u> B890	□	▲	□	◆	□	▲
<u>Rps.viridis</u> B1015	□	▲	□	◆	□	▲
<u>Rb.sphaeroides</u> B875	○	▲	○	◆	○	▲
<u>Rb.capsulatus</u> B875	○	▲	○	◆	○	▲
<u>Rb.sphaeroides</u> B800-850	○	▲	○	◆	○	▲
<u>Rb.capsulatus</u> B800-850	○	▲	○	◆	○	▲
β-POLYPEPTIDES						
<u>Rs.rubrum</u> B890	□	▲	□	◆	□	▲
<u>Rps.viridis</u> B1015	○	▲	○	◆	○	▲
<u>Rb.sphaeroides</u> B875	○	▲	○	◆	○	▲
<u>Rb.capsulatus</u> B875	○	▲	○	◆	○	▲
<u>Rb.sphaeroides</u> B800-850	○	▲	○	◆	○	▲
<u>Rb.capsulatus</u> B800-850	○	▲	○	◆	○	▲

FIGURE 1.2c. Conserved aromatic amino acid residues in the α and β antenna polypeptides of B875/B890, B1015 B800-350 antenna complexes from Rhodospirillaceae. Aromatic residues are found in all α and β polypeptides (\blacktriangle) in the B875/B890 complex (\blacklozenge), in the B800-850 complex (∇), in the B890 complex of Rs.rubrum or in the B1015 complex of Rps.viridis (\square), and in the B875 complex of Rb.sphaeroides and Rb.capsulatus (\circ) [Zuber, 1985][Youvan and Ismail, 1985]. Conserved putative bacteriochlorophyll binding sequences are boxed.

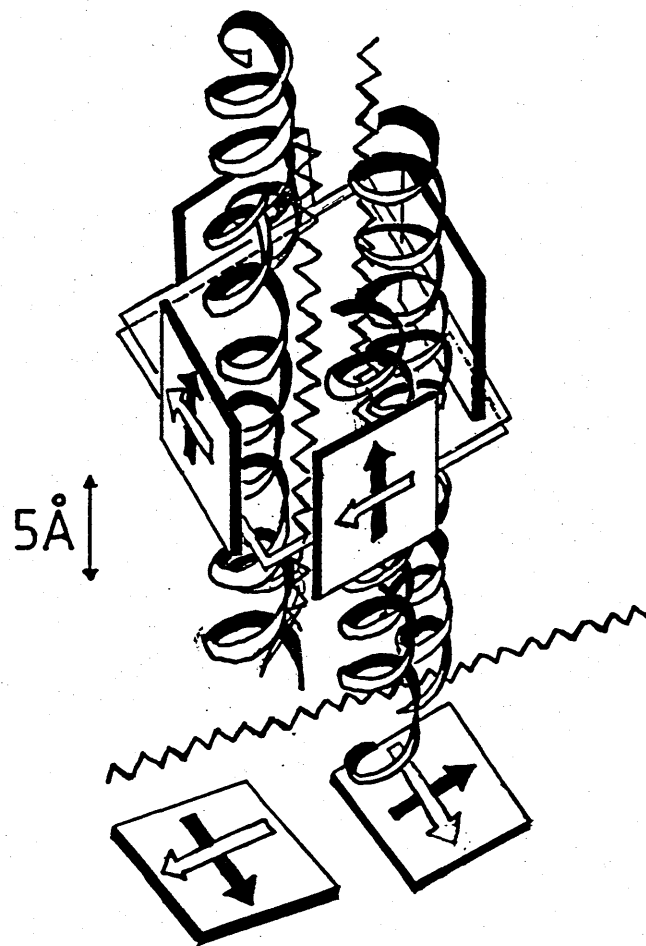
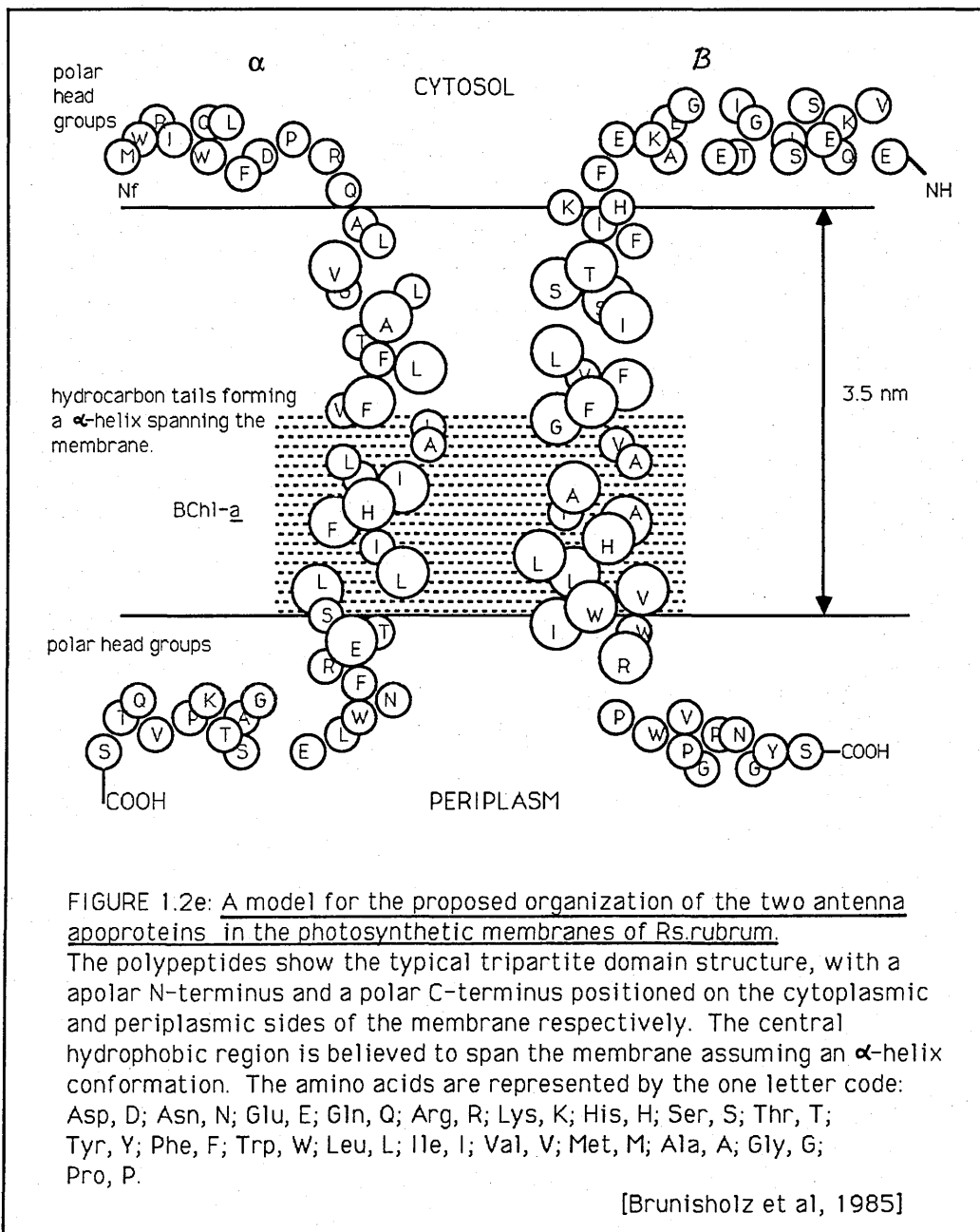


FIGURE 1.2d Schematic Model of the B800-850 Antenna Complex of *Rhodobacter sphaeroides*.

In the model presented the spirals represent protein helices, the polar stretches of the apoproteins are not shown. Squares represent bacteriochlorophyll *a* porphyrin rings with Q_y (open arrows) and Q_x (solid arrows) transitions. The upper four squares belong to BChl *a* 850, and the lower ones are those of BChl *a* 800. Zig-zag lines are carotenoids. The plane of the membrane is thought to be horizontal [Kramer *et al*, 1984].

On the basis of these experiments, and from the measurement of linear dichroism and fluorescence polarization, which provide information about the orientation of pigments [(Bolt *et al*, 1981)(Bolt and Sauer, 1979)(Breton *et al*, 1981)(Breton and Vermeglio, 1982)(Kramer *et al*, 1984a)(Sauer and Austin, 1978)], a fairly detailed model of the minimal basic unit of the B800-850 complex of *Rhodobacter sphaeroides* has been proposed [Kramer *et al*. 1984a]. Figure 1.2d illustrates the proposed model.

The structure of the B870 (B890) antenna complex is believed to be similar to that of the B800-850 complex with respect to both protein structure, pigment content and organization. Figure 1.2e proposes a model for the organization of the α and β polypeptides of the B890 complex of *Rhodospirillum rubrum* S1. The proteins show the tripartite domain structure also observed in the respective polypeptides of the B800-850 antenna complex of *Rhodobacter sphaeroides*. The composition has been examined extensively in *Rhodospirillum rubrum* strain S1 in which the B890 complex accounts for the total BChl *a* content [(Brunisholz *et al*, 1984a&b)(Sauer and Austin, 1978)]. In *Rs. rubrum* S1 the BChl *a* :carotenoid (spirilloxanthin) ratio is 2:1 [(Cogdell and Crofts, 1978)(Thornber *et al*, 1983)], although in *Rb.sphaeroides* the ratio is closer to 1:1 [Broglie *et al*, 1980]. The B875 (B890) antenna complex of both these species also contain two different peptides [(Cogdell *et al*, 1982)(Gogel *et al*, 1983)(Picorel *et al*, 1983)] whose primary structures show a clear homology to the α - and β -polypeptides of the B800-850 complex of *Rhodobacter sphaeroides* and *Rhodobacter capsulatus*. Additionally, these polypeptides possess the conserved AxxxHis sequence (refer again to Figure 1.2c) [(Brunisholz *et al*, 1981 and 1984)(Gogel *et al*, 1983)(Theiler *et al*, 1984a&b)(Tadros *et al*, 1984)(Kramer *et al*, 1984b)].



The Reaction Centre.

Purified RC complexes have been obtained by the detergent treatment of isolated membranes or chromatophores, a method pioneered by Reed and Clayton (1968). The RC have been characterized in terms of their chemical constituents [(Feher and Okamura, 1978)(Okamura *et al*, 1982)] and consist of 4 molecules of BChl a, 2 bacteriopheophytin a molecules, 1 carotenoid, 1 nonhaem iron, and 1-2 ubiquinone molecules (or menaquinone as found in *Chromatium vinosum* D and *Rhodopseudomonas viridis*). These constituents are bound noncovalently to a protein which consists of three polypeptides (L, M and H) in a 1:1:1 ratio [(Clayton and Haselkorn, 1972)(Feher and Okamura, 1978)(Okamura *et al*, 1982)]. Treatment of isolated reaction centres with chaotropic agents can effectively remove the H-polypeptide. The resultant structure, although less stable, shows no change in its binding capacity for bacteriochlorophyll, iron, cytochrome or primary and secondary quinone acceptors (Q_A and Q_B). It also has no observable effect on the primary photochemical activities of photosynthesis [(Okamura *et al*, 1974)(Agalides and Reiss-Husson, 1983)(Feher and Okamura, 1984)]. Removal of the H-polypeptide however, has been seen to effect the transfer of energy from Q_A to Q_B [Debus *et al*, 1985]. These results, therefore, do indicate that the chemical constituents of the reaction centre are only associated with the L and M polypeptides. The primary structures of the reaction centre polypeptides have been determined primarily from the sequencing of structural genes. This is in contrast to the analysis of antenna polypeptides which have been determined using the technique of automated Edman degradation [Brunisholz *et al*, 1981]. By this method the primary sequences of the L, M and H subunits have been determined for the species *Rhodobacter sphaeroides* [Williams *et*

al, 1983, 1984 & 1986], *Rhodobacter capsulatus* [(Youvan *et al*, 1984)(Youvan and Ismail, 1985)] and *Rhodopseudomonas viridis* [Michel *et al*, 1985, 1986]. The percentage identity of residues conserved for all three species is 53% for L, 46% for M and 31% for H. Those residues that interact with the cofactors, such as Histidine binding to bacteriochlorophyll and ligands to nonhaem iron [Deisenhofer *et al*, 1985], are very well conserved. Although the overall conservation of the H-subunit is poor, regions of H in contact with the conserved regions of L and M are highly conserved, for example residues H30 - H42 (69%) and H229 - H240 (66%). Analysis of the L and M subunits has revealed five segments which are rich in hydrophobic amino acids [Williams *et al*, 1983], and which may form membrane-spanning helices lying perpendicular to the membrane [Nabedryk *et al*, 1982]. Hydropathy plots of these sequences provide evidence suggesting that each hydrophobic segment is long enough, being of at least twenty residues, to span the membrane in an α -helix [Williams *et al*, 1983]. These structural predictions have been confirmed by X-ray crystallographic analysis of crystals, successfully produced of the reaction centre of the bacteriochlorophyll b-containing species *Rps. viridis* [(Michel, 1982)(Deisenhofer *et al*, 1984, 1985)], and, more recently, of the BChl a-containing species *Rb. sphaeroides* R26 [Allen *et al*, 1987a & b]. The reaction centre from *Rb.sphaeroides* is composed of three protein subunits L, M and H, and the following cofactors; 4 bacteriochlorophyll a and 2 bacteriopheophytin a molecules, 2 ubiquinones and 1 nonhaem iron. The reaction centre from *Rps. viridis*, has an additional subunit, a cytochrome with 4 C-type haems. While its bacteriochlorophylls and bacteriopheophytins are of the 'b'-type, and the primary quinone is menaquinone. The electron density maps produced for the RC of these species ie. *Rps. viridis* and *Rb. sphaeroides* R26

(produced at resolutions of 2.9 Å and at 2.8 Å respectively), have been used to construct a model describing the arrangement of reaction centre cofactors. The main features of the structure are very similar for the two species, despite differences in their compositions. The model (illustrated in Figure 1.2f for the RC of *Rps. viridis*) shows a roughly two-fold symmetrical arrangement of bacteriochlorophyll and bacteriopheophytin pyrrole ring systems. Two closely associated non-covalently-linked BChl a/b molecules, the "special pair", are positioned near to the axis of symmetry [(Deisenhofer *et al*, 1984, 1985)(Yeates *et al*, 1987)]. These bacteriochlorophyll molecules, known as P870, interact to give an absorption band near to 870nm and constitute the primary electron donor [(Norris *et al*, 1971)(Feher *et al*, 1975)]. The positions of the centres of tetrapyrrole rings are well conserved, but there are, some differences between the two species, in the relative orientation of the rings and placement of sidechains. A striking feature of the structure is the presence of eleven transmembrane helices consisting of approximately 22 - 31 residues; 5 membrane helices in both the L and M subunit, and 1 in the H subunit [Allen *et al*, 1987b]. The bulk of the H-subunit lies in the cytoplasmic side and makes many contacts with the cytoplasmic sides of the L and M subunits. In relating these data with those obtained by sequence analysis, it can be observed that the similarity in the three-dimensional structure of the reaction centre, of the species *Rps. viridis* and *Rb. sphaeroides* is consistent with the similarity apparent in their primary structures.

Having described above what is understood about the basic components of the photosynthetic apparatus, their relative organization with respect to each other, and to the

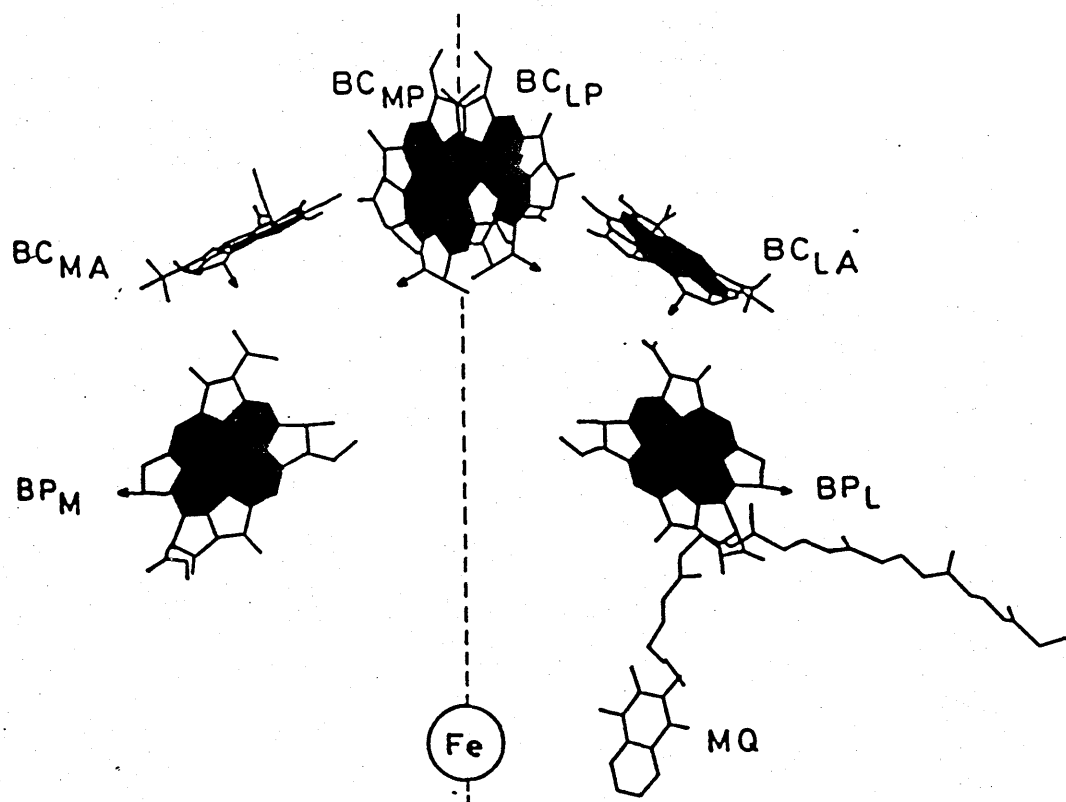


FIGURE 1.2f A Model Illustrating the Arrangement of chromophores in the Reaction Centre of the BChl *b*-containing species *Rhodopseudomonas viridis*.

The model shows four bacteriochlorophyll *b* (BC), two bacteriopheophytin *b* (BP) molecules and the menaquinone (MQ). The models are arranged in two branches L and M.

Summary of letter codes observed in the figure:

- BC_{(MP)L} The BChl *b* primary donor 'special pair'.
- BC_{MA} Monomeric BChl *b* on the 'M' subunit side.
- BC_{LA} Monomeric BChl *b* on the 'L' subunit side.
- BP_L Monomeric bacteriopheophytin *b* on the 'L' subunit side.
- BP_M Monomeric bacteriopheophytin *b* on the 'M' subunit side.
- MQ Menaquinone.
- Fe Ferrous iron.

[(Deisenhofer *et al*, 1984)(Zinth *et al*, 1985)]

intracytoplasmic membrane, can now be considered. The following paragraphs outline current thinking on the topology of the photosynthetic apparatus within the intracytoplasmic membrane.

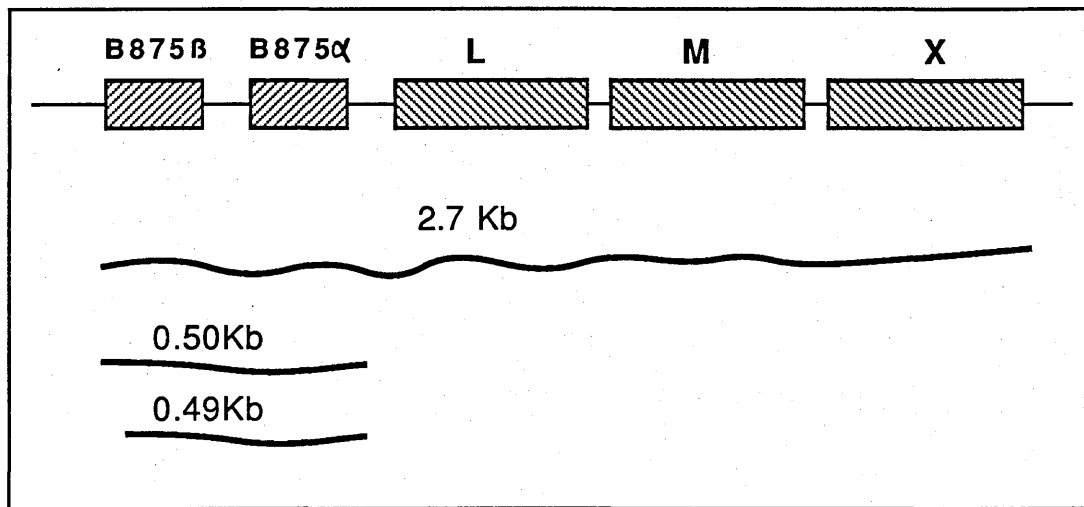
It was Aagaard and Sistrom (1972) who recognized the existence of the two main types of antenna complex in BChl a-containing species of purple bacteria. These early studies also suggested that the amount of RC.BChl a remained relatively constant with respect to the longest wavelength component ie. B875. This gave birth to the idea that a fixed stoichiometry exists between the RC and the B875 complex, an idea which was soon supported by evidence from developmental studies, and from the examination of cells adapting to changes in environmental conditions, particularly to changes in light intensity and partial pressures of oxygen. Examination of these cells showed that the ICM responded to changes in the environment, and adapted accordingly by regulating the size of the ICM itself, by modifying the size of the photosynthetic unit, or in some species, for example *Rhodospirillum rubrum* S1, by modulating the number of photosynthetic units per unit area of membrane. The size of the photosynthetic unit depends largely on the synthesis of B800-850 BChl a which, unlike the coordinated synthesis of the RC and B875 BChl a, is influenced by prevailing environmental conditions, such that low light intensities induce its synthesis and consequently increase the size of the photosynthetic unit [Firsow and Drews, 1977]. A number of developmental studies also revealed that during the formation of the photosynthetic membrane, the RC and B875 components are produced first and the B800-850 complex is added subsequently [(Aagaard and Sistrom, 1972)(Takemoto, 1974)(Niederman *et al*, 1976)(Drews *et al*, 1977)(Firsow and Drews, 1977)(Pradel *et al* 1978)(Schumacher and Drews, 1978)(Hunter *et al*, 1982)]. It was also shown that the syntheses

of the RC and the B875 complex are coordinated, whereas the synthesis of the B800-850 complex proceeds independently [(Aagaard and Siström, 1972)(Lien and Gest, 1973)(Niederman *et al*, 1976)]. This coordinated synthesis can also be observed at the molecular level. The recent success in sequencing the DNA fragment containing the *puf* operon (formerly referred to as the *rxcA* locus) has shown that the genes encoding the α and β pigment-binding proteins of the B870 antenna complex and the photochemically-essential L and M subunits of the reaction centre complex, in the species *Rhodobacter capsulatus* and *Rhodobacter sphaeroides*, are arranged in a single *puf* operon (Figure 1.2g) [Youvan and Ismail, 1984](Taylor *et al*, 1983)]. The genes encoding the polypeptides of the B800-850 antenna complex are not included within this gene cluster but are coded for elsewhere. It is worth noting however, that the identical organization of α and β structural genes, and the sequence homologies between the two α and two β polypeptides, particularly with respect to the conservation of the bacteriochlorophyll binding sequence, suggest that both complexes arose by gene duplication from a single ancestral light-harvesting complex [Youvan and Ismail, 1985]. Transcription of the polycistronic *puf* operon, which is regulated by oxygen tensions [(Clark *et al*, 1984)(Zhu and Hearst, 1986)(Zhu *et al*, 1986)] allows for coordinated gene regulation but does not control the differential expression of different gene products ie. in accordance with the observations that the B875 complexes present are in considerable molar excess over the reaction centre [(Schumacher and Drews, 1978)(Kaufmann *et al*, 1982)]. In this particular case, differential expression results predominantly from differences arising in the stability of the *puf* transcript. The 3' portion of this transcript is rapidly degraded, giving rise to two slowly decaying mRNA remnants encoding the light-harvesting

Figure 1.2g: Genetic Map of the puf Operon

The polycistronic arrangement of genes encoding for the α - and β -pigment-binding polypeptides of the B875 antenna complex and the photochemically essential L and M subunits of the reaction centre is indicative of their coordinated transcription.

[Youvan et al, 1984]



— Messages

- X Open translation reading frame of unknown function.
- L and M Genes encoding the L and M subunits of the reaction centre, the genes actually overlap by 5 nucleotides
- B875 α } Genes encoding the α and β polypeptides of the B875
B875 β } complex.

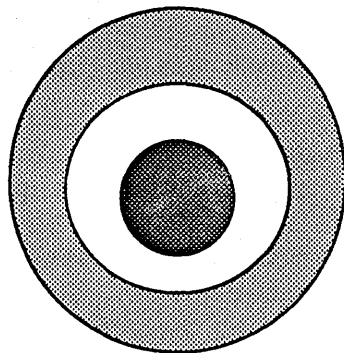
polypeptides. The greater stability of these remnants accounts for nearly all the differences between the concentration of light-harvesting and reaction centre proteins [Belasco *et al*, 1985]. This evidence provides additional support for the coordinated synthesis of reaction centre and B875 light-harvesting complexes. In light of all these results it seems that the light-harvesting apparatus is composed of a fixed B875, and a variable B800-850 component. In obtaining a measurement for the size of the fixed component, studies proposed that the RC is associated with between 20 and 30 B875-BChl *a* molecules [(Aagaard and Sistrom, 1972)(Hayashi *et al*, 1982a&b)(Kendall-Tobias and Seibert, 1982)(Ueda *et al*, 1985)] although values of between 1:30 and 1:40 have also been reported [(Aagaard and Sistrom, 1972)(Firsow and Drews, 1977)]. If the B800-850 pigment-protein complex is also present, then this ratio varies inversely with the light intensity at which the cells are grown, and can range from 50 to 300 BChl *a* molecules per RC [(Aagaard and Sistrom, 1972)(Drews *et al*, 1983)]. A number of models have been proposed to describe the relationship between the RC and light-harvesting complexes. The one that receives the most experimental support is that described by Monger and Parson (1977) who suggest that the RC shares a common pool of interconnecting B875 complexes surrounded by a sea of the B800-850 antenna complex. Two variations of this model are recognized; one describes the independent separation of reaction centres, known as the Puddle Model, and the second predicts the interaction of a number of reaction centre molecules within a sea of the B875 antenna complex ie. the Lake Model (these two models are illustrated in Figure 1.2h). This arrangement of complexes relative to each other is supported by experimental evidence from energy transfer studies, which show that energy is transferred with high efficiency from short wavelength BChl *a*

FIGURE 1.2h: Models describing the proposed organization of reaction centre and light-harvesting components.

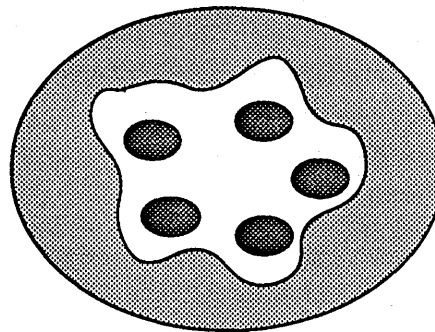
Two models have been proposed, the Puddle model and the Lake model, describing the organization of the reaction centre and the light-harvesting complexes: the Puddle Model suggests an independent separation of reaction centres, whereas the Lake Model suggests that several reaction centres associate within a lake of the B875 antenna complex.

[Monger and Parson, 1977]

■ Reaction centre. □ B875 LHC. ▣ B800-850 LHC.



PUDDLE MODEL



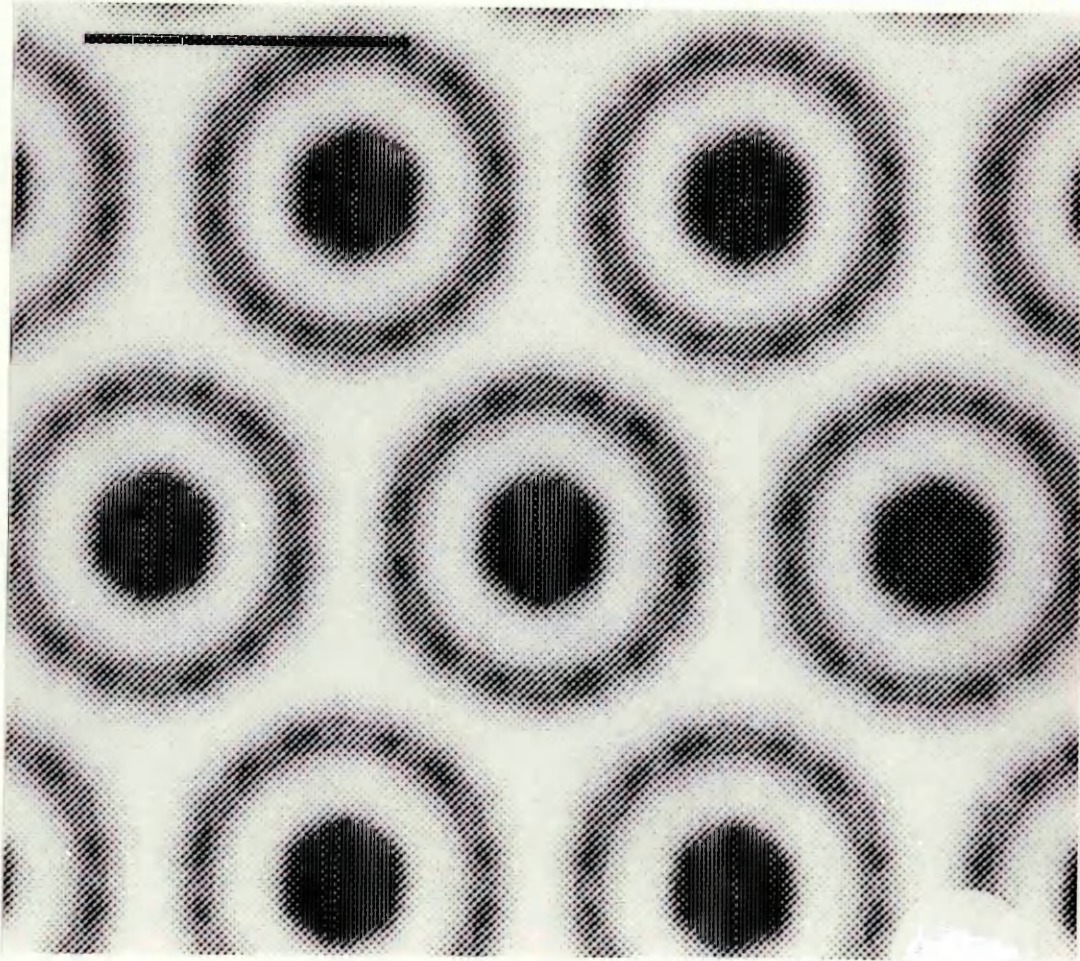
LAKE MODEL

such as BChl a 800 and 850, to long wavelength BChl a ie. B875 and hence to the reaction centre [(Clayton, 1980)(Hayashi *et al*, 1982b)]. The cyclic arrangement of complexes as depicted by the model is a probable consequence of the highly packed, twisted arrangement of the α and β polypeptides in conjunction with the probable interaction of amino acid side chains [Zuber, 1985].

Investigations of the photosynthetic membranes isolated from the BChl b-containing species *Rhodopseudomonas viridis* and *Ectothiorhodospira halochloris*, using high resolution electron microscopy and image processing techniques, have led to the low resolution elucidation of the three-dimensional structure of their photosynthetic apparatus [Engelhardt *et al*, 1983]. They are shown to consist of a large central core structure which protrudes from both surfaces of the membrane [(Miller and Jacob, 1983)(Stark *et al*, 1984)] and is surrounded by six smaller centres of mass (Figure 1.2i) [Miller, 1982]. The successful production of three-dimensional crystals of the reaction centre of *Rhodopseudomonas viridis* [Deisenhofer *et al*, 1984, 1985] and their subsequent analysis shows that the central core of the photosynthetic unit has dimensions comparable to those determined for the reaction centre molecule [(Miller, 1982)(Jay *et al*, 1984)(Stark *et al*, 1984)]. The surrounding ring is believed to consist of twelve light-harvesting complexes arranged in six dimers [Miller, 1979, 1982]. Estimates of the bacteriochlorophyll-b content of the reaction centre-antenna complex, determined from the ratio of antenna absorbance at 1020 nm to that of reaction centre absorbance at 830 nm, suggest that approximately 24 BChl-b molecules are associated with each reaction centre [Breton *et al*, 1985]. Assuming that each antenna complex contains four BChl-b molecules (as is suggested by some B875-type BChl-a-protein complexes [Zuber, 1985]), this would suggest that each reaction centre is associated

FIGURE 1.2 i Contour Maps of the*Plasmic Side of Triton X-100-Treated Membranes of *Rhodopseudomonas viridis* Obtained by Fourier Processing of Electron Micrographs.

The single membrane sheet shows the characteristic pattern of hexagonally packed circular units. The structural unit on the plasmic side resembles a ring of 120 Å diameter, with a central core measuring 45 Å across which rises steeply to a plateau. Within the ring twelve units arranged in six pairs can be observed. Bar scale = 10 nm. (100 Å).



(*Plasmic refers to periplasmic side)

with six B1020 antenna complexes. These results also suggest a six-fold symmetrical structure. However, cross-sectional analysis of two-dimensional [Miller and Jacob, 1983] and three-dimensional [Deisenhofer *et al*, 1984] crystals of isolated reaction centres, and the examination of photosynthetic membranes by means of scanning transmission electron microscope mass determination and mass mapping [Engelhardt *et al*, 1986] show it to be roughly elliptical (Figure 1.2 j). This would imply that reaction centre and antenna associations cannot have a rotational symmetry greater than two fold [Stark *et al*, 1984]. The apparent six-fold symmetry therefore, probably reflects a rotational average of a number of reaction centre-antenna conjugates packed in various orientations into a two-dimensional hexagonal lattice [(Welte and Kreutz, 1982)(Miller, 1979, 1982)(Engelhardt *et al*, 1983)(Miller and Jacob, 1983)(Stark *et al*, 1984)]. The lattice structure of the thylakoid membrane has also been observed in other BChl *b*-containing species including *Thiocapsa pfennigii*, *Ectothiorhodospira abdelmalekii*, and *Rhodopseudomonas sulfoviridis* [Eimhjellen *et al*, 1967].

These studies provoke the question as to whether the constant statistical relationship apparent in some BChl *a*-containing species reflects the existence of a similar well-defined core-complex. A number of techniques have been adopted to see whether a similar type of RC-core complex is common to all BChl *a*-containing species. The earliest, although indirect, study was that of Thornber (1970) in which a fraction, the so-called fraction A, was successfully isolated from *Chromatium vinosum* strain D, containing the B875 light-harvesting spectral form together with the RC in a ratio of 45:1 respectively. Since then the idea that the B870 complex is intimately associated with the RC has received experimental support from a number of sources [(Lien and Gest,

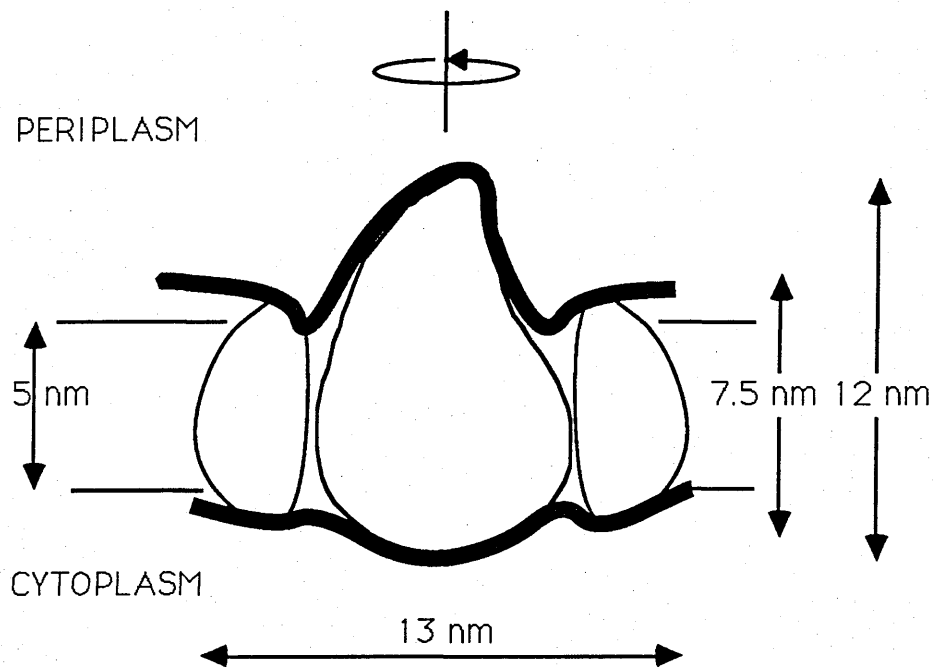


FIGURE 1.2j: Schematic model of a transmembrane section through the photosynthetic complex.

Data on the shape and dimensions were drawn from surface relief reconstructions and averages of negatively stained and unstained membranes. The results suggest that the reaction centre protrudes substantially from both membrane surfaces, and being roughly elliptical in shape, may assume various orientations within the LHC ring. [Engelhardt et al, 1986].

1973)(Monger and Parson, 1977)(Takemoto *et al*, 1982)(Drews *et al*, 1983)(Peter *et al*, 1983 and 1984)(Ueda *et al*, 1985)(Varga and Staehelin, 1985)(Youvan and Ismail, 1985)] in particular from the mild treatment of the photosynthetic apparatus with detergents [Jay *et al*, 1984], and by immunofractionation techniques [Takemoto *et al*, 1982]. Cross-linking studies also indicate that the H-subunit has 'close-neighbour relationships' with polypeptides of the B875 (B890) antenna complex [Peter *et al*, 1983] and that it plays an important structural role in the membrane in the coordination of the reaction centre-antenna interactions [(Takemoto *et al*, 1982)]. Glazer (1983) also claimed that the two are functionally associated and consequently called the associated complex the "Photochemical reaction centre". A different approach was made by Varga and Staehelin (1985), who on isolating and characterizing the large oligomeric complexes of the photosynthetic unit of *Rhodopseudomonas palustris*, ie. RC-B880 core, B800-850 and RC-B880-B800-850, inserted them into phospholipid liposomes. In correlating the size and composition of such complexes with other data available on the morphology, biochemistry and biophysics, a model describing spatial relationships between individual components was proposed (Figure 1.2k). The model suggests that in *Rhodopseudomonas palustris* the reaction centre forms a core-complex with twelve B880 antenna complexes, which may also combine with B800-850 antenna to yield a larger complex. This model therefore, provides a basis for future experimental examination of component organization *in vivo*, and also provides additional experimental support to existing evidence. The work of Ueda *et al* (1985) employing non-equilibrated electrophoretic techniques on a range of bacteriochlorophyll-a containing species of purple bacteria yielded similar results. However it must be stressed that the conclusions

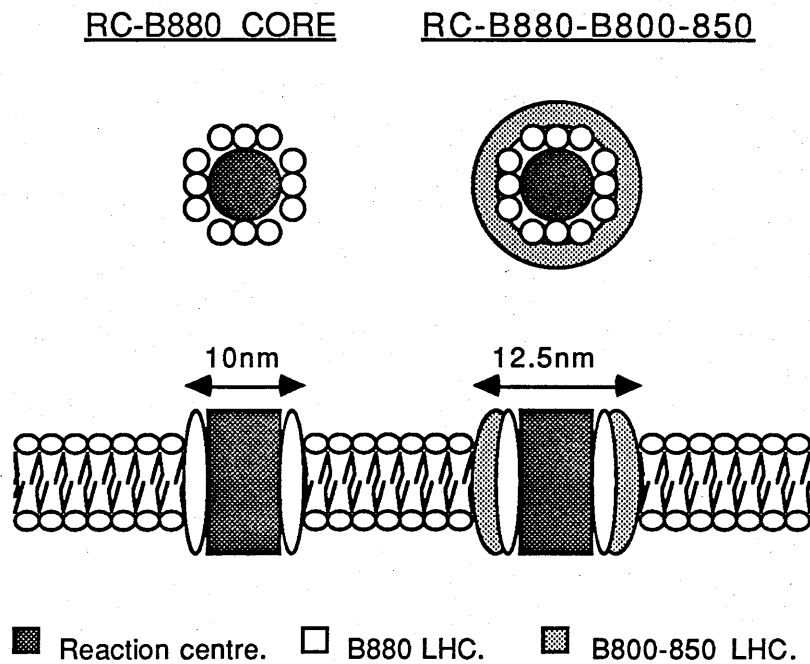


FIGURE 1.2k : Models for the major pigment-protein oligomers in *Rps.palustris* photosynthetic membranes, top and side views.

The model suggests that the reaction centre forms a core-complex with 12 B880 antenna complexes. The B800-850 may also associate with this core structure to yield a larger oligomer.

[Varga and Staehelin, 1985]

drawn in this case are based on poor analysis of data, and rely upon inaccurate determinations of protein molecular weights. These seemingly supportive data therefore, are best considered as a product of coincidence rather than the result of reliable experimental protocol.

The precise association between these components is still not entirely clear although experimental evidence obtained to date does suggest the existence of a stoichiometric association. It still remains to be seen however, whether the apparent numerical relationship between these two components reflects a fixed stoichiometry, or whether it is simply a statistical phenomenon, a coincidental average of several RC-B875 photosynthetic units which exhibit individual variation. It is also of importance to examine whether this relationship is true for all BChl a-containing species. This study involves the isolation of this apparent 'core structure' from a number of BChl a -containing species and its examination with respect to antenna-RC associations.

CHAPTER 2

Methodology

The reaction centre-B875 antenna complex has been isolated from the photosynthetic units of bacterial membranes, using the method of detergent solubilization and sucrose density-gradient centrifugation, as described by Firsow and Drews (1977) but modified and adapted to suit the range of bacteriochlorophyll a - containing species examined in this study. Prior to describing the actual experimental protocols employed to examine the structural and functional integrity of this complex, the concepts behind each technique will be discussed.

Methodology 2.1

Spectral Characterization.

The photosynthetic membranes of purple bacteria show distinctive variations in the near infrared region of their absorption spectra [Pfennig, 1978]. Nearly all of the absorption bands in this region are due to bacteriochlorophyll a (BChl a) absorption with the spectral variation being a consequence of its interaction with the immediate environment ie. BChl-BChl [Drews *et al*, 1977], BChl-protein [Vrendenberg and Ames, 1967] and BChl-carotenoid interactions and to a lesser extent BChl-lipid interactions [Pfennig, 1978].

Three main types of BChl-protein complexes are recognized and are differentiated according to their NIR absorption spectra:

- (i) B875 (B890) complex - This exhibits bulk absorption in the region at or around 875 nm.
- (ii) B800-850 complex - shows two absorption bands at 800

nm and 850 nm.

(iii) B800-820 - this pigment-protein complex shows peak absorption at 800 nm and 820 nm.

The presence or absence of these components is used to characterize, and categorize, bacteriochlorophyll a-containing species of purple bacteria [Cogdell and Thornber, 1979]. To briefly recap, the three major groups recognized are Type I (these bacteria possess only the B875 (B890) antenna complex), Type II, which possess the B800-850 antenna complex in addition to the B875 (B890) complex, and finally Type III which have all three types of bacteriochlorophyll-protein complexes recognized ie. B875 (B890), B800-850 and B800-820.

The relative ratio of absorption at B800 to B850 can be attributed to changes in environmental parameters such as partial pressures of oxygen and light intensity [Firsow and Drews, 1977]. Bacteriochlorophyll production is regulated by the partial pressure of oxygen, and the level of pigmentation is finely tuned by the prevailing light intensity [(Aagaard and Sistrom, 1972)(Firsow and Drews, 1977)] such that pigmentation is strongly suppressed by a combination of light and oxygen. Anaerobic conditions will, however, stimulate BChl a production, and the light intensity will modulate relative proportions of B850:B875 with very weak light causing an increase in the ratio, and high light reducing the ratio [(Aagaard and Sistrom, 1972)(Clayton, 1980)(Firsow and Drews, 1977)].

The examination of the NIR absorption spectra of purple bacteria is regarded as a useful tool for the characterization of different purple bacterial species [(Angerhofer *et al*, 1986)(Pfennig, 1978)(Gomez *et al*, 1982)] and is also useful for ascribing changes in the shape of the spectrum to changes in environmental conditions [Drews *et al*, 1977]. In addition to this

invaluable method of differentiation, the NIR spectrum provides a rapid and a sensitive monitor of membrane or complex integrity [(Thornber *et al*, 1978)(Cogdell and Thornber, 1979, 1980)]. Since spectral information is a direct result of pigment interaction, any disruption of the intramolecular organization will be easily detected. The monitor is particularly sensitive since the different spectral forms absorb at wavelengths far removed from that of monomeric BChl a , which in organic solvents or detergents shows an absorption peak at approximately 772 nm [Clayton, 1963]. Lesser shifts can also be detected with only slight changes in interaction [Thornber *et al*, 1978]. This is of particular importance since the isolation of hydrophobic protein is fraught with difficulty, and it is essential that we have a rapid and a sensitive assay to confirm that native configurations have been retained during the isolation and purification procedures.

This useful assay has been employed in a number of studies [(Aagaard and Siström, 1972)(Cogdell and Crofts, 1978)(Sauer and Austin, 1978)(Cogdell and Thornber, 1979, 1980)(Bolt *et al*, 1981)(Kramer *et al*, 1984a&b)(Sebban *et al*, 1985)(Angerhofer *et al*, 1986)]. It has ensured that the isolated and purified complexes are still representative of their *in vivo* counterparts, and thus has permitted further characterization studies to be completed. Also, in being able to isolate and characterize the components of the photosynthetic apparatus it has been possible to account for the NIR absorption spectra of whole cells [Cogdell *et al*, 1983].

Methodology 2.2

The Isolation of the Light-Harvesting and Reaction Centre Complexes from Membrane Preparations.

The method first described by Firsow and Drews (1977) was adapted here for the isolation of the reaction centre-antenna complex from a range of BChl *a* -containing species of purple bacteria. The method essentially involves the solubilization of membranes, and their fractionation by sucrose-density gradient centrifugation.

Detergents, offering a useful and convenient method of membrane solubilization, have been used widely in the study of biological membranes: their properties have been utilized for the isolation of the two main components of the photosynthetic apparatus ie. the reaction centre (RC) and light harvesting complexes (LHC) [Sauer and Austin, 1978], for the isolation of purified reaction centres [Reed and Clayton, 1968], and have also been employed for the further breakdown of isolated complexes into their constituent polypeptides and pigments [Weber and Osborn, 1969].

The choice of detergents depends upon a number of important factors including properties of the membrane to be solubilized, properties of the complex(es) to be isolated and of course properties of the detergent itself:

(1) Properties of the membrane and membrane proteins: Bacterial membranes form multimolecular aggregates composed largely of phospholipid bilayers interspersed with proteins to which pigments, carbohydrates etc, are bound. Membrane proteins are generally classified into two categories (i) Extrinsic or peripheral

proteins [Singer and Nicolson, 1972]. (ii) Intrinsic proteins [Capaldi and Green, 1972]. The classification method is operational and is based on the way these proteins can detach themselves from the membrane [Singer, 1974]:

(i) Extrinsic proteins - presumably bound by ionic interactions these proteins can be easily removed from the membrane by manipulations of ionic strength and pH or by other mild treatments. A typical example of an extrinsic protein is the cytochrome c_2 protein of *Rhodospirillum rubrum* S1 [Dickerson *et al*, 1971].

(ii) Intrinsic proteins have an intimate association with the membrane and can only be removed by disrupting the membrane with organic solvents or detergents. These proteins possess hydrocarbon regions which associate with the hydrocarbon tails of the phospholipid bilayer [(Thornber *et al*, 1983)(Cogdell and Thornber, 1980)]. The proteins making up the LHC of purple photosynthetic bacteria are typical examples of intrinsic proteins; these polypeptides possess a tripartite domain structure, consisting of polar C and N termini and a central hydrocarbon core which forms an α -helix spanning the membrane [(Francis and Richards, 1980)(Brunisholz *et al*, 1984a&b)].

(2) Properties of Detergents: Detergents belong to the heterogeneous group of molecules called lipids: possessing the basic lipid structure consisting of an apolar group of aliphatic or aromatic nature, and a polar group. It is the relative balance between the hydrophobic and hydrophilic moieties of the detergents which distinguishes them from those lipids important in biological membranes which have a greater hydrophilic nature [Helenius and Simons, 1975]. As a result of this molecular structure, detergent molecules aggregate themselves into thermodynamically stable structures called micelles, which can

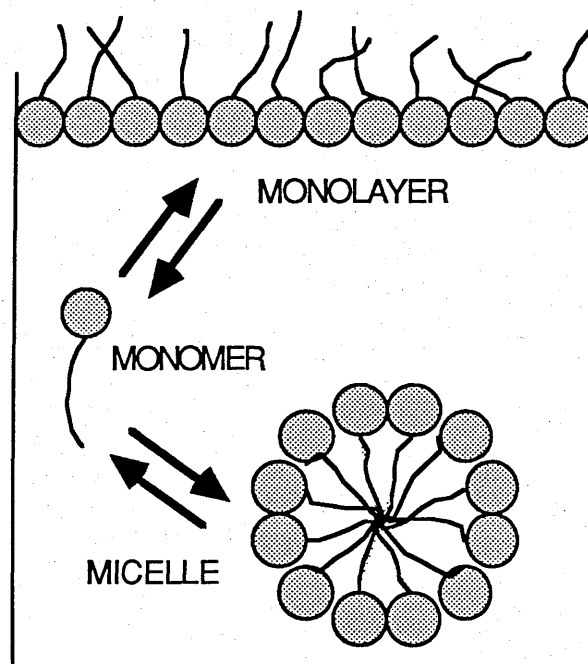


FIGURE 2.2a. Schematic Representation of the Equilibrium or Surfactant Between Monomer, Monolayer and Micellar Forms.

The formation of this thermodynamically stable micelle structure is a spontaneous reaction, driven by hydrophobic forces. The reaction, however, is dependent upon the CMC and the CMT.

[Helenius and Simons, 1975].

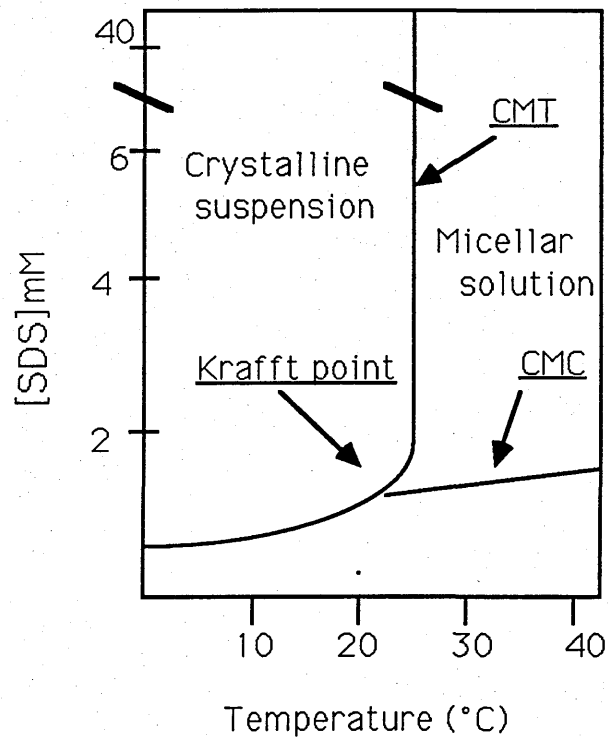
take on the form of spheres, discs, oblate or prolate ellipsoids, cylinders or even bilayered vesicles (Figure 2.2a) [Helenius and Simons, 1975]. The micelle core can be regarded as a tiny volume of liquid hydrocarbon owing to the disordered arrangement of hydrocarbon chains. Hydrophobic membrane lipids can be incorporated into the micellar core and be distributed evenly throughout the solution. Micelle formation is a spontaneous reaction driven by hydrophobic forces but is nevertheless dependent upon a critical micellar concentration and a critical micellar temperature:

Critical Micellar Concentration (CMC) - When concentrations of dissolved detergent are low, part of the detergent will exist as a monolayer at the air-water interphase and part will be dissolved as monomers. Increasing the detergent concentration consequently increases the monomer level to a critical value after which micelle formation will take place. At high concentrations the detergent exists as both monomers and micelles. For practical purposes the CMC is thought of as the highest monomeric detergent concentration obtainable [Helenius and Simons, 1975] (Figure 2.2b).

Critical Micellar Temperature (CMT): Below the CMT, which is specific to a particular detergent, the detergent will form insoluble crystals and the monomer level in equilibrium with the crystals will be below the CMC. Increments of temperature consequently increase the monomer concentration until the CMC is obtained at the CMT. This is usually visualized by the clearing of the cloudy crystalline suspension [Tanford and Reynolds, 1976](Figure 2.2b).

The size of the micelle depends mainly upon the size of the apolar moiety of the detergent molecule, and also, although to a much lesser extent, upon the polarity of the polar groups i.e. an increase in the size of the apolar moiety will serve to lower the

Figure 2.2b: Examining the Effects of Temperature and Detergent Concentration on Micelle Formation.



The Figure shows a temperature-concentration phase diagram of SDS in 0.1 M NaCl/ 0.05 M sodium phosphate, pH 7.4. (CMC = Critical micellar concentration; CMT = Critical micellar temperature). At low temperatures ie. below CMT, the detergent will form insoluble crystals, the level of monomers, therefore, will be below the CMC. As the temperature is increased the monomer concentration will also increase, until the CMT is reached, at which point, provided the detergent concentration is above its CMC, micelle formation will occur. This point is referred to as the Krafft Point.

[Becker et al, 1975]

CMC and will subsequently increase the micelle size.

Detergent Types: detergents can be roughly classified into two groups depending upon their ability of showing 'lyotropic mesomorphism', that is the formation of liquid crystals at high concentrations . This property is a characteristic common to all detergents of Type A but not of Type B (Table 2.2).

Type A detergents: These detergents are subdivided into two groups:

(i) Alkyl ionic detergents: These detergents nearly always denature proteins at the concentrations and temperatures normally used for membrane solubilization. Having the ability to dissociate proteins into their constituent polypeptides these detergents, for example sodium dodecyl sulphate (SDS), are often used to analyse, isolate and characterize individual peptide chains of proteins, [(Weber and Osborne, 1969)(Fairbanks *et al*, 1971)] . Generally speaking anionic alkyl detergents are more disruptive than cationic detergents, however the effect will also depend on the sensitivity of the protein to the detergent, the presence of prosthetic groups and ligands, and protein-protein interactions which may serve as stabilizers to denaturation [Helenius *et al*, 1979]. Lauryl dimethylamine N-oxide (LDAO) is also an alkyl ionic detergent; it has a zwitterionic head group which gives it milder detergent properties, and as such is most commonly used in the solubilization of bacterial photosynthetic membranes, providing fairly high yields of solubilized antenna in the absence of extensive denaturation [(Clayton and Clayton, 1972)(Simon and Helenius, 1975)(Cogdell *et al*, 1982)].

(ii) Non-ionic detergents: These detergents, for example Iso-octyl phenoxypolyoxyethanol or Triton X-100 (trade name), are effective at breaking lipid-lipid or lipid-protein interactions but

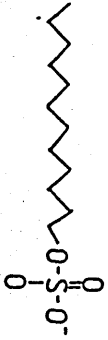
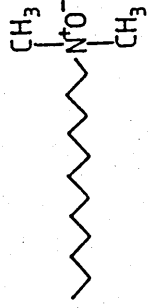
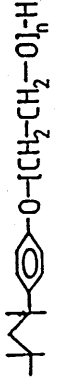
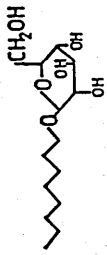
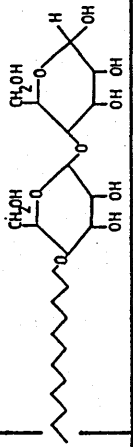
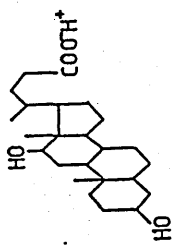
CHEMICAL NAME	Abbreviation/ Trade name.	Structural Formula.	Head group Charge
<u>Type A surfactant.</u> Sodium dodecyl sulphate	SDS		Anionic
Lauryl dimethylamine N-oxide	LDAO		Zwitterionic
Iso-octylphenoxy- polyoxy ethanol	Triton X-100		non-ionic
β-D-octylglucoside	OG		non-ionic
Lauryl maltoside	LM		non-ionic
<u>Type B</u> Deoxycholic acid	—		Mildly anionic

TABLE 2.2 Detergent Types and their Classification.

are ineffective at breaking interactions between proteins, thus they tend to be used for the characterization of membrane proteins in their native state [(Helenius and Simons, 1975)(Helenius *et al*, 1979)].

Type B Detergents or Bile Salts: These detergents differ in their basic structure to those detergents of Type A. Bile salts have a rigid steroid ring structure with hydroxyl groups distributed along the length of the molecule and an ionic group positioned at the end of a short, flexible branched aliphatic chain [(Helenius and Simons, 1975)(Helenius *et al*, 1979)]. This organization causes the 'bean-shaped' molecule to orientate itself "flat" on the air-water interphase. Above the CMC, bile salts will form small aggregates of 2-8 molecules aligned back to back to form the 'primary micelle' structure, at higher concentrations these micelles interact to form a relatively globular cluster of 12-100 molecules, referred to as 'secondary micelles' [(Helenius and Simons, 1975)].

Deoxycholate and cholate are examples of bile salts. These two detergents differ in the number of hydroxyl groups distributed on their steroid rings, having 2 and 3 hydroxyl groups respectively. Generally speaking dihydroxy salts, such as deoxycholate, can effectively dissociate interactions between proteins and are much more powerful membrane solubilizers than the trihydroxy bile salts, and more non-ionic detergents [Tanford and Reynolds, 1976].

Summarizing on detergent properties, it seems that the combination of charged head group and the flexible apolar tail is instrumental to the disrupting capacities of denaturing detergents [Tanford, 1973 and 1980]. Comparatively less disruptive, or mild detergents, have a tendency to be more rigid with bulky apolar moieties which probably fail to penetrate the crevices of protein surfaces as effectively as the flexible alkyl chains [Helenius and

Simons, 1975].

From the above information it can be seen that there can be no one "most effective" detergent, and that effectivity depends upon the complex nature of interactions between the proteins and lipids in a particular membrane, and upon the chemical nature of the detergent itself. Effectivity or solubility is also dependent upon the nature of the protein, upon the extraction conditions such as temperature and pH, and also upon the ultimate aim of the isolation procedure. Thus the choice of an 'optimum detergent and detergent concentration' for any solubilization must be determined by empirical means, although a basic understanding of detergent properties can effectively reduce the field of 'trial and error'.

Methodology 2.3

Characterization of the 'Core Complex'

A. Determination of the Bacteriochlorophyll *a* : Reaction Centre Ratio.

It appears from a number of studies, both direct and indirect, that the B875 (B890) antenna complex is always associated with the reaction centre (RC) in a fixed stoichiometric ratio. Studies on a select number of different bacteriochlorophyll *a* (BChl *a*)-containing species of purple bacteria, conclude that between 20 and 30 BChl *a* molecules are associated with each RC [Hayashi *et al*, 1982a] although values of between 30 and 40 per RC have also been reported [(Aagaard and Sistrom, 1972)(Firsow and Drews, 1977)(Lien and Gest, 1973)]. Evidence therefore, points towards the existence of a fixed stoichiometric relationship between the RC and the B875 antenna complex although the precise association is not clear.

(1) Determination of the RC-Concentration. Determining the concentration of RC depends upon the measurement of spectral changes induced by its photochemical reactions. That the RC is responsible for carrying out the primary processes of photosynthesis was first proposed by Duysens *et al* (1956). They observed a reversible light-induced bleaching of a component which absorbed light near 870 nm in chromatophores of *Rhodospirillum rubrum*. This was manifested as a small (approximately 2%) decrease in absorption in the major long wavelength absorption band of BChl *a*. This reversible bleaching reflects the oxidation of a 'special pair' of BChl *a* molecules termed P870 ('P' refers to 'pigment' and 870 indicates the

wavelength of maximum absorption) which has an intense absorption band near 870 nm (or 960 nm in *Rhodopseudomonas viridis*), consequently it is termed P870 (or P960). After activation by light an electron is released which causes the reduction of the intermediate electron acceptor, a bacteriopheophytin a (or b) molecule [Fajer *et al*, 1975]. A monomeric bacteriochlorophyll molecule has also been postulated to exist between the special pair and the bacteriopheophytin [Shuvalov and Asadov, 1979]. From the intermediate acceptor the electron is stabilized on a primary quinone acceptor, Q_A, before being transferred to a secondary quinone acceptor, Q_B [(Wraight, 1979)(Parson *et al*, 1984)]. The primary quinone in *Rhodobacter sphaeroides* and *Rhodospirillum rubrum* is ubiquinone [(Feher *et al*, 1972)(Cogdell *et al*, 1974)(Morrison *et al*, 1977)], whereas in the species *Chromatium vinosum* and *Rhodopseudomonas viridis* it is menaquinone [Pucheu *et al*, 1976].

As already mentioned these photochemical reactions can be monitored by measuring spectral changes (Figure 2.4a); in addition to the bleaching of absorption at about 865 nm (in *Rhodobacter sphaeroides*) photo-oxidation also causes a shift in the 800 nm absorption band towards shorter wavelengths, giving rise to increased absorption at 789 nm and reduced absorption at 808 nm . The bleaching centered at 275 nm is due mainly to the reduction of ubiquinone (UQ) [Clayton, 1980]. The spectral changes observed with the photo-oxidation of the RC can also be mimicked using a chemical oxidant such as ferricyanide [Clayton, 1973].

Light or chemically induced spectral changes have been used in a number of studies to determine the concentration of RC molecules ie. by measuring the degree of bleaching in the region of 870-890 nm [(Clayton, 1971)(Clayton and Yau, 1972)(Clayton *et al*, 1972a&b)] using the extinction coefficient value of $113.\text{mM}^{-1}.\text{cm}^{-1}$

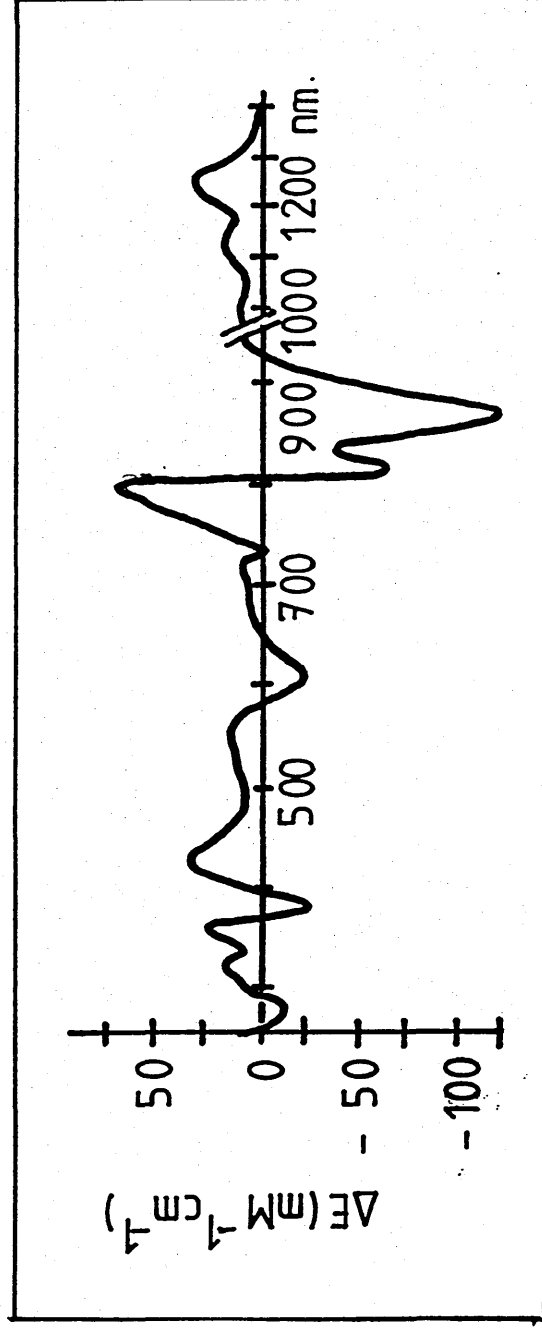


FIGURE 2.4a A Typical Spectrum Showing Reversible Light-Induced Changes in a Reaction Centres Isolated from Carotenoidless Mutant *Rhodospirillum rubrum*.

The bleaching seen at 870 nm and 600 nm, the band shift effect at 800 nm, the positive absorption bands at 435 nm, between 460 nm and 570 nm, and at 1250 nm, are all spectral changes indicative of the oxidation of the special pair of BChl a molecules by transfer of a single electron to UQ, the reduction of which contributes to the bleaching effect observed at 275 nm. The ordinate is the millimolar extinction coefficient $\Delta\epsilon$, based on the molarity of reaction centres regarded as macromolecules.[Clayton, 1980]

which has been predetermined for *Rhodobacter sphaeroides* [(Clayton, 1966)(Firsow and Drews, 1977)]. The extinction coefficient value has been determined for *Rhodobacter sphaeroides* however the methods used were relatively crude and were also based on the assumption that the photochemical unit contained a trimer of BChl a molecules per reaction centre [(Ke *et al*, 1968)(Clayton, 1971)(Clayton and Yau, 1972)(Clayton *et al*, 1972b)(Firsow and Drews, 1977)]. (The photochemical unit is so defined because it is capable of transferring no more than one electron at a time despite the presence of more than one BChl a molecule). More recent evaluations of the molecular composition of the photochemical unit however yield results indicating a pigment composition of 4 molecules BChl a per RC. This new perception of its morphological entity in conjunction with refined methods for RC purification has led to the reevaluation of the extinction coefficient such that ϵ_{865} is equal to $128 (\pm 6) \cdot \text{mM}^{-1} \cdot \text{cm}^{-1}$ [(Lien and Gest, 1973)(Straley *et al*, 1973)] or $133 \cdot \text{mM}^{-1} \cdot \text{cm}^{-1}$ [Clayton *et al*, 1972a].

In pure RC preparations all the absorption at 870 nm is due to P870 however in preparations of RC-B875 conjugate complexes most of the absorption at 870 nm is due to LH BChl a [Clayton, 1971]. This poses a problem particularly when oxidation is carried out chemically ie. by the addition of ferricyanide, since results have indicated that bleaching at 870 nm is not fully reversible; believed to be a consequence of the irreversible bleaching of bulk or light harvesting BChl a [Aagaard and Sistrom, 1972]. In such circumstances it is favourable to measure the blue shift as opposed to that of bleaching. Although these represent qualitatively different spectral changes ie. shift and bleaching, they do occur in the same proportions and it is generally accepted that the shift apparent at around 800 nm is a reflection of

bleaching occurring at longer wavelengths [Thornber, 1970].

The concentration of RC molecules is expressed relative to the total BChl a content of the RC-B875 conjugate; total BChl a is determined by the spectrophotometric evaluation of absorption changes at the IR maximum at about 875 nm, using the predetermined extinction coefficient $\epsilon_{875}=120.\text{mM}^{-1}.\text{cm}^{-1}$ [Clayton,1971].

Methodology 2.4

The Polypeptide Composition of the Isolated Reaction Centre-Antenna Conjugates.

The polypeptide composition of the isolated reaction centre (RC)-antenna conjugates was examined using gel electrophoresis, or rather to be more specific sodium dodecyl sulphate polyacrylamide gel electrophoresis (SDS-PAGE).

Polyacrylamide gel electrophoresis offers a rapid and reliable method, and when used in conjunction with a detergent, commonly SDS, provides a powerful and efficient technique [Laemmli, 1970] for the determination of specific polypeptide contents, their size and their purity [(Shapiro *et al*, 1967)(Shepherd and Kaplan, 1978)]. This technique has been utilized extensively in the characterization of the photosynthetic apparatus of purple photosynthetic bacteria from the simple estimation of the molecular weight (M_r) of proteins and their subunits [(Clayton and Clayton, 1972)(Broglie *et al*, 1980)(Tanaka *et al*, 1983)] to the determination of the specific polypeptide content, assembly and distribution [(Thornber, 1970)(Clayton and Clayton, 1978)(Hunter *et al*, 1979,1982)(Cogdell *et al*, 1983))(Ueda *et al*, 1985)(Klug *et al* 1986)].

The use of polyacrylamide as a supporting medium for zone electrophoresis was proposed by Raymond and Weintraub (1959), prior to this many other forms of media had been proposed. The advantages of polyacrylamide were that the gel is chemically inert, is stable over a wide range of temperature and ionic strength, and is flexible and transparent [(Hames, 1981)(Raymond and Weintraub, 1959)]. The use of PAGE for the separation and

isolation of proteins was recognized in the early 1960's, after which it became a routine method in most protein laboratories [Rothe and Maurer, 1986]. The system was also later shown to be invaluable for estimating the molecular weight of polypeptides from a variety of proteins, the results themselves being highly reproducible [Weber and Osborne, 1969].

Polyacrylamide is the result of polymerization of acrylamide monomers into long chains which become cross-linked by N,N'-methylenebisacrylamide (Bis-acrylamide) [(Davis, 1964)(Raymond and Weintraub, 1959)]. The reaction is initiated by the addition of either ammonium persulphate or riboflavin, with the addition of N,N,N',N',-tetramethylethylene diamine (TEMED) accelerating the reaction: in the ammonium persulphate-TEMED system, the TEMED catalyses the formation of free radicals from persulphate which in turn initiates polymerization. In the riboflavin-TEMED system, free radicals are produced from the photodecomposition of riboflavin, with TEMED acting to stabilize the system [(Hames, 1981)(Rothe and Maurer, 1986)].

Acrylamide gels are used as a support medium for electrophoresis through which proteins carrying a net charge will migrate; their mobility depending upon their respective charge densities ie. the ratio of charge to mass: the higher the ratio the faster the molecules will migrate. Polyacrylamide gels also separate proteins according to their size. The pores generated from cross-linkage of acrylamide monomers are the same order of size as proteins and thus produce a molecular sieving effect [Hames,1981]. The effective pore size can be regulated by the total acrylamide concentration and the proportion of cross-linker used, such that at higher concentrations the effective pore size is reduced.

A vast majority of studies employ dissociating buffers, these

usually contain detergents such as SDS which serve to dissociate proteins into their monomeric constituents (denaturation is achieved by heating the protein sample at 100°C in the presence of excess SDS and a thiol reagent which cleaves disulphide bonds). When a detergent such as anionic SDS is used in PAGE the intrinsic charges of polypeptides become insignificant relative to the negative charge provided by the bound detergent. In SDS-PAGE polypeptide complexes migrate strictly according to polypeptide size [(Shaphiro *et al*, 1967)(Weber and Osborne, 1969)]-thus the correct porosity of the polyacrylamide gel becomes important.

There are two extremes of gel concentration; too high would result in the exclusion of proteins which are unable to penetrate the gel, or too low where there is no or little fractionation of the proteins. Between these two extremes the protein will be separated to variable extents depending on the concentration. There will be no one concentration that will resolve all proteins/polypeptides perfectly or equally and thus it is important to select a concentration which gives adequate display of all components. Alternatively polyacrylamide gradient gels or 'pore gradients' can be used [Margolis and Kenrick, 1968]. These gels allow the separation of proteins over a wide range of molecular masses, and improve band resolution since electrophoresis passes through a gradient of low to high gel concentrations.

The buffer system used in PAGE is also important to polypeptide resolution. Two systems are recognized (Appendix 4): (i) Continuous buffer system and (ii) Discontinuous buffer system. The continuous buffer system contains the same buffer ions, although at different concentrations, and maintains constant pH throughout the sample, gel and electrode vessel reservoirs. Protein samples are loaded directly onto the resolving gel of this system. In the discontinuous system however, there are variations

in the buffer ion and pH in the gel compared with the electrode reservoirs. In this system protein samples are loaded onto a large-pore 'stacking' gel polymerized on top of the small pore resolving gel. The advantage of the discontinuous gel is that it permits the loading of relatively large volumes of dilute sample whilst maintaining good resolution [(Davis, 1964)(Ornstein, 1964)(Raymond, 1964)].

Methodology 2.5

Examining the Functional Integrity of the Isolated Reaction Centre - Antenna conjugate.

The process of photosynthesis depends upon the capture of light energy by complex organic pigments, and its transfer to the RC where it will be trapped and utilized. However, not all light quanta absorbed will be used and are therefore dissipated; the reemittance of light energy as fluorescence is one method of dissipation [(Amesz, 1978)(Clayton, 1980) (Drews, 1985)]. Although fluorescence is a seemingly wasteful process, its detection and measurement has been invaluable in providing information on electron transfer efficiencies [(Vredenberg and Amesz, 1967)(Kramer *et al*, 1984a)(van Grondelle, 1985)], photophysical processes, on the state of the reaction centre (RC) [(Clayton *et al*, 1972)(Vredenberg and Duysens, 1963)] and on the organization of the photosynthetic apparatus itself [(Monger and Parson, 1977)(Hunter *et al*, 1979)(van Grondelle *et al*, 1982)].

Vredenberg and Duysens (1963) observed that the fluorescence yield of B890 in the intact cells of *Rhodospirillum rubrum* is correlated with the oxidation-reduction level of the primary electron donor, P890, such that light-induced bleaching at around 890 nm will cause a rise in fluorescence. This is expected since the extent of bleaching, or oxidation, signifies the saturation of the RC [(Clayton, 1967)(Vredenberg and Duysens, 1963)]. The fluorescence yield therefore, will itself reflect the photochemical state of the RC, since there exists an inverse relationship between photochemistry and fluorescence (Figure 2.5a) [(Clayton, 1967)(Hunter *et al*, 1979)]. This inverse relationship can also be

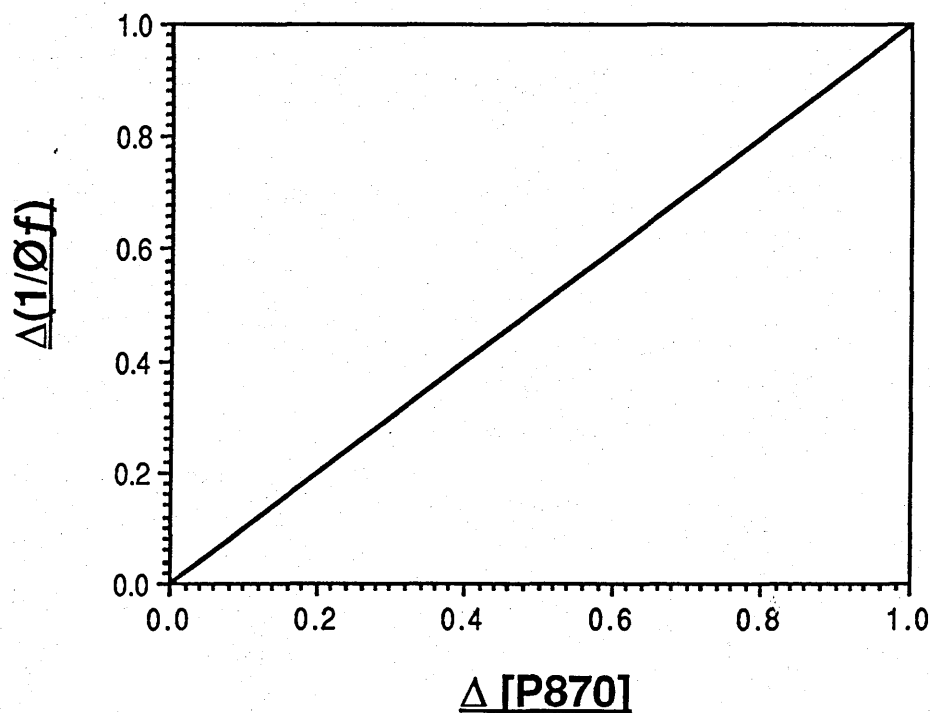


FIGURE 2.5a The Relationship Between the Yield of Bacteriochlorophyll fluorescence and the state of the Trapping Pigment, P870, in an Aerobic Suspension of *Rb.sphaeroides* cells.

The change in reciprocal of fluorescence yield ($\Delta 1/f$) is plotted against the change in concentration of P870 ($\Delta[P870]$). These changes were light-induced and were measured during the transition between dark and light steady states. Bleaching at P870 was recorded as the changes in absorbancy at 870 nm. Units of both ordinate and abscissa have been normalized to maximum values of 1.0.

It can be observed from the figure that an inverse linear relationship exists between the two parameters. [Clayton, 1967].

expressed quantitatively in the form of the equation:

$$\phi_p = 1 - \phi_f / \phi_{f_{\max}}$$

Where ϕ_p is the quantum efficiency of photosynthesis defined as the fraction of deexcitations that lead to photochemistry,

$$\text{ie. } \phi_p = K_p / (K_f + K_d + K_p).$$

{ K_p = Rate constant for photochemical utilization; K_d = Rate constant for radiationless deexcitation; K_f = Rate constant for fluorescence dissipation}.

and ϕ_f is the quantum yield of fluorescence

$$\text{ie. } \phi_f = K_f / (K_f + K_d + K_p).$$

The value of ϕ_f reaches a maximum value ie. $\phi_{f_{\max}}$ when K_p is reduced to zero [Clayton, 1971, 1980].

If the fluorescence yield is measured and expressed against time three main stages of fluorescence can be detected (Figure 2.5b):

F_0 is the minimum level of fluorescence always emitted; this level is detected immediately upon onset of illumination within the resolution time of the measuring instrument [Hunter *et al*, 1979]. At this level all photochemical traps are open. When the system is saturated ie. all of the photochemical traps are operatively closed a maximum, F_{\max} , level of fluorescence will be achieved. The rate at which F_{\max} is attained depends upon a number of factors, such as the level of illumination and the rate of electron transport to and from the RC, and also upon the functional integrity of the system: in an intact system the level of

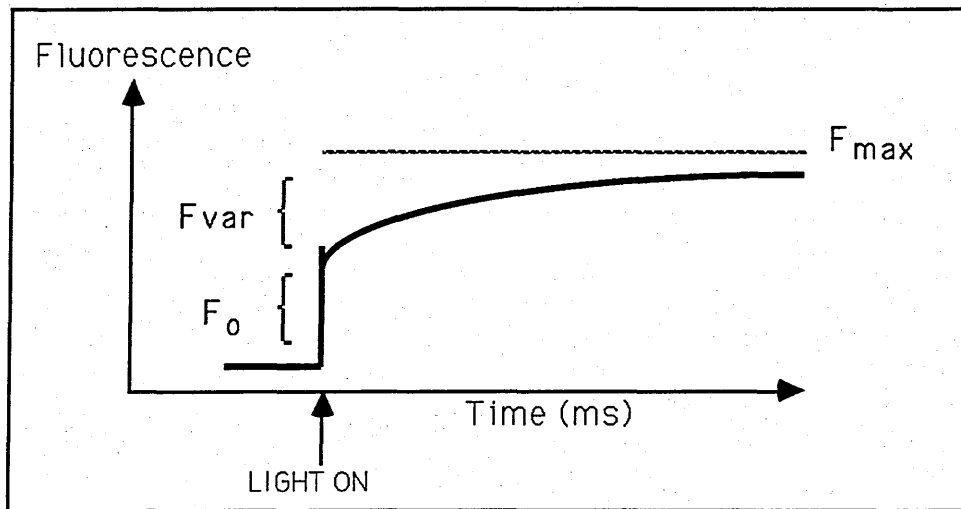


FIGURE 2.5b Demonstrates the relationship between fluorescence yields and time in an intact system. Three stages are typically recognized:

- F_0 - indicative of the minimum level of fluorescence always emitted.
- F_{max} - representative of the maximum level of fluorescence output.
- F_{var} - indicates the gradual increase in fluorescence yields observed between the F_0 and F_{max} values.

fluorescence will increase gradually corresponding to the gradual reduction in the number of RC traps available for photochemistry, hence variable fluorescence (F_{var}) will be detected. If the system is in some way disrupted, for example by chemical blockage or physical separation of pigments [Thornber, 1970], the F_{max} level of fluorescence will be attained very rapidly and there will be no, or very little, detectable variable fluorescence.

Fluorescence induction kinetics were employed in this study in order to examine the functional integrity of the isolated RC-antenna conjugates. Fluorescence was generated and detected on equipment diagrammatically illustrated in Figure 3.5. The basic process of fluorescence generation and detection is described below: radiation from a white light source is passed through a monochromator or glass filter(s) which removes light of wavelengths similar to those to be measured, but retains those bands of light necessary for sample excitation [(Clayton, 1980)(Skoog and West, 1980)]. The light is then passed through the sample and the fluorescence generated is passed through interference filters which remove scattered and reflected radiation. The fluorescence then passes into a photon-detecting device, such as a photomultiplier or a photodiode. The electrical signal produced is then passed through an amplifier, through an analogue-digital converter and is then displayed on an oscilloscope [(Clayton, 1980)(Hipkins and Baker, 1986)]. The reliability of the system depends on it being tight from external light. The choice of filters is also crucial, a variety of types are available and are briefly described below:

Interference Filters Two main types are recognized: 'Destructive' - which cancel out wavelengths of radiation not required for transmission, and 'Constructive' which reinforce wavelengths of light to be transmitted.

Absorption Filters allow the transmission of specific bands of radiation. There is the 'Long Pass' which transmits radiation of long wavelengths and rejects short wavelengths and the 'Short Pass' which acts in the converse manner.

Neutral Density Filters are used to attenuate radiation without significantly modifying its spectral distribution [Hipkins and Baker, 1986]

The choice of filters therefore depends upon the absorption properties of the sample, and the wavelength of fluorescence emitted. Excitation spectra of fluorescence can be used to determine which light wavelengths elicit fluorescence. In an isolated RC-antenna conjugate, fluorescence is emitted with a maximum near 900 nm which corresponds (according to Stoke's Shift) to the absorption maximum at 870 nm [Clayton, 1980]. The sample is therefore, excited with light corresponding to the blue region of the spectrum and fluorescence is detected in the red region.

Methodology 2.6

Crystallizations - Conclusive Evidence for the Existence of a Well-Defined Core Complex.

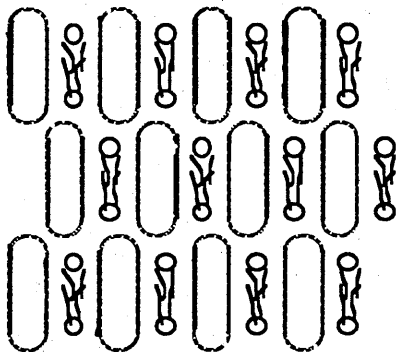
The ability to crystallize the isolated reaction centre (RC)-antenna conjugate requires the molecules, in the solid state, to be arranged in a symmetrical and periodically repetitive fashion [McPherson, 1982]. Thus successful crystallizations would reinforce the idea that there is a fixed and well defined stoichiometric core structure. The examination of crystals using X-ray diffraction and image processing techniques, would also allow the determination of the fine structure and spatial organization of proteins, which have, until recently, only been considered in the light of indirect experimental information from conventional methods such as photoselection, linear dichroism and neutron diffraction [(Michel, 1983)(Thornber *et al*, 1983)].

Membrane proteins however, are inherently difficult to crystallize, the main problem being, as mentioned in section 2.2, the solubilization of membranes composed of proteins embedded in liquid bilayers. Detergent solubilization of membranes is therefore required, a technique which itself is fraught with difficulties. Just to briefly recap on the activity of detergents; detergents form micelles which during membrane solubilization incorporate the lipids and proteins and thus in some respect replace the lipid bilayer. One problem with solubilization methods of this type, is the potential distortion of native protein configurations. Although any major conformational changes may be detected by changes in spectral properties, or in functional integrity, very slight changes, perhaps one or two amino acids, may not be detected by conventional

assays. If, however, a change of this type affected the symmetrical arrangement of the overall structure, then crystallization would be prevented. It is possible that changes of this sort have limited the success of crystallization attempts made so far, although as yet, not enough is understood about protein-lipid interactions in photosynthetic membranes to speculate on the magnitude of this problem, or indeed its potentiality. Detergents therefore, must be selected for their ability to solubilize membrane proteins whilst maintaining their conformation and integrity, at least as far as can be detected [(Helenius and Simons, 1975)(Michel, 1983)]. As well as being important in the initial preparation of proteins for crystallization, detergents also play a crucial role in the actual formation of some three-dimensional crystals. Two basic three-dimensional membrane crystals are formed: Type I consist of two-dimensional crystals arranged into stacks which gives a third dimension with respect to up and down orientations, rotations and translation. Lipids surround the proteins in a lipid bilayer type fashion thereby creating hydrophobic interactions which stabilize the crystals in the two-dimensions of the membrane. Polar interactions are important in all three dimensions (Figure 2.6a). Type I crystals are generally small and as such are only useful for electron microscopic investigations [Henderson and Shotton, 1980]. Crystals of the Type II category consist of membrane proteins crystallized with bound detergents which compensate for the hydrophobicity of their original intramembranous surfaces. Although the crystal lattice is made up preferentially with the protein (Figure 2.6b) the size and chemistry of the detergent have an important influence in crystal packing; if for example a detergent is too large to fit perfectly into the crystal lattice the lattice structure itself may be disrupted. In these circumstances it is favourable to replace the detergent with a smaller detergent or with

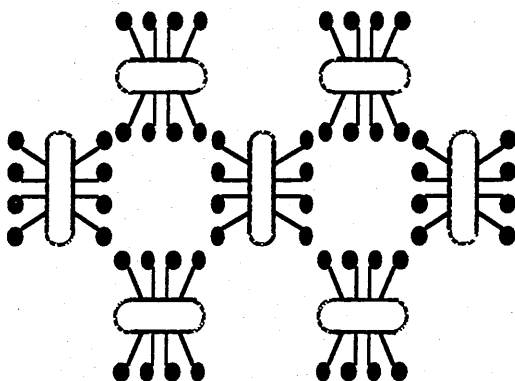
FIGURE 2.6 a&b. Diagrammatic Representation of the Two Basic Types of Membrane-Protein Crystal Recognized.

TYPE I



Stacks of two-dimensionally crystalline membranes ordered in the third dimension ("membrane crystal").

TYPE II



A membrane crystallized with detergents bound to its hydrophobic protein surface*.

*The hydrophilic surface of a protein is indicated by the dashed lines.



Lipids.



Detergents.

[Michel, 1983]

a small amphiphile molecule [(Garavito and Rosenbusch, 1980)(Michel, 1983)], for example 1,2,3 heptane-triol (HPT) and benzamidine hydrochloride (BH). The latter molecules are believed to bind to the protein in much the same manner as detergents but fit much better into the lattice. They may also act by forming mixed micelles with detergents resulting in the formation of much smaller micelles than those produced with pure detergent. [Michel, 1983]. They have also been shown to prevent the separation of detergent and aqueous phases which could have inhibiting influences on crystal formation [Michel and Oesterhelt, 1980].

Protein molecules within detergent micelles therefore represent the starting material for crystallization. For crystallization to be achieved however, it is necessary to create a situation where the molecules are driven into some kind of three-dimensional order. The driving force, like in all thermodynamic systems, being free energy minimization: full solvation represents one free-energy minimum, and conditions approaching supersaturation another, for example, in an extremely concentrated solution where there is insufficient water to maintain hydration or to shield molecules from one another, molecules may aggregate, a process which forms the basis of crystal formation. If this state of equilibrium is approached too quickly molecules may aggregate as an amorphous precipitate, alternatively, if a gradual approach is made molecules are given a chance to maximize favourable interactions with neighbouring molecules and minimize dispersive forces. In the latter situation crystallization is possible [Michel, 1983].

The specific kinetic and thermodynamic parameters of this equilibrium ie. the solute is partitioned between a soluble and solid state, will depend on the chemical and physical properties of the solvent and solute involved and by the influence of physical parameters such as pH and temperature. It is necessary therefore,

to create a situation which favours the precipitation of proteins. The strategy usually employed involves the use of some precipitant agent or agents, and to examine the solubility of the protein at various concentrations as a function of other relevant parameters such as pH, temperature and small amphiphile concentration. Three main types of precipitant are recognized:

(1) Salts for example ammonium sulphate cause the water molecules, which would normally be available for solvation of protein, to form bonds with the small ions. If the concentration of ions becomes sufficiently high the proteins are driven to neutralize their surface charges by interacting with one another and thus we get selective precipitation. The solubility minimum is effected by specific ion concentration, protein concentration, pH and temperature. In general the solubility function for proteins is logarithmic and exponentially decreases as the ion strength is increased. The rate is a function of the protein and ions involved [(Dixon and Webb, 1961)(McPherson, 1982)].

(2) Organic solvents are believed to cause precipitation by means comparative to 'salting out': organic solvents bind water molecules to themselves thereby effecting the capacity of the system to fully solvate the macromolecules. They also lower the dielectric constant of the medium which reduces the effective electrostatic shielding between individual macromolecules. Although solvents such as 2-methyl-3-D-pentenediol (MPD) or hexanediol are gentle and efficient precipitants [Michel, 1983], most organic solvents have denaturing effects on many proteins - a property which severely limits their use as a precipitating agent [Dixon and Webb, 1961].

(3) Polyethylene glycol (PEG) confers several advantages with respect to both crystal formation and crystal analysis, and for these reasons is used extensively in crystallization. Beneficial properties are listed below:

(a) PEG is effective at low ionic strength and therefore provides a low electron density medium. The low ionic strength serves to encourage higher ligand binding affinities which, as a consequence, generates protein-ligand complexes and isomorphous heavy atom derivatives more easily. These are then examined by difference Fourier techniques [McPherson, 1982]. The low electron dense medium also implies a lower background level for protein structures derived from the X-ray diffraction of crystals.

(b) The crystallization of proteins with PEG is possible within a fairly narrow range of concentration ie. from approximately 5-15%, and the exact concentration at which crystal formation occurs is rather insensitive and can be successful within 2-3% of the optimal value. This can compare with the precipitant agents salts and organic solvents which rely on concentrations being within 1-2% of the optimum value which may lie between 15-85% saturation.

(c) When examined for its ability to induce crystallization in a range of proteins (some of which had been crystallized previously by conventional means and the rest had had no previous success in crystallization), PEG was shown to exhibit greater generality than any of the previously used reagents. Also of those crystals previously crystallized PEG produced crystals of similar habit and morphology, indicating that it is unlikely that PEG produces any major conformational distortions or anomalies [McPherson, 1976]. It was also concluded from this study that "PEG may be the best initial trial reagent for crystallization of proteins for X-ray diffraction analysis".

A number of physical methods are available for crystallization, bulk dialysis, microdialysis, sequential extraction and free interface diffusion are but a few. The method in most frequent usage, particularly if supersaturation is to be attained by precipitation, is that of vapour diffusion: with this method droplets

of protein sample, or sample solution as it is so called, are placed in depressions on spot plates or microscope slides. The spot plates are held by some means above a reservoir of precipitating solution within a sealed container. Through the vapour phase the concentration of PEG, salt or organic solvent in the reservoir equilibrates with that in the sample. In the case of salt or PEG precipitation the well solution will contain a level of precipitant lower than the reservoir, and thus equilibrium proceeds by distillation of water out of the droplet into the reservoir [Davies and Segal, 1971]. A particular advantage of this technique is that it requires only small amounts of sample and is ideal for screening a large number of conditions. It also allows freedom in varying conditions such as concentrations, pH and temperature even after the conditions are set up [McPherson and Spencer, 1975].

Vapour diffusion techniques have been successfully employed in a number of studies, of particular note was the success in crystallizing the photochemical reaction centre of *Rhodopseudomonas viridis* which was sufficiently large for study by X-ray crystallographic analysis and image processing techniques which require the crystals to be of a certain minimal size (linear dimensions of greater than 0.2 mm), and have a certain degree of order and mechanical strength [Zeppezauer, 1971]. Crystals have also been obtained for the B800-850 antenna complex of *Rhodobacter capsulatus* [Mäntele *et al*, 1985], *Rhodobacter sphaeroides* strain 2.4.1. [Allen *et al*, 1985a], *Rhodopseudomonas acidophila* strain 7750 [Cogdell *et al*, 1985], and the reaction centre-B875 antenna conjugate of *Rhodopseudomonas palustris* [Wacker *et al*, 1986] using the method of vapour diffusion. These crystals despite being too small or of insufficient internal order [Welte *et al*, 1985], for analysis by X-ray diffraction techniques have been examined by spectroscopy and by polyacrylamide gel

electrophoresis. Protein patterns, absorption spectra, dichroism and in some investigations the reversible photo-oxidation of the reaction centre primary electron donor, all show that the purified complexes have been successfully crystallized without a major change in their composition or conformation [(Allen *et al*, 1985a&b)(Cogdell *et al*, 1985)(Thornber *et al*, 1983)(Zinth *et al*, 1983)(Welte *et al*, 1985)(Wacker *et al*, 1986)]. Successful crystallizations have also revealed how different factors such as precipitant concentration, pH, temperature and type of small amphiphile can affect many aspects of the crystallization process including the rate of formation, and the size and shape of crystals [(Allen and Feher, 1984)(Cogdell *et al*, 1985)(Michel, 1982 and 1983)]. Crystallization therefore is the result of a number of variables interacting together to produce optimum conditions for the crystallization of a particular protein: the number of permutations is extensive and successful crystallization requires systematic screening and endless patience !!!.

CHAPTER 3

Materials and Methods.

3.1 Cell Culture: *Rhodopseudomonas acidophila* strains 7050 and 7750 were grown in Pfennig's medium, using succinate as the main carbon source [Pfennig, 1967] (Appendix 1.1). All other species, *Rhodopseudomonas palustris* strains 'DSM 8252' and 'French', *Rhodocyclus gelatinosus* strains 149 and 151, *Rhodopseudomonas blastica*, *Rhodobacter sphaeroides* strains 2.4.1. , R26 and M21, and *Rhodospirillum rubrum* strain S1 were grown in a well defined nutrient medium that also has succinate as its main carbon source (Appendix 1.2) [Bose, 1963]. *Chromatium vinosum* strain D was grown in the heterotrophic synthetic medium of Fuller [cited Bose, 1963] (Appendix 1.3).

Stock cultures of bacteria were kept as stabs in agar (Appendix 1.4) in M^CCartney bottles. When liquid cultures of cells were required the stocks were overlaid with the necessary growth media and grown up anaerobically in a thermostatically controlled illuminated growth room. After about 24 hours the cells were usually of sufficient density to be transferred into flat-sided bottles (500 ml). When a large quantity of a particular species was required liquid cultures from the standard 500 ml culture bottles were further transferred into 10 l flasks. To prevent contamination the tops of bottles and flasks were flamed before and after the transfer of cells, and all inoculations were carried out in a laminar flow chamber. Serial dilutions of liquid cell cultures were periodically, aseptically, plated out on agar (Appendix 1.4) in petri-dishes. The petri-dishes were placed in a GasPak® jar system (BBL Microbiology Systems) along with a

GasPak® hydrogen and carbon dioxide generator envelope. The jar, then closed and sealed to generate an anaerobic system within, was incubated at 28°C for approximately one week. Single colonies were then selected and used to inoculate agar stabs in McCartney bottles.

All bacterial species were grown at approximately 30°C under conditions of high light (42 W.m⁻²) and of low light (9 W.m⁻²) intensities; high light conditions were provided by banks of 3 x 150 W bulbs placed approximately 150 cm from the culture bottles, and low-light intensity conditions were created by placing culture bottles at least 300 cm away from a single 100 W bulb. Light intensity was measured with a UDT Model 40X OptoMeter in the wavelength range 450 - 910 nm.

The exposure of the carotenoidless strain *Rhodobacter sphaeroides* R26 to light and oxygen will cause the cells to photodestruct. These cells are therefore grown for 24 hours in the dark at 30°C post inoculation, before being exposed to light; most of the oxygen in the medium will be removed by respiration during this period.

3.2 Harvesting the Cells.

The cells were harvested in the MSE 6 I Coolspin centrifuge at 2500 x g, 4°C for 100 minutes. They were then washed by resuspending them in MES (2(Morpholino)ethanesulfonic Acid) buffer (Appendix 1.5) and repelleted by centrifugation at 17 000 x g, 4°C, for 15 minutes in the MSE 18 centrifuge. The cells were resuspended in 20 mM MES-HCl pH 6.8, 0.1 M KCl and either used immediately or stored at -20°C until required.

3.3 Membrane Preparation.

The cells were homogenized and broken by passage through a cooled Aminco 'French' pressure cell at 10 ton.inch^{-2} in the presence of a little DNase (Deoxyribonuclease 1 from Bovine Pancreas, SIGMA Chemical Company) and magnesium chloride. The broken cells were centrifuged at $15\,000 \times g$, 4°C for 10 minutes in a MSE 18 centrifuge. In those bacterial species which contain vesicular-shaped intracytoplasmic membranes (ICM), for example *Rhodobacter sphaeroides*, *Chromatium vinosum* strain D and *Rhodospirillum rubrum* S1, this low speed pellet containing unbroken cells and cell material was discarded. Chromatophores were obtained from the subsequent centrifugation of the supernatant at $243\,000 \times g$, 4°C for 1 hour in a Sorvall OTD-65B Ultracentrifuge. In those bacterial species containing lamellar ICM both pellets were retained and combined. The pellet was resuspended in a minimal volume of 10 mM Tris (Tris(hydroxymethyl)aminomethane)-HCl pH 8.0 and homogenized. Membrane preparations were used immediately or stored frozen (-20°C).

Further evidence, to ascertain that the RC-B875 antenna conjugate represents a stoichiometrically fixed core structure, was obtained from the preparation, and comparison, of cells grown at different light intensities ie. under low-light and high-light conditions. For comparative purposes therefore, the isolation procedures had to be consistent: prior to cell disruption samples of high-light and low-light grown cells were diluted until they were of an equal optical density at 650 nm, usually about 50. Absorption at this wavelength is proportional to cell density and is not obscured by pigment absorption. An equal volume of high-light and low-light grown cells were passed through the 'French'

pressure cell. The pellet(s) obtained from the centrifugation procedures described above were resuspended in equal volumes of 10 mM Tris-HCl, pH 8.0.

3.4 Cell Counts

To compare the amount of reaction centre and light-harvesting complexes in high and low-light grown cells of a particular species, it was necessary to ensure that an equal number of cells was considered. Cell counts were therefore made for each high-light and low-light grown sample, for which the optical density at 650 nm was later determined. The experimental protocol is described below:

Serial dilutions of each sample were made, and their respective absorption at 650 nm was determined. The cells were killed with a small drop of iodine solution, and then counted on a haemocytometer slide using a light microscope. The cell count values were then plotted with respect to the optical density at 650 nm. The relationship existing between these two parameters was used as a point of comparison between high-light and low-light grown cells.

3.5 Spectrophotometry.

A SP8-500 UV/VIS recording spectrophotometer was used for the measurement of absorption spectra at room temperature. At the end of each preparative stage room temperature absorption spectra were recorded.

3.6 Isolation of the Light-Harvesting and Reaction Centre Complexes from Membrane Preparations.

Firsow and Drews (1977) described a method involving the solubilization of photosynthetic membranes using a mild detergent, and their subsequent fractionation by sucrose-density gradient centrifugation. The basic method was as follows; the NIR absorption maximum was determined from the spectrum of the membrane preparation, and the concentration of the photosynthetic membranes was adjusted to an optical density (OD) of approximately 50 at their NIR absorption maximum. A 1 ml aliquot of the sample was then added to 2 ml 10 mM Tris-HCl, pH 8.0 containing detergent. The sample was stirred for 10 minutes at 4°C and any unsolubilized material removed by centrifugation in a Hettich EBA 3S centrifuge at 450 x g for 10 minutes. The supernatant was loaded onto sucrose gradients and centrifuged in a Sorvall OTD-65B Ultracentrifuge at 197 000 x g, 4°C for about 16 hours in the T865 fixed angle rotor, or at 97 000 x g, 4°C for approximately 24 hours in the AH 627 swing-out rotor, or at 200 000 x g in the TST 41.14 swing-out rotor. The temperature was increased to 8°C when the detergent used was sodium dodecyl sulphate (SDS). The sucrose-density gradients employed ie. the molar sucrose concentrations and their relative volumes, were dependent upon a number of conditions including the detergent used for solubilization, the rotor used for centrifugation, and the method employed for isolating the fractionated bands. The type and concentration of detergent used for membrane solubilization was dependent upon the membrane species and to some extent upon the sample batch. Thus solubilization conditions had to be optimized for each species to allow the isolation of light-harvesting and RC complexes still representative of their *in situ*

state. The following detergents were tested: Sodium and lithium dodecyl sulphate (SDS/LDS)(specially purified for biochemical work BDH Chemicals Ltd.), lauryl dimethylamine N-oxide (LDAO)(Fluka AG.), iso-octyl phenoxy-polyoxyethanol (trade name Triton X-100 supplied by BDH Chemicals Ltd.), Dodecyl β -D-maltoside (supplied by Boehringer, W.Germany), cholic acid (sodium salt, SIGMA Chemical Company) and n-octyl- β -D-glucopyranoside (Bachem Feinchemikalien AG. Switzerland).

A number of preliminary experiments varying sucrose concentrations, relative volumes, detergent, sample variety and concentration, centrifuge rotor and isolation method were initially completed in order to determine which conditions yielded the most satisfactory results as regards the isolation of the B800-850 antenna complex and the reaction centre (RC) -B875 antenna conjugate from a particular species. Preliminary experiments were completed to determine the effective volume ratio of the sucrose concentrations. Linear and step gradients were also compared to see whether they improved isolation.

For the isolation of the fractionated bands from the gradient one of two methods was employed:

- (1) Manual fractionation using a pasteur pipette to carefully extract each band.

- (2) Automated fractionation using an Isco-density gradient fraction collector. This instrument collects equivolume fractions throughout the sucrose gradient. The fraction collector, also equipped with an ISCO UA-5 absorbance monitor, made a continuous recording of absorbance at 280 nm throughout fractionation.

The type of extraction method utilized generally dictated the centrifugation method: automated fractionation using the ISCO-density gradient fraction collector required gradients to be prepared in straight-sided centrifuge tubes of the type compatible

with the AH 627, or the TST 41.14, swing-out rotors, which take 6 x 36 ml, or 6 x 14 ml, centrifuge tubes respectively. With manual fractionation, however, it was more convenient to utilize the T865 fixed angle rotor, since this rotor requires a shorter centrifugation period (owing to greater centrifuge speeds possible) and also allows 8 x 27 ml centrifuge tubes to be prepared per spin.

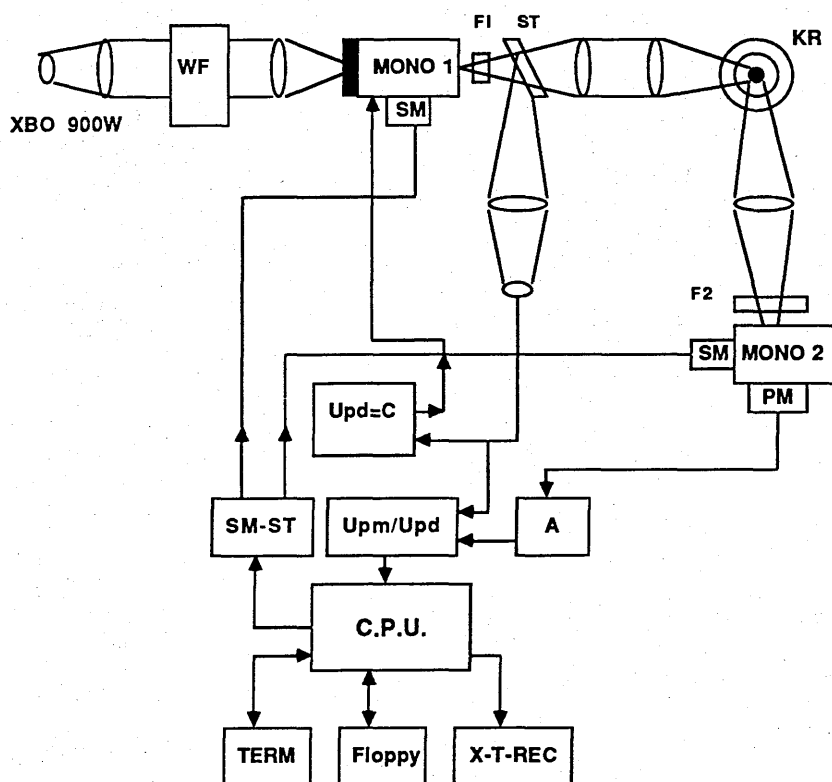
For the isolation of the RC-antenna conjugates from *Rhodobacter sphaeroides* 2.4.1 an alternative method was employed: the cells were washed once with 50 mM Tris-HCl, pH 7.5, 1 mM EDTA (ethylene diamine tetraacetate). The cell pellet was resuspended in the same buffer and the cells were disrupted by one passage through the 'French' pressure cell at 10 ton.inch⁻². All operations were carried out at 4°C. The crude lysate was treated with DNase (1ug.ml⁻¹) for 1 hour with stirring. The lysate was diluted with an equal volume of Tris-EDTA buffer, and the cell debris was removed by centrifugation at 10 500 x g for 2 hours. The membrane pellet was resuspended by homogenization in 0.1 M sodium phosphate buffer (pH 7.5) and the concentration adjusted to give an absorbance at 850 nm of 50.cm⁻¹. The membrane suspension was brought to room temperature and lauryl dimethylamine N-oxide (LDAO) (30%) was added drop-wise to give a final concentration of 0.25% (v/v). The suspension was stirred slowly for 10 minutes at room temperature and then centrifuged in the Sorvall OTD-65B Ultracentrifuge at 158 000 x g for 1 hour. The pellet was resuspended in 10 mM Tris-HCl, pH 7.5 by homogenation and the concentration adjusted to give an absorbance at 850 nm of 100.cm⁻¹ (where the ratio of 850/875 absorbance was approximately 1.6). To determine the optimum concentration of membranes for solubilization the suspension was diluted 1:1, 1:2, 1:3 with 10 mM Tris-HCl, pH 7.5 (4°C). LDAO (30%) was gradually added to give a final concentration of 0.5% (v/v). The solutions

were gently stirred for 10 minutes at room temperature and then loaded in 3 ml aliquots onto 20/40 % (w/v) sucrose step gradients (in 10 mM Tris-HCl, pH 7.5). The sucrose density gradients were centrifuged overnight in the Sorvall AH65 swing-out rotor at 97 000 x g. This preparative procedure was repeated using the detergent N-octyl- β -D-glucopyranoside (OG). To improve the purification of the preparation N-octyl- β -D-glucopyranoside or lithium dodecyl sulphate was added to the 20% (w/v) sucrose solution at a final concentration of 0.1% (v/v) [Kaplan, S. Personal communication].

3.7 Absorption and Fluorescence Spectroscopy.

Room temperature (270K) and low temperature (110K and 10K) absorption spectra were recorded on a Cary 14 spectrophotometer. The concentrated RC-B875 antenna samples were mixed with glycerol in the ratio of 70% glycerol : 30% sample buffer (v/v) in order to obtain a clear glass at low temperatures. Fluorescence emission and excitation spectra were also recorded at room and low temperature (270K, 110K and 10K) on apparatus similar to that illustrated in Figure 3.1. The efficiency of carotenoid to bacteriochlorophyll singlet-singlet energy transfer was calculated from the ratio of carotenoid peak height at 530 nm in the fluorescence action spectrum to the corresponding peak in the absorption spectrum after the spectra were normalized at the 590 nm BChl *a* absorption peak [van Grondelle *et al*, 1982]. Room and low temperature analyses were kindly completed by J. Ullrich at the Physics Institute, University of Stuttgart, W. Germany.

FIGURE 3.1: BLOCK DIAGRAM OF THE FLUORESCENCE APPARATUS USED IN STUTTGART TO MEASURE FLUORESCENCE EMISSION AND EXCITATION SPECTRA.



XBO 900W: Xenon arc

MONO 1: Excitation monochromator.

MONO 2: Emission monochromator.

PM: Photomultiplier.

PD: Photodiode.

Kr: Kryostat.

SM: Stepmotor.

ST: Beam splitter.

Upd=C: Slit-width control

F1/2: Filter

WF: Waterfilter.

C: Comparator

A: Amplifier

TERM: Terminal

X-t-REC: X-t-recorder

CPU: Central Processing Unit.

Upm/Upd: Analogue divider

SM-ST: Stepmotor driver

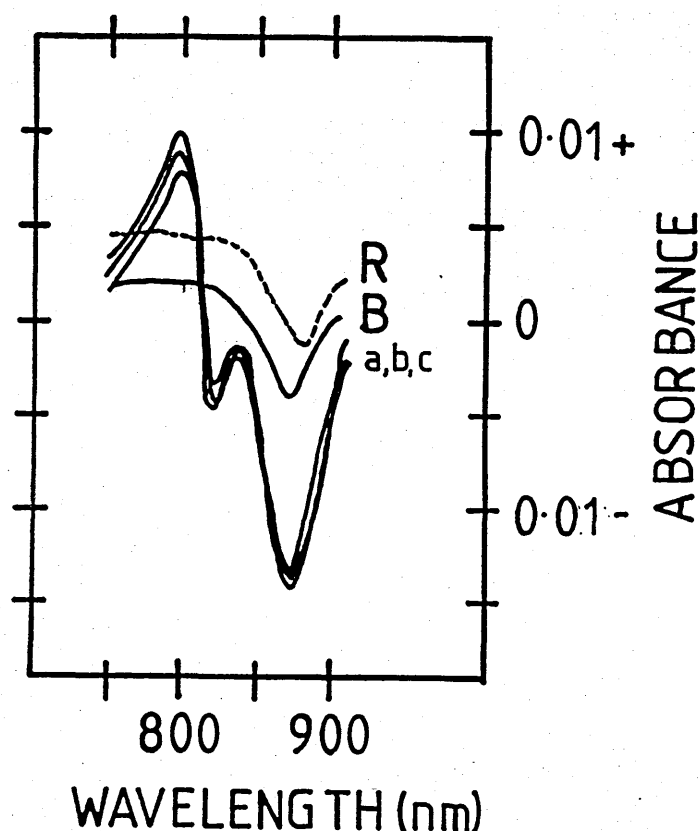
3.8 Determination of the Reaction Centre (RC) : Light-Harvesting Bacteriochlorophyll a Ratio.

The concentration of a freshly isolated sample of RC-B875 conjugate was diluted to give an absorbance at the NIR absorption maxima ie. at about 875 nm, of approximately 1.0 cm^{-1} . A 3 ml aliquot of sample was added to both the reference and sample cuvettes. The absorbance scale was set to 0.2 and the spectrophotometer was zeroed with the zero point centrally positioned on the chart paper. A baseline was recorded from 900 to 700 nm at 50 nm.cm^{-1} (4 nm.s^{-1} chart speed). To ensure complete reduction of the reference cuvette a small amount of sodium ascorbate was added. Potassium ferricyanide was added to the sample cuvette and a difference spectrum was recorded from 900 to 700 nm. Figure 3.2 illustrates a typical oxidation-reduction difference spectrum. Subsequent additions of potassium ferricyanide were made until complete oxidation of the RC had been achieved ie. there is no further increase in the intensity of the blue shift at 800nm and at the point prior to the irreversible bleaching of the LH.BChl a, indicated by a slight shift to the red in the bleaching at 883/870 nm band. Since it has been shown that excessive potassium ferricyanide addition can bring about the irreversible bleaching of light-harvesting BChl a, a small quantity of sodium ascorbate was added to the sample cuvette to ensure oxidation reversibility had been maintained. The RC-concentration was determined from the change in absorption at 800 nm using the predetermined extinction coefficient $133 \text{ mm}^{-1} \text{ cm}^{-1}$ [Clayton *et al*, 1972a].

The concentration of total BChl a was determined from the absorption of the sample at 880 nm using the extinction coefficient, $\epsilon_{880} = 120 \text{ mM}^{-1} \text{ cm}^{-1}$ [Clayton, 1971] or the extinction

FIGURE 3.2 A Typical Oxidation-Reduction Difference Spectrum Produced by a Sample RC-B875 Complex Isolated from the Purple Bacterial Species, *Rhodobacter sphaeroides* R26.

An equivolume sample of RC-B875 antenna complex, in 10 mM Tris-HCl, pH 8.0, isolated from photosynthetic membranes of *Rhodobacter sphaeroides* R26, was added to both reference and sample cuvettes, a baseline reading was recorded, indicated by the line spectra, 'B'. Line spectra 'a', 'b' and 'c' were recorded after consecutive additions of potassium ferricyanide, and ascorbate, to the sample, and reference, cuvettes respectively. Additions were made until there was no further increase in the size of the spectral shift centred at approximately 800 nm. To ensure oxidation reversibility had been maintained, ascorbate was added to the sample cuvette, and the difference spectra (R) was recorded. (Absorption pathlength 1 cm).



coefficient experimentally determined for each species.

3.9 Determination of the Extinction Coefficient at 880 nm for Total Bacteriochlorophyll *a*.

Aliquots of the isolated RC-B875 antenna complex were made to a final volume of 1 ml with 10 mM Tris buffer, pH 8.0. The aliquots ranged from 20 μ l to 300 μ l volumes depending upon the initial sample concentration. The near infra-red absorption peak of each sample was recorded. 4 mls of acetone:methanol (7:2 v/v) were added to each sample, vortexed and centrifuged for 2 minutes in a Hettich EBA 3S benchtop centrifuge at 450 x g. Owing to the sensitivity of free BChl *a* to light, all solvent extraction procedures were carried out in darkened test-tubes. The absorption maxima at 772 nm was recorded. The extinction coefficient for BChl *a* was then determined from the ratio of the *in vivo* and *in vitro* absorption peaks using the *in vitro* extinction coefficient for BChl *a*, $\epsilon_{772} = 76.\text{mM}^{-1}.\text{cm}^{-1}$.

$$\text{ie. } \epsilon_{880} = \frac{A_{880}}{A_{772}} \times 76 \quad (\text{Cohen-Bazire } et al, 1957).$$

An average value for ϵ_{880} was determined.

3.10 Concentrating the Isolated Complexes.

The isolated B800-850 complex and RC-B875 complex were too dilute for subsequent analytical methods. They were, therefore, concentrated on DE52 (Diethylamininoethyl Cellulose preswollen microgranular anion exchanger supplied by Whatman Biosystems Ltd.) columns in 20 mM Tris-HCl, pH 8.0. The sample was washed with the buffer solution and eluted with 250 mM NaCl solution in 20 mM Tris-HCl, pH 8.0 containing 0.1% LDAO (v/v). The

concentrated samples were then dialyzed at 4°C against 20 mM Tris-HCl, pH 8.0. This method was also employed to exchange the detergent present in the sample: once added to the DE52 column the sample was washed several times with the buffer solution and eluted with a salt solution containing the alternative detergent (Appendix 1.6).

3.11 Analysis of the Polypeptide Composition of the Isolated Conjugates.

Protein concentration was determined using the tannin assay as described by Mejbaum-Katzenellenbogen and Dobryszczyka (1959). 1 ml of tannin reagent (Appendix 1.7) was added to 1 ml of protein sample prewarmed for about 5 minutes at 30°C. After 10 minutes at 30°C, 2 ml of 0.1% (w/v) gum arabic solution was added to stabilize turbidity. The mixture was cooled to room temperature, and the absorbance at 500 nm was recorded against a blank containing all the components except protein. The optical density at this wavelength is directly proportional to the amount of protein present at standard conditions. Bovine serum albumin (Fraction V supplied by SIGMA Chemical Company) was used as the protein standard: the optical density of known concentrations of BSA was recorded to produce a standard calibration curve (Figure 3.3).

The polypeptide composition of the isolated RC-antenna conjugates was determined using sodium dodecyl sulphate-polyacrylamide gradient gel electrophoresis (SDS-PAGGE) (Appendix 2.1 describes gel buffer solutions and polyacrylamide gel preparation). The general method of Laemmli (1970) as described by DeMartini *et al* (1978) was used: slab gels as illustrated in Figure 3.4b were employed. The apparatus is a modification of the Studier-type slab gel model (Figure 3.4). The gel was formed

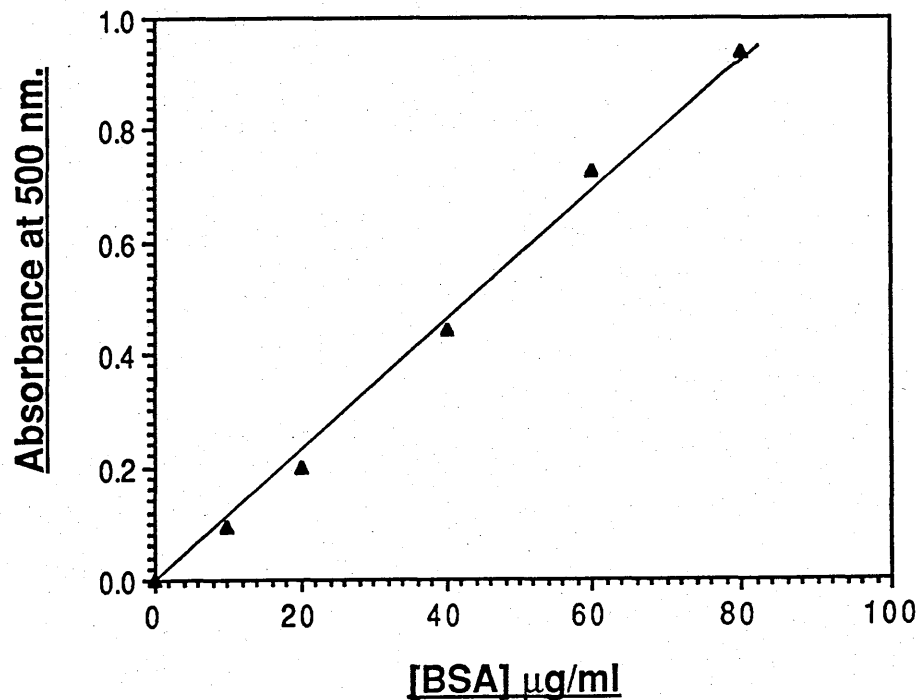


FIGURE 3.3. Typical Calibration Curve Relating the Parameters of Protein Concentration with Respective Absorbance at 500 nm.

The optical density at 500 nm (ordinate) of known concentrations of the protein standard, Bovine serum albumin (BSA)(abscissa), were recorded to produce a standard calibration curve. The calibration curve was used to determine protein concentrations of 'unknown' samples. A tannin assay was carried out on each sample in order to determine its OD_{500} . (Absorbance path length 1cm.).

FIGURE 3.4 A Studier-Type Gel Apparatus (above) and the Notch-Glass-Plate Assembly used to form the Gel Slab (below).

The glass-plate assembly consists of two glass plates of equal side and base dimensions, the top of one glass plate, however, is notched. Dividers of approximately 1.5 mm thickness separate the two glass plates, which are held together with bulldog clips. The side and base edges are sealed with agarose. A perspex comb is placed between the two glass plates to allow wells to be formed. This is removed, along with the base divider, when the gel is assembled on the gel apparatus. The gel-plate sandwich is placed in a vertical position with respect to the gel apparatus, such that the notch of the plate sandwich is aligned with the notch of the upper buffer reservoir. The base of the gel sandwich is emersed in the lower buffer reservoir. The gel is held in position with bulldog clips. The gel apparatus is connected to a power supply such that the upper reservoir is connected to the cathode, and the lower reservoir is connected to the anode electrode. A continuous current flowing from the upper reservoir to the lower reservoir is therefore, generated.

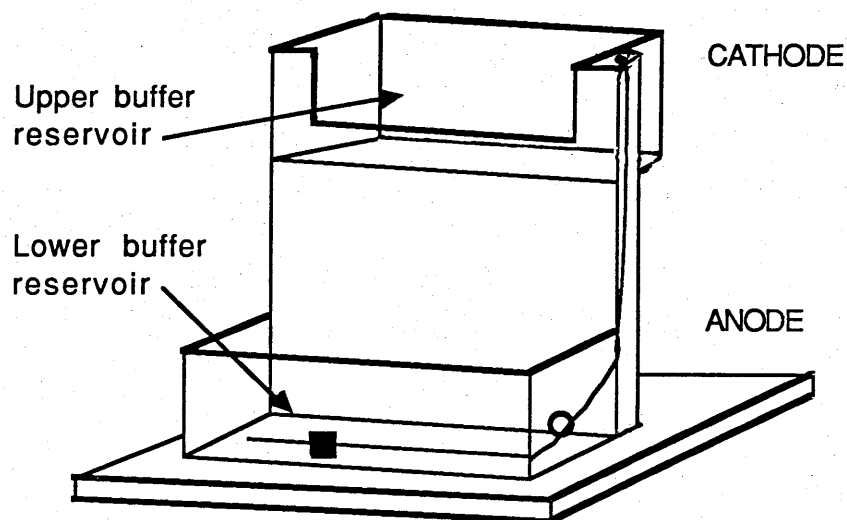
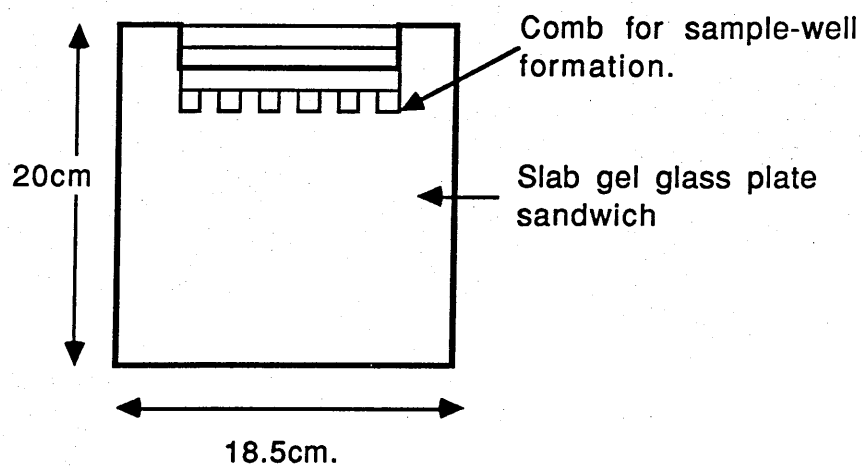


FIGURE 3.4 (Above) A Studier-type gel apparatus
 (Below) The notched glass-plate assembly
 used to form the gel slab.
 [Hames, 1981]



between 2 glass plates, one rectangular in shape with dimensions of 20 cm x 18.5 cm and the other the same size except for a 16 cm x 1.5 cm notch cut into one of the 20 cm edges. The glass plates were placed together and divided by spacers (1.5mm thick) along the base and side edges. The edges were sealed with 2% agarose and clamped together with bulldog clips. The clamped plate assembly was held vertically during the pouring and the running of the gel. A 20% (w/v) polyacrlamide gel solution was poured between the glass plates to a level about 1 cm from the bottom: this simply served as a 'plug' to ensure there was no leakage from the system. When the 'plug' was set the resolving gel mixture was prepared and poured to within 4 cm of the top. A layer of 50% (v/v) H₂O:methanol was poured on top of this to ensure that the gel sets evenly and that no meniscus was formed. Gradient gels of acrylamide concentrations ranging from 11.5% to 18% (w/v) were also prepared. In addition to a gradient in acrylamide concentration, a density gradient of sucrose was also included to minimize mixing by diffusion, an almost inevitable consequence of allowing the gel to polymerize over a period of approximately 12 hours (with shorter setting periods convective disturbances caused by the heat of polymerization must also be reduced). Once the resolving gel was set, the water/methanol layer was removed and the stacking gel was poured. A perspex comb was inserted between the glass plates and into the stacking gel mixture in order to form the sample wells. The stacking gel was left to polymerize for about 30 minutes. The comb and base divider were then removed before attaching the glass plate sandwich to the electrophoresis apparatus: the plates were arranged such that the notched glass plate is aligned with, and is adjacent to, the upper buffer reservoir. The bottom of the gel should be immersed in the buffer

in the lower reservoir. Samples containing approximately 35 μg protein were loaded into the wells using a 50 μl glass syringe. The apparatus was connected by leads to a power pack such that the proteins migrate towards the anode ie. the lower reservoir. The gel was electrophoresed at 12 mA for about 16 hours.

Standard protein mixtures containing proteins of known molecular weights were run alongside the sample proteins to give some indication of the relationship of molecular weight and mobility (Appendix 2.2a) in each gel system. The standard mixture contained the proteins Bovine serum albumin (68 kd)(Fraction V supplied by SIGMA Chemical Company), alcohol dehydrogenase (from baker's yeast (1.1.1.1.) supplied by BDH Chemicals Ltd.) (41 kd), myoglobin (from horse heart, salt-free from BDH Chemicals Ltd.)(17.2 kd) and cytochrome C (from horse heart Type II-A supplied by SIGMA Chemical Company)(12.2 kd). The samples were prepared by adding an equal volume of boiling solution (Appendix 2.2b) to the protein sample which was adjusted to a concentration of 2 mg.ml^{-1} . The samples were boiled for 1.5 minutes at 100°C or heated to 70°C for 30 minutes.

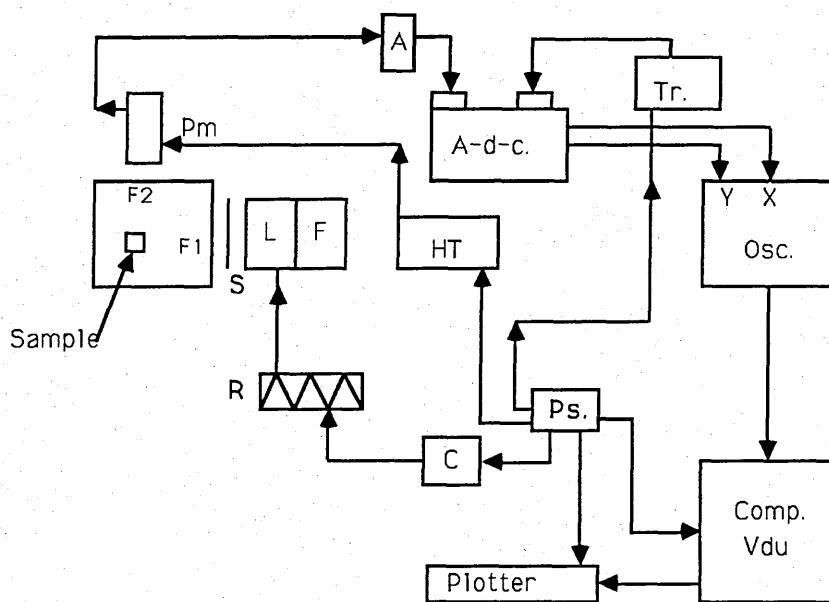
When the dye front had reached the bottom of the resolving gel, the gel plates were removed from the apparatus and separated. The gel itself was carefully lifted from the plates and put into staining solution (Appendix 2.3) for at least 2 hours. The gels were then destained in 10% methanol, 10% acetic acid. The protein bands were observed by lowering the destained gel onto a light box.

3.12 Measuring the Fluorescence Properties of the Isolated RC-B875 Conjugate.

Fluorescence emitted from the complex was detected with a home-built fluorometer (Figure 3.5). Excitation was provided by passing light powered by a 150 W Quartz-halogen lamp through a 587 nm red cut-off filter. Fluorescence was collected at right-angles to the direction of excitation, passed through a RG 715 nm cut-off filter and a Balzer's 913 nm interference filter and detected on an extended S20 Thorn EMI photomultiplier tube (Type number 9592B). The signal was amplified and passed through an analogue-to-digital converter and into a PDP 11/23 microcomputer supplied by D.E.C. (Digital Electrical Corporation), this device allowed the capture and storage of rapid transient data (The computer programme for fluorescence analysis was designed by Dr.M.F.Hipkins). The period of light excitation was controlled by an electromagnetically operated shutter which on onset of shutter opening also triggered the data storage device. The stored data could then, or at a later date, be graphically presented using the attached graph plotter.

The isolated RC-B875 complex had to be of sufficient concentration to allow the detection of fluorescence, but not so concentrated that the phenomenon of self-absorption was introduced. An 'optimum' concentration, or concentration range, therefore, had to be determined: the fluorescence yield was measured for samples with respective optical densities, at their NIR absorption peak, ranging between 0 and 1.0. In the absence of self-absorption, the relationship between the fluorescence yield and absorption maxima should be linear. It was found that samples with OD_{880} greater than 0.25. produced self-absorption effects. Samples were therefore, diluted to

FIGURE 3.5: BLOCK DIAGRAM OF FLUORESCENCE APPARATUS



A	Amplifier
A-d-c	Analogue-digital convertor
C	Constant voltage power supply (Coutant).
Comp.VDU	PDP 11/23 Microcomputer with visual display unit.
F	Fan
F1	587nm red cut-off filter.
F2	RG 715nm cut-off filter and Balzers 913nm Interference filter.
HT	High tension.
L	Quartz halogen lamp (150W)
Osc.	Oscilloscope.
PM	Photomultiplier (S20 Thorn EMI Type number 9592B)
PS	Power supply
R	Rheostat
S	Shutter
Tr	Trigger

concentrations less than, or equal to, this maximum value. Experiments were also carried out to examine the effects of ascorbate, potassium ferricyanide and detergents on the nature and yield of fluorescence: detergents including LDAO, SDS, Triton X-100 and n-octyl β -D-glucopyranoside (OG) at concentrations ranging from 0 to 2.0% (v/v) were examined. It is important to mention here that all samples were given a minimum three minutes dark period prior to excitation. To ensure that experimental conditions, such as heat or time effects, were not influencing the yield of fluorescence, a sample was maintained within the fluorescence apparatus for a period of 70 minutes, and the fluorescence yield was measured, and recorded, at 10 minute intervals during this period. Each experiment generated a fluorescence induction curve from which the relationship existing between the parameters of time and fluorescence yields could be examined.

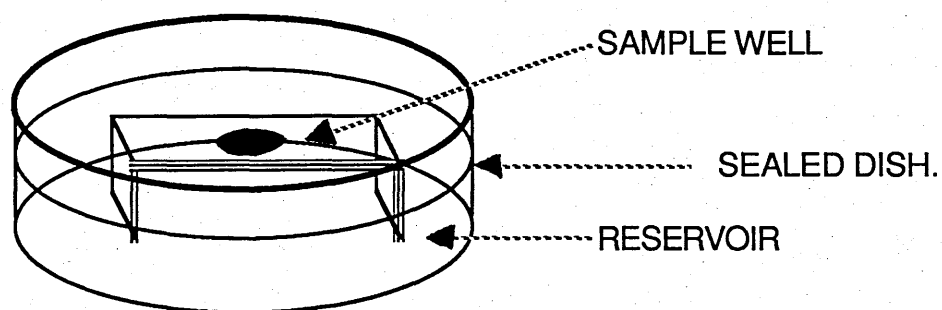
3.13 Crystallization of the Isolated Conjugate.

The method of vapour diffusion was used to produce crystals [Michel and Oesterhelt, 1980]. Prior to crystallization various preparative procedures were carried out on the isolated RC-B875 antenna conjugates, in order to ascertain which methods were favourable with respect to crystal formation. It was shown previously that crystallization is more successful using a more concentrated sample, all samples, therefore, were concentrated on DE52 columns and eluted with a salt solution containing detergent. Four preparative procedures were examined: (i) the RC-B875 conjugate was dialyzed and then concentrated on a DE52 column, the sample was eluted with 250 mM NaCl containing 0.1% LDAO (v/v) (ii) As described in (i) although the eluting buffer consisted of 500 mM NaCl containing the milder detergent 1% dodecyl β -D-

maltoside, which may serve to stabilize the isolated complex. (iii) The sample was concentrated as described in (i) and was then further purified by a single passage over a molecular sieve column (Sephacryl S200 supplied by Pharmacia fine chemicals). The sample was then dialyzed and reconcentrated on a DE52 column and eluted with a solution of 500 mM NaCl containing 1% dodecyl β -D-maltoside (w/v). (iv) As described in (iii) although the final elution buffer contained the detergent 1% (w/v) cholic acid.

Figure 3.6 illustrates the type of apparatus used in these crystallization experiments. The wells on the crystallization platform of the dishes were examined for scratches and thoroughly cleaned before crystallization solutions were prepared. This helps to reduce the possibility, or extent, of nucleation and also aids in the production of larger crystals [M^CPherson, 1982]. An example of the crystallization procedure is detailed below and employs a recipe described by Wacker *et al* (1986) for the crystallization of the RC-B875 conjugate of *Rhodopseudomonas palustris*: an 8 ml volume of the precipitating solution containing 18% (w/v) polyethylene glycol 2000 (PEG 2000 supplied by BDH Chemicals Ltd.), 20 mM MgCl₂ in buffer A (10 mM Tris-HCL, pH 8.0 containing 0.04% (w/w) LDAO (supplied by Fluka A.G.)) was added to the reservoir area of the crystallization dish. A small amount of sodium azide is added to all solutions containing PEG to preclude the growth of bacteria and moulds. The sample solution was prepared in a 1.5 ml eppendorf by combining an equal volume of 17% (v/v) PEG 2000, 20 mM MgCl₂ in buffer A with the protein sample. The solution was thoroughly vortexed and then centrifuged for 2 minutes at 4000 x g in a MSE minor "s" bench-top centrifuge to eliminate any amorphous material which may serve to interfere with crystallization. A 50 μ l droplet of the well solution was pipetted onto the well of the crystallization platform.

FIGURE 3.6 Diagrammatic Representation of the
Type of Apparatus used in Crystallization Experiments



This type of crystallization dish is frequently used in crystallization attempts utilizing the general method of vapour diffusion; the well solution, containing the sample complex and precipitant, is contained within a depression, or well, on the crystallization platform held above a reservoir of precipitating solution. The crystallization dishes are sealed. Supersaturation is achieved through the vapour phase as the concentration of precipitant in the reservoir equilibrates with that in the sample.

Crystallization conditions were changed by systematically modifying parameters such as the temperature of incubation (10°C and 20°C), the pH (pH 8.0-9.5), the concentration of internal (well) and external (reservoir) PEG solutions and the type of detergent in buffer A (0.04% (v/v) LDAO, 0.1% (v/v) DDAO and 0.1% (w/v) dodecyl β -D maltoside). The pH of the sample solution was monitored using an "INGOLD" microelectrode, the pH being modified by the additions of very small amounts of concentrated acid or alkali. The crystallization pots were sealed with plastic tape, labelled and maintained in thermostatically-controlled environments in the dark for 2-3 weeks before examination using a light microscope. Other crystallization recipes employed in this study are described in the results section although the basic procedures adopted are as described above.

CHAPTER 4

Isolation of the Reaction Centre-B875 Antenna Conjugate using the Technique of Sucrose Density-Gradient Centrifugation.

4.1 Optimization of Solubilization Conditions.

Solubilization of photosynthetic membranes of purple bacteria with detergents dissociates the membrane into its two main components, namely the RC-B875 antenna conjugate and the B800-850 antenna complex. These components can be fractionated, in a spectrally pure form, using the general method of sucrose density-gradient centrifugation. The fractionation of solubilized membranes of most bacteriochlorophyll *a* (BChl *a*) -containing species of purple bacteria, therefore, yields two bands, an upper and a lower band, containing the B800-850 antenna complex and RC-B875 antenna conjugate respectively (Figure 4.1a). Species such as *Rs. rubrum* strain S1 and the mutant strains of *Rb. sphaeroides*, R26 and M21, however, yield only the RC-B875 band. The successful solubilization and fractionation of these components in the sucrose-density gradients depends upon the optimization of a number of conditions including:

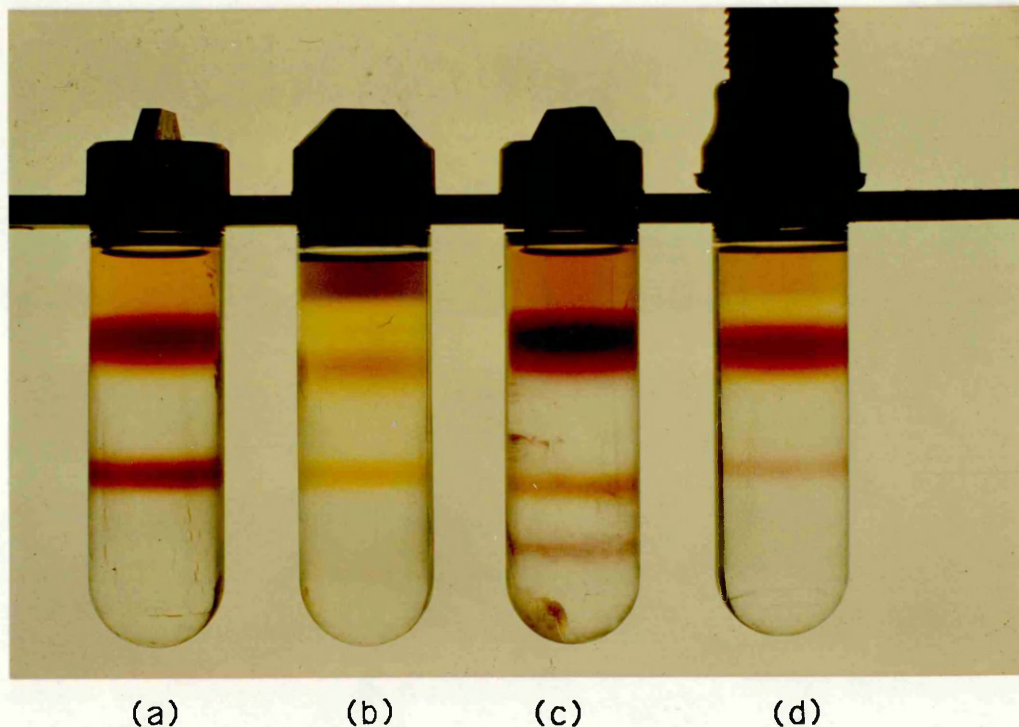
- (i) Detergent type
- (ii) Detergent concentration
- (iii) Sucrose concentrations and the relative volume of each concentration making up the gradient.

Detergents were examined for their ability to solubilize chromatophore preparations of the species, *Chromatium vinosum* strain D (Figure 4.2 presents a spectrum of a typical membrane preparation of *Chromatium vinosum* strain D), and to yield the two

Membranes using the Method of Sucrose Density-Gradient Centrifugation.

Fractionation of detergent-solubilized membranes by sucrose density-gradient centrifugation typically yields two bands, Band I (upper band) and Band II (lower band). The figure shows fractionated membranes of the species (a) *Rps. palustris* 'DSM8252', (b) *Rc. gelatinosus* 151, (c) *Rps. acidophila* 7050 (grown under low-light intensity conditions) and (d) *Rps. acidophila* 7750. The membranes were prepared as described in section 3.3, the OD₆₅₀ was adjusted to approximately 50. cm⁻¹ and solubilized with the detergent LDAO at concentrations of 0.75% (*Rps. palustris* 'DSM8252' and *Rc. gelatinosus* 151) and 1.0% (*Rps. acidophila* strains 7050 and 7750). A 3 ml aliquot of solubilized membrane was layered onto the top of sucrose density-gradients prepared with equivolumes (8 ml) of 1.2 M, 0.6 M, and 0.3 M sucrose in 10 mM Tris-HCl, pH 8.0 containing 0.2% (v/v) LDAO. The gradients were centrifuged in a Sorvall OTD-65B Ultracentrifuge (fixed-angle rotor T865) at 196 000 x g, 4°C, for approximately 16 hours.

The two bands have spectral properties characteristic of the two main components of the photosynthetic apparatus, ie. the B800-850 light-harvesting complex (Band I) and the RC-B875 antenna complex (Band II). Spectral analysis of the pigmented material banding at the top of the gradient shows it to be denatured material.



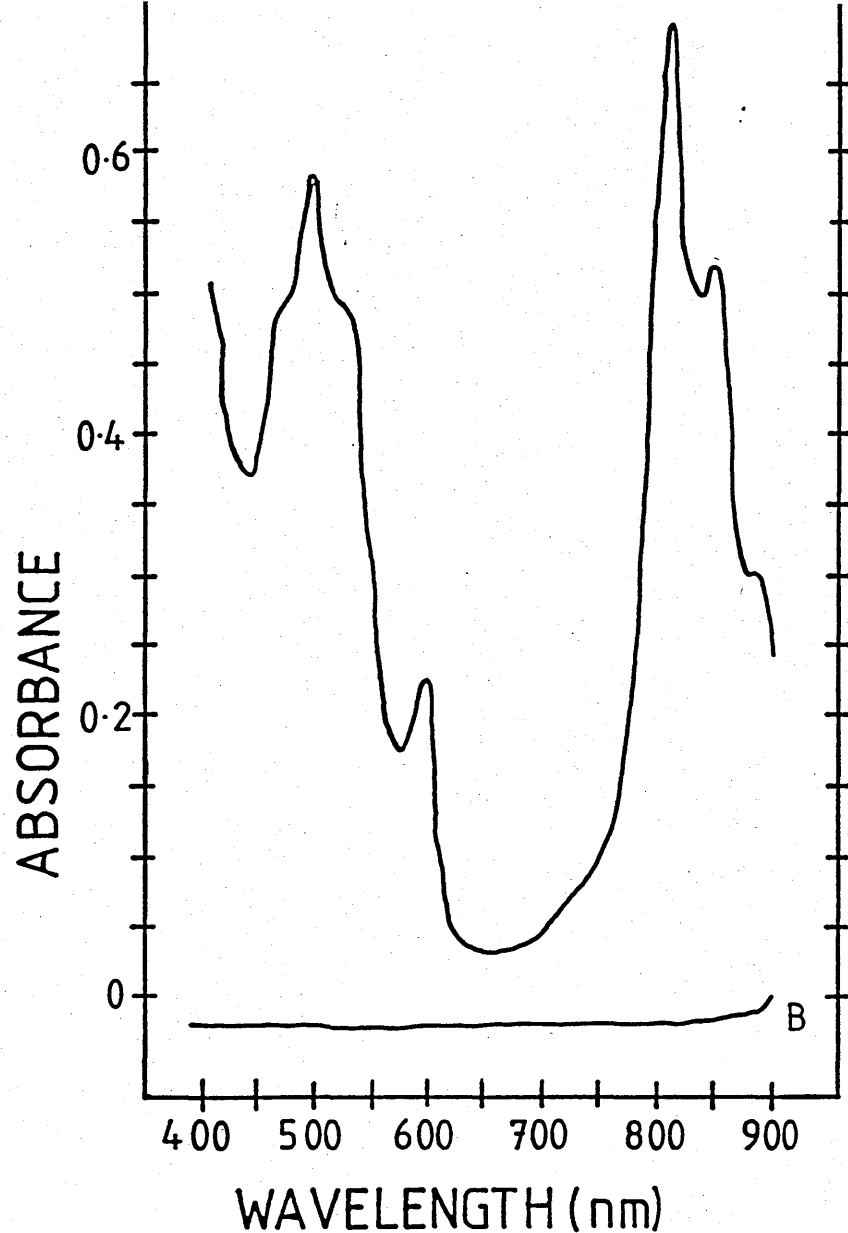


FIGURE 4.2 Typical Spectrum of a Chromatophore Preparation of the Purple Bacterial Species *Chromatium vinosum* Strain D.

The absorption properties of the light-harvesting antenna complexes B800-850, B800-820 and B875, and the reaction centre complex, produce characteristic absorbance peaks typical of those observed in the NIR region of spectrum shown above. The peak observed at approximately 590 nm is also the product of BChl a absorption. Carotenoid absorption produces the spectral peaks typically observed in the spectral range from approximately 440 nm to 570 nm.

The chromatophores were prepared as described in section 3.3 and resuspended in 10 mM Tris-HCl, pH 8.0. The absorption spectrum was recorded using an SP8-500 UV/VIS spectrophotometer at wavelengths from 900 nm to 400 nm (Absorbance pathlength 1 cm)

main components of the photosynthetic apparatus in a spectrally pure form. The detergents used included lauryl dimethylamine N-oxide (LDAO), sodium dodecyl sulphate (SDS), sodium deoxycholate (SD), Triton X-100, lauryl maltoside (LM), dimethyldecylamine oxide (DDAO) and N-octyl- β -D-glucopyranoside (OG). The effectivity of each detergent was examined with respect to a number of criteria: (a) Its ability to solubilize photosynthetic membranes of purple bacteria, such that subsequent fractionation on sucrose density-gradients yields two bands (except in those species such as *Rhodospirillum rubrum* strain S1 which yields the RC-B890 complex). (b) The band yields should be dense enough for subsequent analysis and there should be no, or a minimum of, unsolubilized material pelleted at the bottom of the gradient and/or denatured material at the top of the gradient and (c) spectral analysis of the fractionated band(s) should show them to be representative of the different components of the photosynthetic apparatus.

(a) Sodium deoxycholate (SD): membranes of *Chromatium vinosum* strain D solubilized in SD at concentrations less than 3% (w/v) produced two bands in the sucrose gradient, however, spectral analysis revealed incomplete fractionation indicated by the presence of a shoulder on the left arm of the B875 absorption peak, and also the presence of a pellet of unsolubilized material at the bottom of the gradients. At concentrations of SD ranging from 3% to 7% (w/v) the extent of solubilization, as suggested by the size of the pellet, improved and again two distinct bands were obtained in the sucrose gradient. Spectral analysis revealed no, or little, improvement in the purity of the fractions; the small peak, of Band I, evident at 850nm is indicative of contamination of the RC-B880 complex, and likewise, the large absorption peak of Band II at 800nm suggests that the RC-B880 complex has only been

FIGURE 4.3 (a & b) Typical Absorption Spectra of Complexes isolated from Photosynthetic Units of *Chromatium vinosum* D by Solubilization of Membranes Using the Detergent, sodium deoxycholate.

Figure 4.3a presents typical spectra of complexes isolated by the fractionation of photosynthetic membrane of *Chromatium vinosum* D solubilized in 3% (w/v) sodium deoxycholate (SD). The spectral properties of these complexes in 10 mM Tris-HCl, pH 8.0, suggest that only partial isolation, of the different spectral components constituent of the photosynthetic unit, had been achieved. Band I has absorption properties characteristic of the B800-820/800-850 antenna complexes, although the large shoulder extending well into the NIR region suggests that some RC-B875 antenna complex was still present. Band II shows that enrichment of the B880 antenna complex had been achieved, although high absorption observed between 800 nm and 850 nm, indicates that there was only partial isolation of the RC-B875 complex from the other antenna component.

Figure 4.3b presents spectra of fractions isolated from photosynthetic membranes of *Chromatium vinosum* strain D solubilized in 6% (w/v) SD. The spectral properties of these bands, in 10 mM Tris-HCl, pH 8.0, are very similar to those observed in Figure 4.3a, suggesting again that isolation of the B800-820/B800-850 (Band I) and RC-B875 (Band II) LHC, in a spectrally pure form, was incomplete. Band II does show some improvement in the isolation of the RC-B875 complex in comparison to that of the previous figure. A small degree of denaturation, however, is also apparent.

(Absorbance pathlength 1 cm).

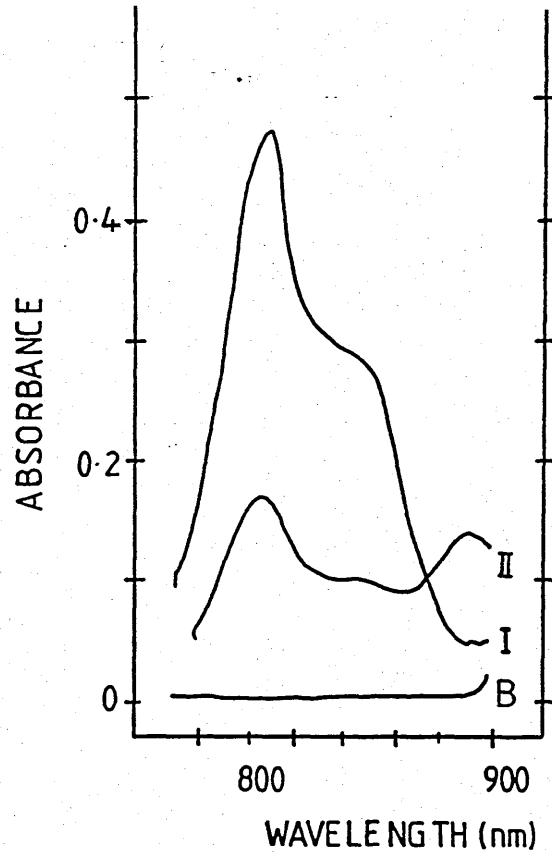
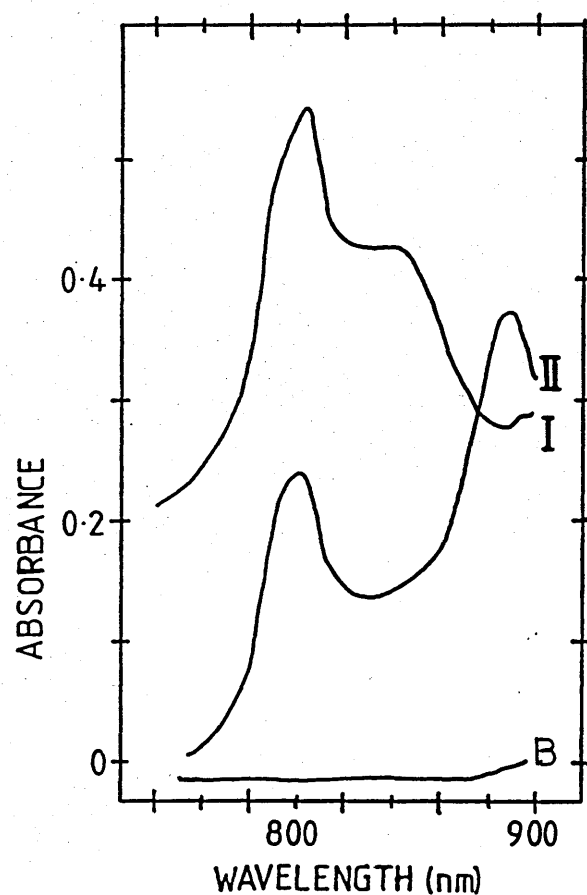


FIGURE 4.3a Solubilization of Photosynthetic Membranes of *Chromatium vinosum* strain D in 3 % (w/v) sodium deoxycholate.



(B - baseline)

FIGURE 4.3b Solubilization of Photosynthetic Membranes of *Chromatium vinosum* strain D in 6 % (w/v) sodium deoxycholate.

partially isolated from the B800-850 antenna complex (Figure 4.3a). At high concentrations of SD ie. above 5% (w/v), a layer of detergent formed in the gradient which interfered with the lower band, making it more disperse. These results therefore, suggest that the SD is fairly ineffective as a detergent for solubilizing the photosynthetic membranes of *Chromatium vinosum* strain D, and for yielding spectrally pure components using the fractionation method of sucrose density-gradient centrifugation (Figure 4.3b).

(b) Sodium dodecyl sulphate (SDS): SDS at concentrations ranging from 0.5% to 1.0% (w/v) produced two bands in the main body of the gradient; analysis of the upper band revealed a spectral pattern characteristic of the B800-850/ B800-820 antenna complex (although the peak at approximately 860 nm suggests partial contamination by the B875 antenna complex). Spectral analysis of the lower, very faint band revealed that only partial isolation of the RC-B875 antenna complex had been achieved. The occurrence of a large, disperse band of green colouration at the top of the gradient suggested that denaturation had occurred. Spectral analysis of this band, showing increased absorption in the spectral region corresponding to monomeric BChl a absorption (approximately 780nm), confirmed this assumption (Figure 4.4 presents a spectrum of membranes of *Chromatium vinosum* D solubilized in 1% SDS). Increasing the concentration of SDS from 1% to 2% SDS only served to increase the amount of denatured material occurring at the top of the gradient and to reduce the amount of Band II (the lower band) to an almost negligible level. The upper band, however, produced the characteristic B800-850/ B800-820 absorption spectra. It seems therefore, that although SDS yields the B800-850/ B800-820 antenna complex, it fails to yield pure fractions of the RC-B875 antenna conjugate. This result is somewhat surprising since Thornber (1970) successfully

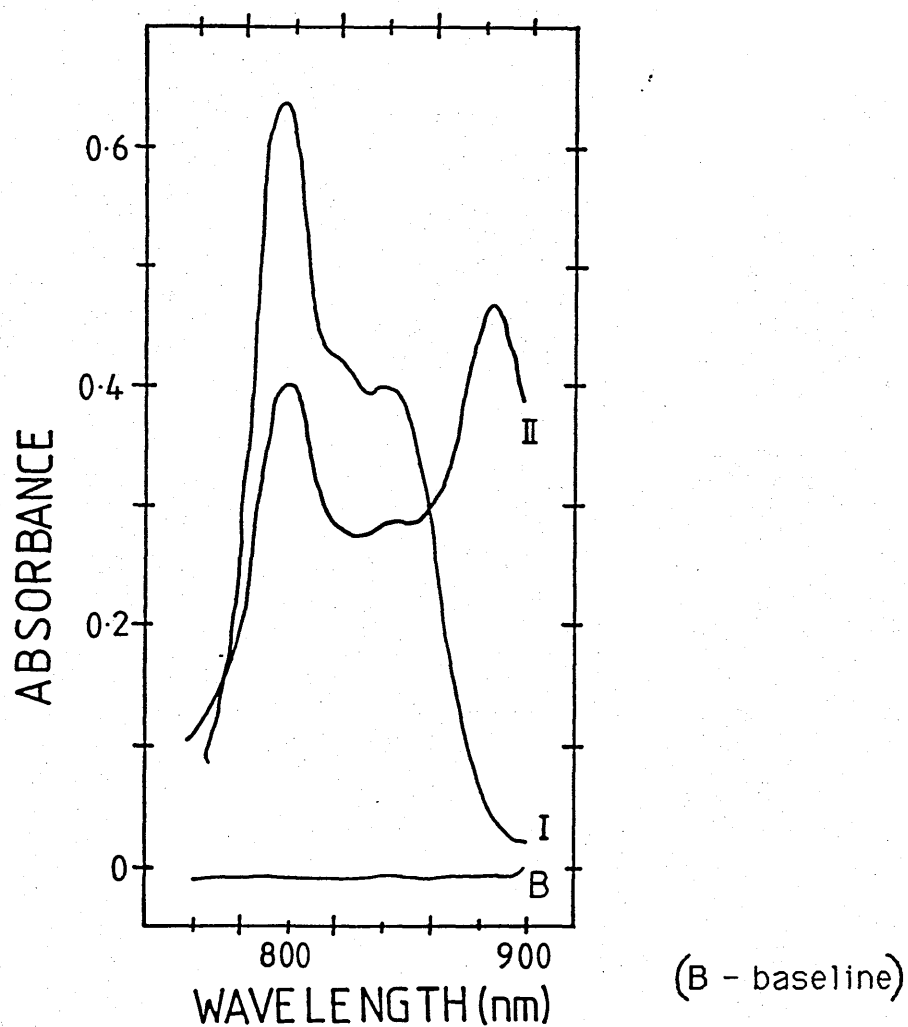


FIGURE 4.4 Spectra of Fractions Isolated From the Photosynthetic Membranes of *Chromatium vinosum* strain D solubilized in 1% (w/v) SDS.

Fractionation of photosynthetic membranes of *Chromatium vinosum* strain D solubilized in 1% (w/v) SDS by sucrose density-gradient centrifugation, typically yields two bands. Figure 4.4 presents typical absorption spectra of these bands in 10 mM Tris-HCl, pH 8.0 (Absorption pathlength 1 cm); examination of Bands I and II indicates that only partial isolation of the B800-820/B800-850, and RC-B890, antenna complexes had been achieved

isolated the B880 spectral form, the so-called Fraction A of *Chromatium vinosum* strain D, by the solubilization of chromatophore membranes in 0.5% (w/v) SDS. However, the large quantity of denatured material produced under the experimental conditions adopted here, certainly suggest that the detergent properties of SDS are too harsh for the solubilization of membranes of *Chromatium vinosum* strain D.

(c) Lauryl dimethylamine N-oxide (LDAO): The successful isolation of spectrally pure fractions of *Chromatium vinosum* strain D was achieved using the detergent LDAO at concentrations ranging from 0.3% to 2.0% (v/v) (Figure 4.5). Since the extent of solubilization and denaturation, induced by a detergent appears to be species, as well as complex, variable (Fyfe, 1985), the general application of LDAO as an effective detergent for fractionating membrane components from a range of bacterial species was examined. The effective solubilization capacity of LDAO, at concentrations ranging from 0.5% to 2.0% (v/v), was tested on membrane preparations of the BChl a-containing species, *Rhodospirillum rubrum* S1, *Rhodobacter sphaeroides* wild type 2.4.1. and the mutant strains R26 and M21, *Rhodocyclus gelatinosus* strains 149 and 151, *Rhodopseudomonas palustris* strains 'French' and 'DSM8252', *Rhodopseudomonas blastica* and *Rhodopseudomonas acidophila* strains 7050 and 7750.

Figures 4.6 (a-h) present spectra showing the successful isolation of the two main components of the photosynthetic apparatus (with the exclusion of *Rs. rubrum* S1 which yields only the RC-B890 complex) using the detergent LDAO. LDAO therefore, proved to be a useful detergent, fulfilling the 'effectivity criteria' described above for most of the species considered: exceptions included wild-type *Rhodobacter sphaeroides* 2.4.1., and its mutant strains M21 and R26. The effective detergent concentration varied

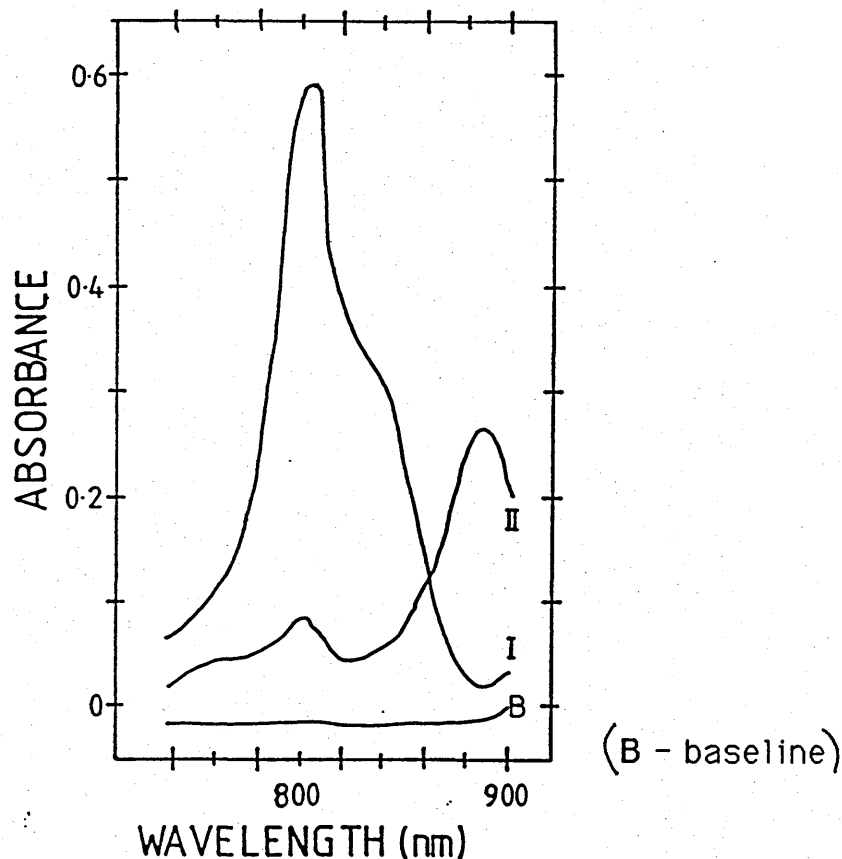


FIGURE 4.5 Solubilization of Membranes of *Chromatium vinosum* strain D using the Zwitterionic Detergent 0.3% (v/v) LDAO.

Photosynthetic membranes of *Chromatium vinosum* strain D solubilized in 10 mM Tris buffer (pH 8.0) containing 0.3% (v/v) LDAO, and fractionated by sucrose density-gradient centrifugation, typically yields two bands, Band I and Band II. The absorbance properties of these bands in 10 mM Tris-HCl, pH 8.0, confirmed that the two main components of the photosynthetic unit had been successfully isolated. Band I has an absorption peak at 800 nm which shoulders at approximately 840 nm. This pattern of absorbance is typically produced by pure B800-820/B800-850 antenna complex. Band II shows an absorbance peak at approximately 890 nm, and a smaller peak arising at 800 nm. The peaks are the result of B890 antenna complex, and RC, absorption respectively, and are indicative of successful isolation of the RC-B890 core component of *Chromatium vinosum* strain D.

FIGURE 4.6 (a - h) Detergent Solubilization of Photosynthetic Membranes Prepared from a Range of BChl *a*-Containing Species of Purple Bacteria.

The Figures 4.6 (a-h) present typical spectra of the two bands generated by the fractionation of membranes solubilized in the detergent LDAO. The effective concentration of LDAO utilized for membrane solubilization was seen to be species specific, with the species *Rps. palustris* strains 'French' and 'DSM8252' requiring 0.75% (v/v) LDAO, *Rps. acidophila* strains 7050 and 7750, 1.0% (v/v), and the species *Rc. gelatinosus* strains 149 and 151, *Rps. blastica* and *Rs. rubrum* S1, a concentration of 0.5% (v/v) LDAO.

It can be seen from the absorption spectra, that the spectral properties of Bands I and II for each species examined, are very similar in the visible region of the spectrum; with peaks in the 450 nm -570 nm range arising from carotenoid absorption, and the peaks at approximately 380 nm and 590 nm, arising from the Soret, and Q_x absorption bands of BChl *a* respectively. In the NIR region of the spectrum, however, the spectral properties of the two bands differ quite significantly. Band I peaks maximally at 800 nm and at 850 nm, whereas Band II produces a prominent absorption peak at approximately 875 nm, and a smaller peak at 800 nm. The absorption properties expressed by each band are typical of the B800-850 and RC-B875 LHC respectively. The spectral properties of respective bands, are seen to be very similar in all species examined; slight differences are observed only in the relative ratio of the 800 nm and 850 nm absorbance peaks of Band I, and in the precise position of the NIR absorbance peak of Band II.

These spectra clearly illustrate that the isolation of the B800-850 and RC-B875 antenna complexes of the photosynthetic unit of a range of BChl *a*-containing purple bacteria, has been successfully achieved using the detergent LDAO.

Membranes from each species were prepared as described in section 3.3, and resuspended in 10 mM Tris buffer, pH 8.0. The absorption spectra were recorded using an SP8-500 UV/VIS spectrophotometer (Absorbance pathlength 1 cm).

FIGURE 4.6a

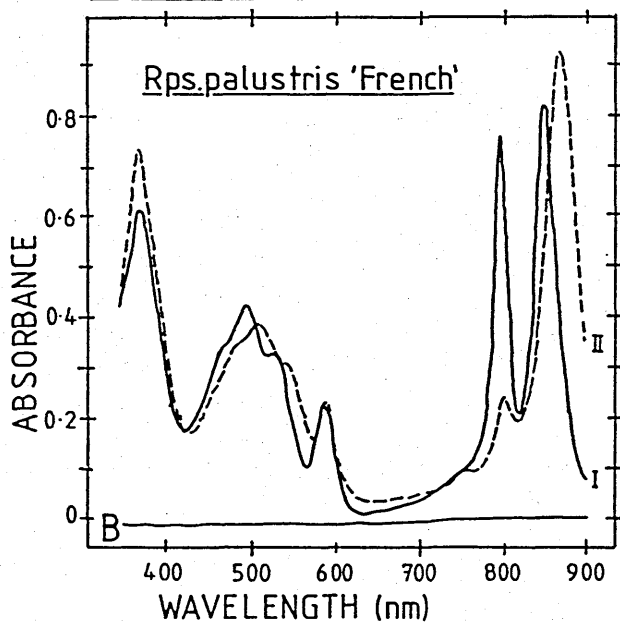


FIGURE 4.6b

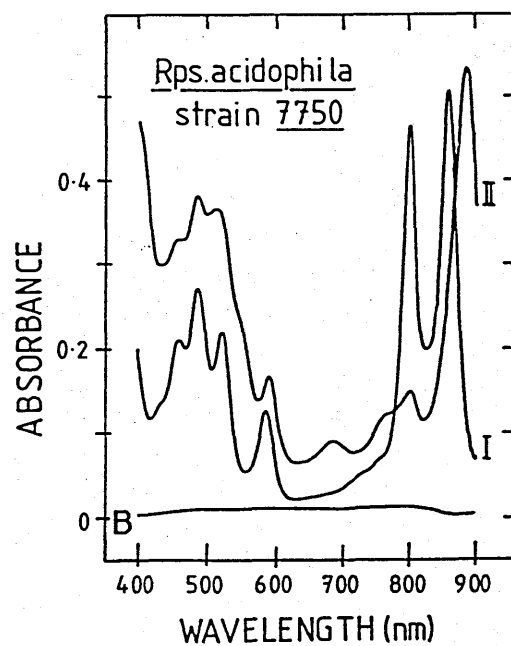
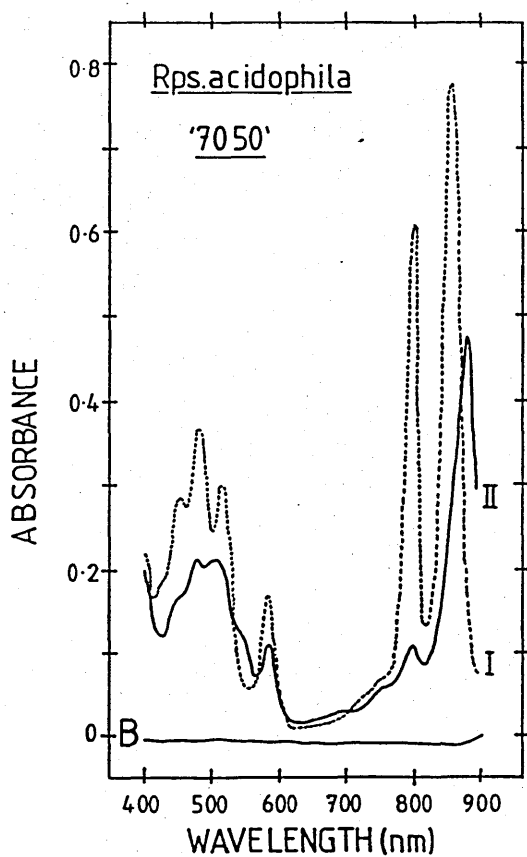
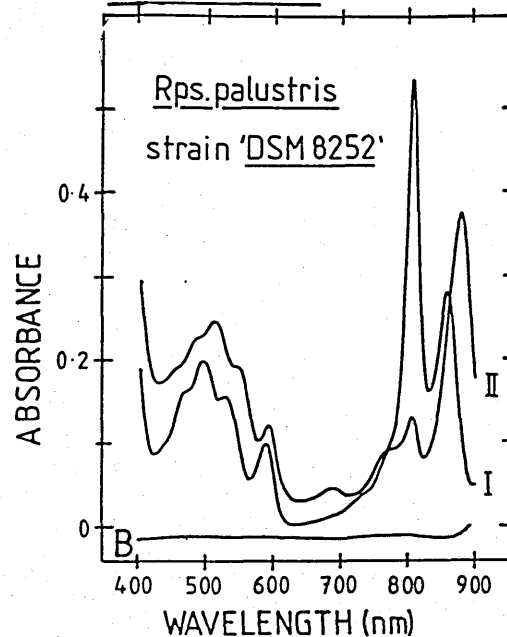


FIGURE 4.6d

FIGURE 4.6c

(B - baseline)

FIGURE 4.6e

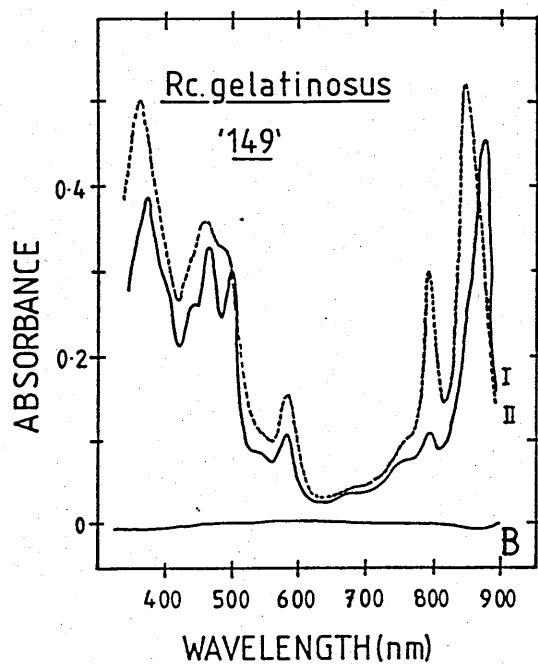


FIGURE 4.6f

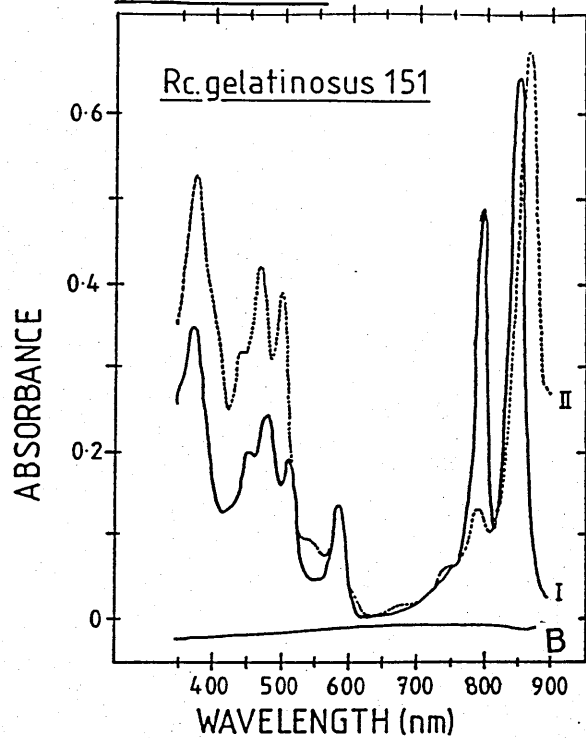


FIGURE 4.6g

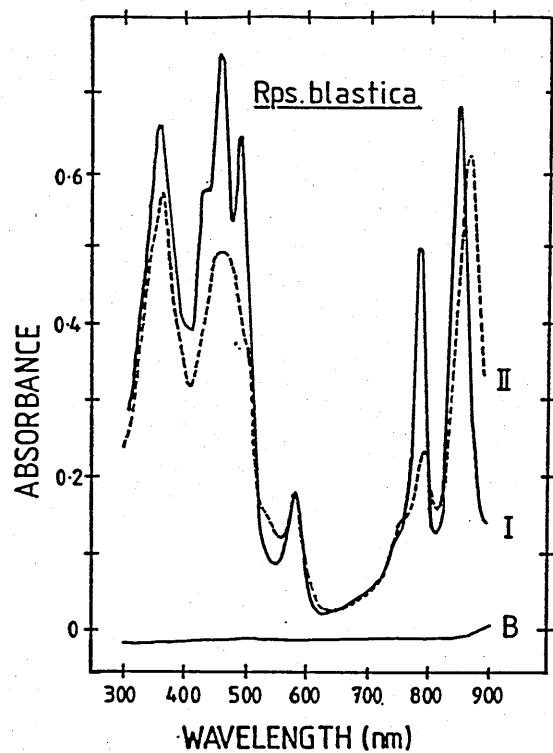
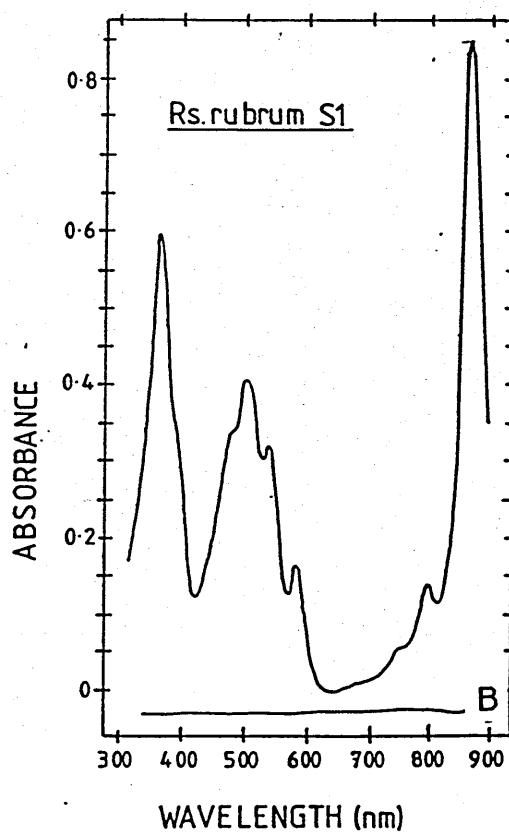


FIGURE 4.6h

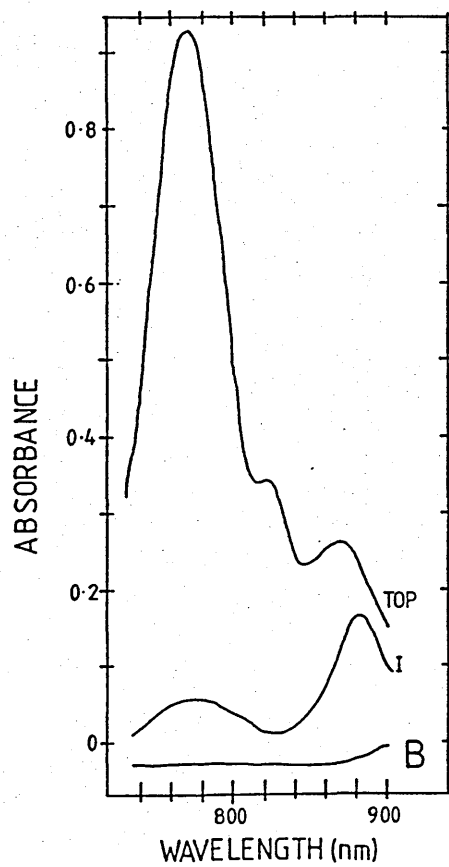


depending upon the species and occasionally, upon the sample batch. Figures 4.7 (a,b & c) present examples of spectra of membranes of *Rs. rubrum* S1 solubilized in the detergents 1% LDAO, 0.5% LDAO and 1% lauryl maltoside respectively. 1% LDAO therefore, can be seen to be too harsh, causing extensive denaturation, whereas the lower concentration of 0.5% LDAO, and the milder detergent 1% LM, allowed the successful isolation of the RC-B890 antenna complex. The solubilization and fractionation of membranes of *Rb. sphaeroides* 2.4.1. with LDAO gave rise to two bands in the sucrose gradient. The first, occurring high up in the gradient, exhibited the characteristic B800-850 absorption spectra, and the second, occurring at the top of the gradient, produced a spectrum typical of denatured material (Figure 4.8). An alternative method of membrane preparation was, therefore, adopted. This method involved the solubilization of membrane preparations of varying concentration with the detergents LDAO and N-octyl β -D-glucopyranoside at final concentrations of 0.5% and 1% respectively [Kaplan, S. Personal communication]. As can be observed in Figure 4.9, this method was unsuccessful in that only enrichment, and not isolation, of the RC-B875 antenna conjugate was achieved. It was observed that the level of denaturation increased as the sample became less concentrated. The mutant strains *Rb. sphaeroides* R26 and M21 were also seen to be very sensitive to the detergent LDAO (Figure 4.10 and 4.11), particularly when it was included in the sucrose solutions in addition to being used in membrane solubilization. It was normal practice in the preparation of sucrose density-gradients to include a low concentration (approximately 0.2%) of the detergent being employed in membrane solubilization in the sucrose solutions, since this appeared to improve band resolution. For the solubilization of R26 and M21 however, improved fractions were

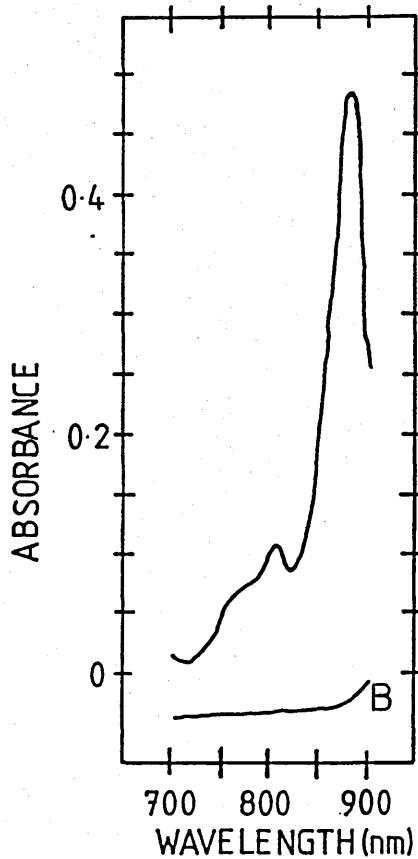
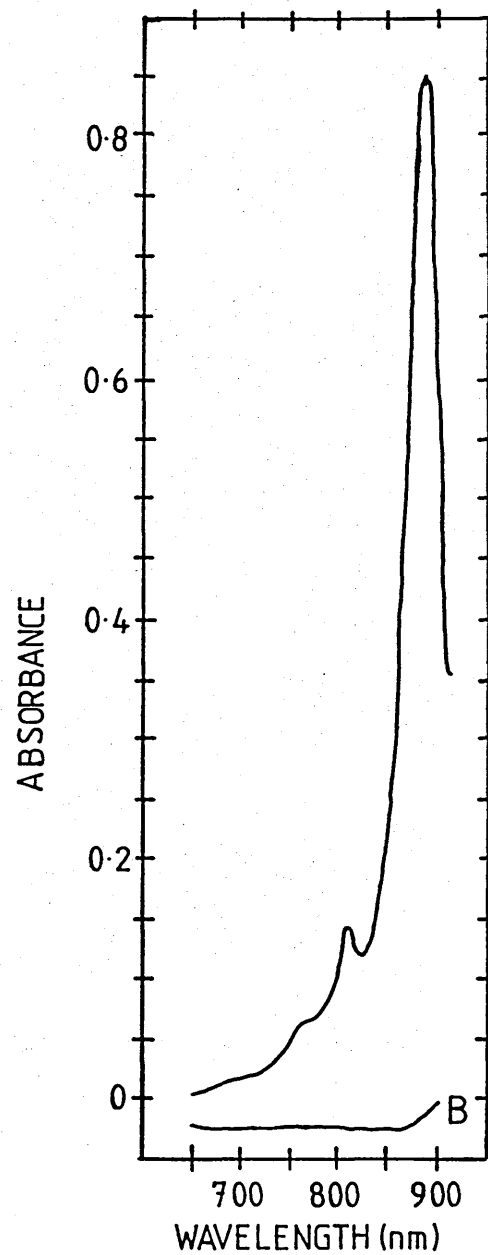
FIGURE 4.7 (a -c) The Effects of Different Concentrations of the Detergent LDAO on the Solubilization of Photosynthetic Membranes Of *Rs. rubrum* S1.

Figures 4.7 a-c present spectra of photosynthetic membranes of *Rs. rubrum* S1 solubilized with the detergents 1.0% (v/v) LDAO, 0.5% (v/v) LDAO and 1% (w/v) Dodecyl β -D-maltoside (LM) respectively. The solubilized membranes were fractionated by the usual method of sucrose density-gradient centrifugation. The isolated fractions were resuspended in 10 mM Tris-HCl, pH 8.0. The spectra clearly show that isolation of the RC-B890 component, has been successful utilizing the detergents 0.5% LDAO and 1% LM. The detergent LDAO at concentrations of 1% and above, however, caused extensive denaturation of membrane components, indicated by the large absorption peak apparent at approximately 770 nm. (Absorbance wavelength 1 cm).

(a) *Rs. rubrum* S1 solubilized in 1% LDAO.



(c) *Rs. rubrum* S1 solubilized in 1% LM.



(B - baseline)

(b) *Rs. rubrum* S1 solubilized in 0.5% LDAO

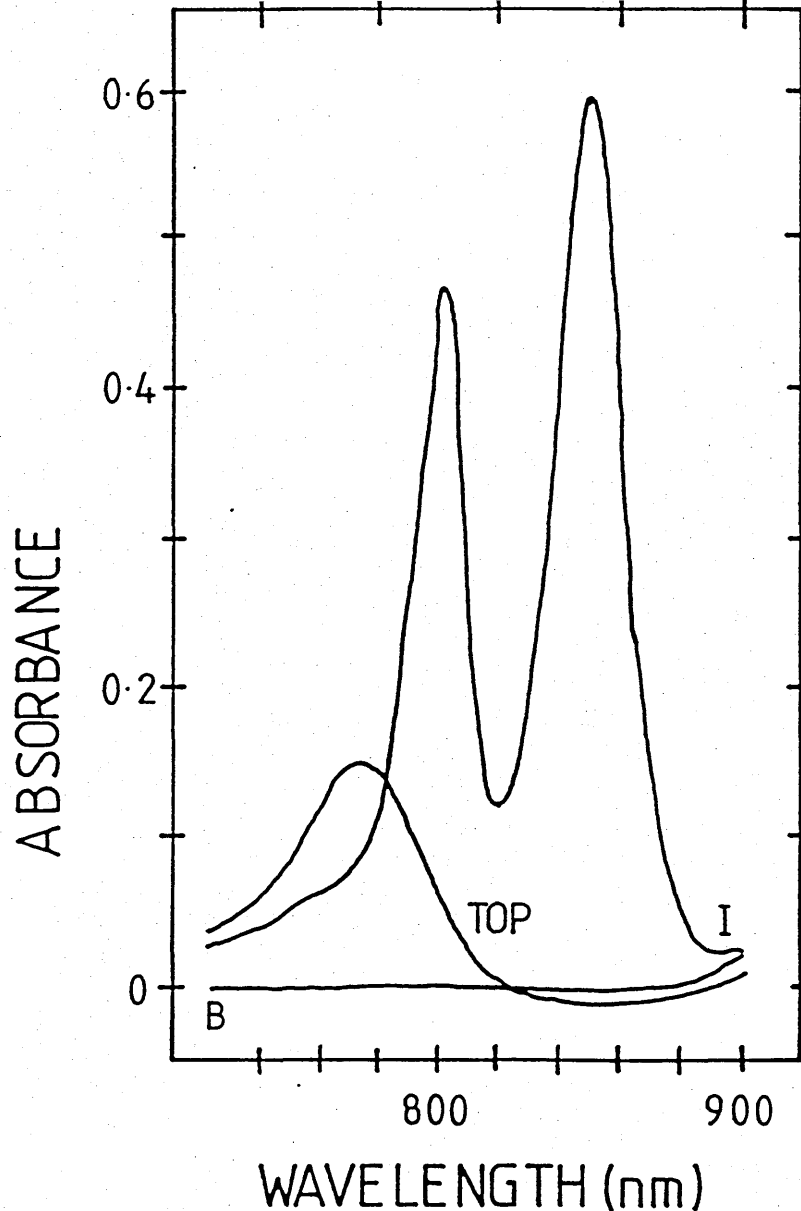
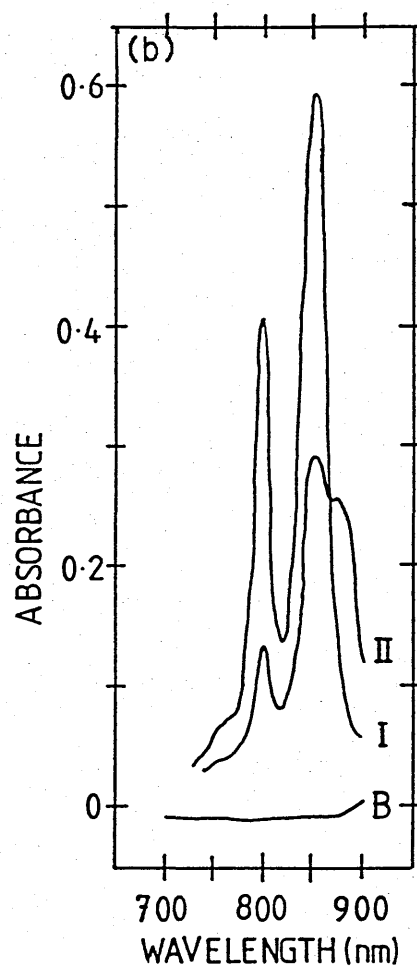
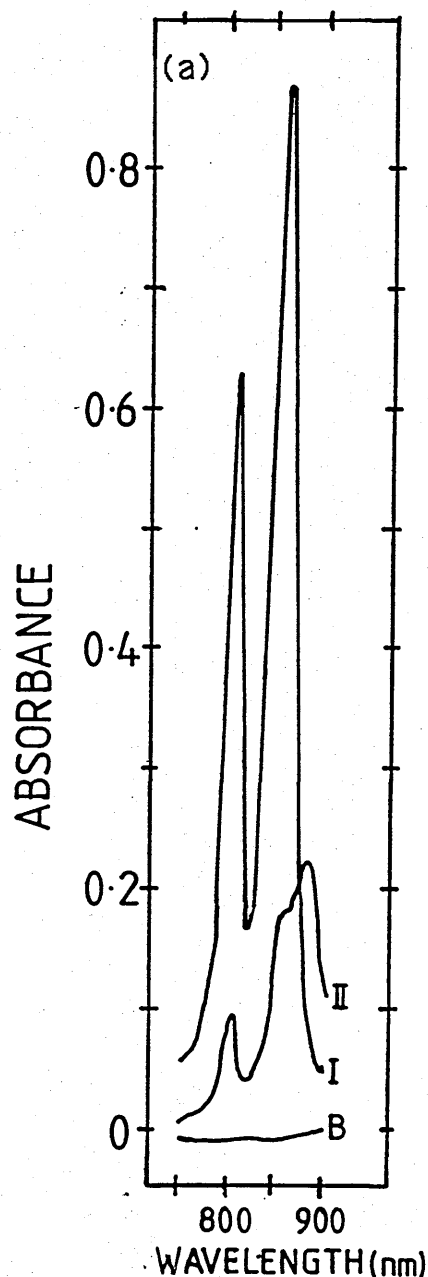


FIGURE 4.8 Solubilization of Photosynthetic Membranes of *Rb. sphaeroides* 2.4.1 in 1% (v/v) LDAO.

The fractionation of photosynthetic membranes of *Rb. sphaeroides* 2.4.1., solubilized with the detergent 1% (v/v) LDAO typically yields two fractions. The absorbance properties of the lower fraction, (I), are characteristic of pure B800-850 antenna complex. Spectral analysis of the second fraction (TOP), which banded at the top of the sucrose gradients, clearly showed that extensive denaturation had occurred. There was no evidence for the isolation, or enrichment, of the RC-B875 antenna complex.

The membranes were prepared as described in section 3.3 and resuspended in 10 mM Tris buffer, pH 8.0. Absorbance pathlength 1 cm.



(B - baseline)

FIGURE 4.9 (a & b) Detergent Solubilization of Photosynthetic Membranes of *Rb. sphaeroides* 2.4.1.

Figures 4.9 a and b present spectra of complexes isolated from membranes of *Rb. sphaeroides* 2.4.1. solubilized in (a) 0.5% (v/v) LDAO, and (b) 1% (w/v) N-octyl β -D-glucopyranoside. The complexes were isolated using the method described in section 3.6 and resuspended in 10 mM Tris-HCl, pH 8.0. It can be observed in both spectra, that although the B800-850 was successfully isolated (Band I), only enrichment of the RC-B875 antenna complex (Band II) was achieved. (Absorbance pathlength 1 cm).

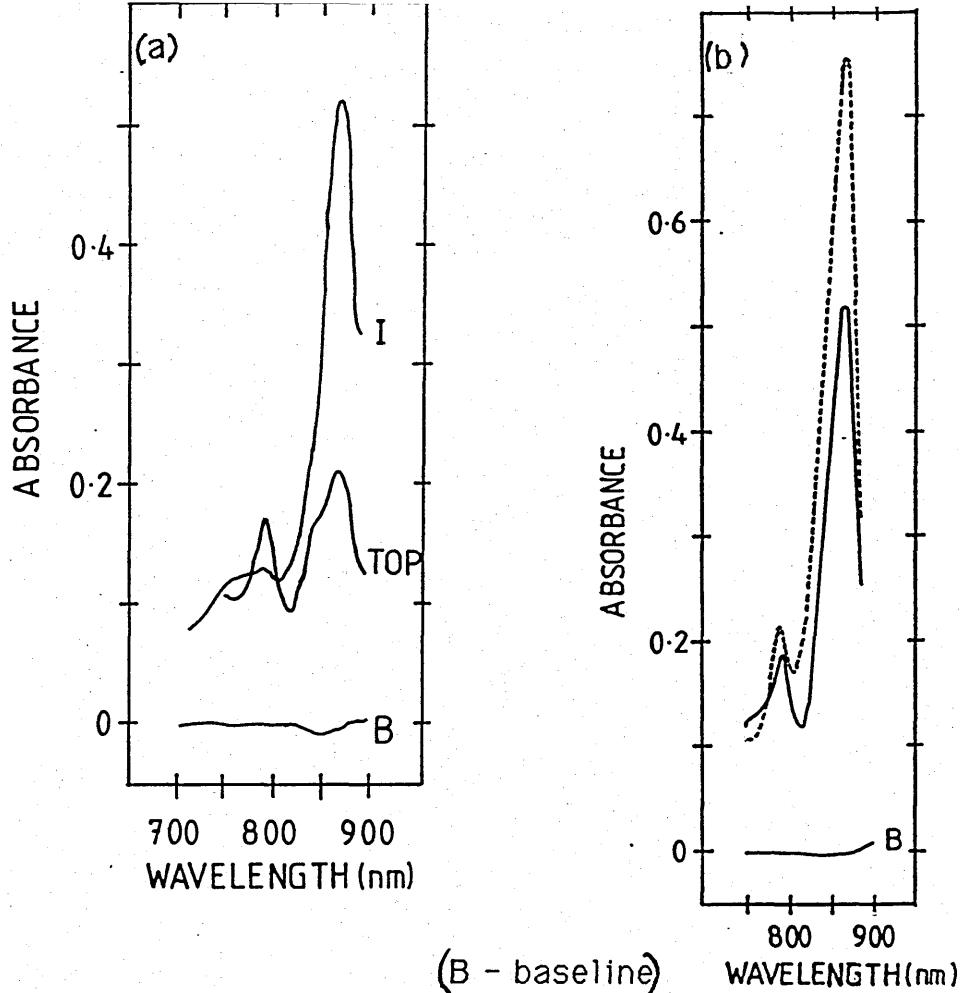


FIGURE 4.10 (a & b) Detergent Solubilization of Photosynthetic Membranes Isolated from *Rhodobacter sphaeroides* mutant strain M21.

Figure 4.10a presents spectra of complexes isolated from membranes of *Rhodobacter sphaeroides* M21 solubilized in 1% (v/v) LDAO in 10 mM Tris buffer, pH 8.0. and fractionated by centrifugation in sucrose density-gradients containing 0.2% (v/v) LDAO. The spectra reveal that partial isolation of the RC-B875 component was achieved (I), although mass denaturation was also evident (TOP).

The spectra presented in Figure 4.10 b illustrate the successful isolation of the RC-B875 complex from *Rhodobacter sphaeroides* M21 using the detergent 1% (w/v) LM for the solubilization of membrane preparations, and incorporating the detergents 0.2% (v/v) DDAO (—), or 0.2% (v/v) LDAO (---) in the sucrose gradients. Both sets of conditions generated spectrally pure RC-B875 antenna complexes.

Membranes were prepared as described in section 3.3 and resuspended in 10 mM Tris buffer, pH 8.0. (Absorbance pathlength 1 cm).

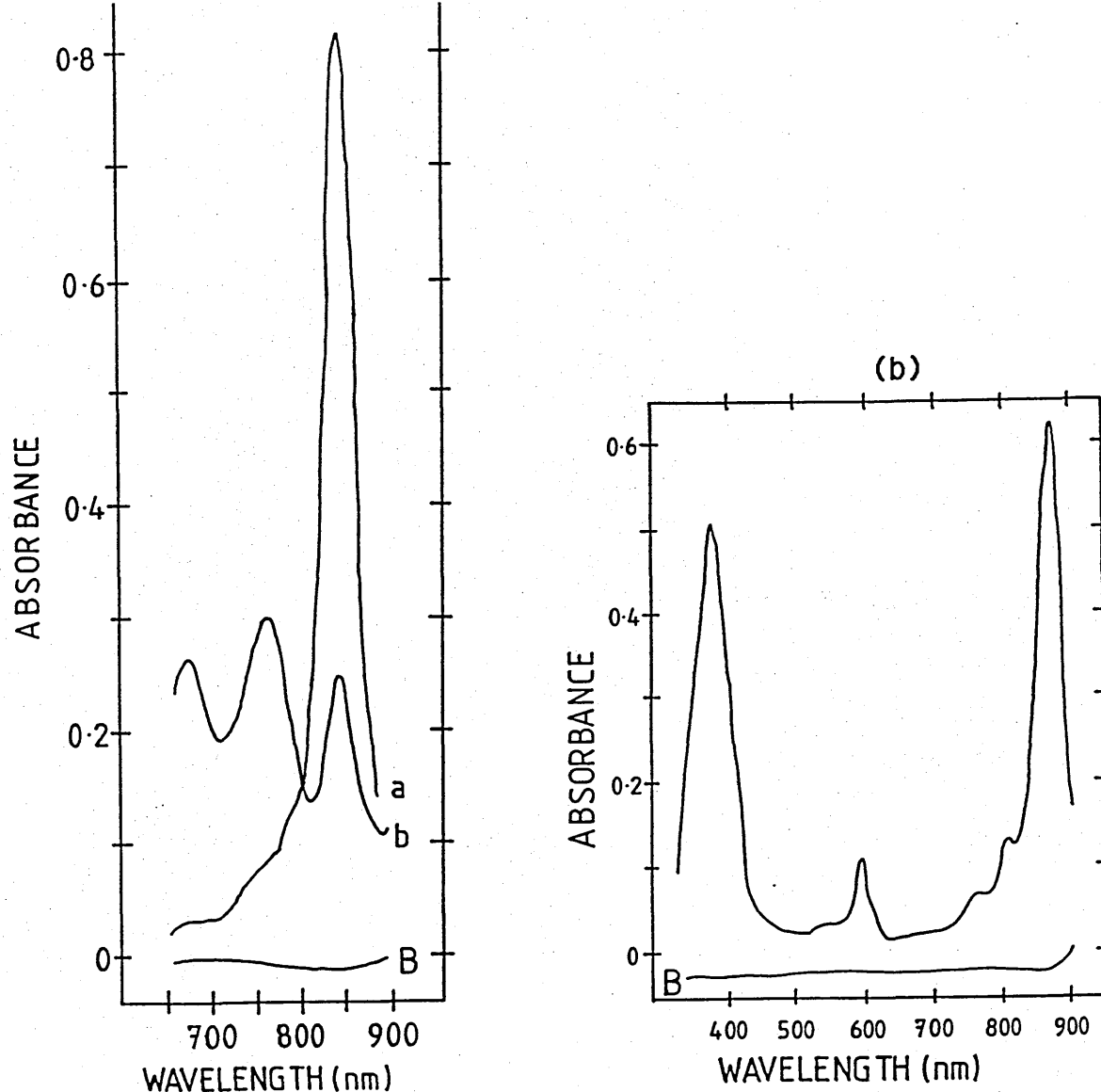


Figure 4.11 (a & b) Detergent Solubilization of Photosynthetic Membranes of *Rhodobacter sphaeroides* Mutant Strain R26.

Figure 4.11a presents spectra of components of the photosynthetic apparatus of *Rhodobacter sphaeroides* R26, isolated from membrane preparations solubilized in 1% (v/v) LDAO and fractionated on sucrose density-gradients containing the detergents (a) 0.2% LDAO or (b) 0.2% DDAO. These spectra show that LDAO employed for both solubilization and fractionation procedures results in extensive denaturation. Isolation is, however, improved if the detergent DDAO is employed in fractionation conditions.

Figure 4.11b illustrates that solubilization of photosynthetic membranes of *Rhodobacter sphaeroides* R26 with the detergent 1% (w/v) LM, and their fractionation on sucrose density-gradients containing 0.2% (v/v) DDAO, results in the successful isolation of the RC-B875 antenna complex.

Membranes were prepared as described in section 3.3 and resuspended in 10 mM Tris buffer, pH 8.0 (Absorbance pathlength 1 cm).

obtained where alternative detergents to those employed in solubilization were included in the sucrose density-gradients. Combinations of the detergents LDAO, DDAO, LM and OG were tested. The use of LDAO in both membrane solubilization and sucrose gradients resulted in extensive denaturation. By exchanging either the detergent in the gradient, or that used in solubilization, for a milder detergent, such as DDAO, LM or OG, denaturation was effectively reduced and spectrally pure RC-B875 components were generated (Figure 4.10b and Figure 4.11b). The use of mild detergents for both membrane solubilization and inclusion in the sucrose solutions resulted in a single, very disperse, lumpy band which produced light-scattering effects when examined spectrophotometrically.

Table 4.1 summarizes the optimum solubilization and fractionation conditions determined for each species examined:

TABLE 4.1

Summary of Optimum Solubilization Conditions

<u>SPECIES</u>	<u>DETERGENT</u>	<u>DETERGENT CONCENTRATION FOR:</u>	
	<u>TYPE</u>	<u>Solubilization</u>	<u>Sucrose gradient.</u>
<i>Rps.acidophila</i> 7050	LDAO	1.0%	(0.2% LDAO)
<i>Rps.acidophila</i> 7750	LDAO	1.0%	(0.2% LDAO)
<i>Rc.gelatinosus</i> 149	LDAO	0.5%-1.0%	(0.2% LDAO)
<i>Rc.gelatinosus</i> 151	LDAO	0.5%-1.0%	(0.2% LDAO)
<i>Rps.palustris</i> 'DSM8252'	LDAO	0.75%	(0.2% LDAO)
<i>Rps.palustris</i> 'French'	LDAO	0.75%	(0.2% LDAO)
<i>Rps.blastica</i>	LDAO	0.5%	(0.2% LDAO)
<i>Chromatium vinosum</i> D	LDAO	0.5%-1.0%	(0.2% LDAO)
<i>Rs.rubrum</i> S1	LDAO/LM	0.5%/1.0%	(0.2% LDAO)
<i>Rb.sphaeroides</i> R26	LM/OG	1.0%	(0.2% DDAO)
<i>Rb.sphaeroides</i> M21	LM/OG	1.0%	(0.2% DDAO)
<i>Rb.sphaeroides</i> 2.4.1.	OG	1.0%	(0.2% DDAO)

Table 4.1 above, summarizes the conditions optimized for the detergent solubilization of photosynthetic membranes. The 'optimal' detergent type and its 'optimal' concentration, in both solubilization and in fractionation procedures, were determined for each species considered.

4.2 The Parameters of the Sucrose Density-Gradients.

The gradient of sucrose concentration, in conjunction with speed and period of centrifugation, governs the fractionation of solubilized material. The parameters of the sucrose gradient are, however, influenced to some extent by the choice of detergent used for solubilization, the type and size of centrifuge tubes (and hence the rotor head) and the extraction method employed. The detergent SDS requires a sucrose density gradient ranging from 1.5M down to 0.5M sucrose, whereas the other detergents used require a gradient ranging between 1.2M and 0.3M concentrations. Isolation of fractionated bands using the ISCO-density gradient fraction collector requires gradients to be prepared in straight-sided centrifuge tubes of the type compatible with the Sorvall AH 651 and TST 41.14 swing-out rotor heads. The rotor head dictates the speed of centrifugation and hence must also govern the centrifugation period required for successful fractionation to be achieved.

Two types of sucrose gradient were prepared (1) Linear gradient, which represents a continuous gradient of sucrose ranging from maximum to minimum sucrose concentrations, or (2) Step gradient, where discrete bands of sucrose are layered on top of each other to form a discontinuous gradient of sucrose ranging from high to low concentrations. By increasing the number of concentration steps within a gradient and thus effectively reducing the concentration difference between adjacent steps, the step gradient can approximate to a linear gradient. Both of these methods were employed and the fractionation results from each were analysed to examine which method provided the better resolution of fractionated bands. The gradients consisted of:

- (a) A linear gradient of sucrose ranging from 0.6M-0.3M

concentrations.

- (b) Equivolume step gradients consisting of 0.6M and 0.3M sucrose.
- (c) Equivolume step gradients consisting of 0.4M and 0.2M sucrose.
- (d) Equivolume step gradients consisting of 0.6M, 0.4M, 0.3M and 0.2M sucrose.

The gradients, loaded with a sample of *Rhodopseudomonas acidophila* 7750 membrane solubilized in 1% LDAO, were centrifuged in the AH 651 swing-out rotor at $97\,000 \times g$ for twenty hours and then fractionated using the ISCO-density gradient fraction collector. Absorption at 280nm was monitored continuously during the fractionation process, and each fraction was analysed for its absorption at 800nm and 880nm. Whole absorption spectra, from 350nm to 900nm, of fractions representative of peak absorptions at 800nm and 880nm were also recorded. It appears from the absorbance recordings monitored at 280nm, that band resolution is greater in the continuous gradients, or those approximating to a linear gradient. Despite this apparent difference in resolution qualities, subsequent spectral analysis of each fraction revealed no significant differences in the purity of components isolated from each gradient. Figure 4.12 shows absorption at 280nm as it was monitored throughout the 0.6:0.4:0.3:0.2M sucrose density-gradient. This absorption pattern, revealing two distinct absorption peaks, was typical of each gradient-type examined. By measuring the optical density of each equivolume fraction, at 800nm and at 880nm, it can be seen that fractions corresponding to the two different 280nm absorption peaks possess different absorption properties with respect to their relative absorption at 800nm and 880nm (Figure 4.13 (a-d)). Fractions corresponding to peak 1 showed a relatively high ratio of

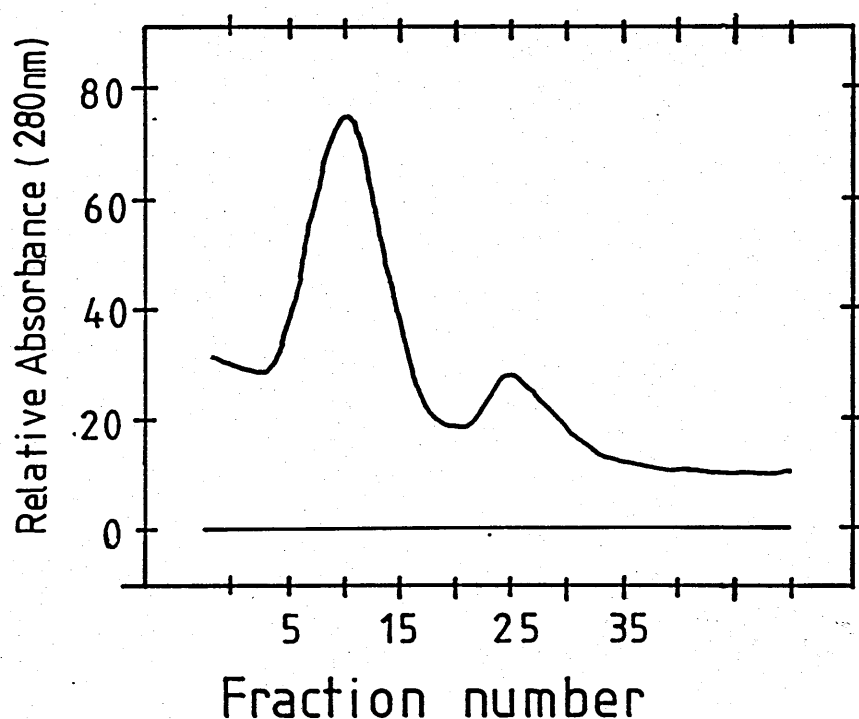


FIGURE 4.12 Monitoring the Fractionation of Bands Isolated From Sucrose-Density Gradients.

A membrane sample of the species *Rhodopseudomonas acidophila* 7750 was solubilized in 1.0% (v/v) LDAO and fractionated by sucrose density-gradient centrifugation. Two bands were visible in the gradient post centrifugation. The gradients were fractionated into equivolume aliquots (0.5 ml) using an ISCO-density-gradient fraction collector. The fraction collector, also equipped with an ISCO UA-5 absorbance monitor, recorded the absorbance, at 280 nm, of the gradient as it was being fractionated. A cross-sectional picture of the sucrose gradient, in terms of relative absorbance at 280 nm, was therefore produced; an example of which is presented above. The two peaks typically observed provide an indication of the resolution quality of the bands in the gradient and more importantly indicate which fractions are representative of each band.

FIGURE 4.13 (i - iv) Absorbance Properties of Fractions Isolated from each of the Four Different Gradient Preparations.

The parameters of sucrose concentration, relative sucrose volumes and type of gradient, were modified in an attempt to examine their effect on the quality of fraction resolution. Resolution quality was subsequently examined by comparing the absorbance properties of fractions isolated from each gradient preparation using the ISCO-density-gradient fraction collector. Four different gradient preparations were examined and compared, these consisted of:

(i) 0.6 M - 0.3 M Linear gradient.

(ii) 0.6 M / 0.3 M Equivolume step gradient.

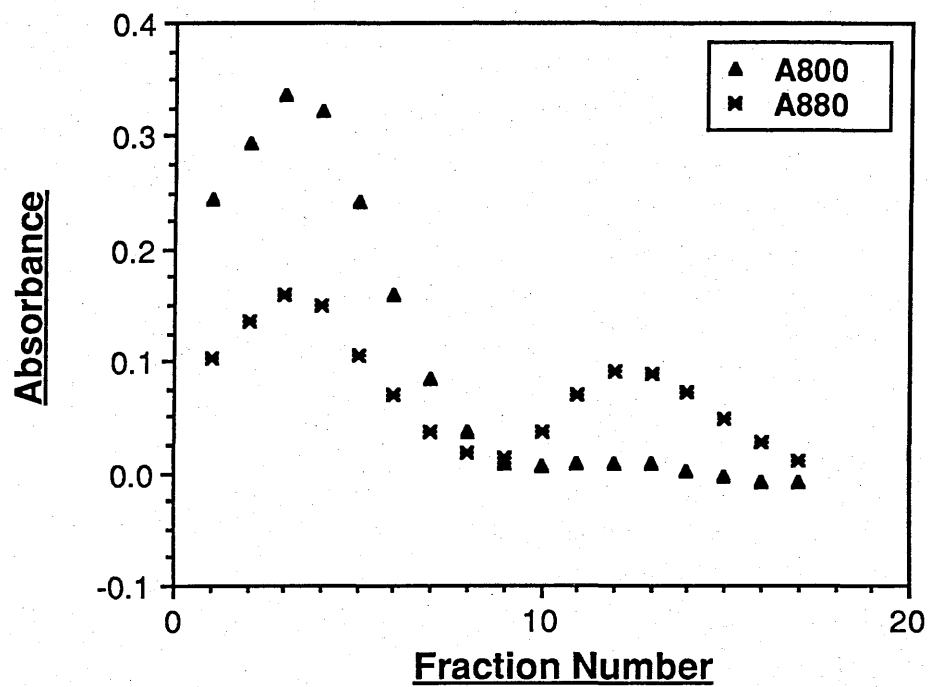
(iii) 0.4 M / 0.2 M Equivolume step gradient.

(iv) 0.6 M / 0.4 M / 0.3 M / 0.2 M Equivolume step gradient.

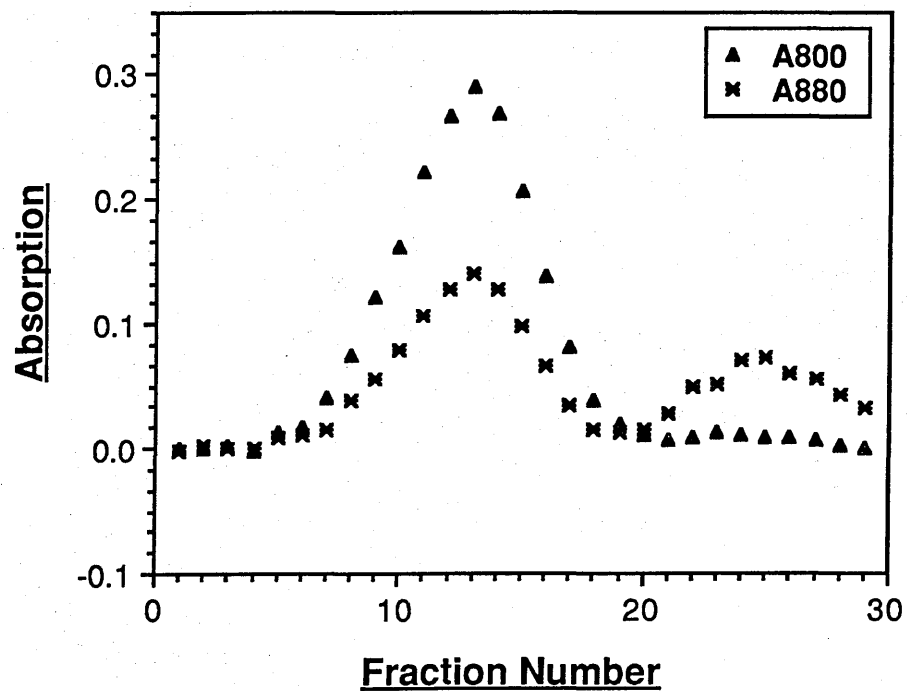
Equivolume fractions (0.5 ml) collected from each gradient and diluted to 3 ml with 10 mM Tris-HCl, pH 8.0, were measured for their absorbance at 800 nm (\blacktriangle) and at 880 nm (\ast) (Absorbance pathlength 1 cm). Each figure shows that fractions removed from high-up in the gradient (corresponding to the first 280 nm absorbance peak shown in Figure 4.12) exhibited a greater relative absorbance at 800 nm to that at 880 nm than those fractions corresponding to the second 280 nm absorbance peak i.e. those fractions isolated from the lower half of the gradient which showed little, or no, absorbance at 800 nm.

It can be observed by comparing the four figures that each gradient preparation was observed to yield fractions with comparable absorbance properties.

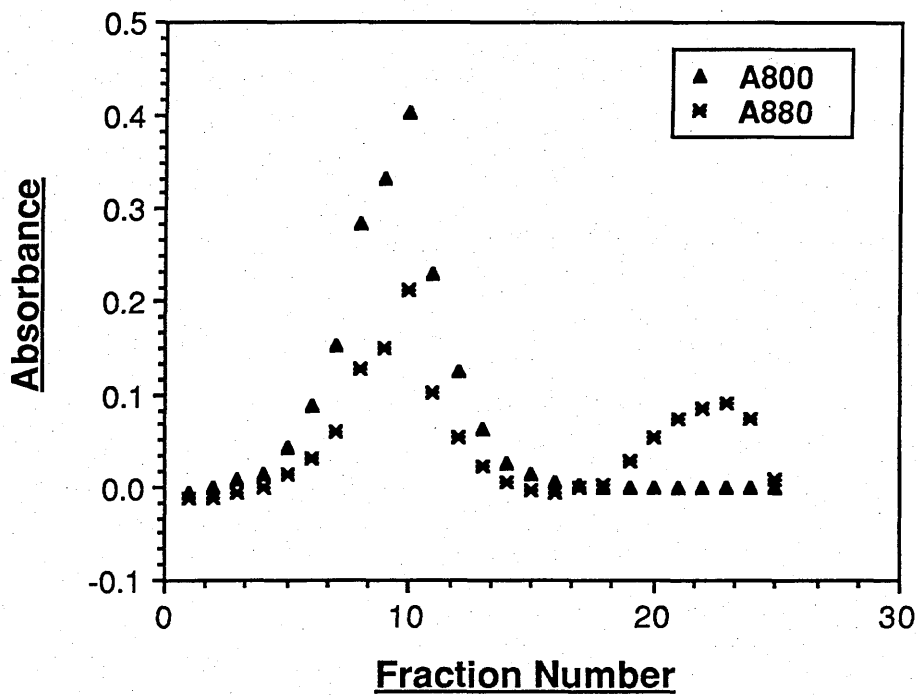
Fractionation on a 0.6-0.3M Linear Gradient



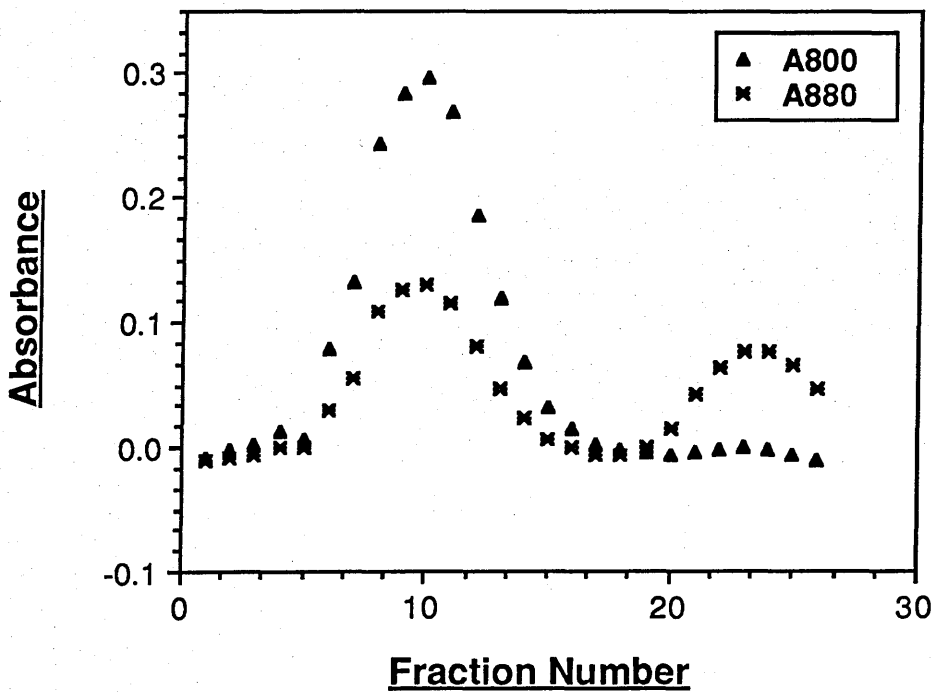
Fractionation on a 0.6M:0.3M Step Gradient



Fractionation on a 0.4/0.2M Step Gradient



Fractionation on a 0.6/0.4/0.3/0.2M Step Gradient



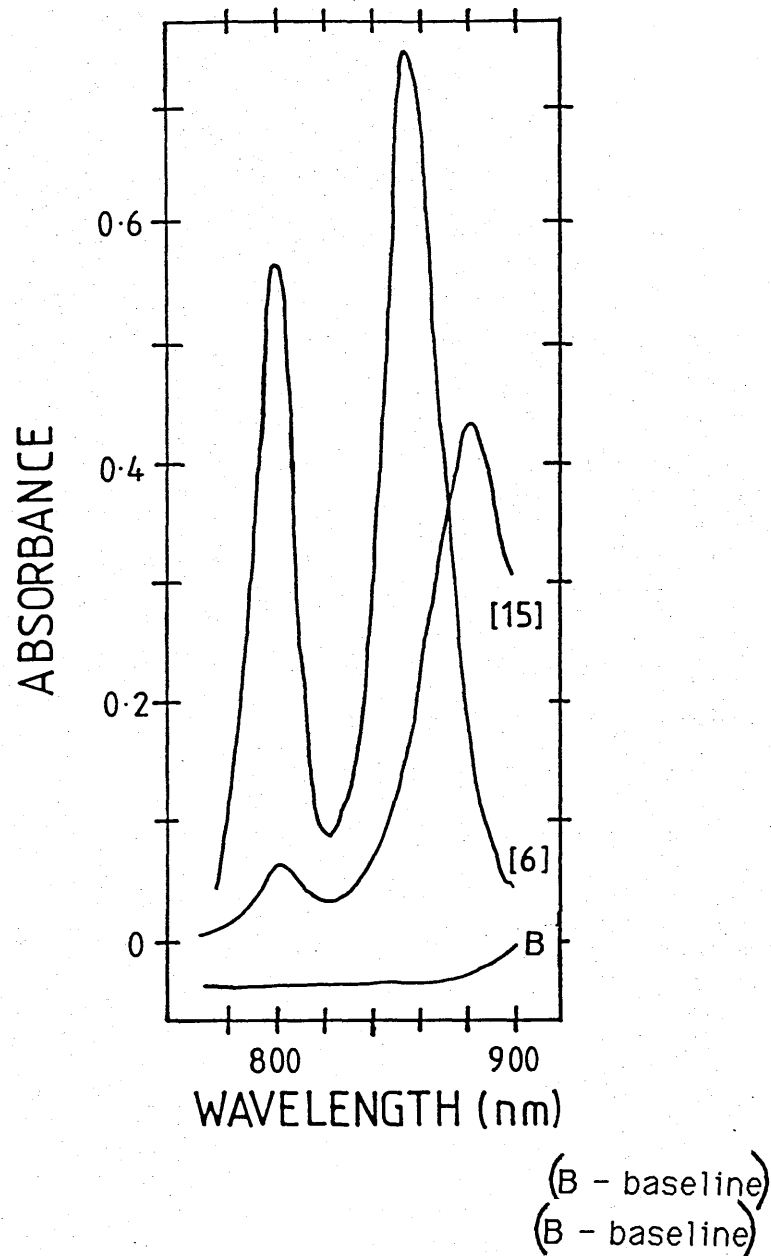


FIGURE 4.14 Absorbance Spectra of those Fractions Showing Peak Absorption Properties at 800 nm and at 880 nm.

Absorption spectra were recorded for those fractions observed in Figures 4.13 (I-IV) showing peak absorbance at 800 nm, and 880 nm. The spectra shown above were recorded for fractions (6) and (15) isolated from the 0.6 M - 0.3 M linear gradient preparation (Figure 4.13 I).

It can be observed from these absorption spectra, that the two fractions [(6) and (15)] have spectral properties typical of the B800-850 and RC-B875 antenna complexes respectively. The spectra shown above are typically representative of 'peak fractions' isolated from each gradient examined. There were no apparent differences observed in the spectral purity of fractions isolated from each gradient.

800:880 nm absorbance and fractions corresponding to the second, smaller peak, showed the converse absorbance ratio ie. having a relatively low 800:880 nm absorbance ratio. The absorption spectra, from 350nm to 900nm, of fractions from each gradient preparation corresponding to peak 800nm and 880nm absorption were also recorded (Figure 4.14). These spectra were characteristic of the different spectral components constituting the photosynthetic apparatus, ie. the first fraction maxima, Fraction I, produced a spectrum typical of purified B800-850 antenna complex, whereas Fraction II exhibits a spectrum characteristic of RC-B875 complex. In summarizing this section it can be concluded that spectrally pure fractions can be obtained irrespective of the 'type' of gradient preparation. However, to ensure this was not simply a consequence of the fractionation method employed, the experiment was repeated with respect to gradient preparations although this time the bands were removed by manual fractionation ie. careful removal using a pasteur pipette. Analysis of these bands showed them to be spectrally pure. As a result of these experiments, routine fractionations were carried out on equivolume step gradients and bands were carefully removed by manual fractionation. Sucrose gradients were centrifuged in the T865 fixed-angle rotor at $197\,000 \times g$ for approximately 16 hours. The procedure generally produced good, spectrally pure fractions. On occasion, however, band resolution was finely attuned by the simple modification of relative sucrose-density volume ratios. This provided sufficient adjustment to account for variations in band resolution due to differences existing between batches of membrane preparations from the same, or from different, species.

TABLE 4.3

Summary of NIR absorption maxima of RC-B875 antenna
complexes determined at room and low temperatures.

<u>SPECIES</u>	<u>ABSORBANCE (nm)</u>		
	<u>270K</u>	<u>110K</u>	<u>10K</u>
<i>Rps.palustris</i> 'French'	806,885	756,806,895	756,806,897
<i>Rps.palustris</i> 'DSM'	752,804,879	804,893	756,804,894
<i>Rc.gelatinosus</i> 149	804,881	802,891	801,891
<i>Rc.gelatinosus</i> 151	801	799	801
<i>Rps.blastica</i>	801	752,799	754,799,
<i>Rs.rubrum</i> S1	804,879	803,889	804,891
<i>Rps.acidophila</i> 7050	799,887	801,986	801,898
<i>Rps.acidophila</i> 7750	799,891	799,902	801,902
<i>Rb.sphaeroides</i> R26	758,806,872	758,804,883	756,804,887

Absorbance spectra of RC-B875 antenna complexes isolated from a range of BChl a-containing purple bacterial species were recorded at 270 K, 110 K and 10 K . The table above summarizes the wavelengths (within the NIR region of the spectrum) corresponding to absorbance peaks for each species at each of the temperatures 270 K, 110 K and 10 K.

4.3 Spectral Analysis of RC-B875 and B800-850 Antenna Complexes.

Spectral analysis of the RC-B875 antenna conjugate was kindly completed by J. Ullrich at the Physics Institute, University of Stuttgart, W.Germany. Using a Cary 14 spectrophotometer the room temperature (270K) and low temperature (110K and 10K) absorption spectra were recorded. Room temperature and low temperature emission and action spectra were also recorded on apparatus similar to that illustrated in Figure 3.1. Figures 4.15(a,b & c) show typical absorption spectra representative of the three spectral types of purple bacteria ie. Type I (*Rhodobacter sphaeroides* R26), Type II (*Rhodocyclus gelatinosus* 149) and Type III (*Rhodopseudomonas palustris* 'French') respectively. Table 4.3 summarizes, for each species, the wavelength corresponding to peak absorption bands at each temperature investigated. The absorption spectra of the RC-B875 antenna conjugate of each species exhibit characteristic peaks at 380nm, 590nm and 880nm which arise from the Soret and the Q_x and Q_y absorption bands of bacteriochlorophyll *a* respectively. At 800nm, reaction centre absorption produces a fourth characteristic peak. The absorption spectra of *Rhodopseudomonas palustris* 'French' and *Rhodocyclus gelatinosus* 149 also display absorption peaks in the spectral range 440nm to 570nm due to carotenoid absorption. *Rhodobacter sphaeroides* R26 however, is a carotenoidless mutant and consequently does not exhibit absorption peaks over this range. Reducing the temperature has the effect of sharpening the absorption peaks and in the NIR region of the spectrum, of shifting peaks slightly towards the red. This is particularly apparent with the Q_y absorption peak at 880nm. At low temperatures, the absorption spectra of *Rhodopseudomonas palustris* 'French' and

FIGURE 4.15 (a, b & c) Absorption Spectra Recorded at Room and at Low Temperatures of the RC-B875 Antenna Complex Isolated From the Species *Rhodobacter sphaeroides* R26, *Rhodocyclus gelatinosus* 149 and *Rhodopseudomonas palustris* 'French'.

Absorbance spectra were recorded for each sample at the temperatures (T) 270 K, 110 K and 10 K using a Cary 14 spectrophotometer within the spectral range 350 – 920 nm (λ). The RC-antenna complex from each species was isolated by sucrose density-gradient fractionation of detergent solubilized membranes. The isolated complexes were then concentrated on DE52 columns and eluted with salt buffer (250 mM NaCl in Tris-HCl, pH 8.0) containing 0.1% (v/v) LDAO. The concentrated samples were then diluted with glycerol buffer (70% (v/v) glycerol:30% 10 mM Tris-HCl, pH 8.0) in order to maintain a clear glass at low temperatures.

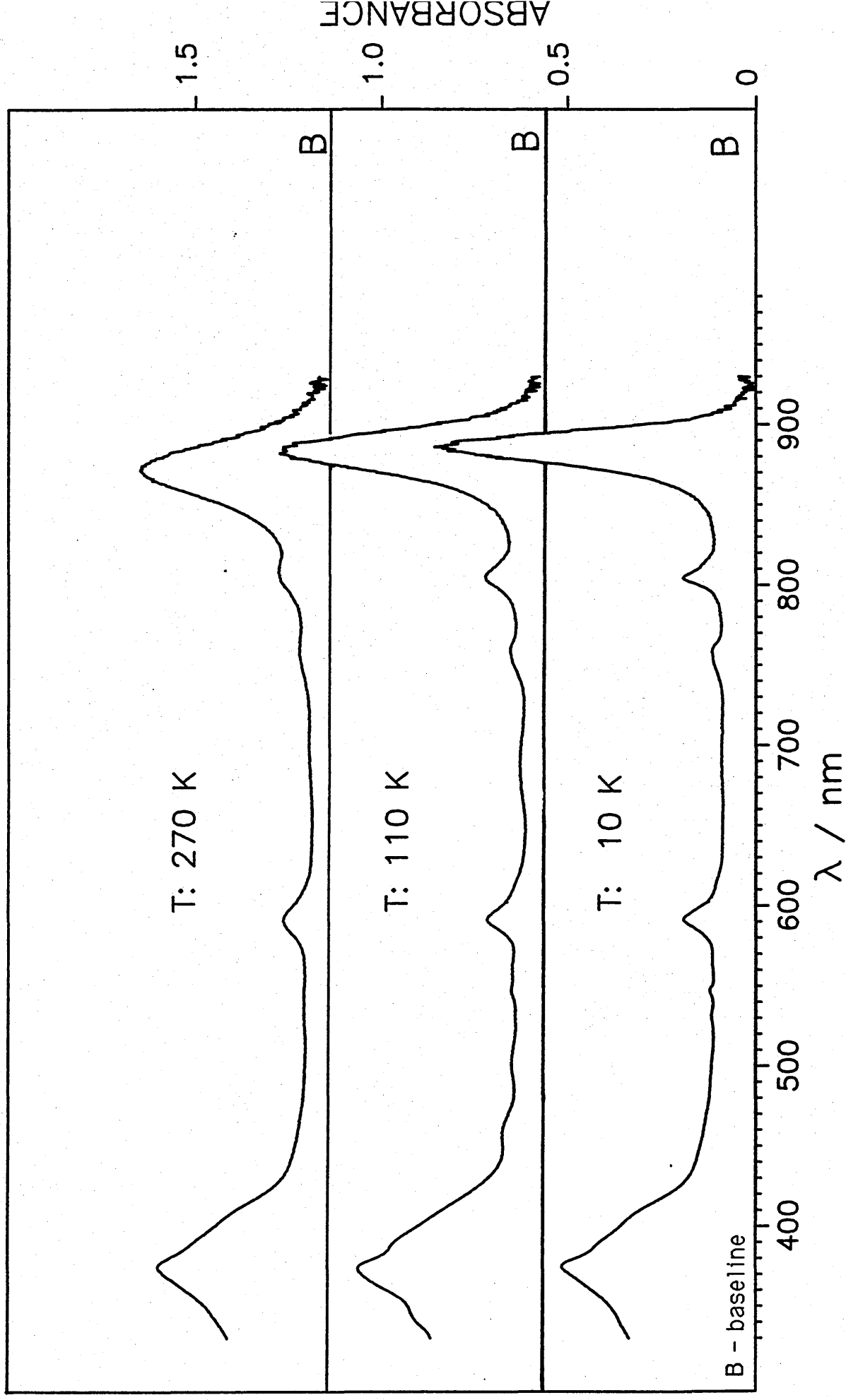


FIGURE 4.15a Absorption Spectra Recorded at Room and at Low Temperatures for the RC-B875 Antenna Complex of *Rh. sphaeroides* R26.

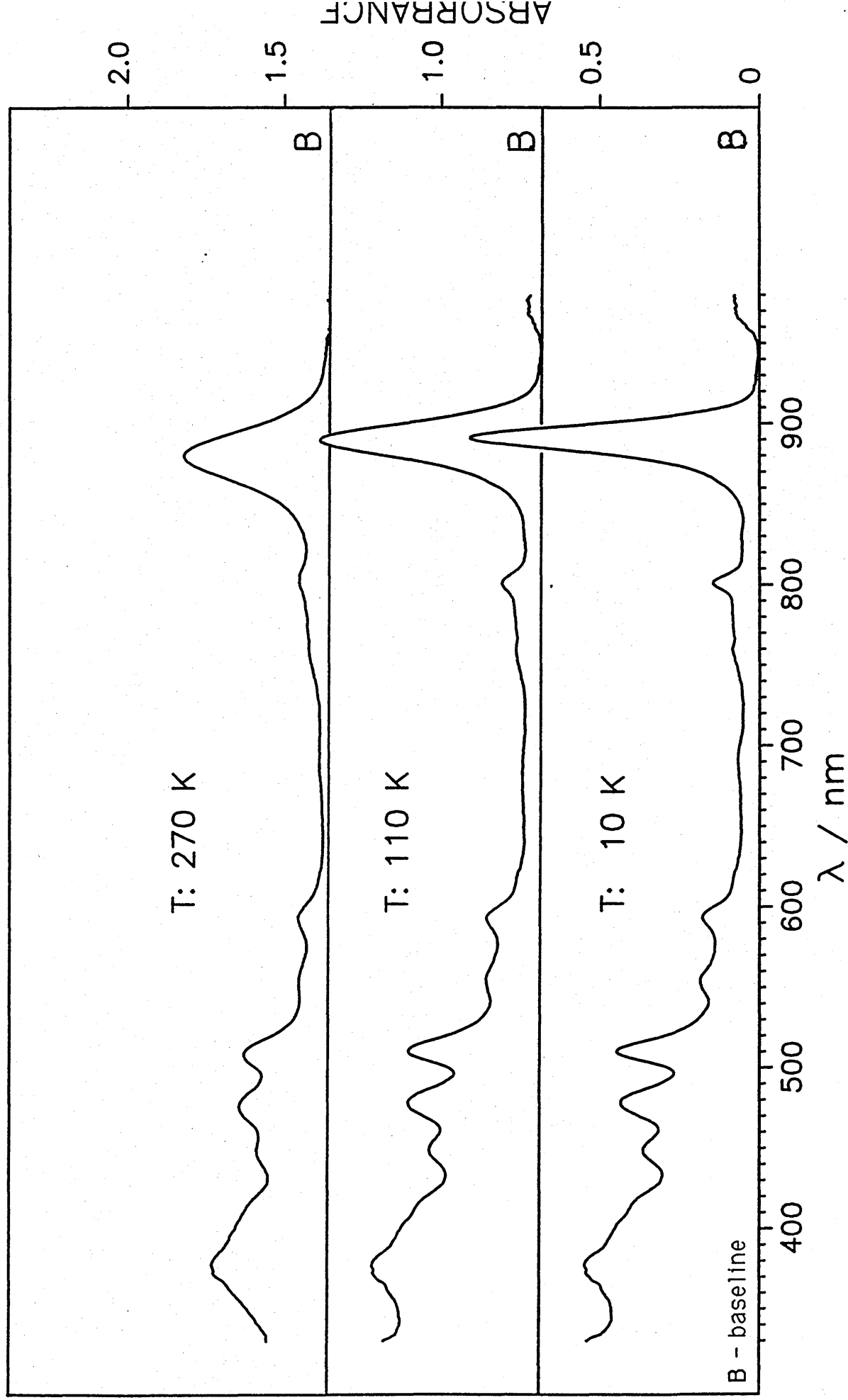


FIGURE 4.15b Absorption Spectra Recorded at Room and at Low Temperatures for the RC-B875 Antenna Complex of *R. gelatinosus* 149.

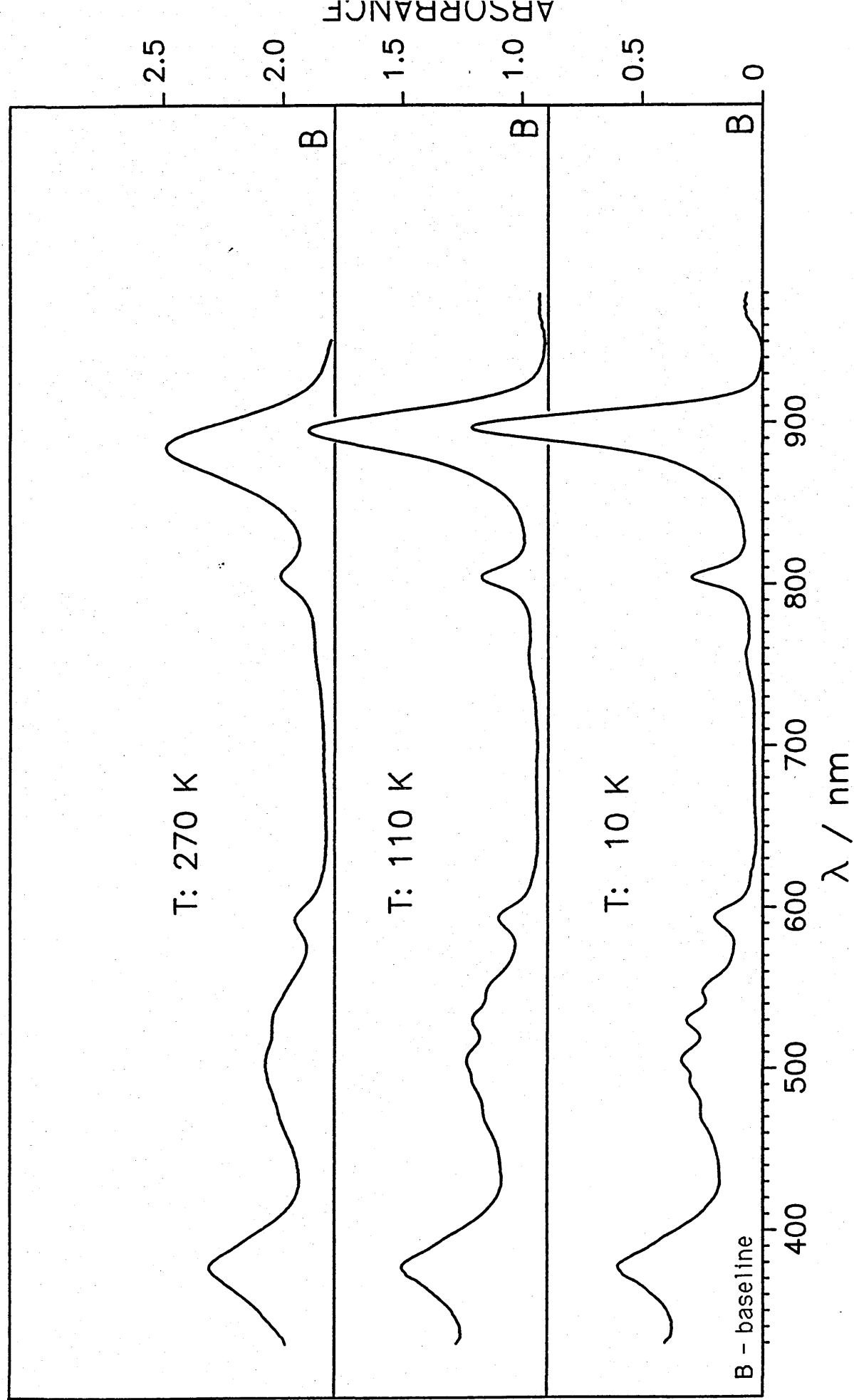


FIGURE 4.15c Absorption Spectra Recorded at Room and at Low Temperatures for the RC-B875 Antenna Complex of *Rps. palustris* French.

'DSM8252' also reveal a shoulder at 870nm which is due to the absorption of the reaction centre 'special pair' of bacteriochlorophylls [Clayton, 1980]. Low temperature absorption spectra also often reveal a small peak at 752nm which is due to reaction centre bacteriopheophytin absorption [Prince and Thornber, 1977].

In summarizing this chapter, it can be said that the method of detergent solubilization and sucrose density-gradient fractionation is useful in providing spectrally pure samples of the different components constituting the photosynthetic apparatus. Examination of their spectral properties confirms their purity and their spectral integrity. Further investigations concerning the nature of the RC-B875 antenna conjugate are discussed in the following chapters.

CHAPTER 5

Determination of the Ratio of Bacteriochlorophyll a to Reaction Centre Molecules in the Isolated RC-B875 Antenna Conjugates.

Evidence from a number of studies [(Aagaard and Sistrom, 1972)(Firsow and Drews, 1977)(Hayashi *et al*, 1982)(Lien and Gest, 1973)], suggests that the B875 antenna complex is associated with the reaction centre in a fixed stoichiometric ratio. These studies, although varying in experimental design, have tended to consider a small number of different species. Determinations of this ratio were, therefore, made for the RC-B875 antenna complex isolated from a wide range of BChl *a* - containing species of purple bacteria.

The concentration of reaction centre molecules was determined from the absorption changes occurring upon chemical oxidation of the reaction centre. Figures 5.1 - 5.4 present oxidation-reduction difference spectra for the species *Rhodopseudomonas palustris* 'DSM8252', *Rhodobacter sphaeroides* R26, *Rhodopseudomonas blastica*, and *Rhodobacter sphaeroides* M21 respectively. These represent typical examples of the difference spectra obtained for each species examined. The various line spectra are: (i) the baseline; both sample and reference cuvettes contain sample of an equal concentration. (ii) Oxidation-reduction difference spectra; addition of sodium ascorbate to fully reduce the reference cuvette, and potassium ferricyanide addition to oxidize the sample, produces these characteristic difference spectra: reduction of the RC 'special pair' of BChl *a* molecules results in the reduction of absorption at 870nm, a spectral change which is also reflected in

the blue shift occurring at 800nm (which gives rise to increased absorption at 789nm and reduced absorption at 909nm). Measurement of this spectral shift provides a more reliable estimate of the RC concentration than bleaching occurring at about 870nm, which may also reflect the irreversible oxidation of light-harvesting bacteriochlorophyll a. Potassium ferricyanide is, therefore, added to the sample cuvette until there are no further changes in the spectral shift at 800nm. To ensure that irreversible bleaching has not occurred, a final addition of sodium ascorbate is made to the sample cuvette. In the absence of irreversible bleaching, a response characteristic of those shown in Figures 5.1b - 5.4b is produced.

The concentration of total bacteriochlorophyll a was determined from sample absorption at its NIR absorption maximum, at approximately 875nm (Figure 5.1a - 5.4a).

The mean ratio of these values ie. the mean concentration of RC:total BChl a was determined for each species considered, and are presented in Table 5.1 (col. 1; pp 82). Observation of these mean values reveals a fairly large amount of variation (as indicated by the standard deviation) about the mean values. In calculating the standard deviation, a normal distribution of sample values is assumed; it can be seen in Figures 5.5 a-j, illustrating the distribution of ratio values, that a normal distribution is evident for most species examined: the low standard deviation calculated for *Rps.palustris* 'French' and *Rps.blastica*, is illustrated in Figure 5.5a & b respectively., by the very narrow normal distribution of values, with a mode value approximating to that of the mean. The species *Rps.acidophila* 7750 (Figure 5.5c) and *Rc.gelatinosus* 151 (Figure 5.5d) show a similar, although a slightly wider, normal distribution, which also reflects the slightly larger standard deviation. The large standard deviation

FIGURES 5.1 - 5.4 Determination of the RC:BChl *a* Ratio.

The following Figures, 5.1 (a & b) - 5.4 (a & b) present typical absorption spectra (a), and the corresponding oxidation - reduction difference spectra (b) for the species *Rhodopseudomonas palustris* 'DSM8252' (Figure 5.1), *Rhodobacter sphaeroides* R26 (Figure 5.2), *Rps. blastica* (Figure 5.3) and *Rhodobacter sphaeroides* M21 (Figure 5.4). Referring to the oxidation-reduction difference spectra recorded for each species, B represents the baseline recording, and the line spectra a, b, c...etc. represent successive additions of potassium ferricyanide to the sample cuvette. Potassium ferricyanide was added until complete oxidation of the RC was achieved ie. there were no further changes in the intensity of the spectral shift centred at 800 nm. The point of complete oxidation was also indicated by spectral bleaching observed at approximately 870 nm; a slight shift of this band towards the red is indicative of the irreversible bleaching of light-harvesting BChl *a*. To ensure that oxidation reversibility had been maintained ie. there had been no oxidation of LH BChl *a*, a final addition of ascorbate was made to the sample cuvette; this effectively reduces the RC molecules, and thus should, in the absence of irreversible bleaching, eliminate the spectral changes observed at 800 nm and 870 nm.

The concentration of RC molecules was determined from the spectral shift observed at 800 nm using the extinction coefficient $\epsilon_{800} = 133.\text{mM}^{-1}.\text{cm}^{-1}$ (the largest shift value, representative of reversible oxidation, was used for this determination).

The concentration of BChl *a* molecules was determined from the absorption recorded for the RC-B875 complex. The absorption maximum, observed at approximately 880 nm, was used in association with the extinction coefficient, $\epsilon_{880} = 120.\text{mM}^{-1}.\text{cm}^{-1}$. (Absorbance pathlength 1 cm).

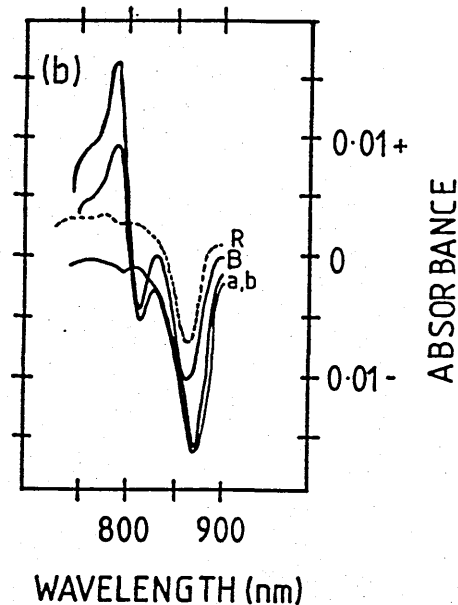
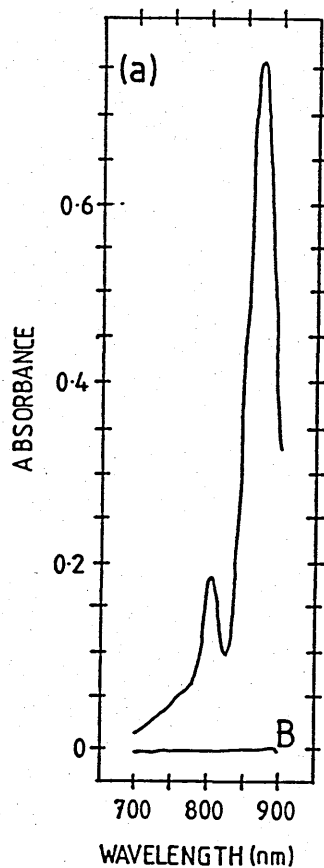


Figure 5.1 (a & b) presents a typical absorption spectrum (a) and corresponding oxidation-reduction difference spectrum (b) of the species *Rps. palustris* 'DSM8252'. The RC:Bchl a ratio value is calculated as 1:22.

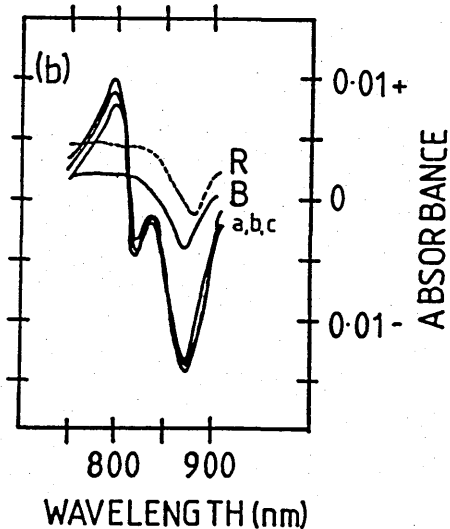
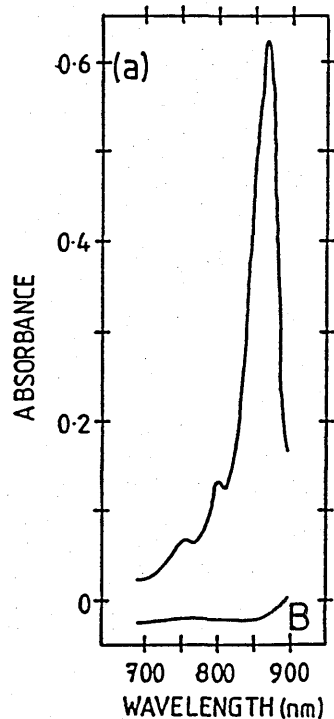


Figure 5.2 (a & b) presents a typical absorption spectrum (a) and corresponding oxidation-reduction difference spectrum (b) of the species *Rb. sphaeroides* R26. The RC:Bchl a ratio value is calculated as 1:25.

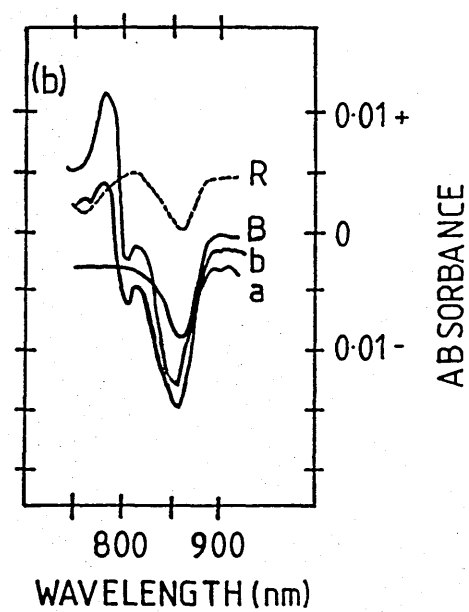
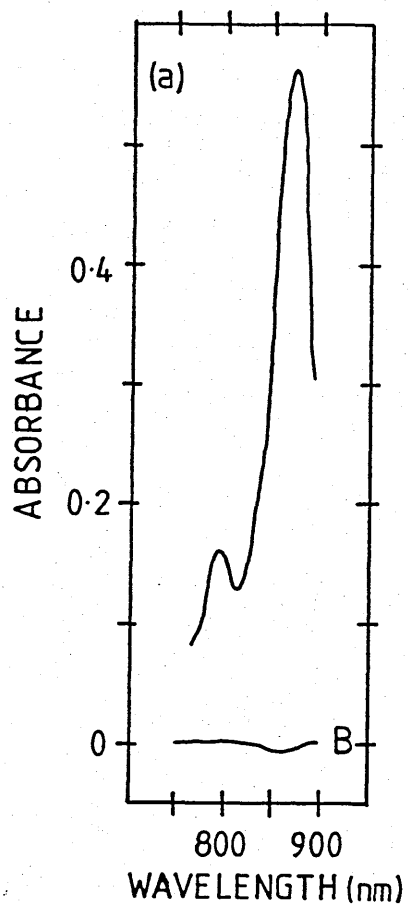


Figure 5.3 (a & b) presents a typical absorption spectrum (a) and corresponding oxidation-reduction difference spectrum (b) of the species *Rps. blastica*. The RC:BChl α ratio value is calculated as 1:22.

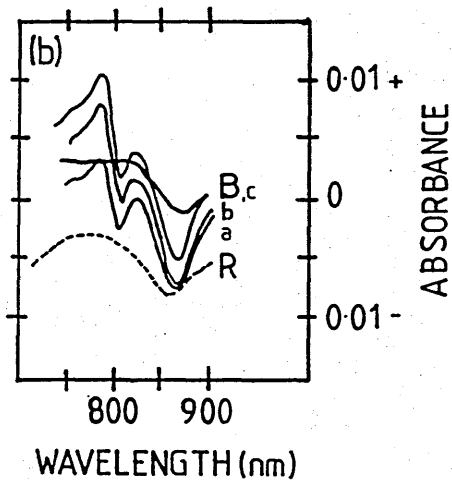
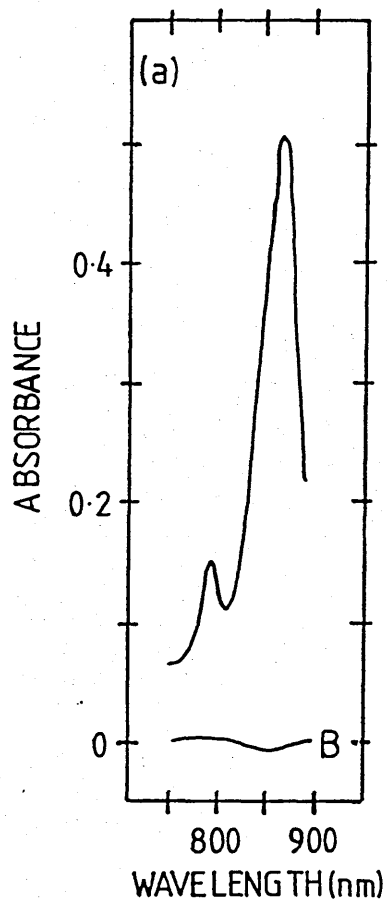


Figure 5.4 (a & b) presents a typical absorption spectrum (a) and corresponding oxidation-reduction difference spectrum (b) of the species *Rb. sphaeroides* M21. The RC:BChl α ratio value is calculated as 1:31.

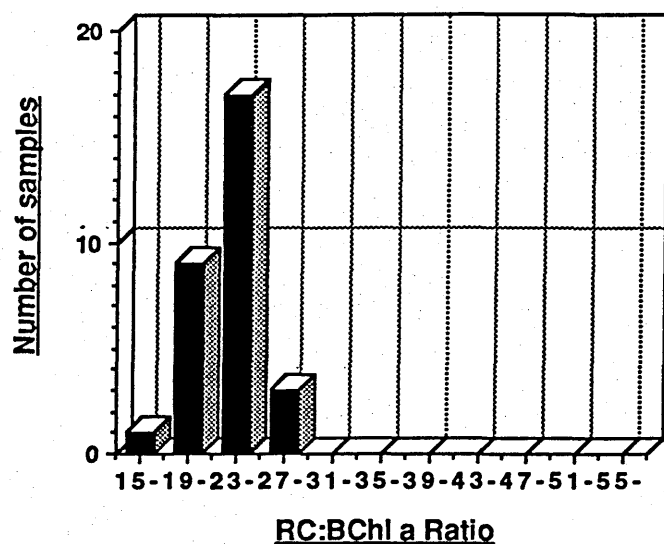
FIGURE 5.5 (a - j) Bar Charts Illustrating the Distribution of RC:BChl a Ratio Values Determined for the RC-B875 Antenna Complex Isolated from a Range of Purple Bacterial Species.

Each chart figure illustrates the spread of measured RC:BChl a ratio values determined for a particular species. The 'RC:BChl a ratio size' on the abscissa of each chart refers to the ratio value determined for a particular sample. The number of samples (ordinate) indicates the number of independent samples having a ratio value within a specific ratio range.

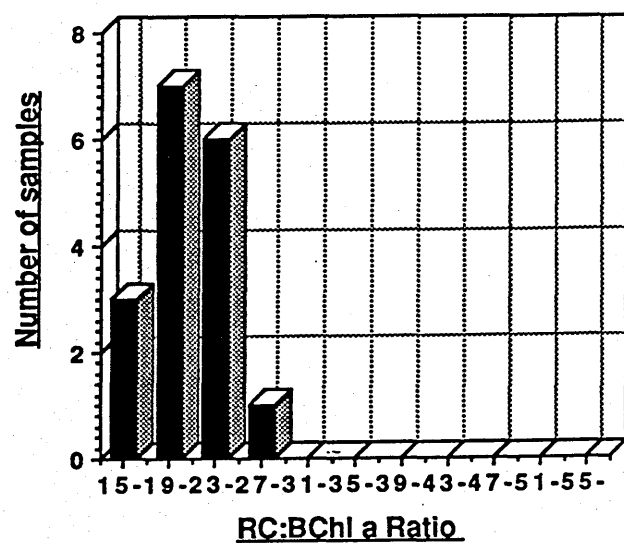
The RC concentration was determined from the oxidation-reduction difference spectra of each sample using the extinction coefficient, $\epsilon_{800} = 133.\text{mM}^{-1}.\text{cm}^{-1}$. The BChl a concentration was determined from the absorption spectrum recorded for each sample, using the extinction coefficient, $\epsilon_{880} = 120.\text{mM}^{-1}.\text{cm}^{-1}$.

It can be observed from these figures that the ratio values determined for most species examined, have a spread approximating to that of a normal distribution, and, for each species, a modal ratio value range can be recognized. (The mean ratio value determined for a particular species is indicated (within brackets*) in each figure.

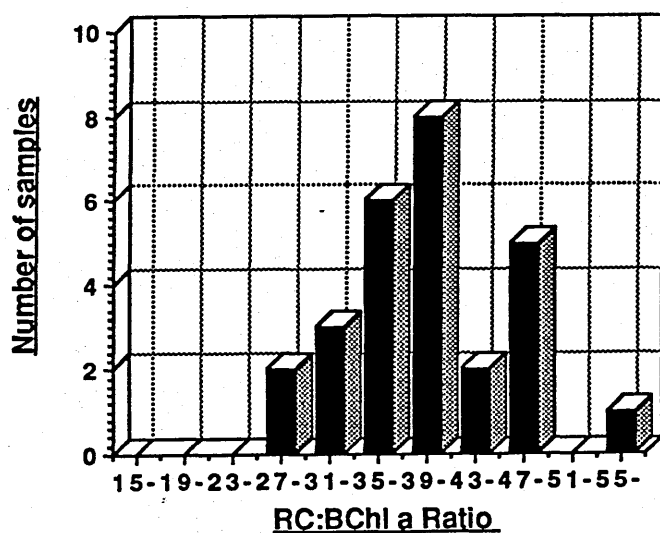
(a) *Rps. palustris* 'French' (*1:23)



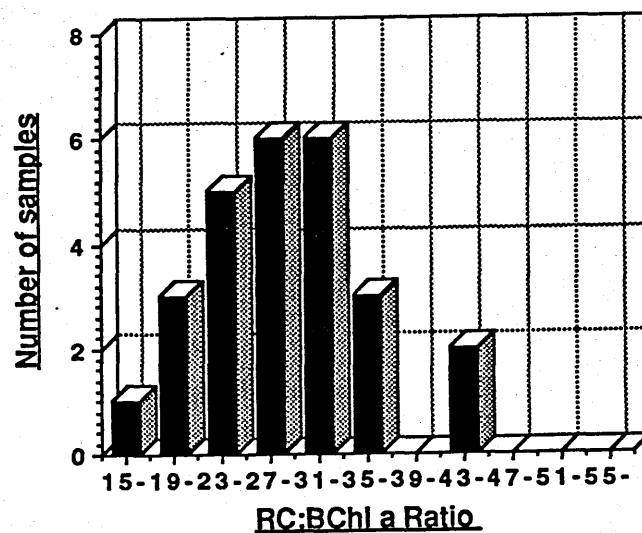
(b) *Rps. blastica* (*1:21)



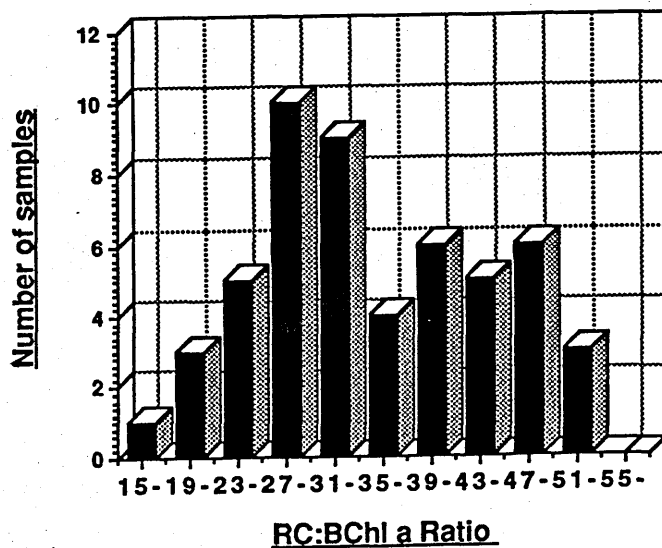
(c) *Rps. acidophila* 7750 (*1:39)



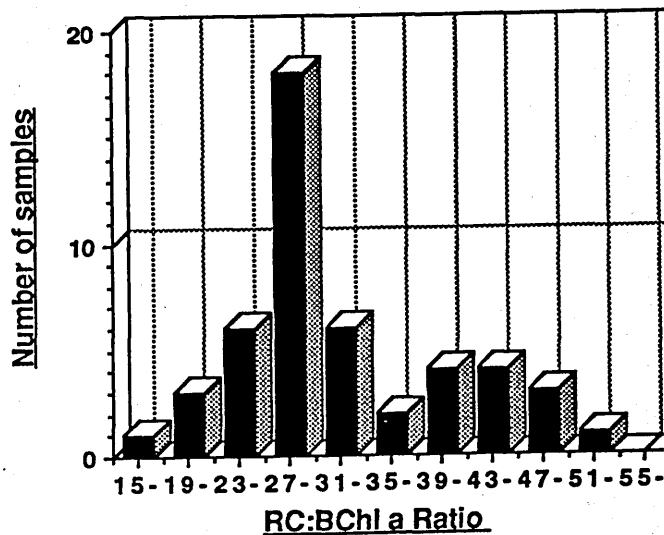
(d) *Rc. gelatinosus* 151 (*1:29)



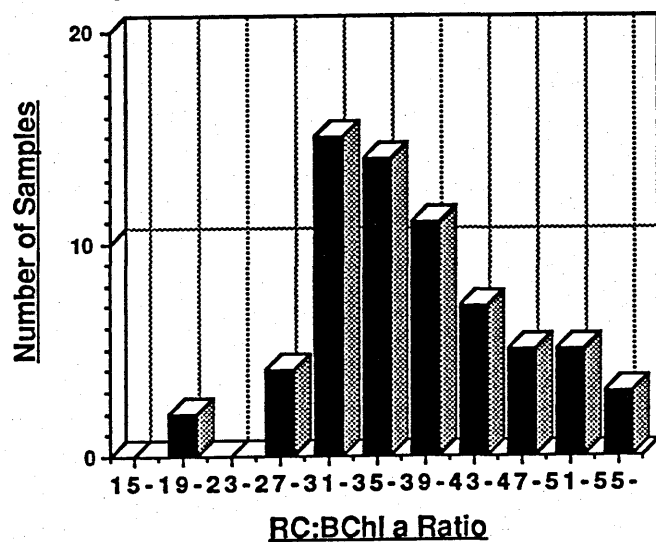
(e) *Rc. gelatinosus* 149 (*1:35)



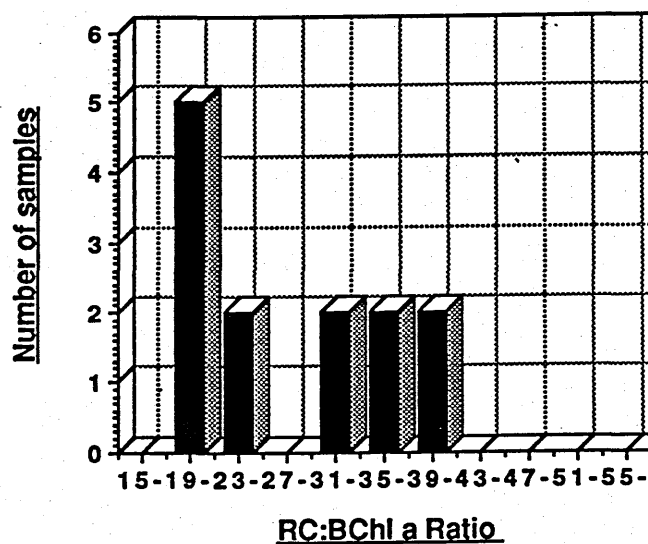
(f) *Rs. rubrum* (*1:33)



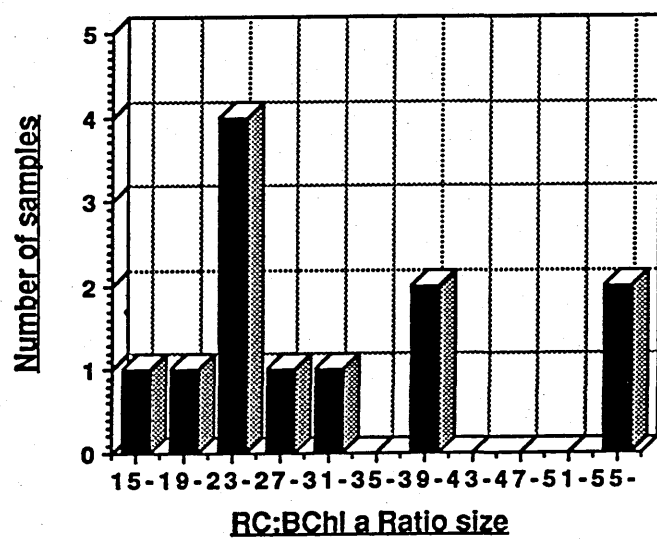
(g) *Rps. acidophila* 7050 (*1:41)



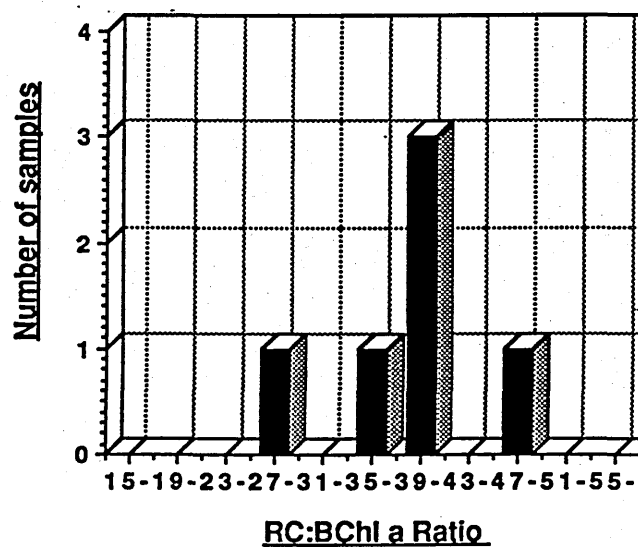
(h) *Rps. palustris* 'DSM 8252' (*1:27)



(i) *Rb. sphaeroides* R26 (*1:33)



(j) *Rb. sphaeroides* M21 (*1:33)



obtained for the species *Rc.gelatinosus* 149 (Figure 5.5e) and *Rs.rubrum* S1 (Figure 5.5f) can be accounted for by the very disperse normal distribution of ratio values ranging from 1:15 to 1:55. These two distributions, and also that for *Rps.acidophila* 7050 (shown in Figure 5.5g), which represents a more dramatic example, show a skew in the normal distribution towards higher ratio values. In all three cases it can also be seen that the mode value is lower than that of the calculated mean, suggesting that this is the result of one, or two unusually high ratio values affecting the ratio such that an artificially high standard deviation, and also mean value, is obtained. A rather erratic distribution is observed for the species *Rps. palustris* 'DSM8252' and *Rb. sphaeroides* strains R26 and M21 (Figure 5.5 h,i & j), which, may be a consequence of the small number of samples analysed. It also appears to be the case for these species that the high mean and standard deviation values determined are a consequence of one or two unusually high ratio values. In cases such as these it may be more accurate to consider the mode value of the distribution rather than the mean and standard deviation.

Variation, within a particular species, about the mean values will be partially due to natural sample variation, but may also be caused by slight changes arising in solubilization conditions, or the result of any other sources of error; the effects these could have on ratio determinations can be examined practically, as well as theoretically. A typical sample, for example, may have an optical density (OD) of $0.8.\text{cm}^{-1}$ at its NIR absorption maxima, chemical bleaching inducing a spectral change of 0.032 units of OD at the point of complete oxidation, will, therefore, yield a RC:B875 ratio value of 1:28. If, however, the RC 'special pair' of BChl a molecules is incompletely oxidized, and a spectral change of only 0.03 units of OD is produced, a final ratio value of 1:30 will be obtained.

Conversely, in the situation of over-oxidation ie. from the irreversible bleaching of antenna BChl-a, a spectral change of 0.034 units of OD may be produced giving a final ratio value of only 1:26. It can be seen from this example, therefore, that spectral changes of only 0.002 units of optical density can have a significant effect on the ratio outcome.

The examples described do represent real sources of error since the method employed demands the careful addition of potassium ferricyanide to the point of complete oxidation, a point indicated by only very slight spectral changes. It also assumes that the addition of ascorbate to the reference cuvette serves to reduce all reaction centre molecules, and thus provides a reference sample representing incomplete oxidation.

Statistical tests were employed to determine whether these values were all approximately equal, both within and between species, or whether significant differences existed between values, as a consequence of natural species variation, or 'artificial' variation induced by treatment effects. The statistical test employed was Analysis of Variance (Appendix 5): this test compares estimates of sample means and standard deviations ie. it compares overall mean values obtained for each species, whilst taking into account variation of individual measurements ie. allowing for random variation within each sample species [Bishop, 1971]. Thus in effect it was employed to determine the statistical probability (at 99% confidence levels) that the mean value determined for each species is the same. Analysis of variance (ANOVA) was performed first to compare all the species as a group, and then smaller combinations of species. Looking at Table 5.1, columns 1, 2 and 3 represent overall mean values (\pm standard deviation) of the RC:BChl a ratio determined using three different extinction coefficients for calculating the concentration of total

TABLE 5.1

Ratio of RC:BChl a determined for the RC-B875 antenna conjugate isolated from a range of BChl a-containing purple bacterial species.

<u>SPECIES</u>	<u>RC:BChl a¹</u>	<u>RC:BChl a²</u>	<u>RC:BChl a³</u>	<u>n</u>
<i>Rps. blastica</i>	1:21 ± 4.0	1:30 ± 6.0	1:27 ± 5.0	18
<i>Rps. palustris</i> 'French'	1:23 ± 3.0	1:30 ± 4.0	1:25 ± 3.5	30
<i>Rps. palustris</i> 'DSM8252'	1:27 ± 7.0	1:26 ± 7.0	1:24 ± 6.0	13
<i>Rc. gelatinosus</i> 149	1:35 ± 9.0	1:36 ± 10.0	1:33 ± 9.0	52
<i>Rc. gelatinosus</i> 151	1:29 ± 7.0	1:29 ± 7.0	1:26 ± 6.0	26
<i>Rps. acidophila</i> 7050	1:41 ± 7.0	1:50 ± 9.0	1:45 ± 8.5	66
<i>Rps. acidophila</i> 7750	1:39 ± 7.0	1:46 ± 7.0	1:42 ± 7.0	27
<i>Rb. sphaeroides</i> M21	1:33 ± 6.0	1:45 ± 8.2	1:40 ± 7.1	6
<i>Rb. sphaeroides</i> R26	1:33 ± 13.0	1:31 ± 12.3	1:28 ± 11.0	10
<i>Rs. rubrum</i> S1	1:33 ± 9.0	1:36 ± 9.0	1:33 ± 9.0	48

(Ratios represent mean values ± standard deviation)

RC:BChl a¹	Ratios have been calculated using the pre-established extinction coefficient $\epsilon_{880}=120.\text{mM}^{-1}.\text{cm}^{-1}$
RC:BChl a²	Ratios have been calculated using an extinction coefficient experimentally determined for each species (see Table 5.2)
RC:BChl a³	Ratios have been calculated using the adjusted experimentally determined value of ϵ_{880} : this value has been adjusted in accordance with the error margin existent between the established and experimentally determined value of A_{880} for <i>Rs. rubrum</i> S1.
n	Number of repeat samples

BChl a at the NIR absorption peak of the RC-B875 antenna complex: in column 1 an extinction coefficient of value 120 mM⁻¹.cm⁻¹ predetermined for *Rs. rubrum* S1 [Clayton, 1971] was employed. In column 2, the extinction coefficient value was determined experimentally for each species examined.

TABLE 5.2.

**Experimentally Determined Extinction Coefficient (at
NIR-maxima) values.**

<u>SPECIES</u>	<u>£880¹</u>	<u>£880²</u>
<i>Rps. blastica</i>	84.mM ⁻¹ .cm ⁻¹	94.mM ⁻¹ .cm ⁻¹
<i>Rps. palustris</i> 'French'	93	104
<i>Rps. palustris</i> 'DSM8252'	125	140
<i>Rps. acidophila</i> 7050	91	102
<i>Rps. acidophila</i> 7750	101	113
<i>Rc. gelatinosa</i> 149	116	130
<i>Rc. gelatinosa</i> 151	121	136
<i>Rb. sphaeroides</i> M21	89	100
<i>Rb. sphaeroides</i> R26	130	146
<i>Rs. rubrum</i> S1	107	120

- £880¹** Extinction coefficient value experimentally determined from the NIR absorption maxima ie. at approximately 880nm.
- £880²** Experimentally-determined value adjusted according to the error margin between the experimentally-determined value and the established value for *Rs. rubrum* S1.

Table 5.2 summarizes the extinction coefficient value determined for each species. It is perhaps important to mention here that the values of £880 experimentally determined for each of the different

strains of a particular species may be expected to be approximately equal. This, however, was not found to be the case for some species, for example *Rhodopseudomonas palustris* 'French' and 'DSM8252', and the two strains of *Rhodobacter sphaeroides*, R26 and M21. It is not known whether these variations reflect true strain variation, or whether it is simply a consequence of some unknown factor associated with the solubilization and/or isolation procedures.

It can also be observed that the experimentally determined value obtained for *Rs. rubrum* was lower than the established value of $120.\text{mM}^{-1}.\text{cm}^{-1}$. Assuming an error in techniques, either as a consequence of solvent extraction or the result of the original isolation procedures adopted, the experimentally determined extinction coefficient values were adjusted according to the error margin observed between the established value for *Rs. rubrum* S1, and the experimentally determined value. Reaction centre:BChl a ratios calculated using these modified values constitute column 3.

Analysis of variance tests were carried out on each column of values to determine whether RC:BChl a ratios for each species were comparable, or whether significant differences existed between individual species or groups of species. AOVO between the mean values and standard deviations in column 1 revealed significant differences (at 99% confidence levels) amongst certain groups of species such that three groups are recognized:

Group a consists of species with a comparatively low RC:BChl a, and includes the two species *Rps. blastica* ($1:21 \pm 4.0$) and *Rps. palustris* 'French' ($1:23 \pm 3.0$).

Group b, the largest group, consists of those species with a RC:BChl a approximating to 1:32 ie. species *Rps. palustris* 'DSM8252' ($1:27.5 \pm 7.0$), *Rc. gelatinosus* 151 ($1:29 \pm 7.0$), *Rc. gelatinosus* 149 ($1:35 \pm 9.0$), *Rb. sphaeroides* R26 ($1:33 \pm 13$) and

Rb. sphaeroides M21 ($1:33 \pm 9.0$).

Group c contains the two strains of *Rps. acidophila* 7050 and 7750 which have comparatively higher RC:BChl a ratios of $1:47 \pm 7.0$ and $1:39 \pm 7.0$ respectively.

Analysis of variance carried out on the values in columns 2 and 3 also revealed subdivisions between species, although they were less defined and overlaps between the groups were apparent. Columns 2 and 3 show a similar trend in grouping arrangements to those observed in column 1, although the sample means and standard deviations cover a slightly different range of values. The main group consists of those species with a mean ratio approximating to 1:26 in column 2 and 1:29 in column 3 ie. *Rc.gelatinosus* 151, *Rps.palustris* 'French' and 'DSM8252', *Rps.blastica* and *Rb.sphaeroides* R26. This latter species can also be included in the second group, along with *Rb.sphaeroides* M21, *Rc.gelatinosus* 149 and *Rs.rubrum* S1 which share an average ratio value of 1:36 (column 2) and 1:33 (column 3). The third group, overlapping group 2, also contains the *Rb.sphaeroides* strain M21 in addition to the two *Rps.acidophila* strains 7050 and 7750, having a mean ratio of 1:44 (column 2) or 1:45 (column 3).

The prime question provoked by these results is whether these subdivisions denote a true variation existing between species or whether they simply reflect the sensitivity of a particular species, or group of species, to the isolation and analysis procedures. For example, a particular species, or a group of species, may be particularly sensitive to detergent treatment, such that during the solubilization and fractionation procedures, bacteriochlorophyll a molecules may become denatured and selectively isolated by fractionation. Alternatively, the detergent may serve to denature, or part denature, reaction centre molecules; either of these possibilities would yield artificially low or high RC:BChl a ratios

respectively. It would also be expected, assuming that the reaction centre concentration was constant amongst species, that the relative 'peak height' ratios ie. the ratio of absorption at the NIR absorbance peak to absorption at 800nm, of the isolated RC-B875 antenna conjugate, would have values reflecting those determined for the RC:B875 BChl a ratio. That is, if the RC:B875 BChl a ratio is high, a high 'peak height' ratio would also be expected, the converse would also be expected to hold true. Table 5.3 presents values of 'peak height' ratios determined from absorption spectra of the RC-B875 antenna complex isolated from each species under examination.

TABLE 5.3

Comparing the ratio of absorption at 880nm:800nm of the
isolated RC:B875 antenna conjugates.

<u>Species</u>	<u>A₈₈₀[*]</u>	<u>A₈₀₀</u>	<u>Ratio of A₈₈₀[*]/A₈₀₀</u>
<i>Rps. blastica</i>	0.58±0.75	0.20±0.06	1:2.9 ± 0.9 (n=48)
<i>Rps. palustris</i> 'French'	0.79±0.20	0.27±0.10	1:2.9 ± 0.8 (n=20)
<i>Rps. palustris</i> 'DSM8252'	0.66±0.18	0.23±0.07	1:2.8 ± 0.9 (n=27)
<i>Rc. gelatinosus</i> 149	0.85±0.28	0.20±0.07	1:4.3 ± 0.9 (n=61)
<i>Rc. gelatinosus</i> 151	0.63±0.25	0.16±0.08	1:3.9 ± 1.0 (n=47)
<i>Rb. sphaeroides</i> M21	0.59±0.15	0.21±0.07	1:3.2 ± 1.0 (n=13)
<i>Rb. sphaeroides</i> R26	0.68±0.18	0.19±0.06	1:4.4 ± 1.9 (n= 9)
<i>Rs. rubrum</i> S1	0.81±0.19	0.21±0.07	1:3.9 ± 1.2 (n=60)
<i>Rps. acidophila</i> 7050	0.88±0.24	0.28±0.13	1:3.7 ± 1.3 (n=85)
<i>Rps. acidophila</i> 7750	0.76±0.22	0.20±0.08	1:3.9 ± 0.9 (n=69)

A₈₀₀ : Average absorbance at 800nm ± standard deviation.

A₈₈₀^{*}: Average absorbance (± standard deviation) at the NIR maximum for a particular species ie. at approximately 880nm.

These results show that the 'peak height' ratio, determined for a particular species remains relatively constant. This constancy also extends between strains of a particular species. However, comparison of all the ratio values obtained, reveals that the different species can be divided into three groups according to the relative value of their peak height ratios. The three groups consist of those species with a relatively low peak height ratio of approximately 3.0 ie. *Rhodopseudomonas blastica*, *Rhodopseudomonas palustris* 'French' and 'DSM8252' and *Rhodobacter sphaeroides* M21, those species with a higher peak

height ratio approximating to 4.0 including the species *Rhodocyclus gelatinosus* 149 and 151, *Rhodospirillum rubrum* S1 and *Rhodopseudomonas acidophila* 7750, and falling mid-way between these two extremes are the two species *Rhodobacter sphaeroides* R26 and *Rhodopseudomonas acidophila* 7050, having an approximate peak height ratio value of 3.6. Observing the absorption values independently at 800nm, and at the NIR absorption peak at approximately 880nm, it can be seen that despite the consistency of absorption of each species at 800nm, the mean NIR absorption value varies quite significantly amongst the different species; this latter value therefore, gives rise to the variation in peak height ratios, and also reflects to some extent the variation in experimentally-determined ϵ_{880} values (Table 5.2). Since the peak height ratio should represent an approximate reflection of the RC:BChl a ratio, ranking each species according to the relative size of each of these two ratio values should produce comparable patterns of order. This however, was not observed to be true for all species, for example *Rhodopseudomonas acidophila* 7050 which has an average mean peak height ratio but a high RC:BChl a ratio, and *Rhodocyclus gelatinosus* 151 has a high mean peak height ratio and an average RC:BChl a ratio. These variations in order, although apparently minor, may indicate that some factor(s) of the solubilization and/or isolation procedures are affecting the photochemical activities (or chemical oxidation) of the reaction centre, and/or influencing BChl a absorption. In view of these results, the sensitivity, monitored with respect to changes occurring in the RC:BChl a and the 880nm:800nm absorption peak ratios, of a particular species to different detergents, and different detergent concentrations, was therefore examined. The isolated RC-B875 antenna conjugates were exposed to the detergents LDAO, SDS and Triton X-100 at different

concentrations over a period of time, after which the absorption spectra and oxidation-reduction difference spectra were recorded. These results are summarized in Table 5.4.

TABLE 5.4 The effects of detergent on the ratio of RC:antenna BChl a, and also upon the ratio of A₈₈₀/A₈₀₀.

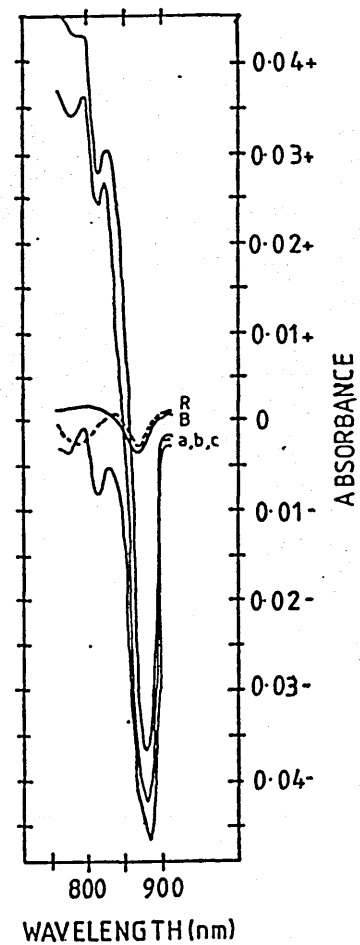
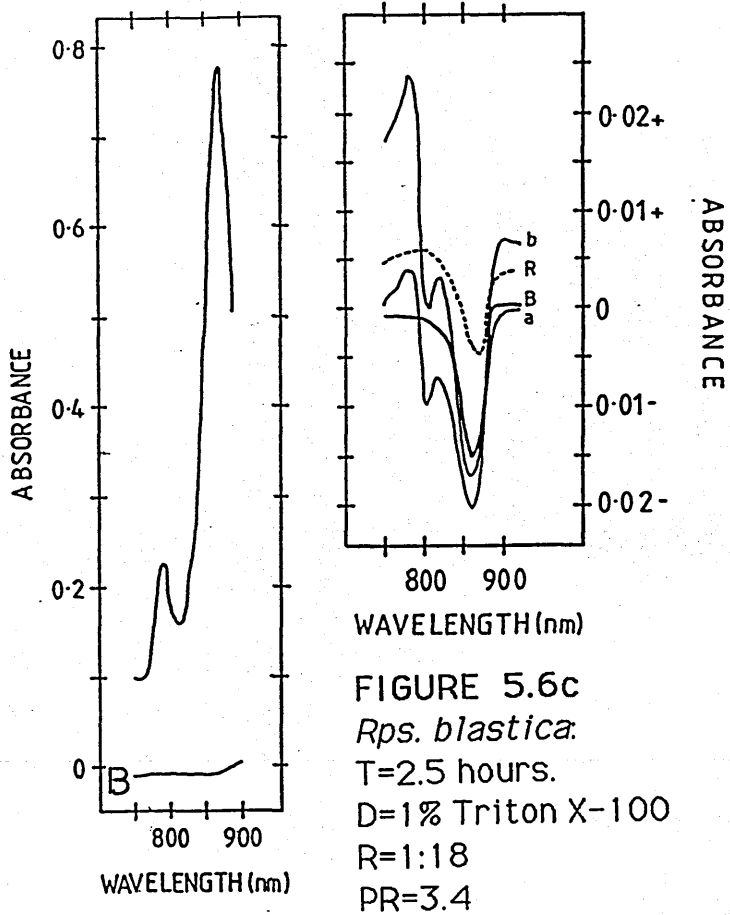
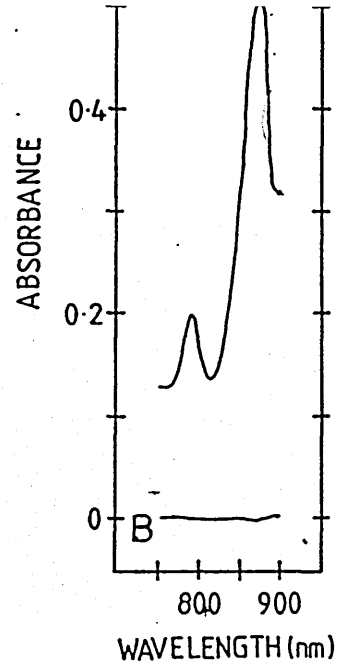
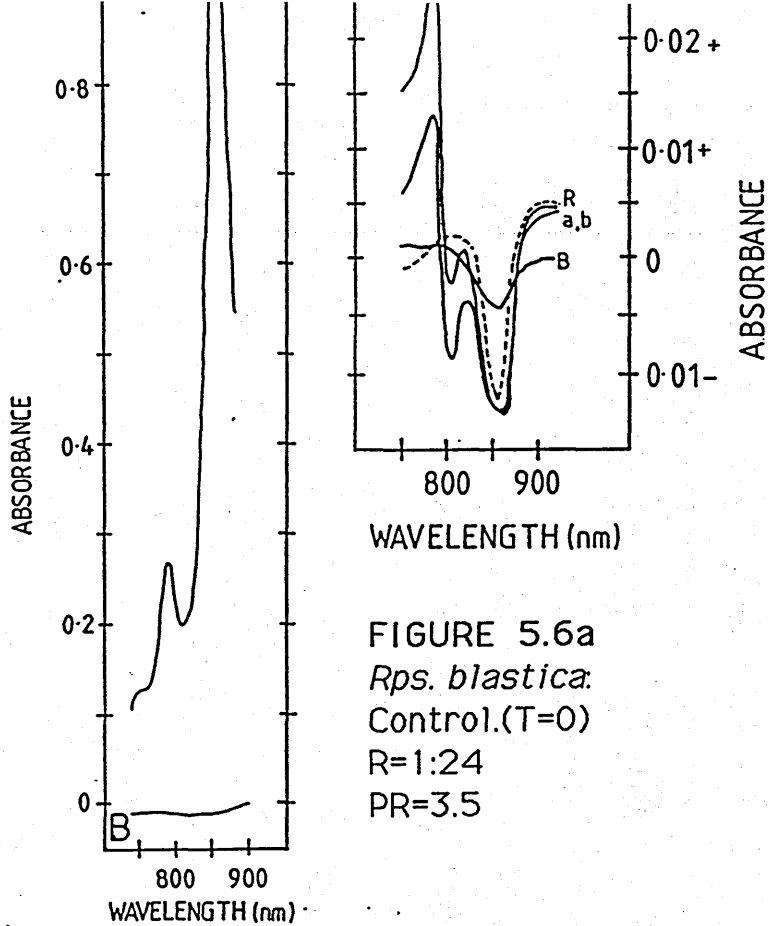
<u>SPECIES</u>	<u>[DETERGENT]</u>	<u>RC:BChl a</u>		<u>A₈₈₀/A₈₀₀</u>	
		<u>1hr</u>	<u>2.5hrs</u>	<u>1hr</u>	<u>2.5hrs</u>
<i>Rps. acidophila</i> 7750	0.1% LDAO	1:31	1:32	3.1	3.1
	0.5% LDAO	1:25	1:64	3.7	3.8
	1.0% LDAO	1:29	1:32	3.7	4.0
	1.5% LDAO	1:28	1:36	3.7	3.7
	0.5% Triton X100	1:26	1:43	3.5	3.6
	1.0% Triton X100	1:33	1:43	3.6	3.5
	1.5% Triton X100	1:37	1:53	3.6	3.7
	0.5% SD	1:28	1:26	3.2	2.9
	1.0% SDS	Denatured-----			
<i>Rc. gelatinosus</i> 149	0.25% LDAO		1:46		
	0.50% LDAO		1:34		
	0.75% LDAO		1:35		
	1.00% LDAO		1:65		
<i>Rc. gelatinosus</i> 151	0.50% LDAO		1:26		
	0.75% LDAO		1:33		
<i>Rps. blastica</i>	0.00% LDAO	1:24	1:22	3.5	3.5
	0.50% LDAO	1:21	1:21	3.5	3.5
	1.00% LDAO	1:22	1:20	3.4	3.1
	1.00% Triton X100	1:18	1:18	3.4	3.7
	1.00% SDS	1:18	1:19	3.2	2.9
<i>Rps. palustris</i> 'French'	0.00% LDAO	1:24	1:23	3.5	3.5
	0.50% LDAO	1:23	1:25	3.4	3.3
	1.00% LDAO	1:25	1:28	2.9	3.0
	2.00% LDAO	1:30	1:31	2.9	2.9

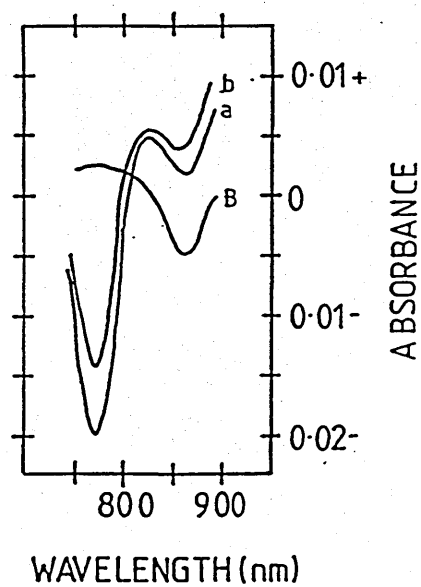
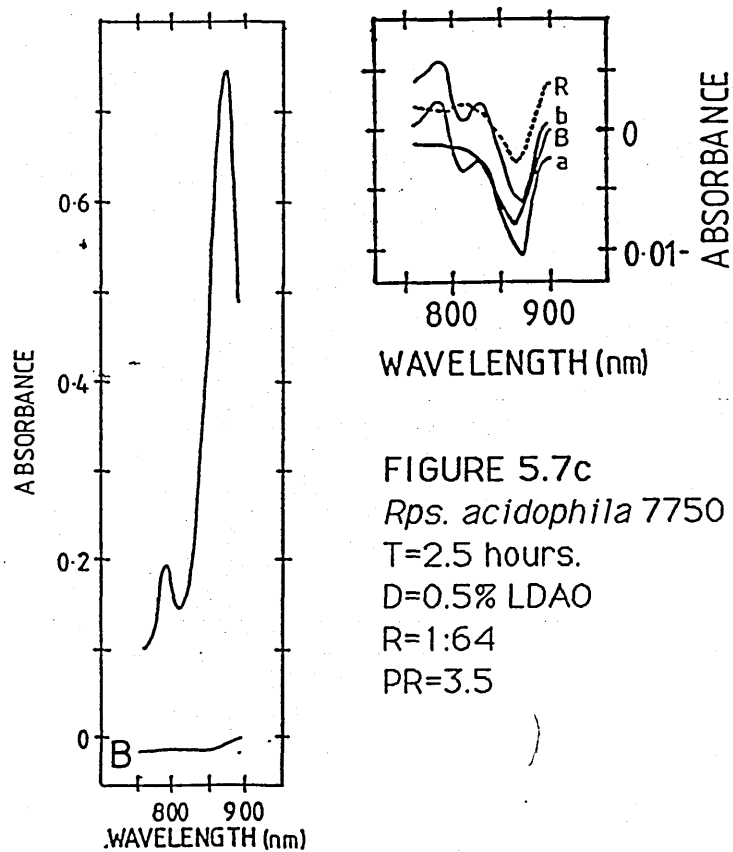
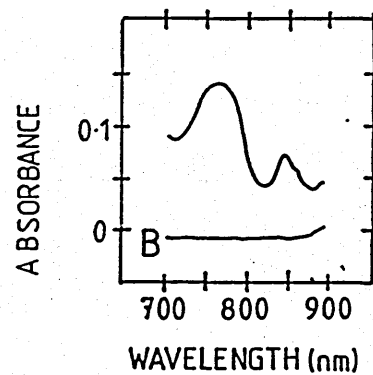
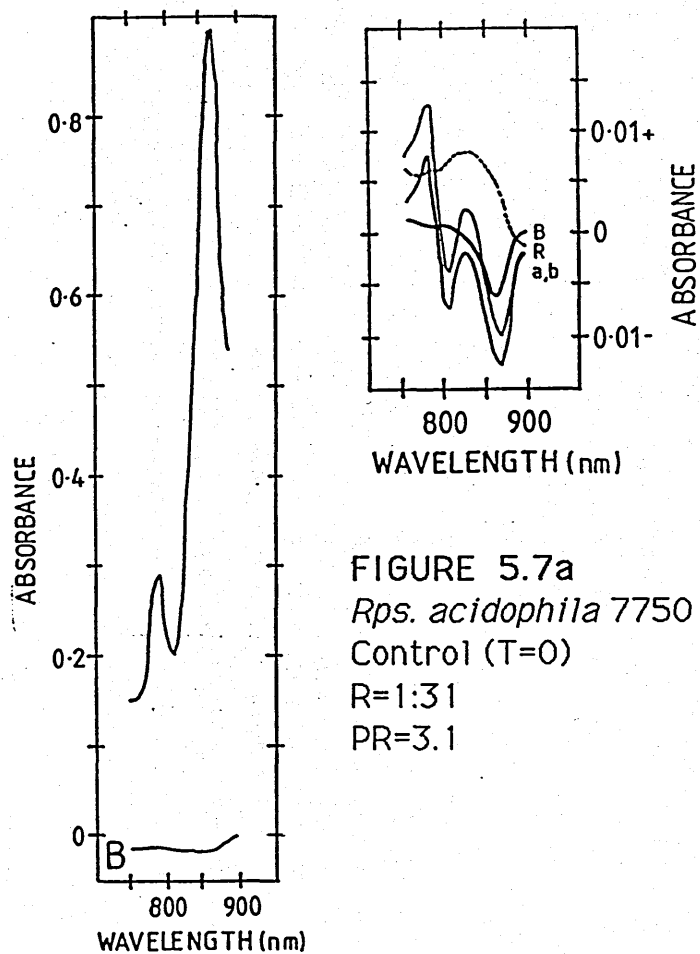
It can be generally observed that the effect of detergent addition is to alter the ratio of reaction centre molecules to light-harvesting BChl a, either by directly influencing the absorption properties or by influencing the oxidation-reduction spectra. The effects on spectral properties can be observed in Figures 5.6–5.8. Examining the difference spectra of *Rps.blastica* it can be seen that detergents such as SDS have a very disruptive effect on the oxidation-reduction difference spectra, to such an extent that it becomes very difficult to determine, with any degree of accuracy, the point of complete oxidation. A reduction in the peak height ratio observed in the absorption spectrum, with respect to the control, was also clearly evident. For the species *Rhodopseudomonas acidophila* 7750, SDS at concentrations of 0.5% caused a similar erratic effect, and at concentrations of 1% SDS complete denaturation was observed. The addition of other detergents, for example Triton X-100 and LDAO, generally maintained 'normal' spectral responses, and no uncharacteristic effects were immediately evident, however, the subsequent determination of RC:B875 BChl a and peak height ratios from these spectra clearly revealed detergent effects. It can be seen in the case of *Rhodopseudomonas acidophila* 7750 that the effect of increasing detergent concentration measured with respect to time, is to cause an increase in the RC:BChl a ratio. The ratio of absorption maxima however showed relatively little change, these results therefore suggest that the RC itself was being affected by the external conditions. A comparable increase in the RC:BChl a ratio in response to increments in detergent concentration, was also observed for the two strains of *Rc. gelatinosus* 149 and 151. A contrary response was produced by *Rps. blastica*; an increase in detergent concentration resulted in reduced RC:BChl a

FIGURE 5.6 - 5.8. The Effects of Detergent Addition on the Absorption, and Oxidation-Reduction Difference, Spectra, Recorded for RC-B875 Antenna Complexes Isolated from the Species *Rhodopseudomonas blastica*, *Rhodopseudomonas acidophila* 7750 and *Rhodopseudomonas palustris* 'French'.

The figures present absorbance spectra (Absorbance pathlength 1 cm), and associated oxidation-reduction difference spectra, recorded for the RC-B875 antenna complex isolated from the species *Rhodopseudomonas blastica*, (Figure 5.6) *Rhodopseudomonas acidophila* 7750 (Figure 5.7) and *Rhodopseudomonas palustris* 'French' (Figure 5.8). The RC-B875 antenna complex, isolated by sucrose density-gradient fractionation of detergent-solubilized membranes, was dialysed against 10 mM Tris-HCl, pH 8.0, prior to incubation, at 4°C, in the presence of additional detergents (D) for varying periods of time (T). In each experiment, controls, containing no additional detergent, were prepared and monitored to ensure that other factors, such as time, temperature etc. were not responsible for inducing changes in spectral properties. The effects of detergents on the absorbance, and oxidation-reduction difference spectra were measured with respect to changes in the peak-height ratios (PR) ie. A_{880}/A_{800} , and RC:BChl *a* ratio (R), respectively. The detergents examined included LDAO, Triton X-100 and SDS at concentrations ranging from 0 - 2% (v/v).

Referring to the oxidation-reduction difference spectra, B represents the baseline recording; line spectra a, b & c etc. represent successive additions of potassium ferricyanide to the sample cuvette. Potassium ferricyanide was added until there was complete oxidation of RC molecules. Ascorbate was finally added to the sample cuvette to ensure that oxidation reversibility had been maintained (R). The concentration of RC molecules was determined from the spectral shift observed at approximately 800 nm, using the extinction coefficient, $\epsilon_{800} = 133.\text{mM}^{-1}.\text{cm}^{-1}$. The concentration of BChl *a* molecules was determined from the NIR absorption peak at about 880 nm, using $\epsilon_{880} = 120.\text{mM}^{-1}.\text{cm}^{-1}$. The values obtained are shown with respective spectral figures, and are summarized in Table 5.4.





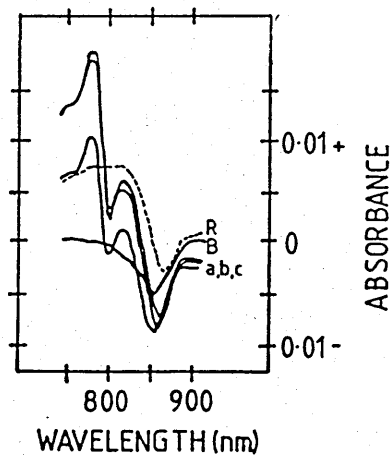
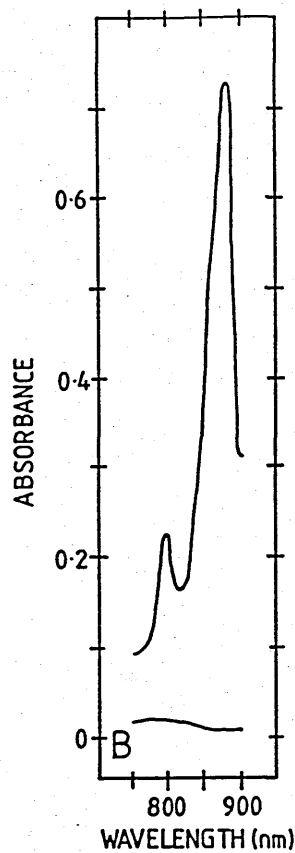


FIGURE 5.8a
Rps. palustris 'French'
 Control (T=2 hours) ;
 R=1:25
 PR=3.29

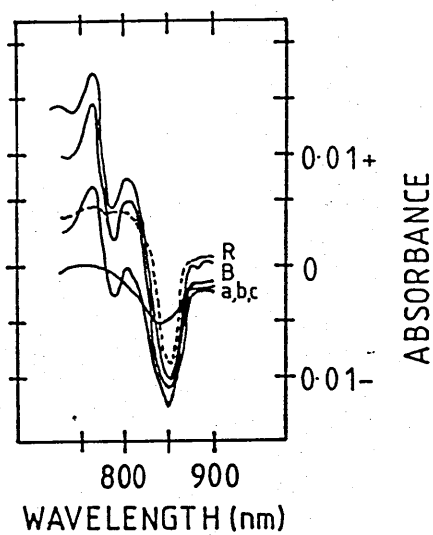
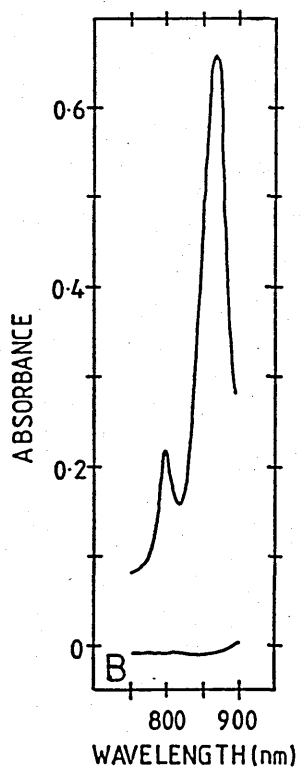


FIGURE 5.8b
Rps. palustris 'French'
 T=2 hours
 D=2% LDAO
 R=1:30
 PR=2.87

determinations and a corresponding reduction in the absorption peak height ratio. Comparable reductions were observed with *Rps. palustris* 'French'. This reduction in the RC:BChl a ratio, particularly when accompanied by an increase in peak height ratios, suggests that the antenna BChl a is being denatured.

Also of particular interest, and worth noting at this point, is the observation that the solubilization and fractionation of the species *Rs. rubrum* S1 on sucrose density-gradients produces two bands; spectral analysis of each band reveals the characteristic response, with peaks corresponding to reaction centre and B890 antenna complex absorption (Figure 5.9). However, the peak height ratio ie A_{890}/A_{800} , of the upper band (band I) from the gradient was observed to be consistently lower than that of band II (the lower band). Determination of the RC:BChl a ratio for each of these bands (summarized in Table 5.5) also revealed that band I was significantly higher, at 95% confidence levels, than band II (although these values were accepted as comparable at 99% confidence levels).

TABLE 5.5

<u><i>Rs. rubrum</i> S1</u>	<u>Average RC:BChl <u>a</u></u>	<u>A_{890}/A_{800}</u>
Band I	1:42 \pm 13 (n=11)	3.4 \pm 0.36
Band II	1:36 \pm 5.6 (n=13)	4.0 \pm 0.66

(Ratio values refer to the mean \pm standard deviation of a number of samples, n).

Sucrose-density gradient fractionation of *Rb. sphaeroides* strains M21 and R26, which, like *Rs. rubrum*S1, have only the B890 antenna complex, also, under some solubilization conditions,

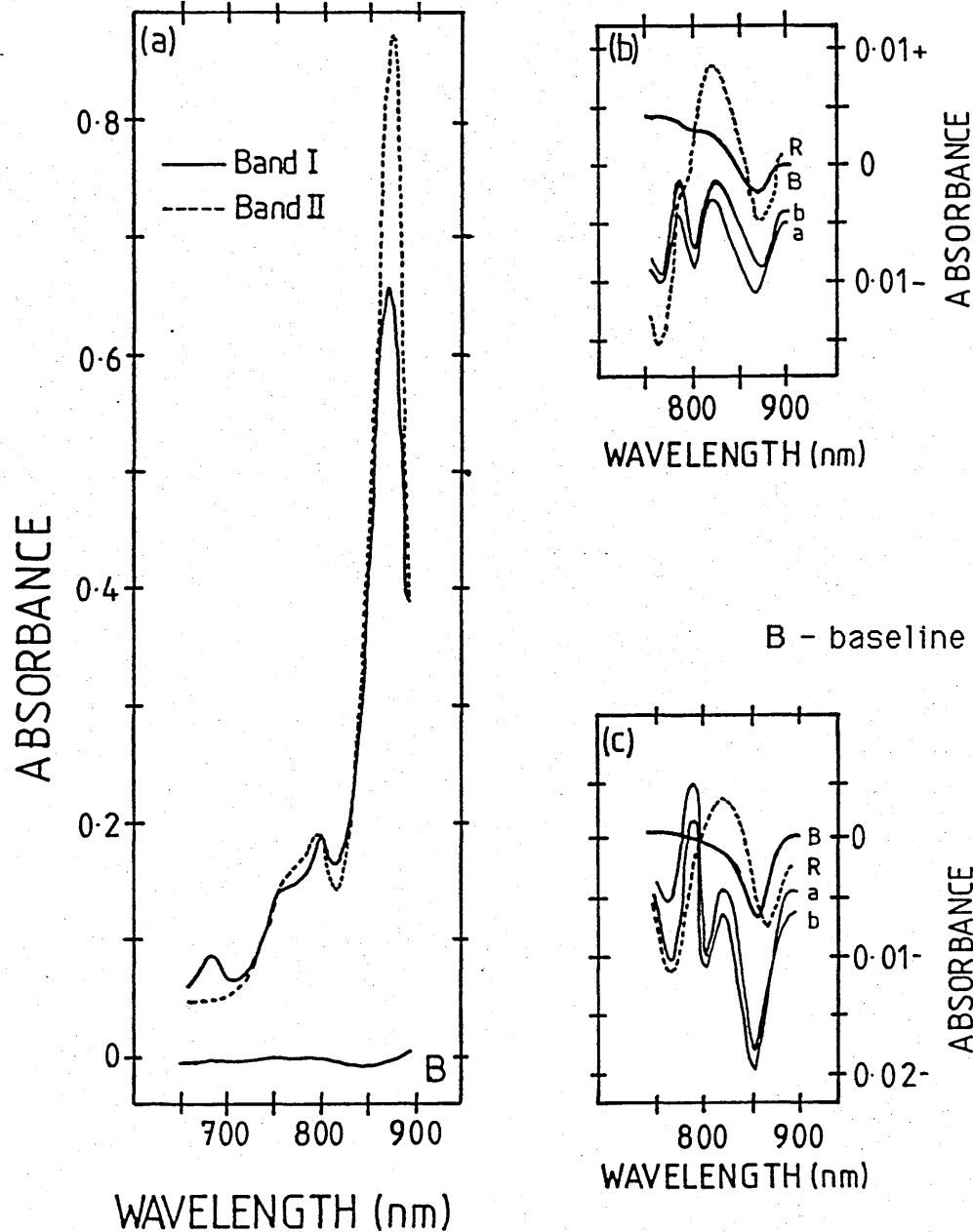


FIGURE 5.9 Spectral Analysis of the Fractionated Products of Detergent Solubilized Membranes of the Species *Rhodospirillum rubrum* S1.

Fractionation of photosynthetic membranes of *Rs. rubrum* S1 solubilized in 0.5% (v/v) LDAO yields two bands (--- and —). Spectral analysis of these bands resuspended in 10 mM Tris-HCl, pH 8.0 show them to have absorption properties characteristic of the RC-B890 antenna complex. Examination of the peak height absorption ratios (Figure 5.9 a) ie. A_{890}/A_{800} , and analysis of the oxidation-reduction difference spectra (Figure 5.9 b & c), however, suggests that significant differences exist between the two bands.

In Figures 5.9 b & c, 'B' refers to the baseline recording, and line spectra indicate successive additions of potassium ferricyanide, until complete oxidation of RC molecules is achieved. A final addition of ascorbate is made to the sample cuvette to ensure that oxidation reversibility has been maintained (R). (Absorbance pathlength 1 cm).

produce two bands; the upper band, however, was invariably denatured. These results can be discussed in the light of earlier experiments which utilized the detergent LDAO to dissociate the reaction centre of *Rs. rubrum*, in an essentially unaltered entity, from its association with most other membrane components [(Reed and Clayton, 1968)(Oelze and Golecki, 1975)(Clayton and Sistrom, 1978)(Loach, 1980)]. It is possible therefore, that the different fractions obtained from LDAO solubilization of membranes of *Rs. rubrum* S1 represent photosynthetic units in different stages of dissociation ie. with the 'light' component, banding high in the sucrose density-gradient, containing a high proportion of reaction-centre depleted photosynthetic components. This would, as a consequence, alter spectral properties and distort the calculated peak-height and RC:BChl a ratios. The dissociation of reaction centre molecules from the RC-B875 antenna complex, by detergent solubilization, may also contribute to variation apparent between ratio values determined for the core complex isolated from different species of purple bacteria. Species may vary in the degree of association existing between the reaction centre and B875 antenna complex, such that core complexes of some species may be dissociated easily, whereas for other species, dissociation may only result from extensive disruption of the photosynthetic unit.

The results examined independently for each species, provide positive evidence supporting the existence of a fixed stoichiometric core structure. Considering the results as a whole, they also suggest that the variation in RC:B875 BChl a and peak height ratios, apparent between different species (and in the case of the former ratio between different strains of the same species), is an artifact of detergent solubilization procedures as opposed to the existence of any natural species variation.

The congruency of the RC:B875 BChl a ratio, determined for a particular species, is also further exemplified by the analysis of the RC:antenna complexes isolated from cells grown under conditions of low, and high, light intensities. Table 5.6 summarizes the mean ratio values determined for high-light (HL) and low-light grown (LL) cells of the species examined.

Statistical tests including analysis of variance and t-tests (which make a comparison between two means and calculate the probability that they are representative of the same population mean [Parker, 1979]) (Appendix 5) conclude that for each species examined there is no significant difference (at 99% and 95% confidence levels) between the high-light and low-light values. To ensure that the samples were indeed representative of HL- and LL-grown cells, the ratio of LL B800-850/B875 to HL B800-850/B875 was determined for each species; these values were determined from the absorption spectra of RC-B875, and B800-850 antenna complexes, isolated from membrane preparations of high-light, and low-light, intensity grown cells [Figure 5.10]. The B800-850 absorption value was determined from the absorption peak at 590nm, which provides an accurate reflection of B800-850 absorption, and the value of RC-B875 absorbance was determined from the NIR absorption peak. Dilution coefficients were taken into account with respect to all measurements. The results are summarized in Table 5.7.

Table 5.6.

Comparison of the RC:B875 BChl a Ratios Obtained for the RC-antenna conjugates Isolated from High-light and Low-light Intensity Grown Cells.

<u>SPECIES</u>	<u>LOW-LIGHT RATIO</u>	<u>HIGH-LIGHT RATIO</u>	<u>t</u>	<u>(f)</u>	<u>PROBABILITY</u>
<i>Rps. acidophila</i> 7050	1:39 - 9.4 (n=30)	1:41 - 10.5 (n=29)	1.12	(57)	0.26
<i>Rps. acidophila</i> 7750	1:39 - 15.8 (n= 4)	1:48 - 6.6 (n= 5)	1.08	(7)	0.12
<i>Rs. rubrum</i> S1	1:29 - 5.5 (n=10)	1:28 - 9.8 (n= 8)	0.10	(16)	0.92
<i>Rps. palustris</i> 'French'	1:24 - 3.5 (n= 7)	1:23 - 4.0 (n= 7)	0.49	(12)	0.63
<i>Rps. palustris</i> 'DSM8252'	1:37 - 2.8 (n= 2)	1:33 - 2.8 (n= 2)	1.41	(2)	0.29
<i>Rc. gelatinosus</i> 149	1:31 - 9.9 (n=13)	1:34 - 7.1 (n=12)	0.78	(23)	0.45
<i>Rc gelatinosus</i> 151	1:32 - 2.5 (n= 3)	1:31 - 1.0 (n= 4)	1.06	(5)	0.34

The RC:BChl a ratios presented, represent mean values - standard deviation, determined for each sample of size, n. The 'low-light' and 'high-light' ratio values obtained for each species were statistically compared in order to determine whether there was any significant difference between them. The level of significance was determined using the t-test. The calculated values of t with their associated degrees of freedom are shown in the table above (t (f)). From the probability, or level of significance determined for each value of t, it can be concluded that there is no significant difference between the 'high-light' and 'low-light' ratio values determined for each species (within 95% and 99% confidence limits).

FIGURE 5.10 Spectra of RC-B875 and B800-850 Antenna Complexes Isolated From Cells of *Rhodopseudomonas palustris* 'French' Grown Up Under Conditions of High-, and Low-, Light Intensities.

The figure presents absorption spectra (absorbance pathlength 1 cm) of the two complexes (Band I (—), and Band II (---)) isolated from detergent-solubilized photosynthetic membranes, of high-light (Figure 5.10a) and low-light (Figure 5.10b) grown cells of *Rhodopseudomonas palustris* 'French', by sucrose density-gradient fractionation. The isolated complexes were resuspended in 10 mM Tris-HCl, pH 8.0.

The two bands isolated from each sample, exhibit absorbance properties characteristic of the two main components of the photosynthetic unit ie. B800-850 (—), and RC-B875 (---), antenna complexes.

Comparing the respective complexes of HL and LL samples, little difference can be observed in the spectral properties of the visible region of the spectrum. In the NIR region of the spectrum, the RC-B875 complexes (---) are also comparable. However, the B800-850 antenna complex is observed to exhibit different NIR absorption properties depending upon the light conditions prevailing during cell development; the most distinctive feature being the difference in the relative absorption of the B800-850 antenna complex at 800 nm and 850 nm. That is, in HL-grown cells two distinct peaks are observed, at 800 nm and at 850 nm. In LL-grown cells, however, the absorbance peak at 850 nm appears as a shoulder on the NIR arm of the prominent peak observed at 800 nm. The relative absorbance ratio ie. A_{850}/A_{800} , of the B800-850 complex from LL-grown cells is consequently much lower than that determined for the B800-850 complex of HL-grown cells.

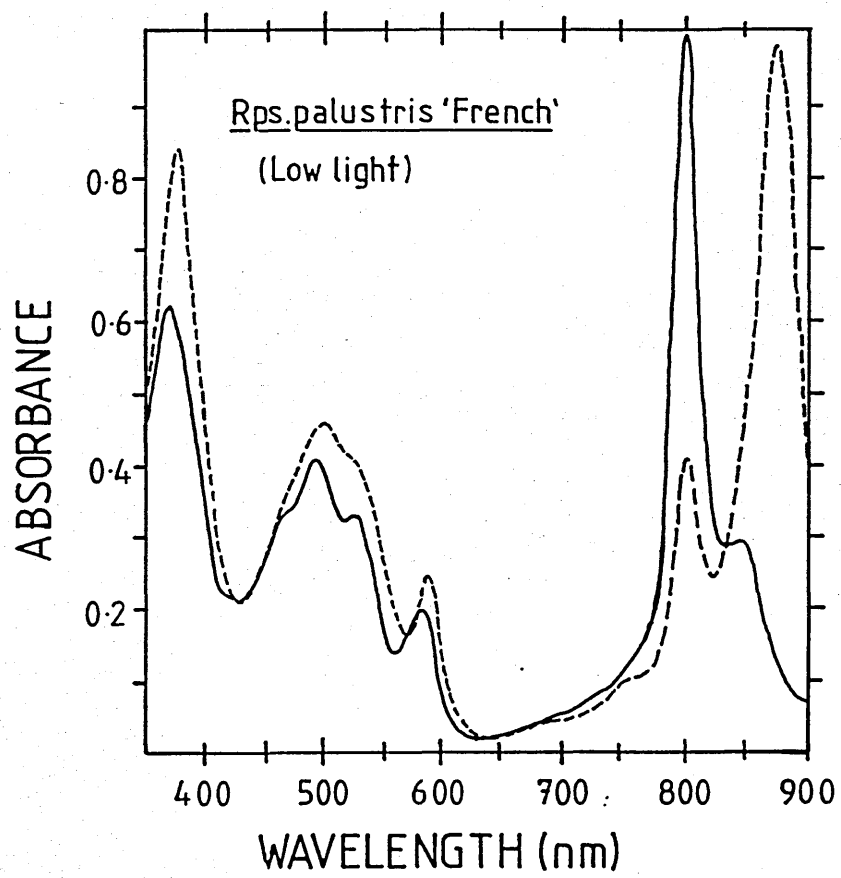
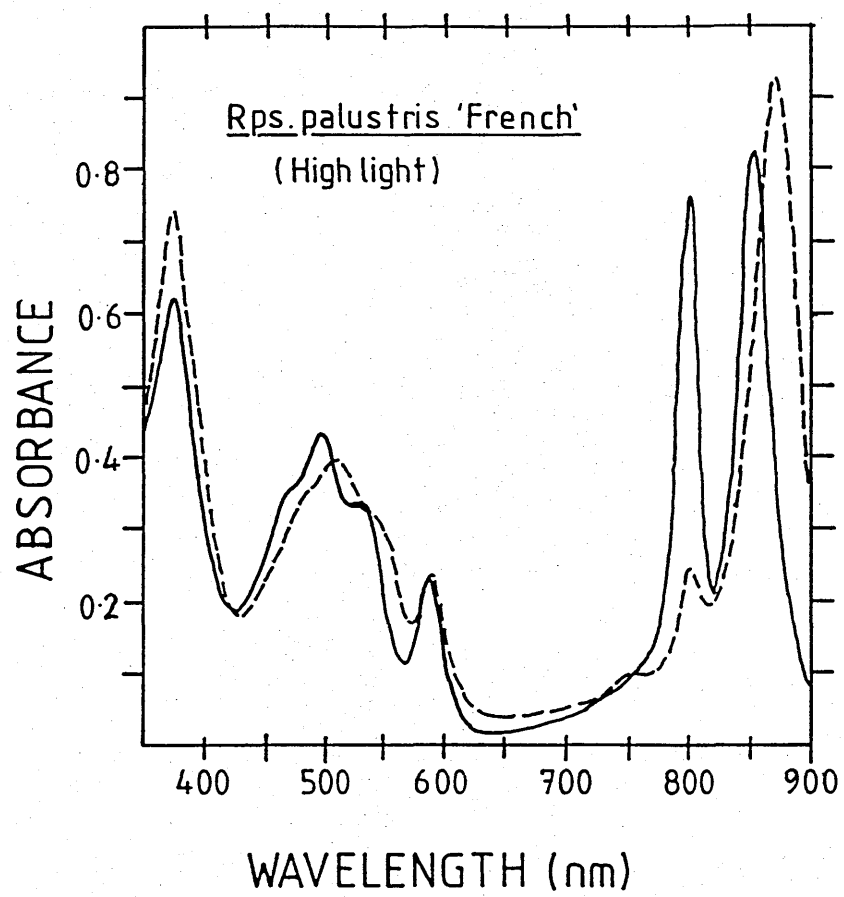


Table 5.7.

**Comparing the Relative Ratios of B800-850 to B875
Antenna Complex in High Light- and Low Light- Grown
Cells.**

<u>SPECIES</u>	<u>RATIO OF LL/HL B800-850/B875</u>	<u>n</u>
<i>Rps. acidophila</i> 7050	2.7 ± 1.4	14
<i>Rps. acidophila</i> 7750	2.1 ± 0.9	3
<i>Rc. gelatinosus</i> 149	3.0 ± 2.3	5
<i>Rc. gelatinosus</i> 151	2.9 ± 0.1	2
<i>Rps. palustris</i> 'French'	2.2 ± 0.0	2

The ratios represent mean values ± standard deviation as determined from a number (n) of independent samples.

The results themselves show a fairly high degree of variation both within and between species, however it is apparent that the total B800-850 BChl a content was higher in cells grown under low-light intensities. The variation in B800-850 BChl a content, apparent both within and between species, could be attributed to some extent, to the effects of growth conditions, and also to the obvious variation existing between different batches of a particular species. Some species, for example *Rc. gelatinosus* 149 and 151 were very difficult to grow under low light conditions, others such as *Rps. blastica*, *Rb. sphaeroides* M21 and R26 would not grow at all, whereas species such as *Rps. acidophila* 7050 and *Rps. palustris* 'French' (which under LL conditions produce an additional B800-820 antenna complex) flourished. Under HL conditions the cells had to be grown to fairly low densities to ensure that 'artificial low-light' conditions were not created due

to shading effects.

The difference in amount of B800-850 antenna complex of HL- and LL- grown cells can be visibly observed by comparing the band densities of fractionated samples of HL and LL solubilized membrane preparations on sucrose gradients. Figure 5.11 shows that whereas the lower RC-B875 bands appear to have approximately equal densities, the upper B800-850 bands clearly differ, with a higher density apparent in the LL preparation. A difference in the overall size of the HL and LL cells of a particular species can also be clearly seen using a light microscope. Comparing the number of cells in a solution corresponding to a particular optical density (measured at 650nm since there is little, or no, BChl a absorption at this wavelength), it can be observed that LL cells appear larger in their overall size, and have a lower cell count, than a sample of HL cells with an equivalent OD₆₅₀. This method of comparing HL and LL cells is useful when examining cells of *Rs. rubrum* S1 which, having only the B890-antenna complex, adapt to LL conditions by increasing the number of photosynthetic units per unit of intracytoplasmic membrane, and also by increasing the amount of intracytoplasmic membrane per cell. Consequently under low light conditions the cells should be larger. Cell counts were made and a calibration curve, relating cell number to relative absorbance at 650 nm, was constructed (Figure 5.12). Calibration curves for high-light and low-light cells of a particular species were then compared; an estimate of the ratio of HL to LL cells was determined by comparing the HL and LL regression lines relating the two parameters of optical density and cell number. The results, shown in Table 5.8, do show that the number of LL-grown cells is indeed much lower than the number of HL cells in a solution of comparative density.

FIGURE 5.11 Fractionation of Detergent-Solubilized Membranes Isolated from Samples of HL- and LL- Grown Cells of *Rhodocyclus gelatinosus* 149 by Sucrose Density-Gradient Centrifugation.

Chromatophore samples prepared from samples of HL and LL cells of *Rhodocyclus gelatinosus* 149 having equal cell numbers (determined from growth curves relating cell number with OD₆₅₀ (Figure 5.12)) were solubilized using detergents, and fractionated by sucrose density-gradient centrifugation. Two bands, Band I and II, having characteristic B800-850, and RC-B875 spectral properties, respectively, were typically generated. It can be observed, by comparing the two gradients shown above that although the density of the lower, RC-B875 complex, band appears approximately equal, the upper, B800-850, band has a considerably lower density in the HL (LHS) preparation. These results provide visual evidence suggesting that although the relative concentration of RC-B875 antenna complex remains constant, irrespective of growth conditions, the relative concentration of the B800-850 complex varies, showing extensive development under LL-intensity conditions.

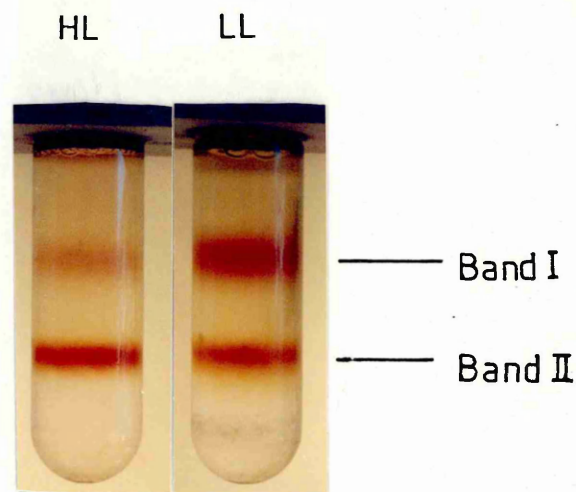
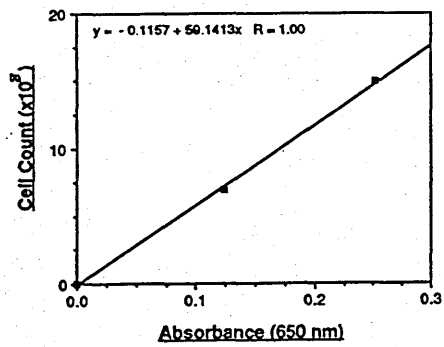


FIGURE 5.12 Calibration Curves Relating the Parameters of Cell Number to Optical Density (at 650 nm) of the Species *R. rubrum* S1, *Rhodopseudomonas acidophila* 7050 and *Rhodocyclus gelatinosus* 151 Grown under HL and LL Intensity Conditions.

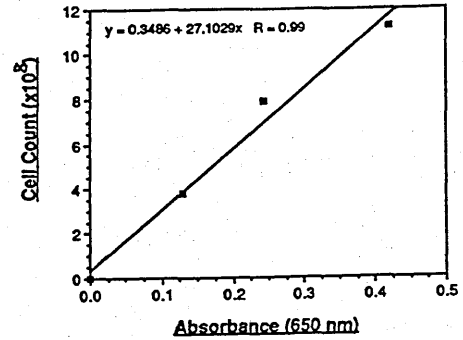
Average cell counts were made using a haemocytometer slide under a light microscope. Cells were killed, to ease counting, with a drop of iodine. The optical density at 650 nm, was measured for each sample. Calibration curves relating cell number per 1 ml sample (ordinate) with respect to OD₆₅₀ (abscissa) were then constructed. A 'best-fit' regression line was determined (R-denotes the 'fit' of the line, and the equation describes the line). The slope of these lines provides an estimation of cell counts expected in a sample with specific OD₆₅₀, and allows comparisons to be made between samples of HL- and LL- grown cells (these results are summarized in Table 5.8).

It can be observed from these calibration curves, that for a given OD₆₅₀ (absorbance pathlength 1 cm), the number of cells is significantly less in samples grown under LL conditions relative to samples grown under conditions of HL intensity. The difference, however, as can be observed by comparing the calibration curves constructed for the species shown, is species specific, and depends to a large extent upon a species ability to grow, or adapt, to prevailing light conditions.

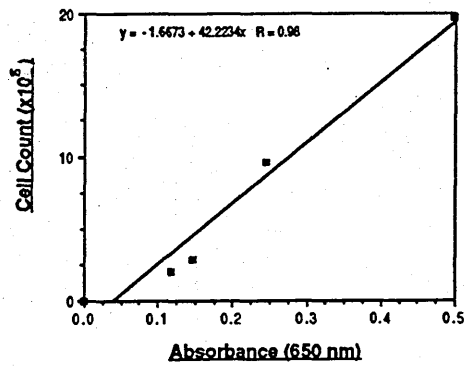
Cell Count of Rs. rubrum S1 LL



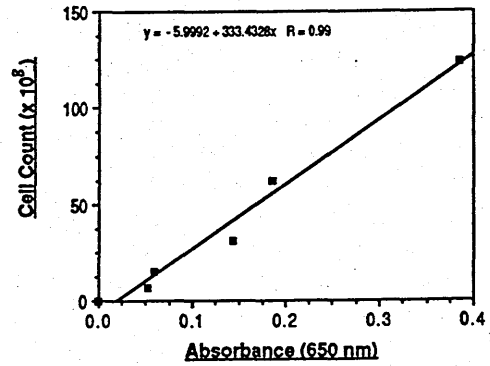
Cell Count of Rs. rubrum S1 HL



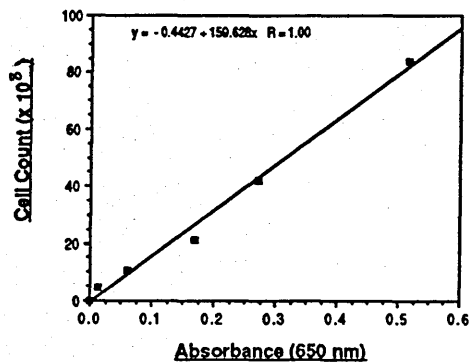
Cell Count of Rps. acidophila 7050 LL



Cell Count of Rc. gelatinosus 151 HL



Cell Count of Rc. gelatinosus 151 LL



Cell Count of Rps. acidophila 7050 HL

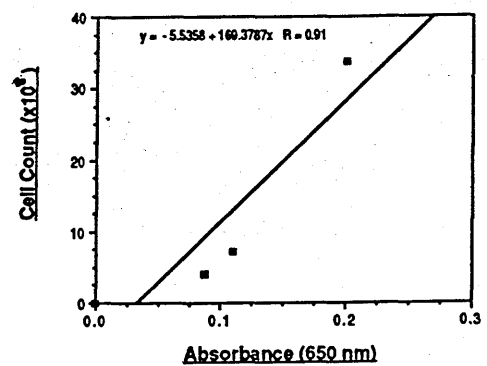


TABLE 5.8

**Examining the Ratio of Cell counts Estimated for a Sample
Species (of specific OD₆₅₀) Grown under Low- and High-
Light Intensity Conditions.**

<u>SPECIES</u>	<u>RATIO OF HL/LL CELL COUNTS</u>
<i>Rps. acidophila</i> 7050	4.0
<i>Rps. acidophila</i> 7750	2.7
<i>Rc. gelatinosus</i> 149	3.8
<i>Rc. gelatinosus</i> 151	2.1
<i>Rs. rubrum</i> S1	2.2

The ratio of HL to LL cells was estimated from the calibration curves (presented in Figure 5.12) relating the parameters of cell number with optical density at 650 nm.

The results presented above clearly show that the number of cells in a sample with specific OD₆₅₀, varies with respect to prevailing growth conditions. Determinations of this type, in conjunction with the examination of spectral properties (particularly of those species capable of producing additional antenna complexes under LL and HL intensity conditions ie. Type III species), and the determination of relative antenna ratios, provide useful assays for discriminating between cells grown under different light-intensity conditions, and can also be employed as indicators that specific HL and LL conditions have been successfully created. This latter confirmation was a prerequisite of those experiments comparing RC:BChl *a* ratios, determined for the RC-B875 antenna complexes isolated from HL- and LL- grown cells. From the results it can be concluded that HL and LL conditions were created, and that cells responded to these changes of light intensity by varying the relative amount of B800-

850 antenna complex. The ratio of RC:BChl a molecules was constant irrespective of prevailing conditions, thereby providing additional evidence to support the existence of a fixed stoichiometric core complex. The results also provide direct evidence supporting the early spectral predictions of Aagaard and Sistrom (1977), who suggested that under varying light-intensity conditions the ratio of reaction centre to B875 antenna complex remained constant, and that the relative amount of B800-850 antenna complex varied.

In conclusion, the results, taken as a whole, strongly support the existence of a variable component, and a fixed stoichiometric component, in the photosynthetic units of purple bacteria. Comparison of the RC:BChl a ratios determined for different species of bacteria reveals a degree of variation, which appears to be a consequence of the solubilization conditions adopted, rather than the result of natural species variation.

CHAPTER 6

Examination of the Polypeptide Composition of the Reaction Centre-B875 Antenna Conjugate.

The polypeptide composition of the reaction centre-B875 antenna conjugate, isolated from a range of bacteriochlorophyll a (BChl a)-containing purple bacterial species, was examined using the method of sodium dodecyl sulphate-polyacrylamide gel electrophoresis (SDS-PAGE). Two different types of gel were prepared; the first, a linear gel which is made up of a uniform acrylamide concentration, whereas the second, a polyacrylamide gradient gel (PAGGE), maintains a gradient of acrylamide ranging from high to low concentrations. Linear gels although producing good resolution of protein bands within a relatively narrow molecular weight range, have insufficient resolving power to separate polypeptides representing a wider range of molecular weights. A 16% polyacrylamide gel, for example, successfully resolves the polypeptide bands of the reaction centre but does not give adequate resolution of the low molecular weight (LMW) polypeptides of the antenna complex. This was overcome by employing linear gels of different concentrations ie. 18% and 12% for resolving components of the light-harvesting complex and reaction centre respectively. Figure 6.1 shows reaction centre components of the species *Rs. rubrum* strain S1 resolved on a 12% polyacrylamide gel. At this concentration the LMW antenna polypeptides are quickly 'run-off' the end of the gel, these polypeptides, however, were successfully separated on a 18% gel, in which the RC bands barely enter the resolving body of the gel.

Gradient gels provide an alternative method to employing two or

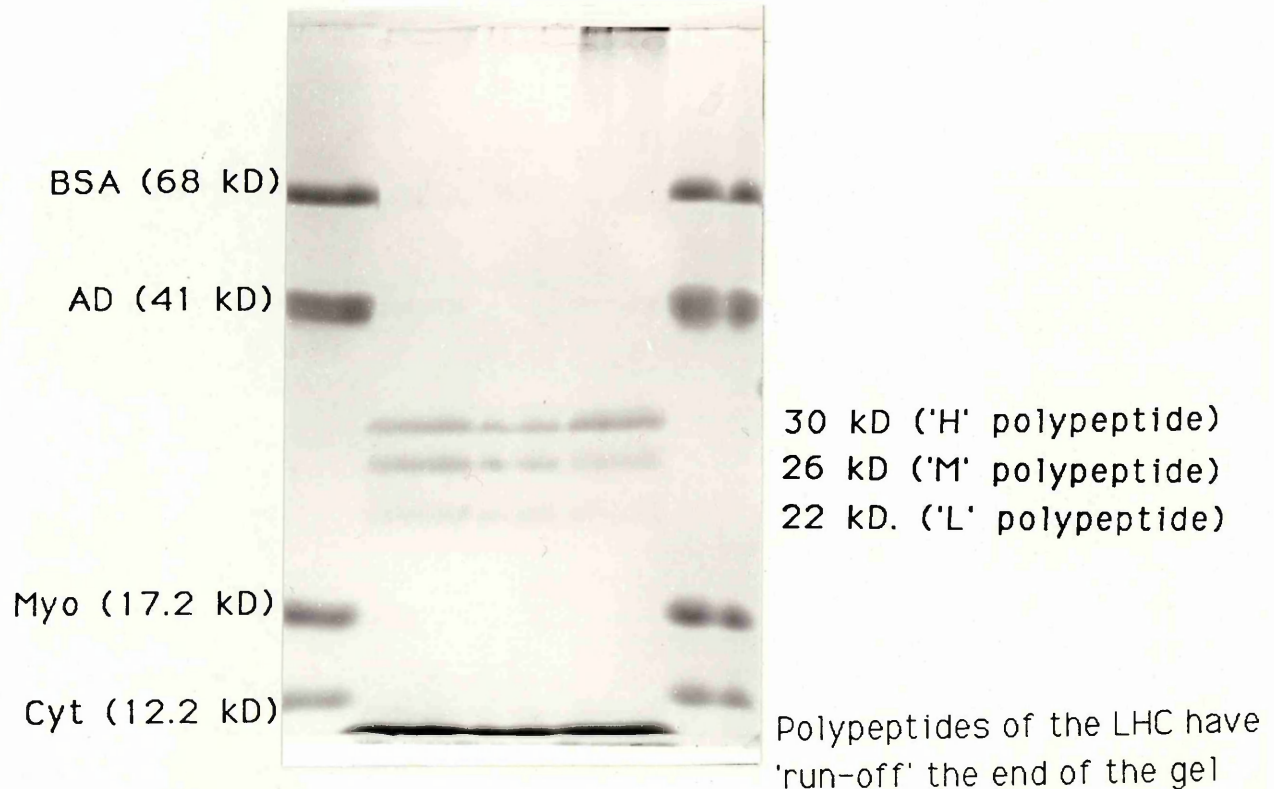


FIGURE 6.1 Separation of the Reaction Centre Polypeptide components of *Rhodospirillum rubrum* S1 RC-B890 Complex on a 12% (w/v) SDS-Polyacrylamide Gel.

The gel figure clearly shows the separation of the triad of polypeptides, H, M and L, characterizing the reaction centre complex. The LMW polypeptide constituents of the light-harvesting complex, are too small to be adequately resolved on a 12 % (w/v) polyacrylamide gel, and have consequently 'run-off' the end of the gel; gels of higher percentage acrylamide are required to resolve these bands.

The RC-B890 protein complex has been resolved along-side standard proteins (Bovine serum albumin (BSA), alcohol dehydrogenase (AD), myoglobin (Myo) and cytochrome c (Cyt)) of known molecular weight; construction of a calibration curve, relating the parameters of protein mobility and molecular weight, provides a technique for estimating the molecular weight of 'unknown polypeptides'. Referring to the calibration curve produced for this gel (presented in Figure 6.4a), the molecular weights of the H, M and L RC polypeptides are approximately 30 kD, 26 kD and 22 kD, respectively.

more gels of uniform concentrations, since, the greater resolving power obtained by electrophoresis through a gradient of acrylamide concentration, permits the resolution of polypeptides corresponding to a wider range of molecular weights. For example, gradient gels with a 'pore-gradient' ranging from 11.5% to 18% acrylamide can resolve polypeptides within the range of 5-40 kD, and can thus successfully resolve the polypeptide constituents of the RC-B875, or B800-850, antenna complexes. Figures 6.2 and 6.3 show the polypeptide composition of the RC-B875 and B800-850 antenna complexes resolved on 11.5%-18% polyacrylamide gradient gels. It can be clearly observed from these figures that, despite the existence of spectral and physiological variations between different species, the pattern of polypeptides, in terms of composition and size of respective components, are very similar. The reaction centre, showing a parallel polypeptide pattern in each species examined, consists of a triad of polypeptides referred to as L, M and H, or 'light','medium' and 'heavy' respectively. It is perhaps important to note here that although L, M and H refer to specific polypeptides of the reaction centre which band typically in the polyacrylamide gels at positions corresponding to light, medium and heavy molecular weight respectively, the actual amino acid compositions suggest that the designated H subunit is in fact the smallest polypeptide, and the M subunit is the largest [(Williams *et al*, 1983)(Youvan *et al*, 1984)]. The polypeptide composition of different species may appear to vary slightly depending upon the absence/presence of tightly associated cytochrome pigments. Those species that contain no tightly bound cytochrome (although they may contain a soluble cytochrome, C₂) are referred to as Type I, and include species such as *Rb. sphaeroides*, *Rb. capsulatus*, *Rs. rubrum* S1 and *Rps. palustris*. Type II species, such as *Rps. viridis*, *Chromatium vinosum*, *Rc.*

FIGURE 6.2 The Polypeptide Composition of the RC-B875 Antenna Complex of *Rhodocyclus gelatinosus* 149, *Rhodopseudomonas blastica* and *Rhodopseudomonas palustris* 'French'.

The figure presents the typical polypeptide composition of the RC-B875 antenna complex of the species *Rc.gelatinosus* 149, *Rps.blastica* and *Rps.palustris* 'French', as resolved by SDS-polyacrylamide gradient gel electrophoresis (SDS-PAGE). The polypeptides were resolved on an 11.5 % - 18 % (w/v) polyacrylamide gel. In all examples the two LMW polypeptides constituent of the B875 antenna complex can be observed to band low-down in the gel; banding at a higher gel position, are the three RC polypeptides (H, M and L). The 'L' polypeptide band of the RC complex, however, is not so clearly distinguished; this polypeptide is frequently observed as a dimer, for example, a dimer of the L polypeptide is observed, in the case of *Rhodopseudomonas blastica*, in a position corresponding to a molecular weight (M_r) of approximately 28 kD.

A distinct band, indicating a polypeptide of approximate molecular weight 49 kD, can be observed by examination of the resolution pattern produced for the RC-B875 complex of *Rhodocyclus gelatinosus* 149. This band is believed to represent the tightly bound cytochrome pigment which is typically associated with the RC-polypeptides of this species.

The sample proteins were resolved along-side standard proteins (Bovine serum albumin (BSA), alcohol dehydrogenase (AD), myoglobin (Myo) and cytochrome c (Cyt)) of known molecular weight. Estimates of the M_r of the sample polypeptides were obtained from the calibration curve (presented in Figure 6.4b) relating the parameters of molecular weight and mobility of these standard proteins.

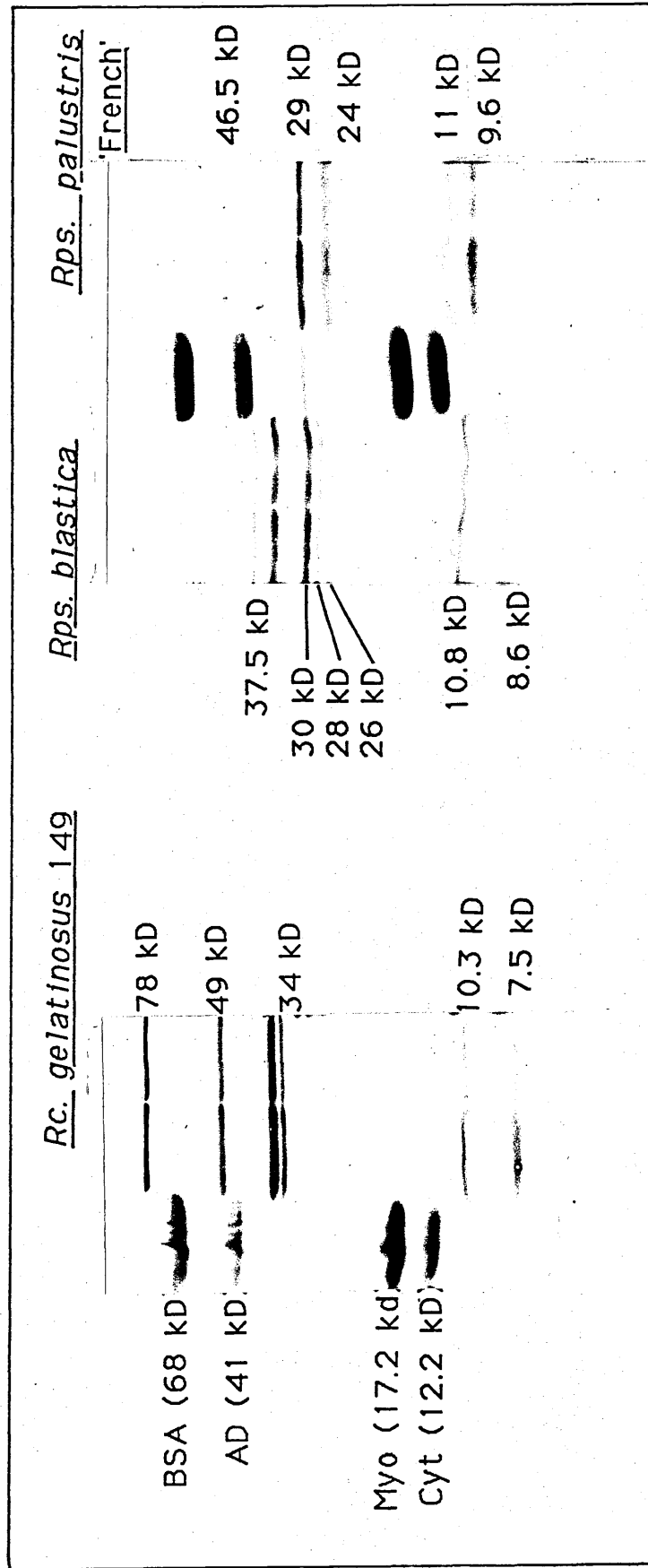
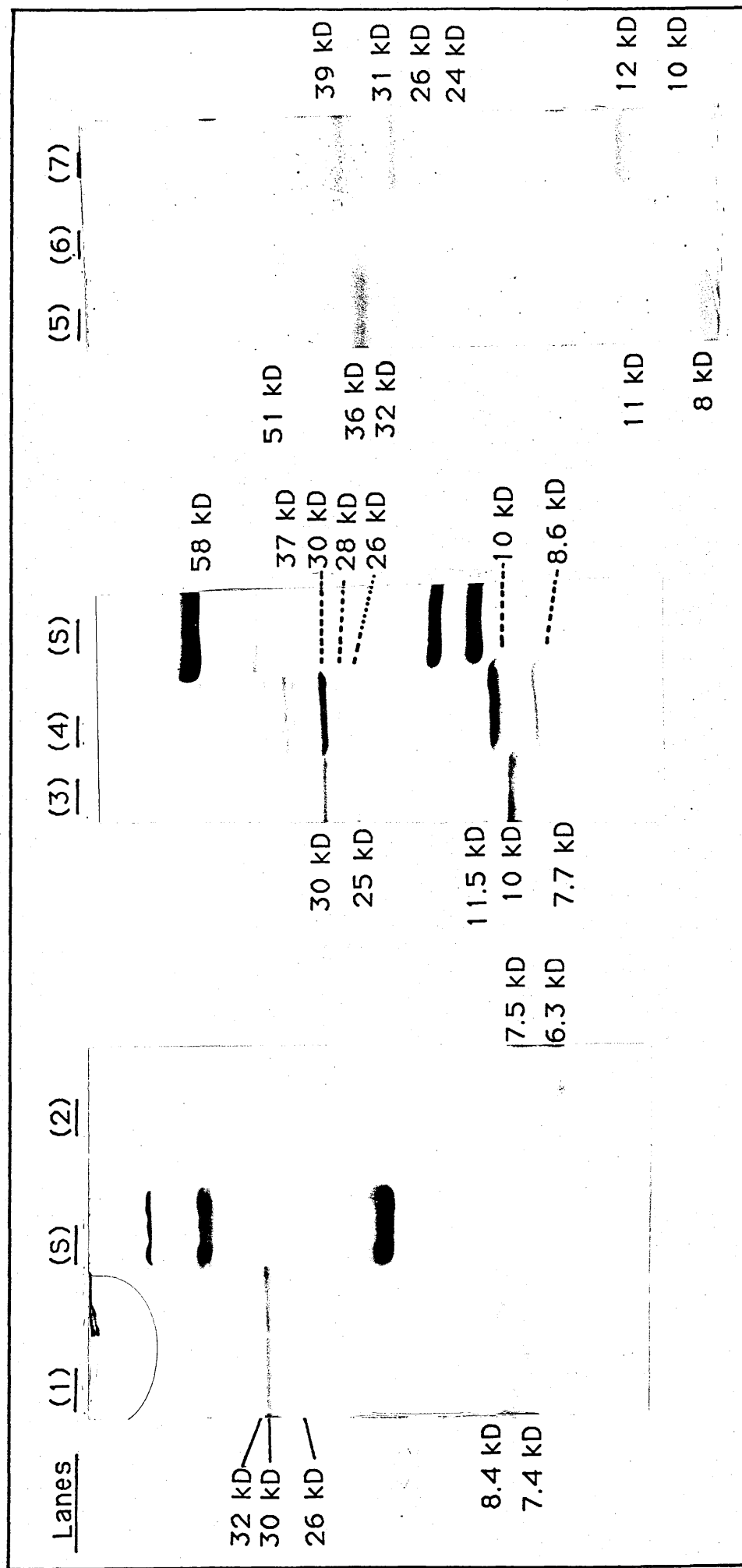


FIGURE 6.3 The Polypeptide Composition of the RC-B875 Antenna Complex of *Rs.rubrum* S1, *Rps. blastica*, *Rps. palustris* 'French', *Rc.gelatinosus* 149 and 151, and the B800-850 antenna complex of *Rps. palustris* 'French'.

The gel figures presented above show the typical polypeptide composition of the RC-B875 antenna complex of *Rs.rubrum* S1 (1), *Rps. blastica* (3, 7), *Rps. palustris* 'French' (4), *Rc.gelatinosus* 149 (5) and 151 (6). In all examples the two low molecular weight polypeptide constituents of the B875 antenna complex band low-down in the gel. The three RC polypeptides (H, M and L) band at a higher gel position. The L-polypeptide is observed here for the RC-B875 complex of *Rps. blastica* and *Rc. gelatinosus* 149 as a dimer.

The B800-850 antenna complex of *Rps. palustris* 'French' has been resolved in lane (2) and is typically observed to consist of two LMW polypeptides.

The polypeptides were resolved on an 11.5 % - 18 % (w/v) SDS-polyacrylamide gradient gel. The sample proteins were resolved along-side standard proteins (S) Bovine serum albumin (BSA), alcohol dehydrogenase (AD), myoglobin (Myo) and cytochrome c (Cyt) with molecular weights 78 kD, 41 kD, 17.2 kD and 12.2 kD respectively. Estimates of the M_r of the sample polypeptides were obtained from a calibration curve relating the parameters of molecular weight and mobility of these standard proteins.



gelatinosus and *Rps. acidophila*, however, do contain a strongly-bound cytochrome (c-type) which serves to donate electrons to the photo-oxidized BChl a dimer [Matsuura and Shimada, 1986]. Examining the polypeptide composition of *Rc. gelatinosus* 149 (Figure 6.2) a distinct band with apparent molecular weight 49 kD can be observed, this probably represents the bound cytochrome subunit.

The B875, and B800-850, light-harvesting complexes, consist of two different types of LMW polypeptides, α and β , although in some species, for example *Rb. capsulatus*, a third, Y, has been observed [(Feick and Drews, 1978)(Amesz, 1979)]. Those species which contain the additional B800-820 antenna complex also appear to have two additional LMW polypeptides, for example *Rps. acidophila* 7050 grown at low-light intensity [Cogdell *et al*, 1983] and *Rps. acidophila* 7750 grown at low temperatures [Schmidt *et al*, 1987].

The polypeptide compositions described are observed in the gel figures ie. the triad of RC bands appearing high up in the gel body, with the two antenna bands appearing lower in the gel plate. In addition to these major bands, a few, generally faint bands of intermediate-high molecular weight, can also be observed. These bands suggest that the sample either contains additional contaminant proteins or alternatively, suggest the presence of polypeptide aggregates. Since no attempts were made to further purify the complex prior to electrophoresis, contamination is plausible. However, since most of the 'additional' bands occur in a relatively high position in the gel they are more likely to represent protein aggregates, either due to incomplete dissociation of polypeptides during sample preparation, ie. samples are prepared by heating at 100°C for 90 seconds in the presence of SDS and β -mercaptoethanol, which serve to break down disulphide bonds and

dissociate the complex into its constituent polypeptide components, or the consequence of excessive heating causing the aggregation of polypeptides [Tanaka *et al*, 1983].

An estimate of the molecular weight of the polypeptide components was determined by comparing the mobility (distance travelled) of each band with those of proteins of known molecular weight. Standard proteins, Bovine Serum Albumin (BSA), alcohol dehydrogenase, Myoglobin and cytochrome *c* with respective weights 68 kD, 41 kD, 17.2 kD and 12.2 kD, were run on each gel and a calibration curve, relating the logarithm of molecular weight with mobility, was then used to determine the molecular weight of each polypeptide band according to its position on the gel (Figure 6.4). Table 6.1 summarizes the molecular weights of the polypeptide constituents of each species complex examined, these can be compared with those estimates already established for a few species which are also summarized in Table 6.1. It can be seen that the molecular weights determined for each species although comparable, do exhibit a small degree of variation both between values obtained from different gels, and also with respect to established values. These results emphasize the fact that molecular weight as determined by SDS-PAGE is best regarded as an 'Rf' value; the absolute value reflecting differences in PAGE-techniques and changes in prevailing experimental conditions. It should also be noted at this point that this estimate is approximately 30% less than the true molecular weight as determined by amino acid sequencing [Loach, 1980]. For example, the molecular weights of those polypeptides isolated from the reaction centre of *Rb. sphaeroides* are 21 kD, 24 kD and 28 kD as determined by SDS-PAGE, or 28 kD, 32 kD and 36 kD respectively, as determined by amino acid analysis [Sutton *et al*, 1982]. It has also been reported that SDS-PAGE should not be used for

FIGURE 6.4 (a & b) Calibration Curves Determined for Standard Proteins; Relating the Parameters of Molecular Weight with Polypeptide Mobility in SDS-Polyacrylamide Gels.

A calibration curve was produced for each gel examined; the molecular weights ($\ln M_r$) of standard proteins were plotted with respect to their mobility (measured as distance travelled, cm) in SDS-polyacrylamide gels. The standard proteins included bovine serum albumin (M_r 68 kD), alcohol dehydrogenase (M_r 41 kD), myoglobin (M_r 17.2 kD) and cytochrome C (M_r 12.2 kD). A line of 'best-fit' (a 'least squares' regression line) was drawn through the points, thereby relating the two parameters (The equation describing the relationship between the two parameters is presented with each calibration curve, R denotes the 'fit' of the line). The molecular weights of unknown polypeptides were determined from their respective calibration curves.

Figures 6.4 a & b present calibration curves produced for gels shown in Figures 6.1 and 6.2 respectively.

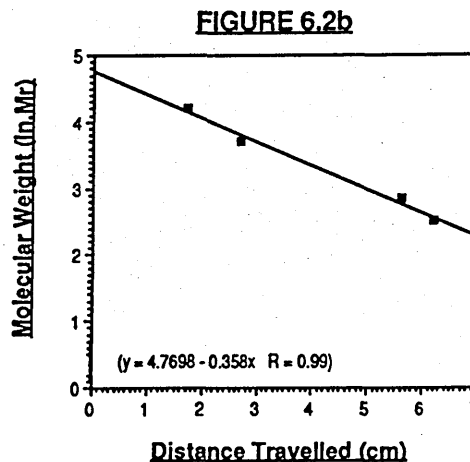
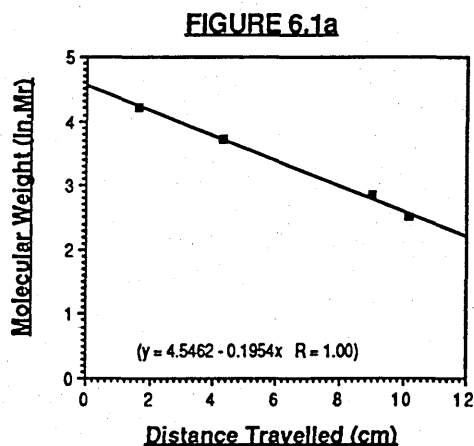


Table 6.1: The size and polypeptide composition of RC-B875 antenna complexes as determined by SDS-PAGE. The average values presented can be compared with those values established by other workers* employing SDS-PAGE.

<u>Strain</u>	<u>Complex</u>	<u>Average Mr.</u> (as determined by SDS-PAGE).	<u>Established Mr.</u> (as determined by SDS-PAGE).
<i>Rps. palustris</i>	B800-850 α	8.0 \pm 0.4 kd (n=3)	9 kd
	B800-850 β	7.0 \pm 0.2 kd (n=3)	8 kd
	RC-B875 H	45 \pm 5.0 kd (n=3)	38 kd
	M	31 \pm 1.1 kd (n=3)	36 kd
	L	27 \pm 2.9 kd (n=3)	33 kd
	α	12 \pm 1.8 kd (n=3)	11 kd
	β	10 \pm 1.4 kd (n=3)	10 kd
<i>Rs. rubrum</i> S1	RC-B890 H	44 \pm 6.8 kd (n=5)*	29 kd
	M	33 \pm 1.6 kd (n=5)*	26 kd
	L	27 \pm 1.3 kd (n=5)*	22 kd
	α	10 \pm 1.2 kd (n=5)	7.6 kd
	β	8 \pm 0.9 kd (n=5)	6.4 kd
(*- The Mr of the H, M and L polypeptides of <i>Rs. rubrum</i> S1 on a linear 12% polyacrylamide gel were determined as 29 kd, 26 kd, and 22 kd respectively)			
<i>Rc. gelatinosus</i> 149	RC-B875 H	36 \pm 2.0 kd (n=3)	33 kd
	M	33 \pm 3.8 kd (n=3)	25 kd
	L	25 \pm 3.5 kd (n=3)	?
	α	11 \pm 1.2 kd (n=3)	—
	β	8 \pm 0.2 kd (n=3)	—
<i>Rc. gelatinosus</i> 151	RC-B875 H	39 \pm 0 kd (n=3)	33 kd
	M	37 \pm 0.9 kd (n=3)	25 kd
	L	30 \pm 1.2 kd (n=3)	—
	α	11 \pm 1.1 kd (n=3)	—
	β	7 \pm 1.1 kd (n=3)	—
<i>Rps. acidophila</i> 7750	RC-B875 H	41 \pm 1.6 kd (n=3)	
	M	34 \pm 1.4 kd (n=3)	
	L	15 \pm 2.3 kd (n=3)	
	α	10 \pm 1.1 kd (n=3)	
	β	8 \pm 0.8 kd (n=3)	
<i>Rps. acidophila</i> 7050	H	51 kd (n=1)	
	L	38 kd (n=1)	
	M	32 kd (n=1)	
	α	15 kd (n=1)	
	β	9 kd (n=1)	

*[(Ueda *et al*, 1985)(Drews, 1985)]

determining the molecular weight of polypeptides less than 15 kD due to the formation of rod-shaped SDS-polypeptide complexes which give rise to anomalous mobilities [Reynolds and Tanford, 1970]. It seems therefore, that SDS-PAGE although providing a rapid and convenient method for examining the polypeptide composition of a protein complex, only provides an estimate of the molecular weight, and that real determinations demand the employment of amino acid or sequence analysis techniques. With respect to these limitations, SDS-PAGE has allowed the examination of the polypeptide composition of the isolated RC-B875 and B880-850 complexes. By comparing these results with pre-established compositions, it can be concluded that the isolated complexes are intact as regards their polypeptide composition.

CHAPTER 7

Examining the Functional Integrity of the RC-B875

Antenna Complex.

Most of the light energy used in photochemistry by purple photosynthetic bacteria is not absorbed directly by the reaction centre but is collected by light-absorbing pigments, namely bacteriochlorophyll (BChl) and carotenoids, which in turn direct the excitation energy to the reaction centre.

The molecules of bacteriochlorophyll are associated with different pigment pools depending upon their spectral properties: the various pools exhibit absorption maxima at, or near to, 800nm, 820nm, 850nm and 875nm (890nm) and are referred to as B800, B820, B850 and B875 (B890) respectively. The exact pigment composition of the photosynthetic apparatus is species variable; for example, *Chromatium vinosum* strain D can exhibit all of the spectral forms, whereas *Rs. rubrum* strain S1 has only the B890 spectral form. However, irrespective of pigment composition the role of light-harvesting complexes is to funnel energy to the photochemical reaction centres where it is harnessed in the electron-transfer reaction yielding oxidized P870. If the reaction centre is not photochemically active the energy is dissipated as fluorescence. These two processes therefore, can be regarded as competitive, and their measurement can provide invaluable information about energy transfer processes, and about the relative organization of light-harvesting complexes and reaction centres. Measurement of excitation spectra of fluorescence, and fluorescence emission spectra, can provide direct quantitative evidence about the efficiency and direction of energy-transfer between pigments. For most bacteriochlorophyll a-containing

purple bacteria it has been shown that nearly all fluorescence excited by visible or NIR radiation is emitted by the antenna BChl absorbing at the longest wavelength, ie. B870 (B890) [(Duysens, 1952)(Goedheer, 1973)]. This provides strong evidence for the efficient transfer of energy from bacteriochlorophylls absorbing at shorter wavelengths to those absorbing at longer wavelengths. Analyses of this type can also be applied to the examination of the functional integrity of isolated complexes, since any blockage in, or disruption of, this energy transfer process will cause an increase in the level of fluorescence emitted. This latter aspect is of importance in this particular area of study, since the RC-B875 antenna complex isolated from each species considered, requires examination to ensure that the light-harvesting BChl a is functionally connected to the reaction centre, and that the conjugate complex is still representative of its *in situ* state. A number of approaches can be made in examining energy transfer processes and efficiencies, but the one of particular importance, and which forms the basis of most techniques, is the measurement of fluorescence yields and/or lifetimes.

Examination of the fluorescence emission spectra of a particular species indicates the wavelength at which peak fluorescence can be detected. This information is, in itself, essential for measuring the action spectra of fluorescence. Figures 7.1 (a,b & c) show typical emission spectra of the species *Rhodobacter sphaeroides* R26, *Rhodocyclus gelatinosus* strain 149 and *Rhodopseudomonas palustris* strain 'French'. These species are representative of the species classification Types I, II and III respectively ie. the division of Types is based on NIR spectral properties, with Type I species exhibiting absorption spectra characteristic of RC and B875 (B880) absorption, Type II exhibiting maximal absorption at 800nm and 850nm in addition to

FIGURE 7.1 (a, b & c) Room and Low Temperature Fluorescence Spectra Produced for the RC-B875 Antenna Complex Isolated From the Species *Rb. sphaeroides* R26, *Rc. gelatinosus* 149 and *Rps. palustris* 'French'.

The fluorescence emission spectra were recorded for each RC-B875 antenna complex sample at the temperatures (T) 270 K, 110 K and 10 K, using a Cary 14 Spectrophotometer. The samples were excited with light of wavelength (λ) 380 nm, and fluorescence emission was monitored in the 700 nm – 1000 nm spectral range. Each sample generated a single emission peak in the NIR region of the spectrum. The intensity of the peak was observed to increase inversely with temperature, ie. as temperature was reduced the intensity of the fluorescence peak increased (the magnitudes of the emission peaks, as presented in the spectra, have been multiplied X fold).

The RC-B875 antenna complexes were isolated by sucrose density-gradient fractionation of detergent solubilized photosynthetic membranes, and then concentrated on DE52 columns. The concentrated samples were diluted with glycerol buffer (70 % glycerol: 30 % 10 mM Tris-HCl, pH 8.0) in order to maintain a clear glass at low temperatures.

Spectral analyses were kindly completed by J. Ullrich at the Physics Institute, University of Stuttgart, W. Germany.

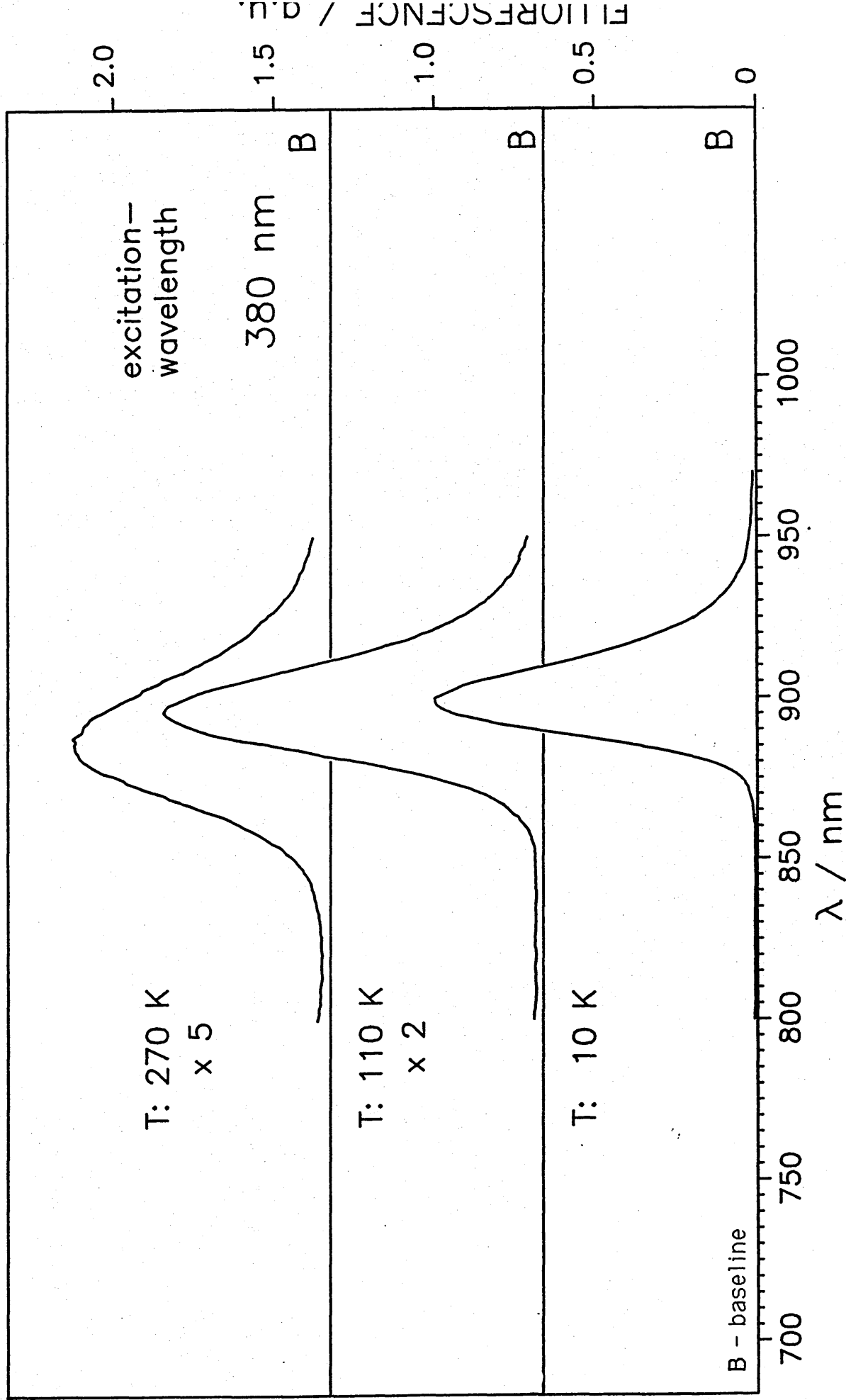


FIGURE 7.1a Room and Low Temperature Fluorescence
Emission Spectra for the RC-B875 Antenna Complex of *Rb.*
sphaeroides R26.

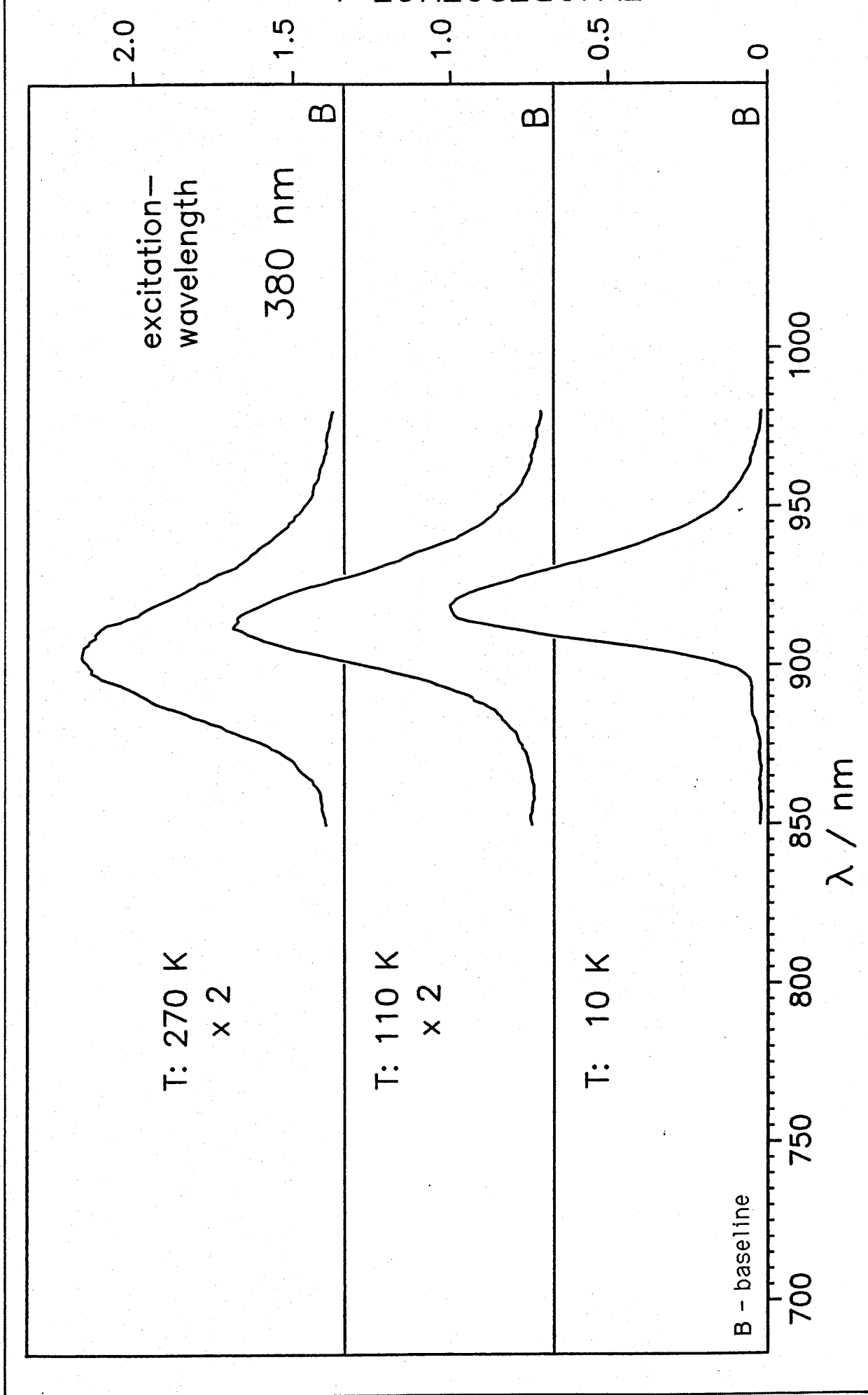


FIGURE 7.1b Room and Low Temperature Fluorescence
Emission Spectra for the RC-B875 Antenna Complex of *RC*.

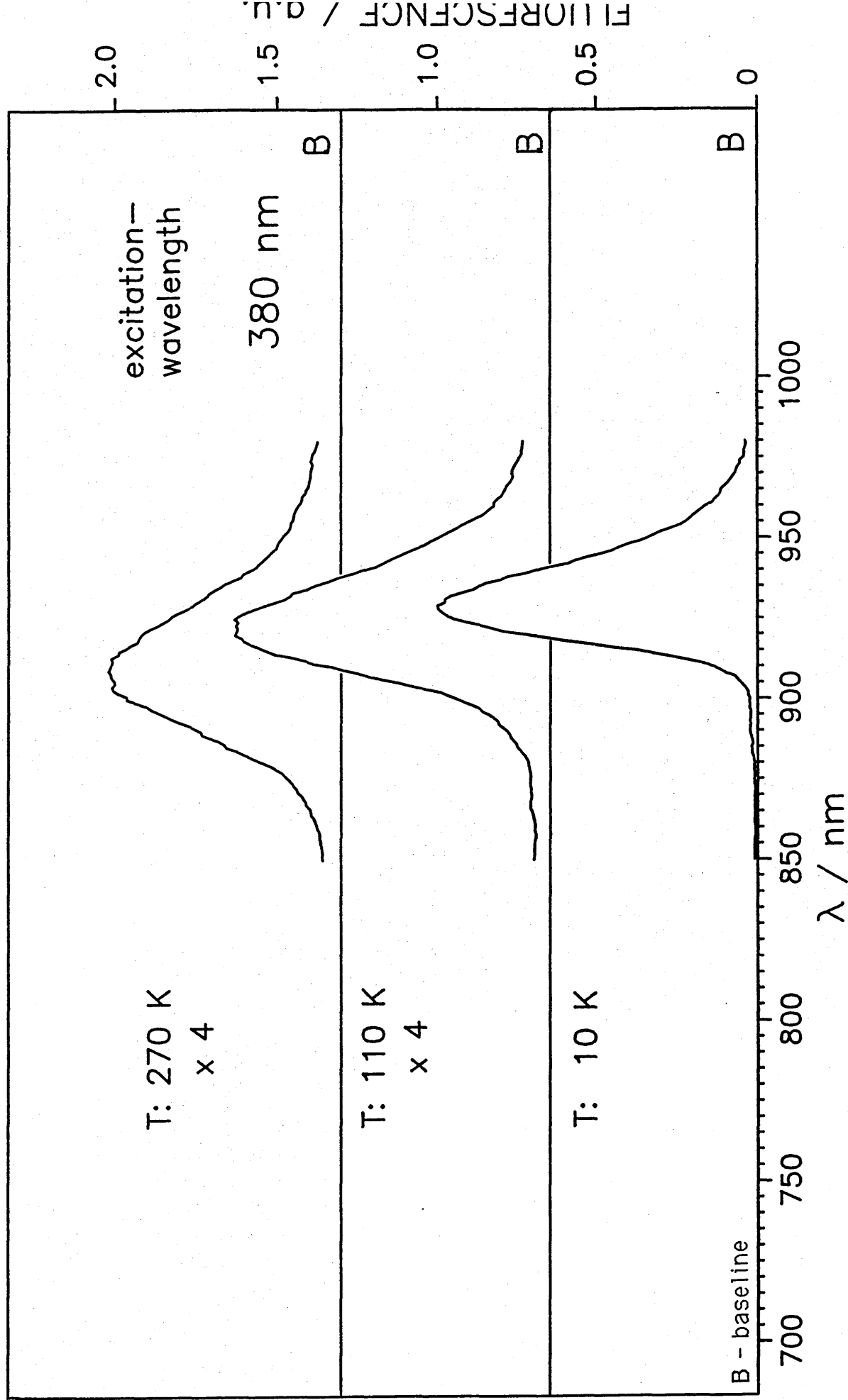


FIGURE 7.1c Room and Low Temperature Fluorescence
Emission Spectra for the RC-B875 Antenna Complex of *Rps.*
rubra 'French'

RC-B875 absorption, and Type III expressing absorption maxima characteristic of the three main BChl *a* pools B800-820, B800-850 and RC-B875. These spectra illustrate the temperature-dependency of fluorescence emission, such that, as the temperature is reduced from 270K to 10K, the emission band becomes sharper, increases in height, and also becomes shifted towards longer wavelengths. This latter effect is clearly seen in the spectra, and also in the information presented in Table 7.1, which summarizes the wavelengths corresponding to peak fluorescence emissions for each species at each of the temperatures 270K, 110K and 10K.

TABLE 7.1

**Summary of the NIR-emission maxima of the RC-B875
antenna complexes determined at room and at low
temperatures.**

<u>SPECIES</u>	<u>EMISSION (nm).</u>		
	<u>270K</u>	<u>110K</u>	<u>10K</u>
<i>Rps. palustris</i> 'French'	908	923	929
<i>Rps. palustris</i> 'DSM'	899	912	895,922
<i>Rc. gelatinosus</i> 149	904	914	919
<i>Rc. gelatinosus</i> 151	902	911	886,918
<i>Rps. blastica</i>	—	915	890,915
<i>Rs. rubrum</i> S1	897	910	916
<i>Rps. acidophila</i> 7050	904	919	921
<i>Rps. acidophila</i> 7750	908	—	929
<i>Rb. sphaeroides</i> R26	887	896	899

Excitation spectra of fluorescence were also recorded for each species, and the effect of temperature on these spectra was examined. Light corresponding to wavelengths throughout the

spectral range of 300nm to 950nm was employed to energize RC-B875 antenna complexes of each species. Fluorescence emission from consecutive excitations was measured at the wavelength corresponding to peak fluorescence emission for a particular species with respect to temperature, ie. since the band of peak fluorescence emission shows a shift to longer wavelengths as the temperature is reduced, so the wavelength of fluorescence detection becomes red-shifted. Figures 7.2 (a, b & c) show typical excitation spectra of fluorescence for the species *Rhodobacter sphaeroides* R26, *Rhodocyclus gelatinosus* 149 and *Rhodopseudomonas palustris* 'French'. The excitation spectra, recorded at room temperature (270K) and at the lower temperatures of 110K and 10K also exhibit temperature dependency such that at low temperatures, bands become sharper and NIR peaks become more red-shifted. The excitation spectra of fluorescence for each species examined show considerable similarity to their respective absorption spectra having peaks arising from the Soret, Qx and Qy absorption bands of BChl *a*. The contribution from the RC absorption band is relatively small, or as in some cases, particularly at room temperature, negligible, for example *Rs. rubrum* S1, *Rc. gelatinosus* 149 and *Rps. sphaeroides* R26. The contribution from the carotenoids is species variable, with some species, such as *Rps. blastica* and *Rc. gelatinosus* strains 149 and 151, showing prominent peaks in the region corresponding to carotenoid absorption. In contrast, *Rps. palustris* strains 'French' and 'DSM8252' show a much smaller contribution, and strains 7050 and 7750 of *Rps. acidophila* and the carotenoidless mutant *Rb.sphaeroides* R26 showing no contribution. The efficiency of carotenoid to bacteriochlorophyll singlet-singlet energy transfer, measured as a function of temperature, was calculated for the species *Rc. gelatinosus* 149 and *Rps. palustris* 'French'. Figure

FIGURE 7.2 (a, b & c) Excitation Spectra. Recorded at Room and Low Temperatures, of the RC-B875 Antenna Complex of *Rb. sphaeroides* R26, *Rc. gelatinosus* 149 and *Rps. palustris* 'French'.

The excitation spectra were recorded for each sample at temperatures (T) 270 K, 110 K and 10 K, using a Cary 14 Spectrophotometer'. The samples were excited with each wavelengths of light throughout the spectral range from 300 nm to 900 nm. Fluorescence from consecutive emissions was measured at the wavelength corresponding to peak fluorescence emission for a particular sample at a specific temperature (predetermined from the fluorescence emission spectra presented in Figure 7.1).

The magnitude of the excitation spectra of fluorescence is observed to be temperature-dependent; with lower temperatures yielding greater fluorescence emissions (the magnitude of the spectral peaks, as presented in the figures, have been increased by X fold).

The RC-B875 antenna complexes were isolated by sucrose density-gradient fractionation of detergent solubilized photosynthetic membranes, and then concentrated on DE52 columns. The concentrated samples were diluted with glycerol buffer (70 % glycerol: 30 % 10 mM Tris-HCl, pH 8.0) in order to maintain a clear glass at low temperatures.

Spectral analyses were kindly completed by J. Ullrich at the Physics Institute, University of Stuttgart, W. Germany.

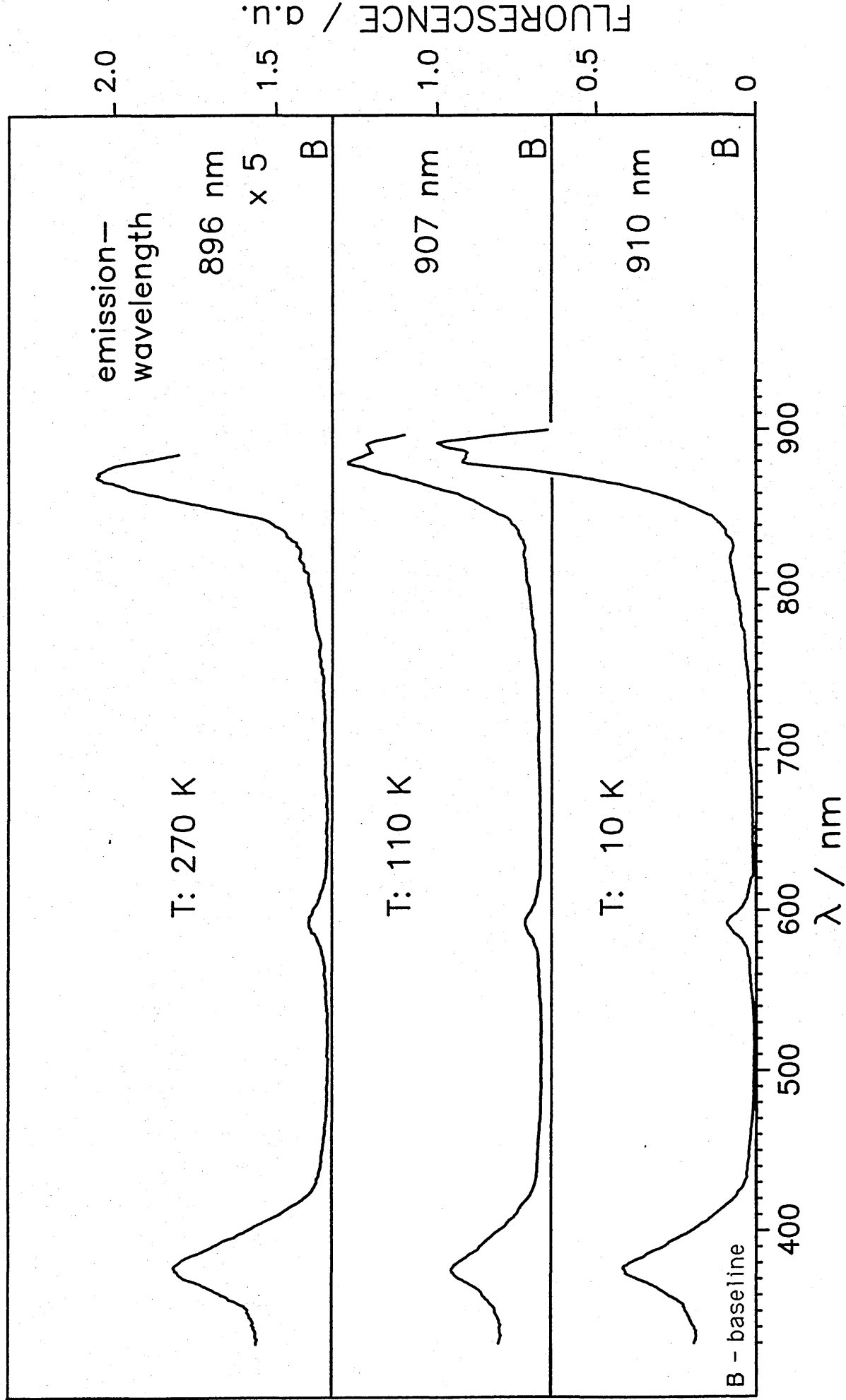


FIGURE 7.2a Excitation Spectra Recorded at Room and Low
Temperatures for the RC-B875 Antenna Complex of *Rb.*
enhanced D26

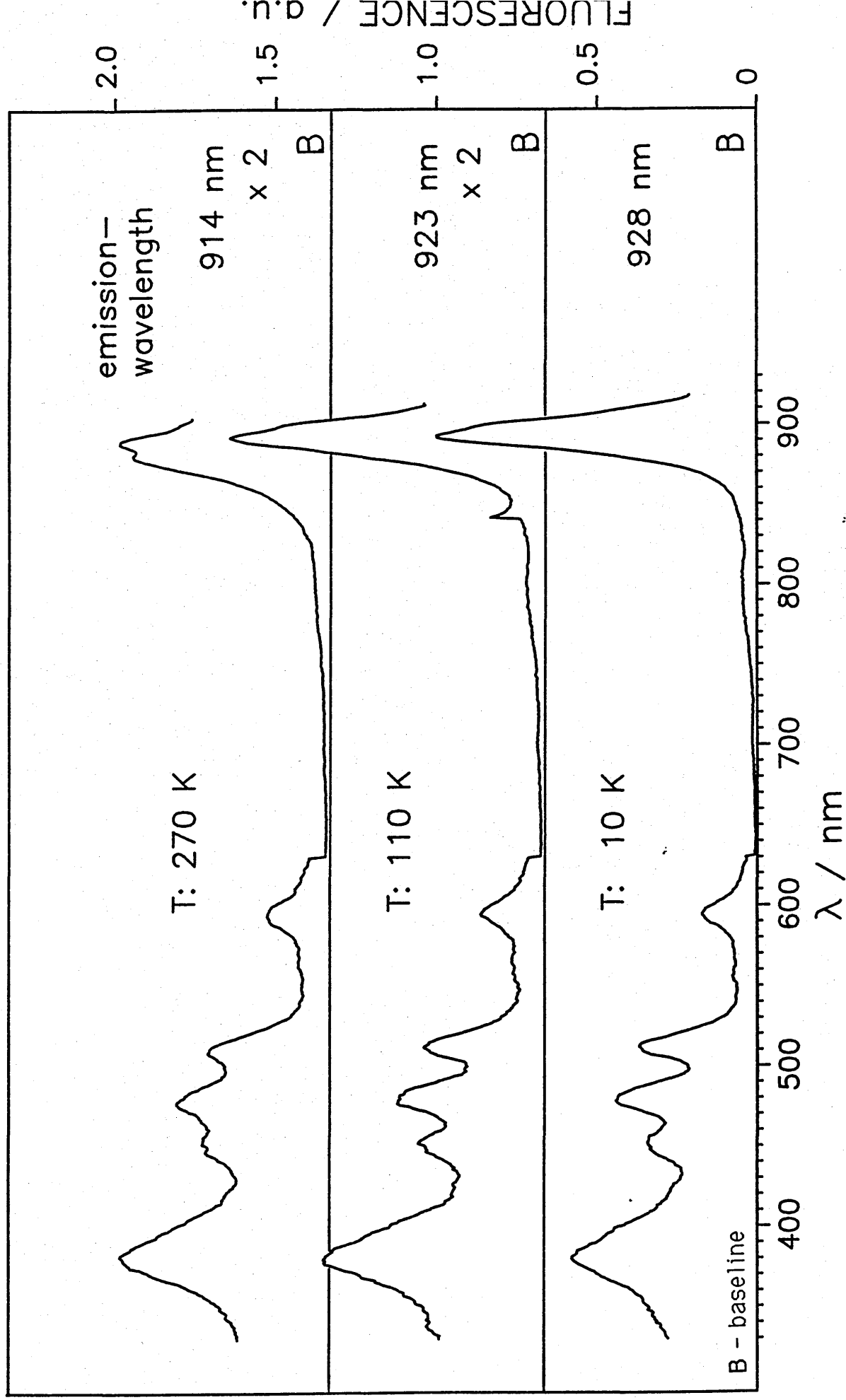


FIGURE 7.2b Excitation Spectra Recorded at Room and Low Temperatures for the RC-B875 Antenna Complex of *Rc. rubrum* 149.

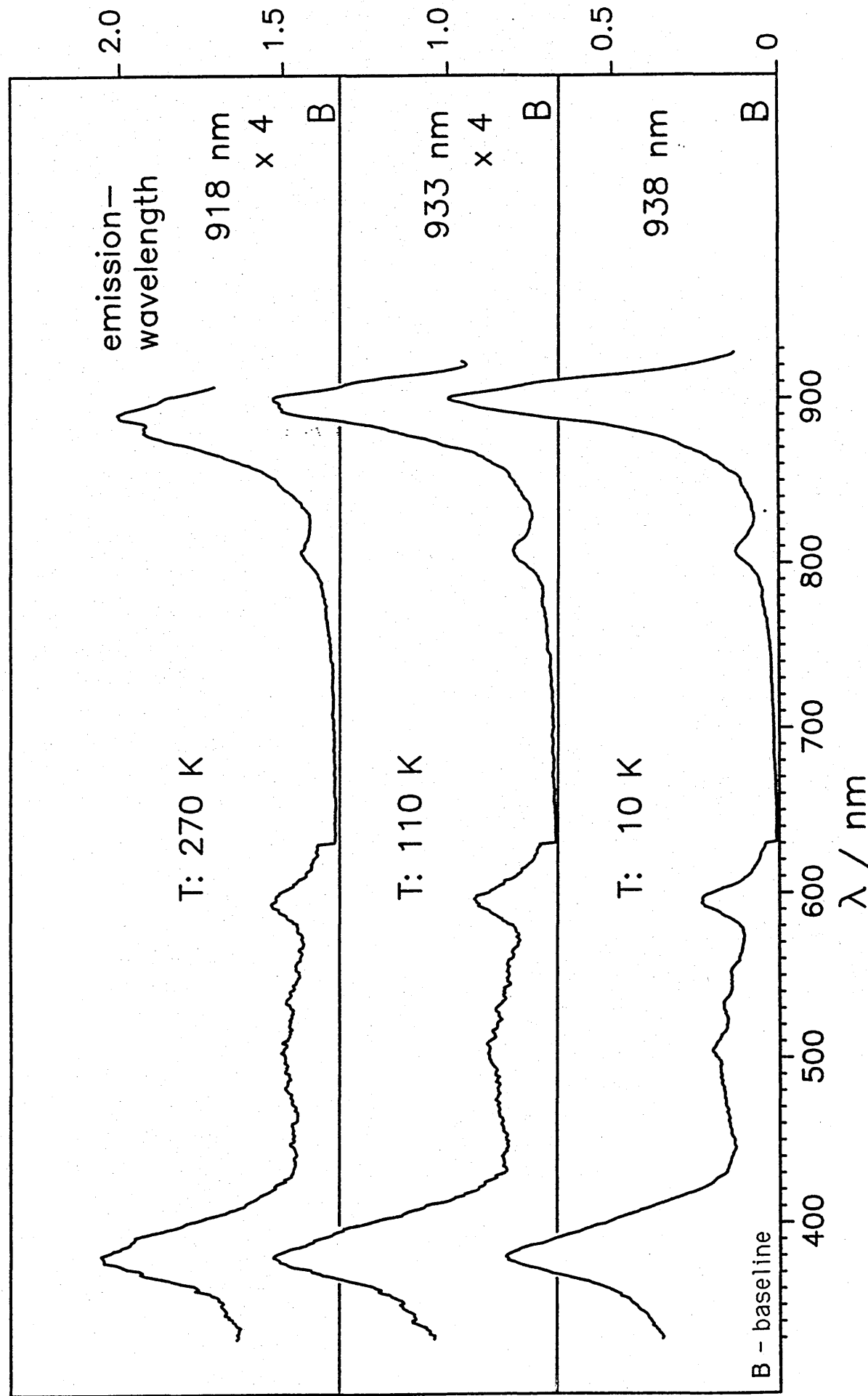


FIGURE 7.2c Excitation Spectra Recorded at Room and at Low Temperatures for the RC-B875 Antenna Complex of *Rps. palustris* French.

7.3 (a & b) and Table 7.2 summarize the energy transfer efficiencies calculated for these two species.

TABLE 7.2.

**Energy Transfer Efficiency from Carotenoid to BChl a in
the RC-B875 complex of *Rc. gelatinosus* 149 and *Rps.*
palustris 'French'**

<u>Species</u>	<u><i>Rc. gelatinosus</i> 149</u>		<u><i>Rps. palustris</i> 'French'</u>	
<u>Temp.(K)</u>	<u>Efficiency</u>	<u>% Error</u>	<u>Efficiency</u>	<u>% Error</u>
10	67	10	31	10
20	68	10	—	—
30	77	10	30	10
70	76	10	32	10
110	62	10	32	10
150	61	10	41	10
190	79	10	42	10
230	67	10	41	10
270	69	10	34	10

The efficiencies of energy transfer, measured as a function of temperature, were calculated from the ratio of carotenoid peak heights at 530 nm in the fluorescence action spectrum to the corresponding peak in the absorption spectrum after the two spectra had been normalized at the 590 nm BChl a absorption peak

It can be observed here, as it has been previously demonstrated [(van Grondelle *et al*, 1983)(Angerhofer *et al*, 1986)], that the efficiency of singlet-singlet energy transfer is temperature independent (the temperature dependence of fluorescence emission

FIGURE 7.3 (a & b) Energy Transfer Efficiencies of the RC-B875 Antenna Complex of *Rc. gelatinosus* 149 and *Rps. palustris* 'French'.

The Figures 7.3 a & b illustrate the efficiency of carotenoid to bacteriochlorophyll singlet-singlet energy transfer, measured as a function of temperature (K), for the RC-B875 antenna complex of the species *Rc. gelatinosus* 149 and *Rps. palustris* 'French' respectively.

The percentage efficiency of energy transfer was calculated from the ratio of carotenoid absorption peaks at 530 nm in the fluorescence action and absorption spectra, after the spectra had been normalized for the BChl a absorption peak at 590 nm. (Error bars indicate percent error in calculating efficiencies of energy transfer).

It can be seen from the figures that energy transfer efficiencies are temperature independent, and are also species-specific, ie. the species *Rc. gelatinosus* 149 is observed to exhibit significantly higher energy transfer efficiencies than *Rps. palustris* 'French', irrespective of temperature.

Spectral analyses were kindly completed by J. Ullrich at the Physics Institute, University of Stuttgart, W. Germany.

FIGURE 7.3a Energy Transfer Efficiencies of the RC-B875
Antenna Complex of *Rc. gelatinosus* 149.

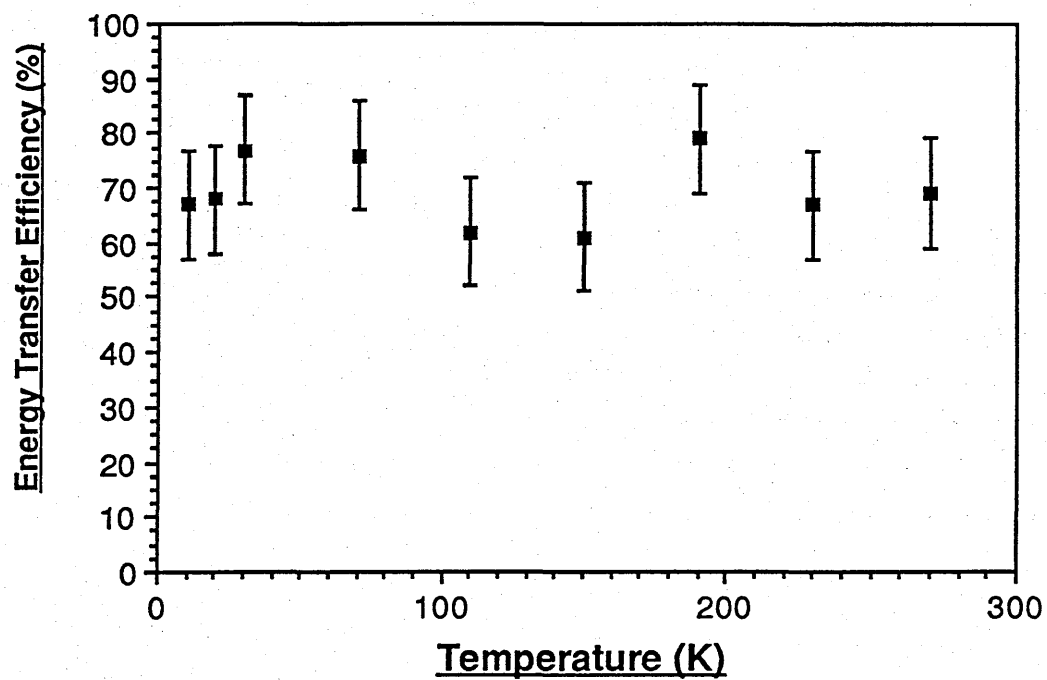
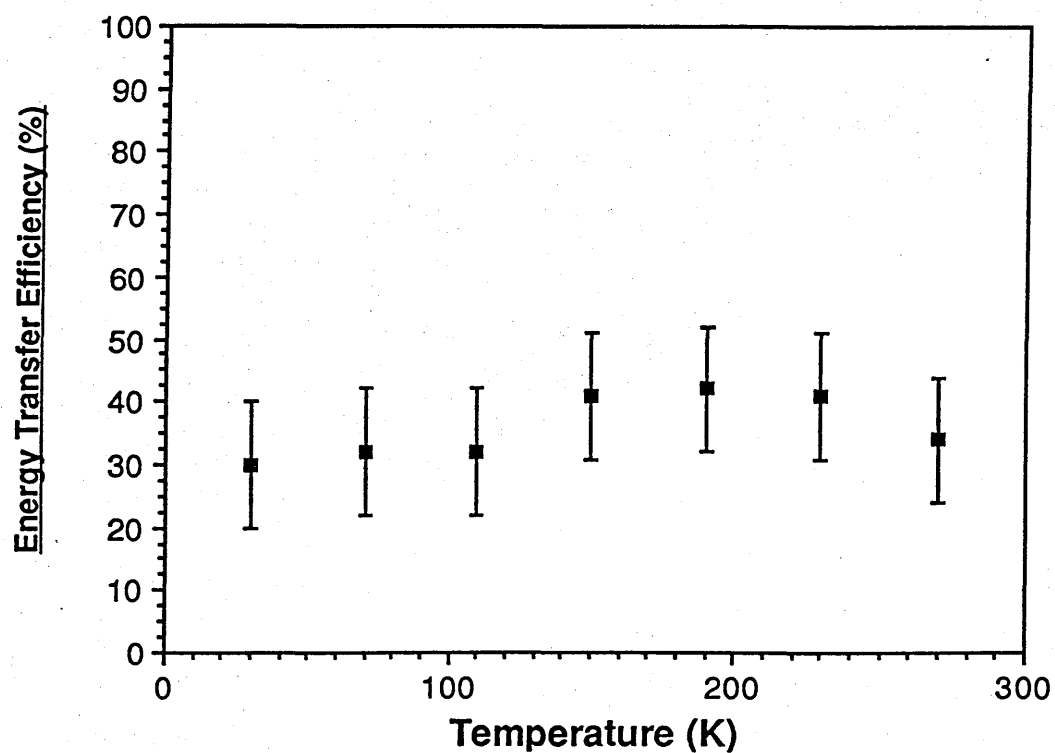


FIGURE 7.3b Energy Transfer Efficiencies of the RC-B875
Antenna Complex of *Rps. palustris* 'French'.



is believed to be due to a decrease in the rate of energy transfer between individual BChl a molecules [Rijgersberg *et al*, 1980]). The relative efficiencies for each species, however, are very different, averaging at $70\pm 6\%$ for the RC-B875 complex of *Rc. gelatinosus* 149, and at only $35.4\pm 5\%$ for the same complex from *Rps. palustris* 'French'. Other values have been determined for the efficiency of singlet-singlet energy transfer from the carotenoid to bacteriochlorophyll, in the RC-B875 complex isolated from other species of purple bacteria. The values average at 25% for the two strains of *Rps. acidophila* ie. 7750 and 7050 [Angerhofer *et al*, 1986], 30% for *Rs. rubrum* S1 [(Pearlstein and Heminger, 1978)(Borisov *et al*, 1982)] and 70% for *Rb. sphaeroides* 2.4.1. [(Hunter *et al*, 1981)(Kramer *et al*, 1984b)].

The emission and action spectra of fluorescence recorded for each species, and the calculation of energy transfer efficiencies determined for the species *Rhodocyclus gelatinosus* 149 and *Rhodopseudomonas palustris* 'French', show that energy is being effectively transferred between BChl a molecules and carotenoids, and between the light-harvesting antenna complexes and the reaction centre. This suggests that the components are connected, and thus provides evidence to substantiate the integrity of the isolated RC-B875 antenna complex, in particular of the antenna complex. The functional integrity of the reaction centre component itself can be examined by observing its fluorescence induction kinetics. In a functionally intact system the level of fluorescence measured, with respect to time, should show a gradual increase corresponding to the 'closure' of reaction centres as they become photochemically activated. This rise in fluorescence, above the initial F_0 level always emitted, is known as variable fluorescence. If a system is disrupted however ie. because of RC inactivation, or a blockage occurring in the electron transport pathway, the initial

level of fluorescence will be very high, and there will be no detectable variable fluorescence.

Fluorescence emission was induced by exciting samples with light corresponding to the blue region of the excitation spectrum, and was detected in the NIR region of the spectrum corresponding to peak emission. The samples themselves had to be diluted to an optimal concentration such that they were of sufficient density to permit the detection of fluorescence, but not so concentrated that self-absorption occurs. The 'optimum' concentration was determined by measuring the fluorescence yield of different concentrations of RC-B890 isolated from *Rs. rubrum* S1. In the absence of self-absorption a straight-line graph should be obtained if the fluorescence yield is expressed with respect to absorption at 890nm. Figure 7.4 illustrates that above an optical density of $0.25.\text{cm}^{-1}$ self-absorption is evident, this was therefore regarded as the optimum concentration and all samples were diluted accordingly. RC-B875 complexes were isolated from each of the BChl *a*-containing species of purple bacteria being investigated, and their respective fluorescence induction kinetics were examined. Figures 7.5 (a-f) show that variable fluorescence was successfully attained for each sample considered with the exception of the two strains 7050 and 7750 of *Rps. acidophila* (Figure 7.6 a&b) for which no variable fluorescence was detected. These two strains produced fluorescence responses typical of a denatured complex, despite the fact that their absorption spectra appeared normal (Figure 7.6 c & d). Since all of the samples had been stored in a concentrated form at -20°C , it was suggested that perhaps the two strains, or rather the RC of the two strains, were in fact sensitive to the storage procedures adopted. Fluorescence induction kinetics were therefore repeated on samples which had been freshly removed from the sucrose density-gradients, however

FIGURE 7.4 Determination of the 'Optimal' Sample Concentration.

The figure presented below describes the relationship between maximum fluorescence yields, as determined from fluorescence induction curves, and sample concentration, as determined by absorption at 890 nm.

The RC-B875 antenna complex sample was isolated from photosynthetic membranes of *Rs. rubrum* S1 by detergent solubilization and subsequent fractionation by sucrose density-gradient centrifugation. The isolated complexes were dialysed against 10 mM Tris-HCl, pH 8.0, and then concentrated on DE52 columns (eluted using a 300 mM salt buffer containing the detergent 1% (w/v) cholate).

It can be observed that a linear relationship exists between the two parameters at sample concentrations corresponding to an OD_{890} of less than 0.25 cm^{-1} . Above this concentration, the linear relationship is disrupted, suggesting that self-absorption is occurring. A concentration corresponding to an OD_{890} of 0.25 cm^{-1} was therefore, considered to be 'optimal' for the examination of fluorescence induction kinetics. (Absorbance pathlength 1 cm).

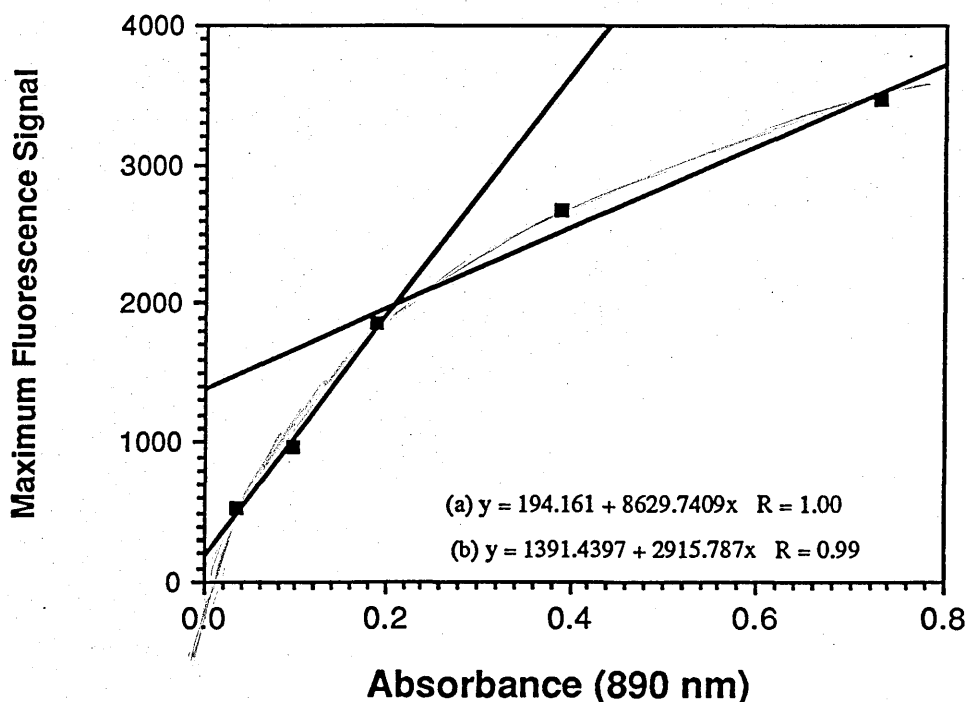


FIGURE 7.5 (a - f) Fluorescence Induction Curves of the RC-B875 Antenna Complex Isolated from a Range of BChl a-Containing Species of Bacteria.

The Figures 7.5 a - f present typical fluorescence induction curves of RC-B875 antenna complexes isolated from the species *Rb.sphaeroides* M21, *Rps.blastica*, *Rps.palustris* 'French', *Rc.gelatinosus* strains 149 and 151, and *Rs. rubrum* S1 respectively.

Fluorescence induction curves were induced, monitored and recorded using a home-built fluorimeter such as that presented in Figure 3.5. Samples were excited with light corresponding to the blue region of the spectrum, and fluorescence was detected in the red. The period of fluorescence (ms - indicated by the bar in each figure) was electromagnetically controlled.

RC-B875 antenna complexes were obtained for each species by fractionation of detergent solubilized membranes, and concentrated on DE52 columns. The concentrated samples were dialysed against 10 mM Tris-HCl, pH 8.0, before being diluted with Tris buffer, pH 8.0 to the 'optimal' concentration.

In each figure two phases of fluorescence emission can be recognized:

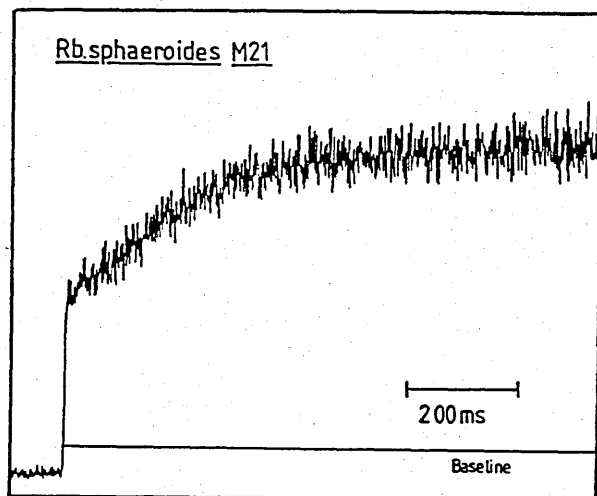
F_0 Indicating the minimum level of fluorescence always emitted.

F_{var} phase showing a gradual increase in fluorescence yields.

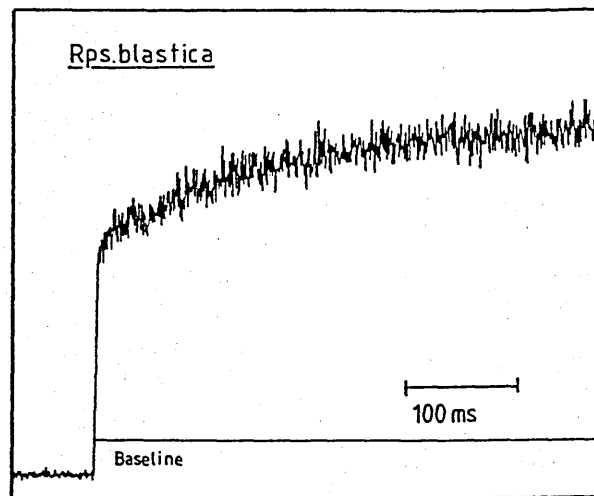
F_{max} represents the maximum yield of fluorescence output.

The production of variable fluorescence suggests that the functional integrity of the complex examined has been successfully maintained. (Absorbance pathlength 1 cm).

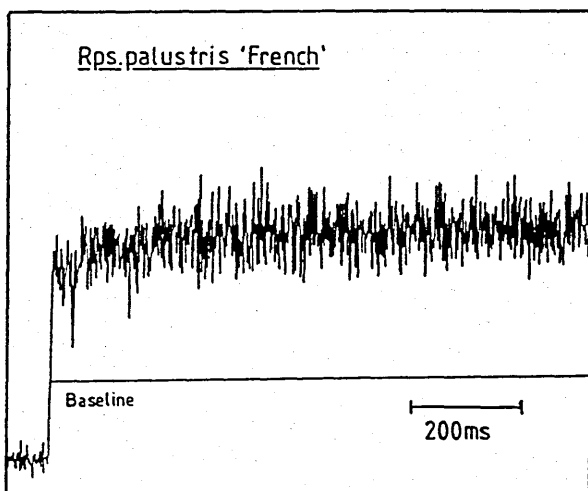
The figures present the relative intensity of fluorescence emission (ordinate) with respect to time (abscissa).



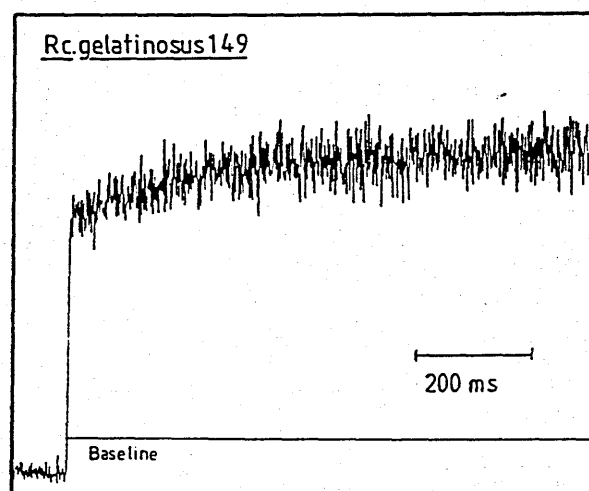
(a)



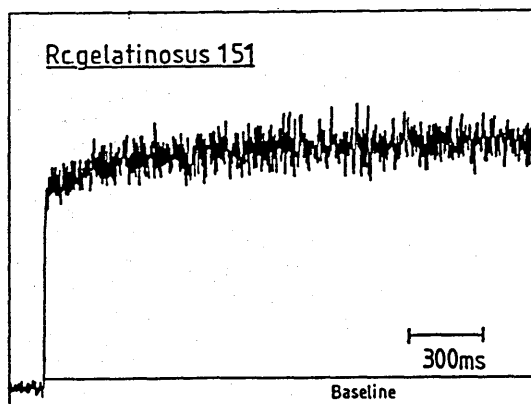
(b)



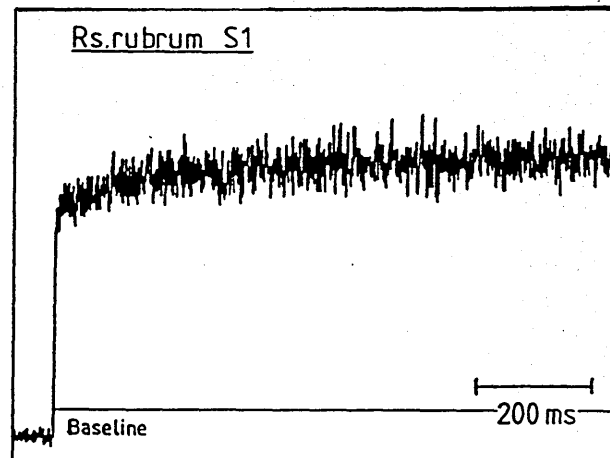
(c)



(d)



(e)



(f)

FIGURE 7.6 (a & b) Fluorescence Induction Curves of the RC-B875 Antenna Complexes of *Rps. acidophila* strains 7050 and 7750.

Fluorescence induction curves were recorded for the RC-B875 antenna complex isolated by the fractionation of detergent solubilized membranes of *Rps. acidophila* 7050 and *Rps. acidophila* 7750. The complexes were concentrated on DE52 columns, and then dialysed against 10 mM Tris-HCl, pH 8.0. The concentrated sample was diluted with 10 mM Tris-HCl, pH 8.0 to the 'optimal' concentration.

The RC-B875 were excited with blue light for a controlled period of time (ms), and fluorescence emission (shown on the ordinate) was detected in the red region of the spectrum. Unlike the fluorescence induction curves presented in Figure 7.5, no variable fluorescence was detected, and the initial F_0 level approximated to the F_{max} level of fluorescence output. These results suggest that the complex is functionally denatured.

Examination of the absorption properties of these complexes, however, shown in FIGURE 7.6 (c & d), provides no evidence for structural denaturation. (Absorbance pathlength 1 cm).

The figures present the relative intensity of fluorescence emission (ordinate) with respect to time (abscissa)

the RC-B875 Antenna Complexes of *Rps. acidophila* strains 7050 and 7750 respectively.

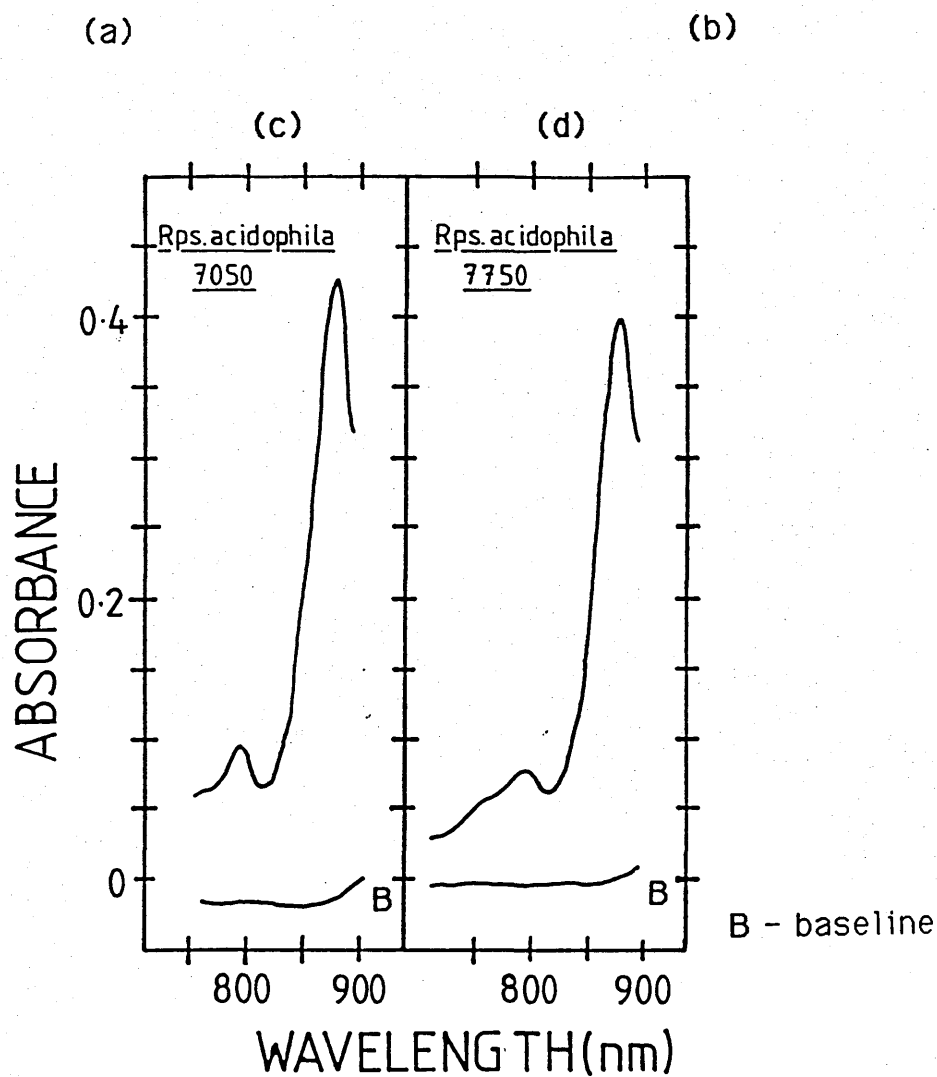
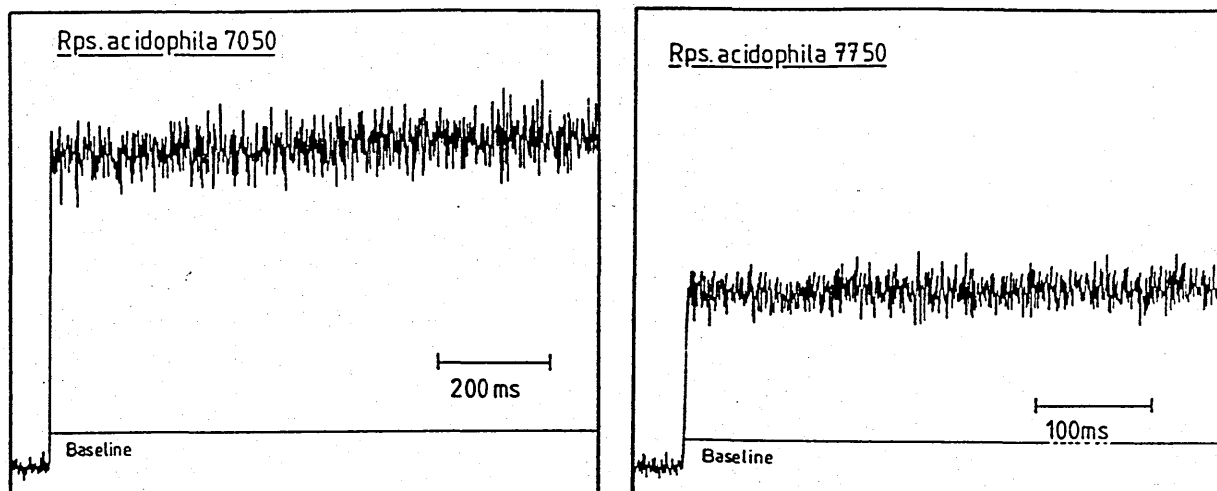


FIGURE 7.6 (c & d) Present Absorbance Spectra of the RC-B875 Antenna Complexes of *Rps. acidophila* strains 7050 and 7750 respectively.

the RC-B875 complex, although producing the characteristic absorption spectrum, failed to yield any variable fluorescence. It was predicted therefore that the solubilization and/or fractionation methods had disrupted the functional integrity of the RC itself, or had caused partial depletion of RC from the 'core-complex' of these two strains of *Rps. acidophila*. The effects of detergents on variable fluorescence are discussed later in this chapter.

The induction and measurement of variable fluorescence kinetics can also provide information about the relative molecular organization or the reaction centre and light-harvesting complexes: Monger and Parson (1977) proposed a model for the *in vivo* organization of the pigment-protein complexes of the photosynthetic unit, which has since received supporting evidence from fluorescence induction studies [Meinhardt *et al*, 1985]. The model suggests that the RC is surrounded by B875 antenna-complex which in turn is surrounded by the B800-850 complex. Two variations of this model are, however, apparent: the first suggests an independent separation of photosynthetic units such that there is no energy transfer between adjacent reaction centres, and the second model suggests that reaction centres are surrounded, and interconnected by a pool of B875-antenna complex, with the B800-850 complexes arranged peripherally around this network. These models are quite appropriately referred to as the Puddle and Lake models respectively (refer back to Figure 1.2h). The two models can be distinguished by examining the relationship between fluorescence yields and the concentration of photochemically active reaction centres [Vredenberg and Duysens, 1963], such that a reciprocal linear relationship between the two variables would suggest that singlet excitations can migrate over large domains of antenna complex (in agreement with the Lake model), and are not

restricted by boundaries separating individual reaction centres (Puddle model). Monger and Parson (1977) studied singlet-triplet fusion (Appendix 6) in *Rb.sphaeroides* chromatophores to obtain information about the movement of singlet excitations, in order to define a 'domain' within the antenna region which is uniform with respect to transfer of singlet excitations [Clayton, 1967]. Using this technique it was found that a reciprocal relationship between fluorescence yield and the concentration of triplet BChl did exist, and thus provided evidence in support of the Lake model of complex organization. The molecular organization of the photosynthetic apparatus can also be probed by measuring electron transfer efficiencies between the RC and B875 antenna complex(es). This technique involves the excitation of a proportion of reaction centres by a flash of light, with light intensity determining the proportion energized. Exposure to a second flash causes excitation of the antenna bacteriochlorophyll which will transfer its energy to the RC. If a particular RC is inactive, or 'closed', the excitation energy can, if the Lake model applies, be transferred to an alternative RC. The Puddle model, however, would permit no such transfer, and energy would be emitted as fluorescence. Expressing the fluorescence yield, or logarithm of fluorescence yield, with respect to time indicates the efficiency of energy transfer, such that an exponential relationship (on a linear scale) signifies the independent separation of reaction centres in accord with the Puddle model, whereas a sigmoidal relationship would support the Lake model of RC-B875 organization. Fluorescence yields procured from the fluorescence curves for each of the RC-B875 complexes were expressed relative to time, and the relationship between these two parameters examined accordingly. Figure 7.7 shows the graphical representation of these values on semi-logarithmic scales. It can be observed that the relationship between these two

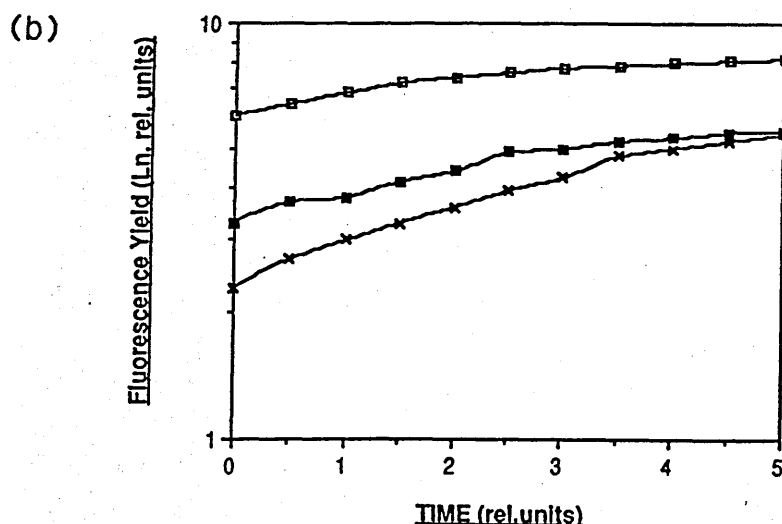
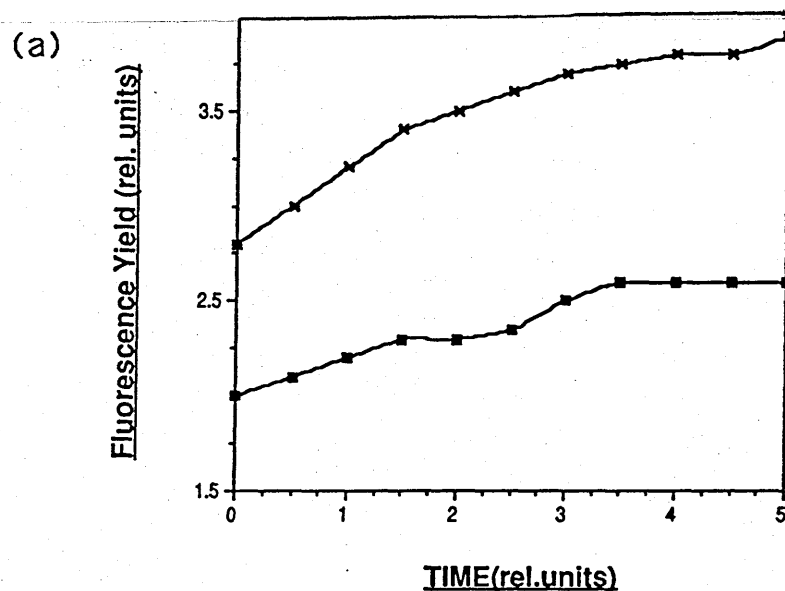
FIGURE 7.7 Examining the Relationship Between Fluorescence Yield and Time for RC-B875 Antenna Complexes Isolated From a Range of BChl a - Containing Purple Bacterial Species.

Figure 7.7a illustrates the relationship between the parameters of time and the fluorescence yields for the RC-B875/B890 antenna complex isolated from the species *Rps. palustris* (x) and *Rs. rubrum* S1 (■)

Figure 7.7b expresses the same relationship on a semi-logarithmic scale for the RC-B875 antenna complex isolated from the species *Rb. sphaeroides* M21 (x) and *Rc. gelatinosus* strains 149 (□) and 151 (■)

The values of fluorescence yield were obtained from the fluorescence induction curves produced for each species (as presented in Figure 7.5).

The relationship between time and log fluorescence is non-linear suggesting that the reaction centre and light-harvesting complexes are arranged in accordance with the lake model of organization.



parameters is non-linear suggesting that the isolated RC-B875 antenna complexes must aggregate in an arrangement comparable to that described by the Lake model such that energy can be transferred between RC-B875 core complexes. Following these experiments the effects of ascorbate, ferricyanide and different detergents on variable fluorescence were examined.

7.1 The effects of ascorbate and ferricyanide addition on fluorescence induction kinetics.

From the oxidation-reduction difference spectra produced in Chapter 5 it was observed that the addition of the chemical oxidant potassium ferricyanide serves to oxidize or bleach the RC BChl a molecule, whereas sodium ascorbate, a chemical reductant, produces the opposite effects. As would be expected, the addition of these two chemicals produce comparable effects on variable fluorescence. Figure 7.8 shows that the addition of ferricyanide reduces the level of variable fluorescence by chemically 'closing' or oxidizing the reaction centre traps. Ascorbate, which serves to effectively open the photochemical traps, consequently increases variable fluorescence.

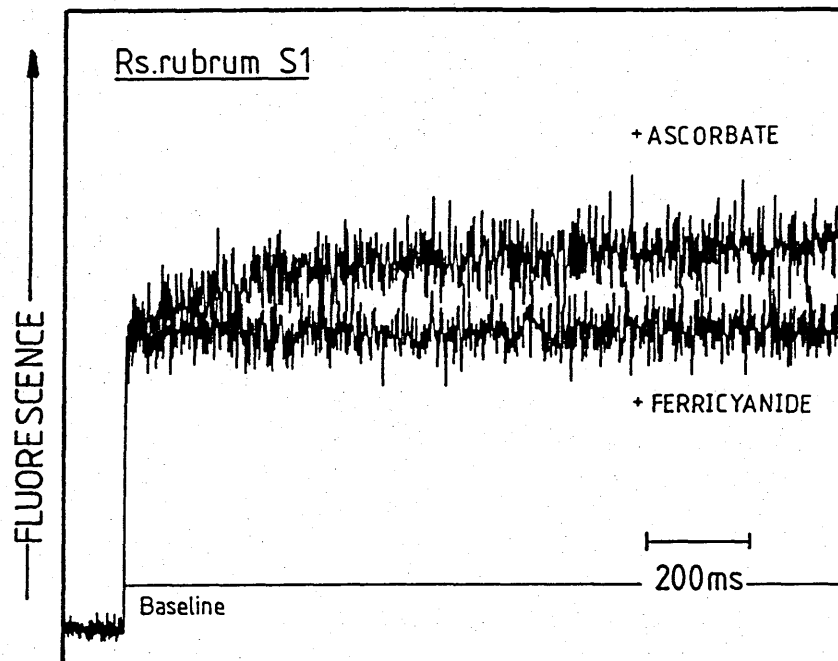



FIGURE 7.8 Examining the Effects of Ascorbate and Ferricyanide on Fluorescence Induction Kinetics

Additions of ascorbate and potassium ferricyanide were made to a sample of *Rs. rubrum* S1 RC-B890 antenna complex. The fluorescence induction kinetics were subsequently monitored. Figure 7.8 presents the induction curves produced. It can be observed that ferricyanide addition to the RC-B890 complex of *Rs. rubrum* S1 abolishes the generation of variable fluorescence, indicating closure of reaction centre traps. Ascorbate induces the opposite effect; opening reaction centre traps and consequently increasing the level of variable fluorescence. (Absorbance pathlength 1 cm).

( 200 ms refers to the time scale of fluorescence induction).

7.2. Looking at the effects of detergent additions on variable fluorescence.

The detergent types examined included sodium dodecyl sulphate (SDS), N-octyl β -D-glucopyranoside (OG), Triton X-100 and lauryldimethylamine N-oxide (LDAO). These detergents were added to a sample of *Rs. rubrum* S1 RC-B890 complex which had been formerly dialysed against 10mM Tris-HCl, pH 8.0 to reduce the concentration of any existing detergent, and diluted to an optical density of 0.27cm^{-1} at 880nm. The effect of detergent addition was to produce a response typical of that expected from a disrupted antenna system; the level of variable fluorescence was reduced, or entirely abolished, and the initial F_0 level of fluorescence increased relative to the maximum fluorescence yield produced by the sample. All of the detergents tested produced this response. They did, however, vary in their effective concentrations, with strong ionic detergents such as SDS eliminating variable fluorescence at concentrations of 0.06% (v/v) and above, and milder detergents, such as OG and Triton X-100, requiring concentrations of approximately 1% and above to produce a similar effect. Figures 7.9 (a-g) illustrate typical responses in fluorescence output upon detergent addition. The weakly zwitterionic detergent LDAO, can be seen to reduce variable fluorescence at concentrations of 0.03% (v/v) LDAO and eliminate it completely at about 0.12% (v/v). Observation of the absorption spectra of the detergent-treated sample at this stage reveals an absorption peak at about 765 nm, corresponding with the absorption of 'free' BChl a, and indicating the structural disruption of the antenna system.

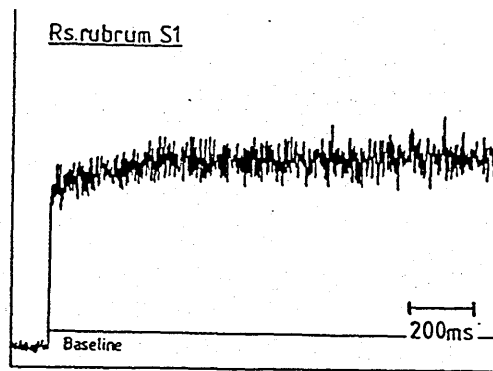
To ensure that neither the heat generated by the apparatus, nor

FIGURE 7.9 (a -g) Examining the Effects of Detergent Addition on Fluorescence Induction Kinetics.

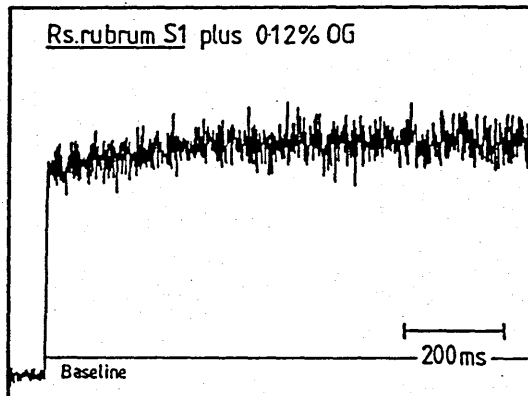
Fluorescence induction curves were recorded for samples of *Rs. rubrum* S1 RC-B890 antenna complex in 10 mM Tris-HCl, pH 8.0 containing the detergents (a) no additional detergent. (b) 0.12% (v/v) n-octyl β -D-gluco-pyranoside (OG). (c) 1.92% (v/v) OG. (d) 0.03% (v/v) Triton X100. (e) 0.96% (v/v) Triton X100. (f) 0.06% (v/v) LDAO. (g) 0.06% (v/v) SDS. (The RC-B875 antenna complex sample was diluted prior to incubation to a concentration corresponding to an OD₈₉₀ of less than 0.25.cm⁻¹. (Detergent effects therefore, are relative to this sample concentration).

It is evident from these figures that detergent additions can affect the production of variable fluorescence. The extent of influence, however, depends upon detergent type and its concentration: detergents such as OG and Triton X-100, at low concentration, have very little observable effect on the production of variable fluorescence. At higher concentrations ie. greater than 1.92% OG and 0.96% Triton X-100, signs of the reduction, or elimination, of variable fluorescence become evident. The detergent LDAO significantly reduces the level of variable fluorescence at concentration of greater than 0.03% (v/v), and the strong, ionic detergent, SDS, was observed to abolish variable fluorescence production at concentrations as low as 0.06% (v/v). (Absorbance pathlength 1 cm).

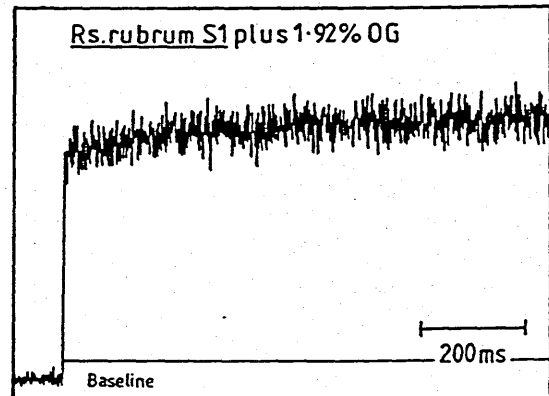
The figures present the relative intensity of fluorescence emission (ordinate) with respect to time (abscissa).



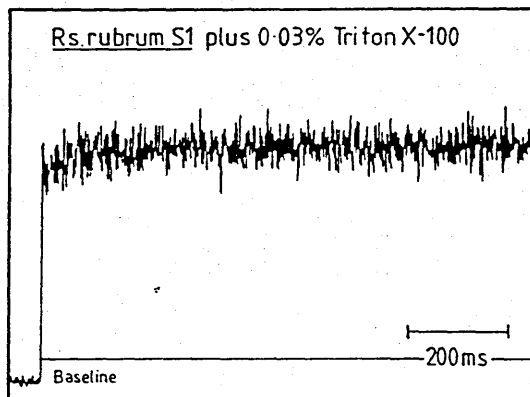
(a)



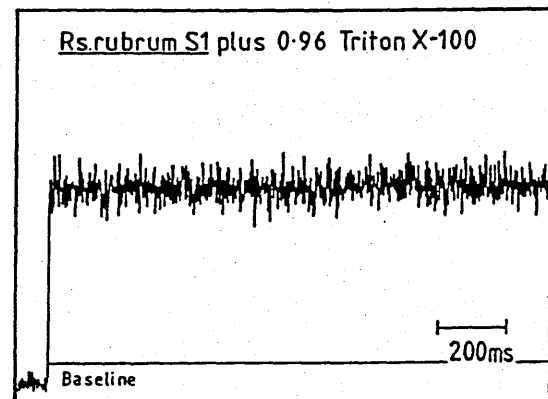
(b)



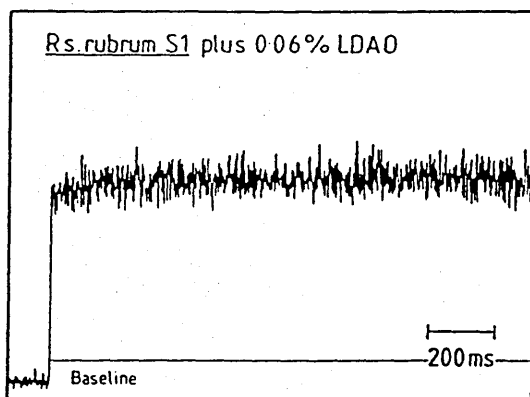
(c)



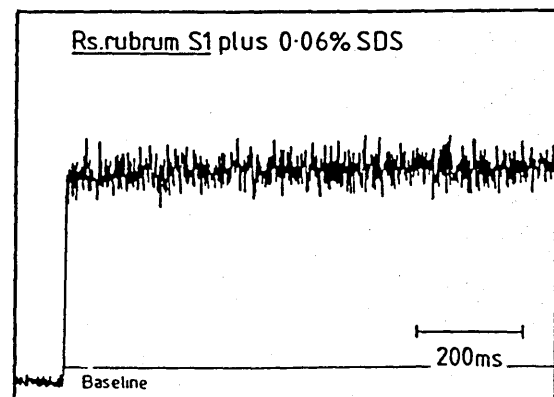
(d)



(e)



(f)



(g)

the age of the complex, produced or assisted in producing, this effect, an experiment was carried out which measured fluorescence yields of a sample maintained within the fluorescence apparatus for a period of 70 minutes. Fluorescence yields were recorded every 10 minutes. Figure 7.10 shows the yield of fluorescence recorded after 2, 30 and 70 minute intervals. Little change in the yield of variable fluorescence was observed during this period of time.

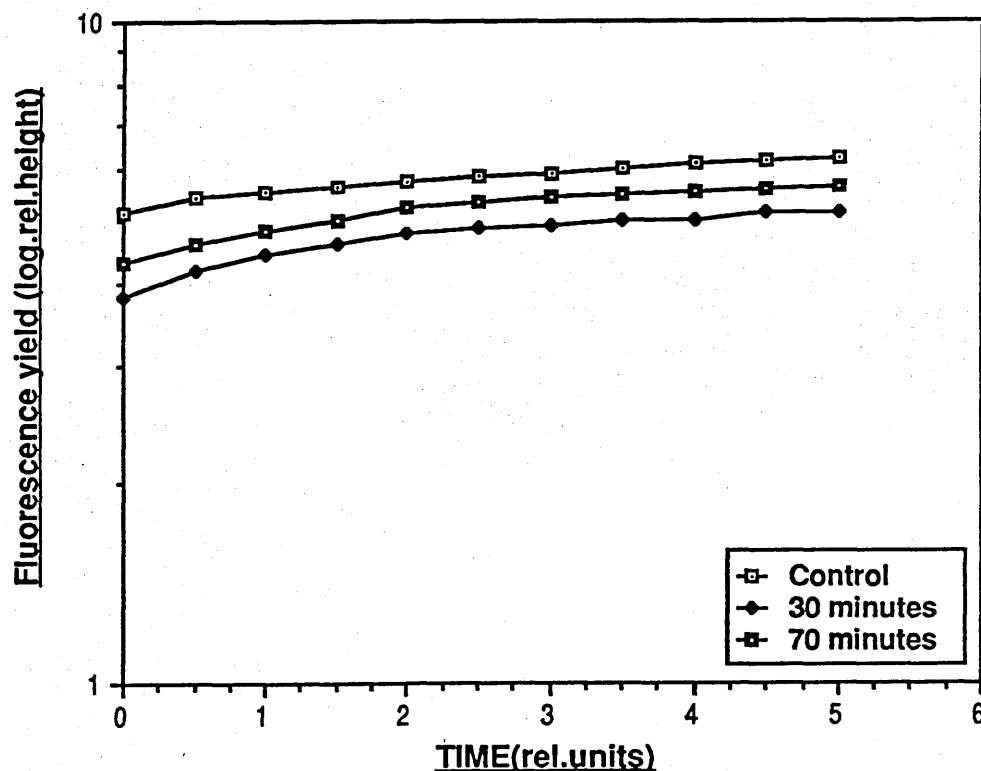
Fluorescence induction experiments therefore, have been conclusive in two respects: firstly in that RC-B875 complexes of all the species examined, with the exception of *Rps. acidophila* strains 7050 and 7750, appear to be functionally intact. *Rps. acidophila* 7050 and 7750 RC-B875 complexes, despite producing characteristic absorption, emission and action spectra, failed to produce variable fluorescence. In examining the effects of detergent on functional integrity they were found not only to be invariably destructive, resulting in the elimination of variable fluorescence, but also to cause structural denaturation, as was indicated by the absorption spectra of some detergent-treated samples.

Secondly, the non-linear relationship existing between the yield of fluorescence and time at low detergent concentrations, suggests that the components of the RC-B875 conjugates are aggregated in such a way that excitation energy can pass between different reaction centres within a 'Lake', or 'domain', of B875 antenna complex. If the detergent concentration is increased however, disaggregation occurs yielding individual, spectrally intact, RC-B875 core complexes. In the presence of excess detergent, or a more disruptive detergent such as SDS, denaturation of individual complexes also becomes evident. A number of studies have been

FIGURE 7.10 The Effects of Time on Fluorescence Induction Kinetics.

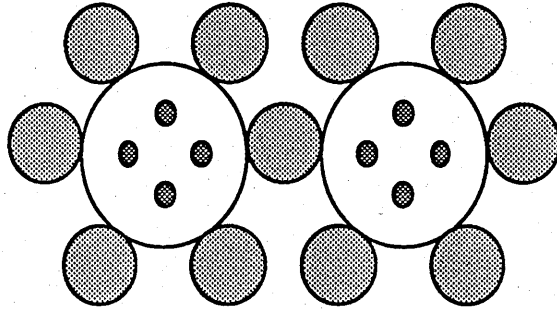
A sample of *Rs. rubrum* S1 RC-B890 antenna complex was maintained within the fluorescence apparatus for a period of 70 minutes. The effects of the prevailing experimental conditions, were examined by observation of the fluorescence induction kinetics of the sample, monitored at 10 minute intervals. Figure 7.10 shows the relationship between the logarithm of fluorescence yield, and time (relative units) recorded for the sample after 0, 30 and 70 minute time intervals. The measurements were procured from the fluorescence induction curves recorded for this sample.

The results show that there is little effect on the level of variable fluorescence production within the time intervals considered, and that the functional integrity of the complex has not been significantly affected by conditions prevailing within the experimental set-up. (Absorbance pathlength 1 cm).

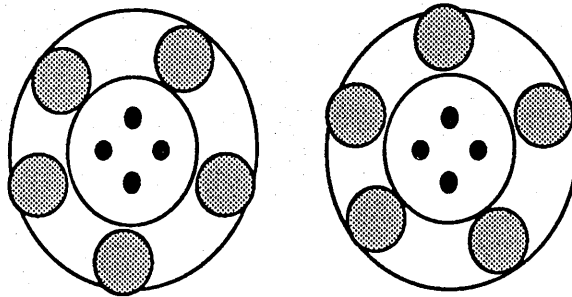


completed examining the size of the B875 domain [(Vredenberg and Duysens, 1963)(Monger and Parsons, 1977)(Campillo *et al*, 1977)(Bakker *et al*, 1983)] and which suggest that the domain size, at room temperature, is large but is reduced significantly at lower temperatures. At room temperature the domain of *Rs. rubrum* S1 consists of approximately 1000 connected antenna molecules, whereas at 4K the size is reduced to approximately 150 connected molecules. Similarly, *Rb. sphaeroides*, at 4K has approximately 100 molecules which connect 4 reaction centres [(Vos *et al*, 1986)(Westerhuis *et al*, 1987)]. The existence of a 'minimal' domain size receives independent experimental support from developmental studies [Hunter *et al*, 1985] which conclude that, even at the earliest stage of development of the photosynthetic membrane, at least four reaction centres are connected. As development proceeds it is suggested [Vos *et al*, 1986] that 'minimal units' combine into larger domains. The barriers between these units are still expected to exist but are believed to be overcome easily by excitations at room temperature and only present difficulties at low temperatures ie. 4K. Vos *et al* (1986) also suggest that at 4K the B800-850 complex of *Rb. sphaeroides* also forms about five domains which transfer energy to B875 via a few contact sites. Thus at low temperatures the Monger and Parson model no longer applies, and a new structure has been proposed [Vos *et al*, 1986]. Figure 7.11 presents 2 models for the proposed antenna structure of *Rb. sphaeroides* at 4K.

Figure 7.11: Models for the Organization of Photosynthetic Units in Rhodobacter sphaeroides Based upon Singlet-Singlet Annihilation Measurements



The model suggests that at 4 K the photosynthetic unit consists of 4 RC connected by approximately 100 B875 BChl a molecules, and that the B800-850 complexes form about 5 domains which transfer energy to the B875 complex, via a few contact sites. Two variations of this general model are proposed; (a) in which the B800-850 complexes are shared between one or more photosynthetic unit complexes (shown above); and (b) in which there is no sharing of the B800-850 complexes between photosynthetic unit complexes.



■ REACTION CENTRE. □ RC-B875 COMPLEX. ▨ B800-850 COMPLEX

(Circles Correspond Approximately to Domain size of B800-850 (45 B850 BChl a) and B875 (≤ 100 B875 BChl a) Determined at 4K).

[Modified from Vos et al, 1986]

CHAPTER 8

Crystallization of the RC-B875 Antenna Complex.

The successful crystallization of the RC-B875 antenna complex isolated from bacteriochlorophyll *a*-containing species of purple photosynthetic bacteria, would provide invaluable evidence to support the existence of a stoichiometrically well-defined core complex.

To date, a number of successful attempts have been made in the crystallization of the various protein components isolated from photosynthetic membranes of purple bacteria, the foremost major success being the crystallization of the reaction centre of the BChl *b*-containing species *Rhodopseudomonas viridis* [Michel, 1982]. The crystals, large and tetragonal in shape, diffracted clearly beyond 2.5 Å and from their X-ray analysis the molecular structure has been elucidated [Deisenhofer *et al*, 1984, 1985]. More recently, further advancements have been made in the crystallization of the other components of the photosynthetic apparatus. Crystals have been successfully obtained of the B800-850 antenna complex from *Rb. sphaeroides* 2.4.1. [(Allen *et al*, 1985)(Cogdell *et al*, 1985)], *Rps. palustris* [(Mäntele *et al*, 1987)(Welte *et al*, 1985)], *Rps. acidophila* [Cogdell *et al*, 1985], *Rb. capsulatus* [(Mäntele *et al*, 1985)(Welte *et al*, 1985)], *Rc. gelatinosus* [Cogdell *et al*, 1987], for the B800-820 complex of *Rps. acidophila* [Cogdell *et al*, 1985] and for the RC-B875 complex of *Rps. palustris* [(Mäntele *et al*, 1987)(Wacker *et al*, 1986)] and *Rs. rubrum* S1 [Cogdell *et al*, 1987]. The crystals produced however, have not been of sufficient size and/or quality for study by X-ray diffraction and image processing techniques, although they do lend themselves favourably

to spectroscopic work [Mäntele *et al*, 1987]. Dichroic spectra recorded for many of these crystals verify that the purified complexes have suffered no compositional or conformational rearrangement as a consequence of crystallization. Examination of these crystals with polarized light reveals an extremely high degree of dichroism, and provides information regarding the orientations of pigment components [(Welte *et al*, 1987)(Mäntele *et al*, 1985)].

All of the studies mentioned above employed the method of vapour diffusion, the crystal-inducing environment created ie. the precipitant, detergent and small amphiphile, generally differed. Two which previously proved successful were adopted, and their parameters modified, and interchanged, in an almost "shotgun" approach to crystallization. The first method (Method 1) described by Allen and Feher (1984) and Welte *et al* (1985) for the crystallization of the B800-850 complex of *Rb. sphaeroides* and *Rb. capsulatus* respectively, employs the method of vapour diffusion in the presence of polyethylene glycol (PEG) , sodium chloride, a detergent and the small amphiphile 1,2,3 heptanetriol. Each of these parameters, including those of pH and temperature, were modified and selectively screened for their ability to induce, or examined for their effects on, crystallization. The precise conditions are summarized in Table 8.1(c, d, f, g, h & i). The second method (Method 2), previously successful in the crystallization of the RC-B875 conjugate of *Rps. palustris* [Wacker *et al*, 1986], incorporates the precipitant PEG, and magnesium chloride dissolved in a 10mM Tris buffer containing a detergent. Again the parameters of relative concentrations, detergent type, temperature and pH were systematically modified (Table 8.1 e, g & j). The sample proteins, which included the RC-B875 complex of *Rs. rubrum* S1, *Rps. acidophila* 7050 and *Rc. gelatinosus* 149, were

isolated by fractionation of detergent solubilized membranes. The isolated RC-NIR antenna complex was then concentrated and further purified employing one of four treatments. These included: (i) concentration of the dialysed RC-B875 complex on DE52 columns and its elution with salt buffer containing 0.1% (v/v) LDAO; (ii) as described in (i) although the elution buffer contained the detergent 1% (w/v) dodecyl β -D-maltoside (LM); (iii) the sample was concentrated as described in (i) and then was further purified by a single passage over a molecular sieve column. The sample was then dialysed, reconcentrated on DE52 and eluted with salt buffer containing 1% (w/v) LM.; (iv) the samples were treated as described in treatment (iii) although the final elution buffer contained the detergent 1% (w/v) cholate. Crystallizations were set up, and left undisturbed for a period of 1-2 weeks prior to examination by light microscopy. Sometimes however, longer incubations were required.

Although most of the conditions described above failed to yield crystals, due to phase separation or the sedimentation of amorphous material, a few did prove successful. However, crystals were only produced for the RC-B890 antenna complex of *Rs. rubrum* S1 dissolved in Tris buffer containing the detergent LM ie. those samples prepared by treatments (ii) and (iii). The RC-B875 complexes isolated from the other two species, *Rps.acidophila* 7050 and *Rc.gelatinosus* 149 could not be induced to crystallize under any of the conditions so described. Successful crystal-inducing environments, created by modifying the parameters of Method 1, are summarized below:

Reservoir buffer: 22% (w/v) PEG 2000

600mM NaCl

Sample buffer: 12% (w/v) PEG 4000

300mM NaCl

1mM EDTA plus 0.1% sodium azide

3.0% HPT at pH 8.5/9.5 and incubated at 10°C/20°C, or

2.5% HPT at pH 8.5 (10°C/20°C) or at pH 9.5 (10°C).

(The sample buffer was then combined with a sample of *Rs. rubrum* S1 RC-B890 complex in a ratio of 1:1).

Figure 8.1 shows a typical crystal formed under the conditions above in the presence of 2.5% HPT at pH 8.5, 10°C. Despite their small, rather irregular-shape, typical of crystals produced using this method, they were very dichroic.

Method 2 was more successful in that crystallization appeared to occur more readily, yielding larger and more regular products. The largest crystals were produced under the conditions described below:

Reservoir buffer: 18% (w/v) PEG 2000

[1]

20mM MgCl₂

Sample buffer: 17% (w/v) PEG 2000

20mM MgCl₂

(The sample buffer was then combined with a sample of *Rs. rubrum* S1 RC-B890 complex in a ratio of 1:1).

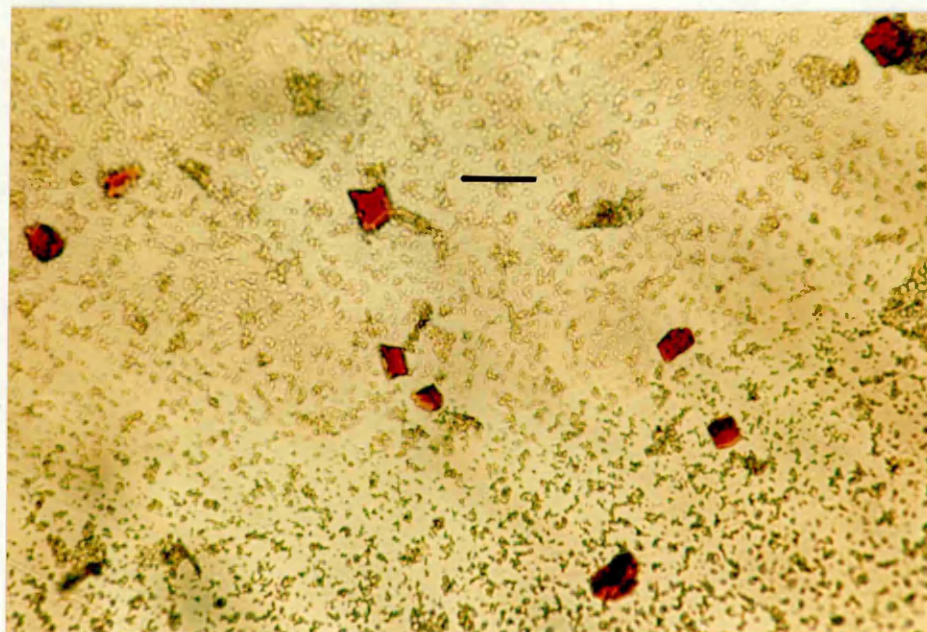
Both buffer solutions were prepared with 10mM Tris-HCl pH 8.0 containing the detergents (a) 0.1% DDAO, (b) 0.04% LDAO. These preparations were incubated for 4 weeks at 20°C before obvious signs of crystal formation were observed. Figures 8.2 a & b show

FIGURE 8.1 Crystallization of the RC-B890 Antenna Complex of *Rs. rubrum* S1.

The method of vapour diffusion in the presence of PEG and the small amphiphile, HPT, as described by Allen *et al*(1984) and Welte *et al*(1985) for the crystallization of the B800-850 complex of *Rb. sphaeroides* and *Rb. capsulatus*, respectively, was adopted and modified to induce crystallization of the RC-B890 complex of *Rs. rubrum* S1. The crystals shown here were induced with internal conditions of 12% (w/v) PEG 4000, 300 mM NaCl, 1 mM EDTA, 2.5% (w/v) HPT, (pH 8.0), combined with *Rs. rubrum*S1 RC-B890 complex in a ratio of 1:1. external reservoir of 22% (w/v) PEG 2000, 600 mM NaCl, and were incubated at 10°C.

The RC-B890 complex of *Rs. rubrum*S1 was prepared by fractionation of detergent solubilized membranes. The isolated complex was then dialysed against 10 mM Tris-HCl, pH 8.0, concentrated on DE52 columns and eluted with salt buffer containing 1% (w/v) LM.

Although the crystals produced were small and irregular in shape, they were dichroic.

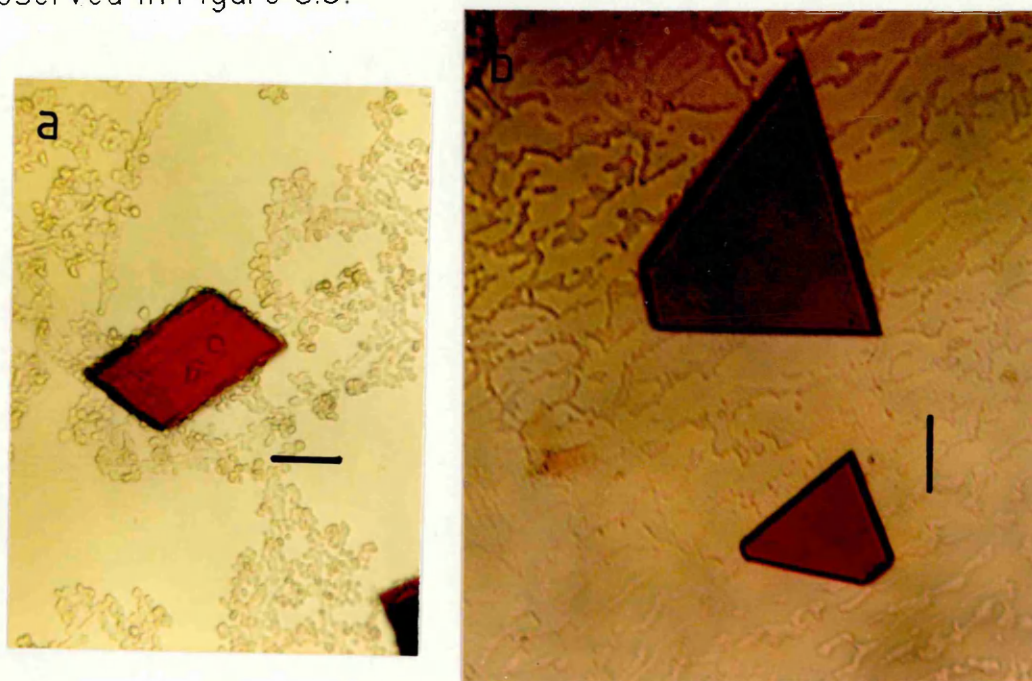


Bar represents 25 μ m.

FIGURE 8.2 (a & b) Crystals of the RC-B890 Antenna Complex of *Rs. rubrum* S1, and the Influence of Detergents on Crystal Form.

Conditions, described by Wacker *et al*(1986) for the crystallization of *Rps. palustris* RC-B875 antenna complex, were adapted to induce crystallization of the RC-B890 antenna complex of *Rs. rubrum* S1. The crystals, shown in Figure 8.2 a & b, were induced by the method of vapour diffusion under conditions of: Sample buffer 17% (w/v) PEG 2000, 20 mM $MgCl_2$ in 10 mM Tris-HCl, pH 8.0. The sample buffer was combined with *Rs. rubrum* S1 RC-B890 complex in a ratio of 1:1. Reservoir buffer 18% (w/v) PEG 2000, 20 mM $MgCl_2$, and incubated at 20°C. The buffers were prepared with 10 mM Tris-HCl, pH 8.0 containing the detergents (a) 0.1% (v/v) DDAO and (b) 0.04% (v/v) LDAO.

It can be seen by comparing the figures (a) and (b) that the size and form of the resultant crystals, are influenced by the detergent present in the crystallization environment. Both crystals have good light polarizing qualities as can be observed in Figure 8.3.



Bar represents 25 μm .

crystals typically produced under the conditions described above. It can be seen that both the size and the shape of the crystals vary depending upon the detergent present in the precipitating solutions: with 0.1% (w/v) DDAO producing rectangular or rhomboid shaped crystals of approximate dimensions $50\text{ }\mu\text{m} \times 32\text{ }\mu\text{m}$ and $52\text{ }\mu\text{m} \times 33\text{ }\mu\text{m}$ respectively. In comparison, 0.04% (v/v) LDAO induced larger crystals but which were, on the whole, irregularly shaped, having 3 to 6 sides. The largest crystal, produced under these conditions, is shown in Figure 8.2b, has dimensions of approximately $94\text{ }\mu\text{m}$, $72\text{ }\mu\text{m}$, $81\text{ }\mu\text{m}$ and $24\text{ }\mu\text{m}$. All of the crystals formed showed good light polarizing qualities: Figures 8.3 a, b, c & d, show examples of crystals photographed under polarizing light, the plane of polarized light is rotated 90° in the two pictures. Comparison of the two photographs shows quite clearly that a high degree of dichroism is exhibited by the carotenoids within these crystals [Cogdell, 1985]. The conditions described above [1] were repeated in an experiment using a different sample of *Rs. rubrum* S1 (but which had been prepared in the same way). Some modifications of crystallization conditions were also made, including changes to the pH of the buffer solutions (pH 8.0 and pH 9.5), and an increase in the concentration of the PEG 2000 in the reservoir buffer (from 18% (w/v) to 20% (w/v)). The results of these experiments suggest that crystal form does not only vary with the type of detergent present in the buffer solution, but may also vary in response to changes in the pH of the sample solution, and to changes in the concentration of the precipitant (Figure 8.4a - Figure 8.4g). The effect of external parameters influencing crystal form, and to some extent size, has also been reported by other workers [(Mäntele *et al*, 1985)(Welte *et al*, 1987)(Cogdell *et al*, 1985,1987)]. In the crystallization experiments described above some of the conditions created were direct repeats of those

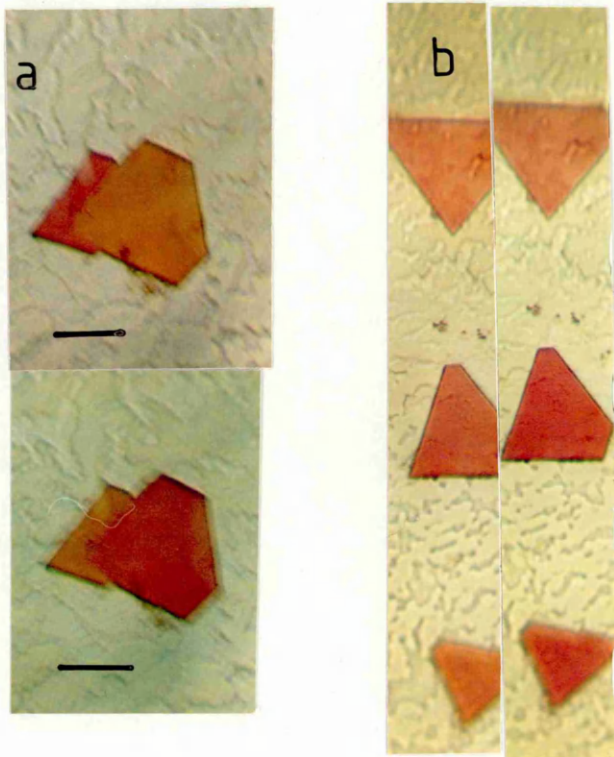
FIGURE 8.3 (a & b) The Dichroic Nature of Crystals.

Crystals of the RC-B890 antenna complex of *Rs. rubrum* S1 can be seen to have good light polarizing qualities. Each figure, a & b, presents two photographs of the same crystal taken under polarizing light. **The plane of polarized light is rotated**

90° in the two photographs. The colour of the crystals, as seen with the naked eye, is dominated by the absorption bands of carotenoid pigments; a change in the colour of the crystals can be observed under polarizing light, demonstrating the high degree of dichroism exhibited by the carotenoids, and is indicative of an internal order.

The quality of Figure 8.3b is, I apologise, not very good (the crystals often form on the surface of the well solution and have a tendency to float about). They do, however, show good light polarizing qualities.

The crystals were formed by vapour diffusion, at 20°C, in the presence of PEG 2000 (18% reservoir and 17% well buffer), 20 mM MgCl₂, in 10 mM Tris-HCl, pH 8.0 containing 0.04% LDAO.



Bar represents 25 μm .

FIGURE 8.4 (a - g) Examining the Effect of pH and Varying Precipitant Concentrations on Crystal Formation.

Crystallization conditions were created which examined the effect of pH and precipitant concentration on the crystallization of *Rs.rubrum* S1 RC-B890 antenna complex. The basic method of vapour diffusion was adopted with standard internal conditions of: 17% (w/v) PEG 2000, 20 mM MgCl₂, and standard reservoir conditions of: 18% (w/v) PEG 2000, 20 mM MgCl₂. Buffers were made up with 10 mM Tris-HCl, pH 8.0 containing a detergent. *Rs.rubrum* S1 RC-B890 complex was added to the internal buffer solution to a ratio of 1:1. Variations in the parameters of internal pH, external concentrations of PEG 2000, incubation temperature, and added detergents, were made, and the effects on crystal formation were examined. Figures 8.4 a-g present crystals typically produced under these conditions (the precise conditions associated with each crystal are described below):

- Figure 8.4a Standard conditions- pH 8.0, detergent 0.1% (w/v) DDAO, incubation temperature 20°C.
- Figure 8.4b Standard conditions- pH 9.0, Detergent 0.1% (w/v) DDAO, incubation temperature 20°C.
- Figure 8.4c Standard conditions- pH 9.0, external concentration of PEG 2000 increased to 20% (w/v) Detergent 0.1% (w/v) DDAO, incubation temperature 20°C.
- Figure 8.4d Standard conditions- pH 8.0, detergent 0.04% (v/v) LDAO, incubation temperature. 10°C.
- Figure 8.4e Standard conditions- pH 9.0, detergent 0.04% (v/v) LDAO, incubation temperature. 10°C.
- Figure 8.4f Standard conditions- pH 8.0, external concentration of PEG 2000 increased to 20% (w/v), detergent 0.04% (v/v) LDAO, incubation temperature 10°C.
- Figure 8.4g Standard conditions- pH 9.0, external concentration of PEG 2000 increased to 20% (w/v), Detergent 0.04% (v/v) LDAO, incubation temperature 10°C.

It is seen, by comparing these figures, that changes in the parameters of pH, relative precipitant concentrations, detergent type, and incubation temperatures, can induce changes in the size and/or form of the crystals.



FIGURE 8.4a

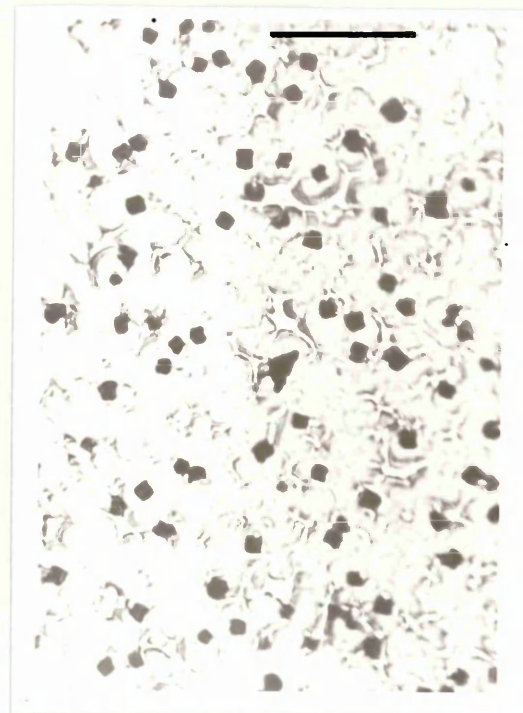


FIGURE 8.4b

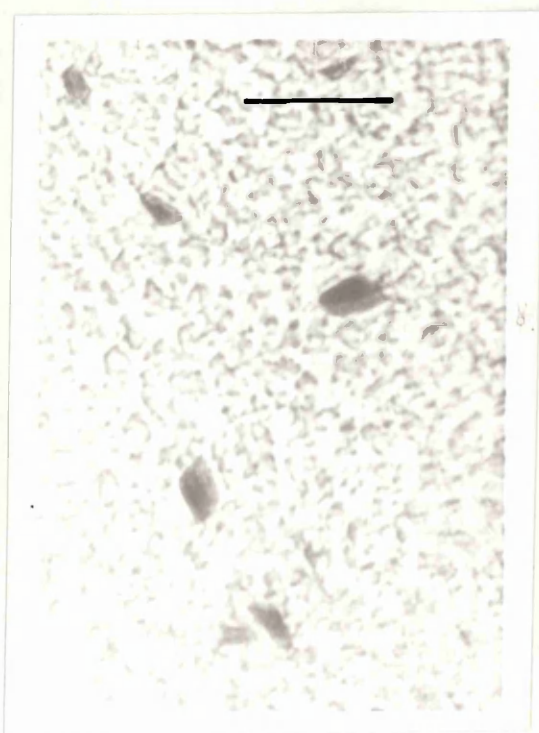


FIGURE 8.4c

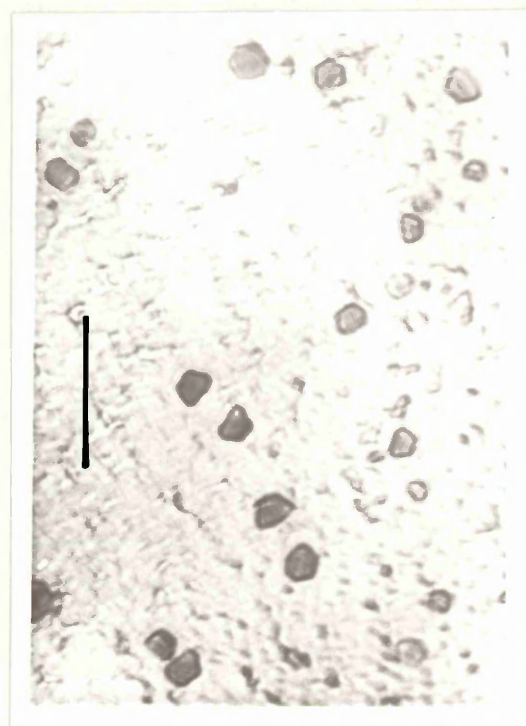


FIGURE 8.4d

Bar represents 25 μm .

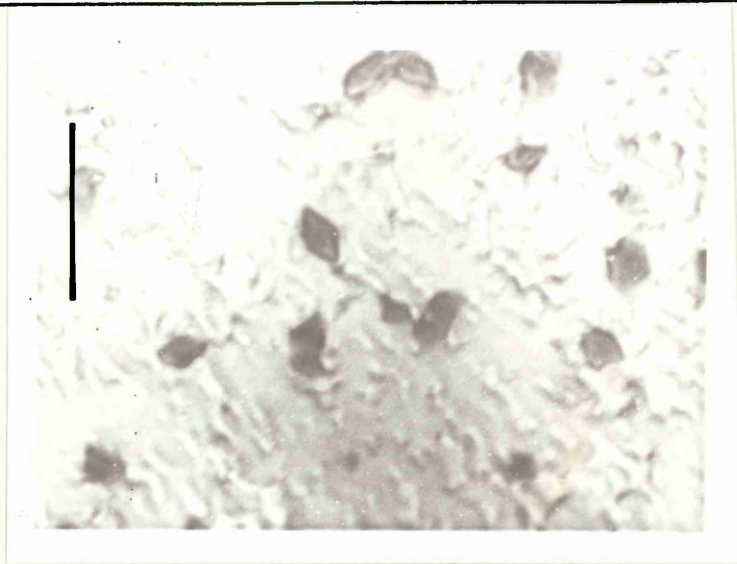


FIGURE 8.4e



FIGURE 8.4f

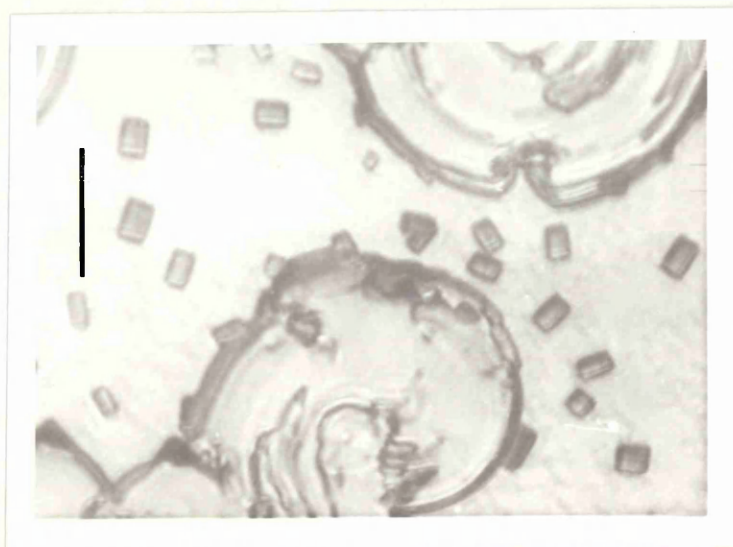


FIGURE 8.4g

Bar represents 25 μm .

described earlier [1]. However, although the resultant crystals were of similar shape they were relatively small, having a maximum dimension of approximately 16 μm (compared with dimensions of approximately 94 μm in crystals obtained in earlier crystallization attempts). These results clearly indicate that the crystallization process is not only sensitive to 'cruder parameter changes', but is also sensitive to slight differences existing between different sample batches of a particular complex, and also to slight differences in preparation procedures.

Attempts at crystallizing the RC-B875 core complex made so far have shown partial success with respect to the crystallization of the RC-B890 complex of *Rs. rubrum* S1. The crystals produced, although too small for examination using X-ray diffraction techniques, did have good dichroic properties, indicative of a well-ordered internal arrangement, and lending strong support to the idea that the complex represents a stoichiometrically well-ordered structure.

TABLE 8.1

A Summary of Crystallization Conditions.

This table summarizes the conditions adopted in each crystallization experiment ([A] - [J]). Parameter variations examined in each experiment are indicated by "/". Only those conditions already described in the text above were successful in inducing crystal formation. All other conditions described failed to induce crystal formation but resulted in the precipitation of amorphous material, or separation of the sample solution into detergent and aqueous phases.

[A]	Reservoir buffer:	45% (w/v) PEG 2000 / 50% (v/v) PEG 2000 (+/- 500mM NaCl)
	Sample buffer:	9% (w/v) PEG 2000 300mM NaCl 3% (w/v) benzamidine hydrochloride hydrate (BH) (supplied by Aldrich Chemical Company Ltd.) 0.1% (v/v) dimethyldecylamine oxide (DDAO) (supplied by OXYL Ltd.) Temperature 10°C/20°C pH 8.5/9.5

Rs. rubrum S1 RC-B890 complex and sample buffer were combined in a ratio of 60%:40% (v/v).

[B] Reservoir buffer: 45%/50% (w/v) PEG 4000/45%/50% (w/v)
PEG 2000
600mM NaCl
Sample buffer: 9% (w/v) PEG 4000 /9% (w/v) PEG 2000
300mM NaCl
3% (w/v) BH
0.1% (w/v) DDAO
Temperature 10°C/20°C
pH 8.5/9.5

Rs. rubrum S1 RC-B890 complex/ 50% *Rps. acidophila* 7050 RC-B875 complex were combined with sample buffer in a ratio of 60%:40% (v/v)/ 50%:50% (v/v), respectively.

[C] Reservoir buffer: 22%/18%/30% (w/v) PEG 2000
600mM NaCl
Sample buffer: 12% (w/v) PEG 2000
360mM NaCl
3% (w/v) 1,2,3 heptanetriol (HPT)(supplied by OXYL Ltd.)
0.1% (w/v) DDAO/0.04% (v/v) LDAO/0.1% (w/v) dodecyl β -D-maltoside (LM) /no extra detergent.
1mM EDTA plus 0.1% sodium azide.
Temperature 10°C/20°C
pH 8.5/9.5

Rs. rubrum S1 RC-B890 complex/ 50% *Rps. acidophila* 7050 RC-B875 complex were combined with sample buffer in a ratio of 60%:40% (v/v)/ 50%:50% (v/v) respectively.

[D] Reservoir buffer: 22% (w/v) PEG 2000
600mM NaCl
Sample buffer: 9%/12%/18% (w/v) PEG 4000
360mM NaCl
0.06% (w/v) LDAO
3.9% (w/v) HPT
Temperature 10°C/20°C
pH 8.5/9.5

Rs. rubrum S1 RC-B890 complex and sample buffer were combined in a ratio of 60%:40% (v/v).

[E] Reservoir buffer: 18% (w/v) PEG 2000
20mM MgCl₂
in 10mM Tris-HCl pH 8.0 containing 0.04%
(v/v) LDAO/0.1% (w/v) DDAO/0.1% (w/v) LM.
Sample buffer 17% (w/v) PEG 2000
20mM MgCl₂
in 10mM Tris-HCl pH 8.0 containing 0.04%
(v/v) LDAO/0.1% (w/v) DDAO/0.1% (w/v) LM.
Temperature 10°C/20°C/room temperature.
pH 8.0

Rs. rubrum S1 RC-B890 complex and sample buffer were combined in a ratio of 1:1 (v/v).

[F] Reservoir buffer: 22% (w/v) PEG 2000
600mM NaCl
Sample buffer: 12% (w/v) PEG 4000
1mM EDTA containing 0.1% sodium azide
2.5%/3.0%/3.5% (w/v) BH/HPT
Temperature 10°C/20°C
pH 8.5/9.5.

Rs. rubrum S1 RC-B890 complex and sample buffer were combined in a ratio of 60%:40% (v/v).

[G] Reservoir buffer: 18%/20%/22% (w/v) PEG 2000
20mM MgCl₂
in 10mM Tris-HCl pH 8.0 plus 0.04% (v/v) LDAO.
Sample buffer: 12%/17% (w/v) PEG 2000
20mM MgCl₂
in 10mM Tris-HCl pH 8.0 containing 0.04% (v/v) LDAO/ 0.1% (w/v) DDAO.
No small amphiphile/3.0% HPT/3.0% BH
Temperature 10°C/20°C

Rs. rubrum S1 RC-B890 complex and sample buffer were combined in a ratio of 60%:40% (v/v).

[H] Reservoir buffer: 22% (w/v) PEG 4000
600mM NaCl
Sample buffer: 12% /18% (w/v) PEG 4000
300mM NaCl
1mM EDTA containing 0.1% sodium azide.
2.0%/2.5%/3.0% (w/v) HPT
Temperature 10°C/20°C
pH 8.5/9.5

Rs. rubrum S1 RC-B890 complex/ *Rc. gelatinosus* 149 RC-B875 complex were combined with sample buffer in a ratio of 1:1 (v/v).

[I] Reservoir buffer: 22%/25% (w/v) PEG 2000
100mM/250mM NaCl
in 10mM Tris-HCl pH 8.0
1mM EDTA plus 0.1% sodium azide
Sample buffer: 8%/10% (w/v) PEG 2000
150mM/250mM NaCl
0.8% (w/v) OG
1.0% (w/v) HPT
1mM EDTA plus 0.1% sodium azide
in 10mM Tris-HCl pH 8.0/8.3
Temperature 10°C/20°C

Rs. rubrum S1 RC-B890 complex/ *Rc. gelatinosus* 149 RC-B875 complex were combined with sample buffer in a ratio of 1:1 (v/v).

(Modified from Frank *et al*, 1987)

[j] Reservoir buffer: 18% (w/v) PEG 2000

20mM MgCl₂

in 10mM Tris-HCl pH 8.0

Sample buffer: 15%/17% (w/v) PEG 2000

10mM/20mM MgCl₂

in 10mM Tris-HCl pH 8.0/9.0/10.0 containing

0.04% (v/v) LDAO

Temperature 10°C/20°C.

Rs. rubrum S1 RC-B890 complex/ *Rc. gelatinosus* 149 RC-B875
complex were combined with sample buffer in a ratio of 1:1 (v/v).

CHAPTER 9

CONCLUSIONS AND DISCUSSION

The RC-B875 antenna complex has been successfully isolated from a range of bacteriochlorophyll *a*-containing purple bacterial species, in which the structural composition and organization, and functional integrity has been examined. Isolation of the RC-B875 antenna complex of these bacteria was achieved by density-gradient fractionation of detergent-solubilized membranes. Owing to variations in detergent effectivity and sensitivities, the exact conditions adopted for each preparation were species dependent.

Determination of the RC:B875 antenna ratio for each isolated complex showed that within a particular species the ratio was constant, irrespective of the light intensity at which the cells were grown; examination of relative absorptions at 800 nm and 880 nm, of each complex, also reflected this consistency. However, comparison of the mean ratio values obtained for different species, showed a degree of variation, such that species could be grouped according to their average ratio value; the majority of species, however, showed a RC:BChl *a* ratio value approximating to 1:32 (or 1:29 when the experimentally adjusted extinction coefficient for absorption of total bacteriochlorophyll at 880 nm was employed in ratio calculations). Species were also differentiated with respect to the ratio of A_{800}/A_{880} ; the pattern of differentiation however, was not an exact reflection of grouping arrangements obtained when the relative size of the RC:B875 antenna ratio was considered. A question was therefore, posed as to whether the apparent divisions existing between groups of species is a consequence of natural species variation, or whether

some factor of the preparative procedure had induced a degree of 'artificial' variation.

Subsequent analysis of the effects of detergent additions on the ratio of RC:B875 BChl a molecules, and on the ratio of A_{800}/A_{880} , revealed that changes could be induced, resulting in an increase, or a decrease, in one, or both, of the measured ratio values. For example, the RC-B875 antenna complex of the species *Rhodopseudomonas acidophila* 7050, when treated with additional detergents showed an increase in the ratio of RC:BChl a molecules, although there was no corresponding increase in the ratio of absorption maxima ie. A_{800}/A_{880} , an effect which suggests that the reaction centre molecules are, in some way, being denatured, or even partially depleted. The results of fluorescence induction studies promote similar conclusions; samples of the RC:B875 antenna complex of *Rhodopseudomonas acidophila* 7050 and 7750 exposed to activating light, fail to produce any variable fluorescence, but instead generate fluorescence induction curves typical of a denatured complex. These results suggest that the reaction centre molecules are either not utilizing the light energy in the electron transfer processes of photosynthesis, or alternatively, if the reaction centre is dissociated, or partially dissociated from the membrane components, then energy may not even be transferred to the reaction centre from the light-harvesting complexes. Either of these possibilities is feasible since (a) there is evidence suggesting that the reaction centre is exposed on both sides of the membrane [(Bachman *et al*, 1981)(Meyer *et al*, 1981)(Valkirs and Feher, 1982)(Wiemken and Bachofen, 1982)], and is therefore, susceptible to denaturation by detergents, and (b) dissociation of the reaction centre from its association with the photosynthetic unit can be achieved using detergents [(Oelze and Golecki, 1975)(Reed and Clayton,

1968)(Clayton and Sistrom, 1978)]. Other species, such as *Rhodopseudomonas blastica*, were also shown to be sensitive to detergent additions, although it appears that the antenna BChl a was affected by the detergent rather than the reaction centre molecules, since an increase in both RC:B875 BChl a and A_{800}/A_{880} ratio values was observed. Examination of the fluorescence induction kinetics of these species, reveals good fluorescence induction curves showing variable fluorescence.

To diverge briefly, the results of a few studies examining the assembly processes of pigment-protein complexes in photosynthetic membranes, have provided a quantitative description of the Monger and Parson model (1977) for *Rhodobacter sphaeroides*. The results suggest that the photosynthetic unit of chromatophores grown under low-light conditions consists of 27 B800-850 complexes, existing as hexamers and higher oligomeric forms in discrete lakes, three dimeric B875 complexes, which may be associated directly with the reaction centre, and 14 B800-850 and 14 B875 complexes, which appear to be functionally associated in various oligomeric states [Hunter *et al*, 1981, 1982]. Additional evidence supporting the existence of two pools of B800-850 antenna complex, one of which is linked directly to B875 forming B800-850-B875 complexes, is obtained from the results of fluorescence yield studies. It is suggested that these heterogeneous complexes represent "fingers" which extend into the B800-850 pool, and in so doing, facilitate energy transfer to the reaction centre from the outer B800-850 array. The existence of "fingers" of B875 antenna complex could partly explain the variation in RC:B875 BChl a ratio values determined for a particular species, and also, perhaps more appropriately, between different species; a "finger" of antenna complex would be more susceptible to 'damage' in fractionation

procedures, and may also be more susceptible to detergent denaturation, than would a solid ring of antenna complex. The variation existent between species could be a consequence of variation in the extent of "finger" formation, and hence variation in sensitivity to detergents. Further examination of the photosynthetic unit of BChl a-containing species is required before any conclusions regarding the existence, or potential existence, of such an arrangement, can be drawn. However, speaking theoretically, an arrangement of this kind would provide a feasible explanation for the variation in RC:BChl a ratios apparent between different species, between different strains and perhaps even within strains of purple photosynthetic bacteria.

Examining the structural composition of the isolated complexes revealed a common polypeptide composition in all BChl a species considered; the pattern of bands in SDS-polyacrylamide gels showed a triad of high-molecular weight reaction centre polypeptides, and the two, low molecular weight polypeptides characterizing the antenna complex.

To draw a conclusion from these results, it seems that the RC-B875 antenna complex forms a 'fixed core structure', although the precise arrangement of components with respect to each other is not fully understood; a tight, well-ordered arrangement is, however, predicted. To complicate matters briefly, it has also been proposed by several groups that the B875 antenna complex is not homogeneous, but contains an additional complex absorbing at approximately 896 nm. [(Bolt *et al*, 1981)(Borisov *et al*, 1982) (Kramer *et al*, 1984b)(Razjuin *et al*, 1982) (Valkunas *et al*, 1985) (Vos *et al*, 1986)]. van Grondelle (1987) studying excited state dynamics of the energy transfer processes using picosecond absorption spectroscopy, "unequivocally established" that B880 of *Rs. rubrum*, and B875 of *Rb. sphaeroides*, contain an

additional, highly-ordered, long-wavelength pigment on which excitations become localized before being transferred to the reaction centre. van Dorssen *et al* (1987) examining *in vitro* spectroscopic properties of the antenna complex, also show in M21, the B875⁻ mutant of *Rb. sphaeroides*, that the antenna complex has optical inhomogeneity causing a weak band at about 899 nm. It is important to emphasize that these studies have all been completed at 4K, and as such, suggest that this component only has a strong influence at low temperatures, and at room temperature its presence, in the first order, may be ignored (since most excitations may be localized on the B875 antenna complex). As yet, however, no model has been proposed incorporating this complex into the core structure [Vos *et al*, 1986]. Irrespective of the presence of this component, the well-ordered internal arrangement of the 'core' structure has received support from the successful crystallization of RC-antenna components, and in this study of the partial success in the crystallization of the RC-B890 complex of *Rhodospirillum rubrum* S1, which, although not of sufficient quality for examination by X-ray diffraction and image-processing techniques, do show strong dichroic properties, indicative of internal order. The crystallization of reaction centre-antenna complexes, however, requires continuous systematic screening both as regards experimental conditions and the range of species examined; the scope for further developments in crystallization methods is extensive; crystals must be improved in both size and quality to ensure that X-ray diffraction and associated techniques can be effectively utilized. Crystallization represents a potentially powerful tool, which could provide invaluable information describing the internal organization of the pigment-protein complexes, and thus may yield the essential evidence required to conclude the argument for the existence of a

"stoichiometric core structure" in the photosynthetic apparatus of all BChl a-containing species of purple bacteria: a prospect which is eagerly awaited.

APPENDIX 1

MEDIA and BUFFERS

1.1 Acidophila Medium (per litre) Adjust final volume to pH 5.2

Potassium di-hydrogen orthophosphate	1.0g
Magnesium sulphate.7H ₂ O	0.4 g
Sodium chloride	0.4 g
Sodium succinate	1.5 g
Calcium chloride.2H ₂ O	0.05 g
Succinic acid	0.065 g
Ammonium chloride	0.5 g
0.1% Ferric citrate solution	5.0 ml
Trace element solution*	10.0 ml
Add H ₂ O to final volume of 1 l. Autoclave at 15 lb.in ⁻² for 20 min.	

Trace Element Solution* (per litre) Adjust final volume to pH 3.0-4.0

Ethylenediaminetetra-acetic acid (EDTA) (disodium salt)	0.5 g
Ferrous sulphate.7H ₂ O	0.01 g
Manganous chloride.4H ₂ O	0.003 g
Boric acid	0.03 g
Cobalt chloride.2H ₂ O	0.02 g
Calcium chloride.2H ₂ O	0.001 g
Nickel chloride.6H ₂ O	0.002 g
Sodium molybdate.2H ₂ O	0.003 g

1.2 C-Succinate Medium (per litre)

Concentration base*	20 ml
di-potassium hydrogen orthophosphate (1M)	10 ml
Potassium di-hydrogen orthophosphate (1M)	10 ml
10% ammonium sulphate	5 ml
Sodium or potassium sulphate (1M)	10 ml
Growth factors**	1 ml
Casamino acids	1 g
Autoclave at 15 lb.in ⁻² for 20 min.	

*Concentration base (per litre)

Nitriloacetic acid	10 g
Magnesium sulphate	14.45 g
Calcium chloride.2H ₂ O	3.4 g
Ammonium molybdate	0.0092 g
Ferrous sulphate.7H ₂ O	0.099 g
Nicotinic acid	0.05 g
Aneurine hydrochloride	0.025 g
Biotin	0.0005 g
Metos 44***	250ml.

Add H₂O to 0.5 of final volume. Adjust to pH 6.8 (the solution should become clear). Add H₂O to final volume of 1 l.

**Growth Factors (per litre)

Biotin	0.02 g
Sodium hydrogen carbonate	0.5 g
-dissolve in 100 ml. H ₂ O	
Nicotinic acid	0.1 g
Aneurine hydrochloride	0.05 g
4-aminobenzoic acid	0.1 g
-Add to water solution. Boil to dissolve.	

Metos 44 ***(per 100 ml)

EDTA disodium salt	0.5 g
Zinc sulphate.7H ₂ O	2.19 g
Ferrous sulphate.7H ₂ O	1.0 g
Manganous sulphate.7H ₂ O	0.308 g
Copper sulphate.5H ₂ O	0.0784g
Colbalt nitrate.6H ₂ O	0.0496 g
disodium tetraborate.10 H ₂ O	0.0354 g
Add 100 ml dH ₂ O and two drops of conc. sulphuric acid.	

1.3 Chromatium Medium

Solution 1	1 litre
Solution 2	1 litre
Solution 3	1 litre
Autoclave at 15 lb.in ⁻² for 20 min.	

Solution 1 (per litre) Adjust to pH 7.8

Sodium chloride	60 g
di-potassium hydrogen orthophosphate	1 g
potassium di-hydrogen orthophosphate	1 g
Ammonium chloride	2 g
Calcium chloride.2H ₂ O	0.25 g
Magnesium chloride.6H ₂ O	1 g
H ₂ O to final volume of 1 l.	

Solution 2 (per litre) Adjust to pH 7.8 - 8.0

Sodium thiosulphate.5H ₂ O	6 g
Sodium hydrogen carbonate	8 g
H ₂ O to final volume of 1 l.	

Solution 3 (per litre)

Ferrous sulphate.7H ₂ O	1.6 g
Ethylenediaminetetra-acetic acid (EDTA) (disodium salt)	3.0 g

1.4 Agar Stabs and Agar Plates. (per 100 ml)

Yeast extract	0.3g
Casamino acids	0.2g
Agar	1.5g

H₂O to final volume of 100 ml. Heat until boiling (the solution should go clear). Pour into McCartney bottles and autoclave for 15 minutes at 15 lb.in⁻². For agar stabs allow the agar to set in the M^cCartney bottles. For agar plates aseptically pour the molten agar into sterile petri dishes, leave to set. Store at 4°C.

1.5 MES solution. Adjust to pH 6.8

2(N-morpholino)ethanesulphonic acid (MES)	20 mM
potassium chloride	100 mM

1.6 Salt Solutions. Adjust to pH 8.0

(1)	Sodium Chloride	350mM
	Tris(hydroxymethyl)aminomethane (Tris)	20mM
	Lauryldimethylamine N-oxide (LDAO)	0.1 % (v/v)
(2)	Sodium Chloride	500 mM
	Tris(hydroxymethyl)aminomethane (Tris)	20 mM
	Dodecyl β -D-maltoside	1.0 % (v/v)

1.7 Protein Assay

Tannin Reagent

Tannic acid	20 g
Hydrochloric acid (1M)	196 ml
Phenol	4 ml

Heat at 80°C. Filter when cool. Store at 4°C.

Gum Acacia

Acacia	0.2%
--------	------

H₂O to volume.

Store at 4°C.

APPENDIX 2

SDS-POLYACRYLAMIDE GEL ELECTROPHORESIS

2.1 Stock solutions for SDS-polyacrylamide gel electrophoresis.

Lower or Separating gel buffer

Tris-HCl 1.5 M ——— 18.2 g/100 ml
Sodium dodecyl sulphate (SDS) 0.4 % (w/v) ——— 0.4 g/100 ml
Adjust to pH 8.8. Make up to 100 ml with dH₂O

Upper or Stacking gel buffer

Tris-HCl 0.5 M ——— 6.05 g/100 ml
Sodium dodecyl sulphate (SDS) 0.4 % (w/v) ——— 0.4 g/100 ml
Adjust to pH 6.8 with HCl, bring up to final volume with dH₂O

Running buffer

Tris-HCl 6.0 g
Glycine 28.8 g
Sodium dodecyl sulphate (SDS) 1.0 g
Should be pH 8.3. Add dH₂O to final volume of 1 l.

Acrylamide stock

Acrylamide 39 g
N,N'-methylene-bis-acrylamide (Bis) 1 g
Add dH₂O to final volume of 100 ml. Filter.

Polyacrylamide Gel preparation

<u>Resolving Gel</u>	Percent gel:	<u>11.5%</u>	<u>18%</u>
Lower gel buffer		4.9 ml	4.9 ml
Acrylamide stock		5.6 ml	9.0 ml
65% (w/v) sucrose		1.5 ml	5.4 ml
20% (w/v) NaCl		0.49 ml	0.49 ml
dH ₂ O		7.5 ml	-----
10% ammonium persulphate (fresh)		31.5 μ l	31.5 μ l
TEMED		3.0 μ l	3.0 μ l
(NNN'N'-tetramethylethylene diamine-BDH Chemicals Ltd.)			

Acrylamide Stacking gel solution (6%)

Upper gel buffer	1.25 ml
Acrylamide stock	0.75 ml
dH ₂ O 3.0 ml	
10% (w/v) ammonium persulphate (fresh)	40 μ l
TEMED	5 μ l

2.2 Preparing Protein samples for SDS-PAGE

Standard Protein Sample

Bovine serum albumin (5 mg.ml ⁻¹)	10 μ l
Alcohol dehydrogenase (5 mg.ml ⁻¹)	10 μ l
Myoglobin (5 mg.ml ⁻¹)	10 μ l
Cytochrome C (5 mg.ml ⁻¹)	10 μ l
dH ₂ O 10 μ l	

Final sample concentration

Protein	1 mg.ml ⁻¹
Tris-HCl pH 6.8	62.5 mM
Glycerol	10 % (v/v)
SDS	2.0 % (w/v)
Bromophenol blue	0.01 % (w/v)
β-mercaptoethanol (BDH Chemicals)	5.0 % (v/v)

2.3 Staining and destaining solutions

Staining solution

Coomassie blue G250	0.25 % (w/v)
Methanol	50 % (v/v)
Acetic acid	10 % (v/v)
dH ₂ O to final volume.	

Destaining solution

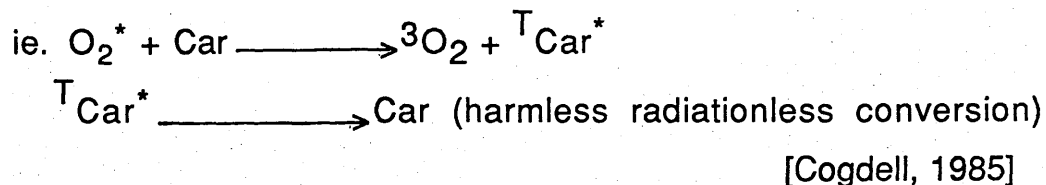
Methanol	10% (v/v)
Acetic acid	10 % (v/v)
dH ₂ O to final volume.	

APPENDIX 3

THE PHOTODYNAMIC EFFECT

Destructive oxidative reactions can occur by the irradiation of chlorophylls, or bacteriochlorophylls, in the presence of oxygen [Krinsky, 1968]. The destructive element, singlet oxygen, is capable of oxidizing chlorophylls, proteins, nucleic acids and lipids, and is formed from the elevation of ground-state triplet oxygen, by the transfer of energy from the excited (*) triplet states of chlorophyll and bacteriochlorophyll ($^3\text{BChl}^*$). The formation of triplet state carotenoid ($^T\text{Car}^*$), however, can protect the organism against these harmful photodynamic reactions by:

(1) Interacting directly with singlet oxygen ($^1\Delta_g.\text{O}_2^*$) to quench it [(Foote 1968)(Foot & Denny, 1968)]



(2) By quenching triplet chlorophylls and bacteriochlorophylls, which are responsible for singlet oxygen production [Krinsky, 1979]



Triplet carotenoid formation takes place in a few nanoseconds, and, therefore, provides an efficient, and an effective, block against the formation of singlet oxygen [(Chessin *et al*, 1966)(Foote,1968)]

APPENDIX 4

BUFFER SYSTEMS EMPLOYED IN POLYACRYLAMIDE GEL ELECTROPHORESIS.

Buffer Systems: two types of buffer system recognized:

(1) Continuous buffer - in which the same type of buffer ions are present throughout the sample, gel and electrode buffer-vessel reservoirs, at constant pH.

(2) Discontinuous buffer - which incorporates different buffer ions, and pH, in the gel compared with electrode reservoirs.

In the continuous buffer system, the samples are loaded directly onto the resolving body of the gel, whereas in the discontinuous system the samples are first loaded onto a large-pore 'stacking gel' polymerized on top of the resolving gel. The latter system, also known as the 'Ornstein-Davis system', allows dilute samples to be applied with no ill effect to the quality of resolution. The theory behind the production of a thin-starting zone can be attributed to the work of Ornstein (1964) and Davis (1964): the sample and stacking gel of the discontinuous system contain Tris-HCl, pH 6.8, whereas, that of the upper electrode buffer contains Tris-glycine buffer (pH 8.3). At pH 6.8, the Tris-glycine buffer is poorly dissociated and the effective mobility is, therefore, low; the mobility of the chloride ions, however, is high, and that of the proteins falls somewhere between the two levels. When a voltage is applied, the chloride ions migrate away from the glycine leaving behind a zone of lower conductivity which, consequently, attains a higher voltage gradient, serving to accelerate glycine mobility in pursuit of the chloride ions. A steady state is established where the products of the mobility and voltage gradient are equal, and,

therefore, move at the same velocity with a sharp boundary between them: the front of this boundary will have a low voltage gradient, whereas at the rear of the boundary the voltage gradient is high. Consequently, as the boundary moves through the sample, and through the stacking gel, any proteins, on account of their intermediate velocity, are swept up into the thin zone between, and are effectively concentrated. As the boundary reaches the resolving gel, the pH value increases causing a greater dissociation of glycine and thereby, increasing its mobility, such that it overtakes the protein and migrates directly behind the chloride ions. At the same time, the pore size of the polyacrylamide gel is reduced, and the mobility of proteins is retarded by the process of molecular sieving. The proteins, therefore, now move in a zone of uniform pH and voltage, and are separated according to size.

APPENDIX 5

STATISTICAL ANALYSES

To compare data from different sample populations it is necessary to apply a test of significance; examples of two such tests are the t-test and the F-Test, or Analysis of Variance. The t-test is employed to examine the difference between two sample means, whereas the F-Test is generally employed when more than two sample means have to be compared.

In applying a test of significance, the main question asked is whether all the samples have the same mean, and thus, have been drawn from a single population, or from populations with the same mean. A test of significance examines the deviation between observed and expected results; if the differences are significant then the alternative hypothesis is adopted, and it is concluded that the samples represent several populations with different means.

In making a test of significance, an estimate must be made of the probability of obtaining a result which deviates from expectation as much as, or more than, the result actually observed. In setting these limits of confidence, the possibility of error must also be considered. Two kinds of error are possible:

Type 1 Error is the rejection of the null hypothesis (H_0) when in fact the population means are equal.

Type 2 Error accepting the null hypothesis when in fact the population means are not equal.

The probability of making either of these errors is dependent upon the critical probability selected, for example, in selecting a probability (P) of 0.001 in place of $P=0.05$, the probability of making a Type 1 error is reduced, and the probability of making a

Type 2 error is increased, and *vice versa*. Therefore in selecting a critical probability level, consideration must first be made of the relative costs of making the two sorts of error. It is from this probability that conclusions regarding the acceptance, or rejection, of the null hypothesis are made. That is, if the observed result is lower than that expected within the level of confidence, then H_0 is accepted. If, however, the estimated probability is low, then H_0 is rejected and the alternative hypothesis is adopted.

The t-test- a test of significance employed to examine the difference between two sample means (X_1 and X_2).

The null hypothesis (H_0) of the t-test assumes that the sample means are equal ie. $X_1 = X_2$. The deviation of the observed result from expectation is simply calculated as the difference between the two means ie. $X_1 - X_2$. To take account of the variability, and number of independent measurements, in both samples, the standard error of the difference between the two means must also be considered. The value of t, therefore becomes:

$$t = \frac{X_1 - X_2}{Sc \sqrt{1/(N_1 + N_2)}} \quad \text{where} \quad Sc = \sqrt{\frac{\sum x_1^2 + \sum x_2^2}{N_1 + N_2 - 2}}$$

where t has $(N_1 + N_2 - 2)$ degrees of freedom (f).

X = Sample mean.

$\sum x^2$ = sum of squares of X ie. $\sum X^2 - ((\sum X)^2/N)$

Analysis of Variance (one-way).

Analysis of variance allows simultaneous comparison of several treatments, testing the hypothesis that all sample means are the same.

The test compares two estimates of overall variance; one

estimate being based on the variance of sample means about the population mean ie. between group variation; and the other is based on the variance of the individual measurements about their group, or sample, mean ie. within group or error variance. The ratio of these variance values denotes the statistic, F. If the null hypothesis ie. that the population means are the same, was true, the ratio of these two estimates would approximate to unity. If the sample means estimate different population means, the value of F should become large ie. indicating that the variation between groups is greater than variation due to random error.

The probability therefore, of obtaining such a ratio value is determined from Tables of Theoretical values of F. Since F is a ratio of two variances, the numerator and denominator must have their own degrees of freedom which are accounted for when entering a calculated value of F into the table.

An example to illustrate the computation of F:

Consider an experiment with K groups, or treatments, with each group having n replicates. Need to compute

(1) Variance between groups, or treatments. ie. the total sum of squares between treatments (SST):

$$SST = \frac{\sum T_K^2}{n} - \frac{(\sum GT)^2}{Kn}$$

where T_{1-K} = totals ie. for each treatment.

GT = total of all treatments ie. $T_1 + T_2 + \dots + T_K$

n = number of samples in each treatment.

Kn = Total number of samples.

(2) Variance within treatments (SSE)

$$SSE = \sum x^2 - \frac{(\sum GT)^2}{kn}$$

where x = each replicate sample ie. there is a total of kn samples.

\bar{x} = treatment mean.

$\sum x^2$ = total sum of squares ie. $\sum (x - \bar{x})^2$

GT = total of all treatments.

n = number of replicates in each treatment.

kn = total number of replicates.

To calculate F , the degrees of freedom (f) of each variance value must also be accounted for ie. the value of f for (a) between treatments is $(k-1)$, and (b) within treatments is $[k(n-1)]$. Therefore the value of F becomes:

$$F = \frac{SST \cdot k(n-1)}{SSE \cdot (k-1)}$$

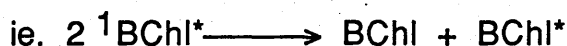
The value of F is entered into the F tables for probability required at $(k-1)$ and $k(n-1)$ degrees of freedom for the numerator and denominator respectively. If the observed value of F is greater than the estimated value, then the null hypothesis is rejected, and the groups are considered to be significantly different within the levels of confidence accepted.

APPENDIX 6

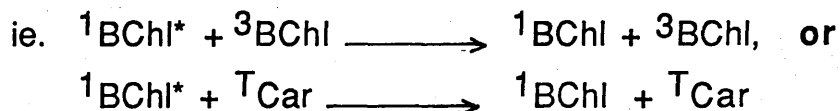
QUENCHING PROCESSES

Energy absorbed by carotenoids is transferred to bacteriochlorophyll and then onto the reaction centre. If, however, the reaction centre traps are closed, subsequent excitation of antenna pigments results in the formation of two types of metastable states; the triplet state of carotenoid pigments ($^T\text{Car}^*$), or, in the absence of carotenoid pigments, the triplet state of bacteriochlorophyll ($^3\text{BChl}^*$). The formation of triplet state carotenoid is probably the result of energy transfer from $^3\text{BChl}^*$, which arises from the intersystem crossing of excited singlet states ($^1\text{BChl}^*$). At relatively weak flashing intensities for intervals of approximately 20 ns, the quantum yield of triplet states is approximately 2%, however, at high-light intensities, quenching processes limit the formation of triplet state antenna pigments; two quenching processes become important:

(1) Singlet-singlet fusion - this process involves the transfer of energy from one $^1\text{BChl}^*$ to another and promotes a higher excited singlet state, which is succeeded by rapid, radiationless relaxation of acceptor BChl to its lowest excited singlet state.



(2) Singlet-triplet fusion - involves energy transfer from singlet excited BChl to a triplet acceptor, followed by radiationless relaxation of the acceptor back to its lowest triplet state.



Quenching processes, therefore, limit the lifetime of excited

singlet states of bacteriochlorophyll.

Examination of quenching by triplet states often employs a dual flash technique: the yield of fluorescence from antenna bacteriochlorophyll during a 20 ns laser flash is measured. This exposure serves to generate $^1\text{BChl}^*$, $^3\text{BChl}$ and ^1Car , any of which may serve to quench fluorescence. After an interval of several μs , during which time the excited states of singlet states have decayed leaving only triplet states, a second weak xenon flash is given which essentially creates steady state conditions and allows an estimate of the quenching effectivity of triplet pigments to be determined [Mauzerall, 1972]. This technique has been employed in a number of studies [(Monger & Parson, 1977)(van Grondelle *et al*, 1983)(Vos *et al*, 1986)] to extract information concerning the movement of singlet excitations within the antenna, and to define a 'domain' [Clayton, 1967] which is uniform with respect to the transfer of singlet excitations.

REFERENCES

- Aagaard, J., and W. R. Sistrom. 1972. Control Of Synthesis of Reaction Center Bacteriochlorophyll in Photosynthetic Bacteria. Photochem. Photobiol. **15**: 209-225.
- Agalidis, I., and F. Reiss-Husson. 1983. Several Properties of the LM unit Extracted with Sodium Dodecyl Sulphate from *Rhodopseudomonas sphaeroides* purified reaction centers. Biochim. Biophys. Acta **724**: 340-351.
- Allen, J. P., and G. Feher. 1984. Crystallization of Reaction Centers from *Rhodopseudomonas sphaeroides*: Preliminary Characterization. Proc. Natl. Acad. Sci. U.S.A. **81**: 4795-4799.
- Allen, J. P., R. Theiler, and G. Feher. 1985a. Crystallization of an Antenna Pigment-Protein Complex from *Rhodopseudomonas sphaeroides*. Biophys. J. **47**: 4a.
- Allen, J. P., R. Theiler, and G. Feher. 1985b. Crystallization and Linear Dichroism Measurements of the B800-850 Antenna Pigment-Protein Complex from *Rhodopseudomonas sphaeroides* 2.4.1. In "Antennas and Reaction Centers of Photosynthetic Bacteria, Structure, Interactions, and Dynamics." (Ed. Michel-Beyerla, M.E.). pp. 82-84. Springer-Verlag. Berlin. Heidelberg. New York. Tokyo.
- Allen, J. P., G. Feher, T. O. Yeates, H. Komiya, D. C. Rees. 1987a. Structure of the Reaction Center from *Rhodobacter sphaeroides* R26: The Cofactors. Proc. Natl. Acad. Sci. U.S.A. **84**: 5730-5734.
- Allen, J. P., G. Feher, T. O. Yeates, H. Komiya, D. C. Rees. 1987b. Structure of the Reaction Center from *Rhodobacter sphaeroides* R26: The Protein Subunits. Proc. Natl. Acad. Sci. U.S.A. **84**: 6162-6166.

- Amesz, J. 1978. Fluorescence and Energy Transfer. In 'The Photosynthetic Bacteria'. (Ed. Clayton, R. K. and W. R. Sistrom). pp. 333-347. Plenum Press. New York. London.
- Amesz, J. 1985. Photosynthesis: Structure of Membrane and Membrane Proteins. Progress in Botany. 47: 87-104.
- Angerhofer, A., R. J. Cogdell and M. F. Hipkins. 1986. A Spectral Characterization of the Light-Harvesting Pigment-Protein Complexes from *Rhodopseudomonas acidophila*. Biochim. Biophys. Acta 848: 333-341.
- Bachman, R. C., K. Gillies, and J. Y. Takemoto. 1981. Membrane Topography of the Photosynthetic Reaction Center Polypeptides of *Rhodopseudomonas sphaeroides*. Biochemistry. 20: 4590-4596.
- Bakker, J. G. C., R. van Grondelle, and W. T. F. Den Hollander. 1983. Trapping, Loss and Annihilation of Excitations in a Photosynthetic System. II. Experiments with the Purple Bacteria *Rhodospirillum rubrum* and *Rhodopseudomonas capsulata*. Biochim. Biophys. Acta 725: 508-518.
- Becker, R., A. Helenius, and K. Simons. 1975. Solubilization of the Semliki Forest Virus Membrane with Sodium Dodecyl Sulfate. Biochemistry 14: 1835-1841.
- Belasco, J. G., J. T. Beatty, C. W. Adams, A. von Gabain, and S. N. Cohen. 1985. Differential Expression of Photosynthesis Genes in *Rps. capsulata*. Results from Segmental Differences in Stability within the Polycistronic *rxsA* Transcript. Cell. 40: 171-181.
- Biebl, H. and N. Pfennig. 1981. Isolation of Members of the Family Rhodospirillaceae. In 'The Prokaryotes - A Handbook of Habitats, Isolation, and Identification of Bacteria.' (Ed. Starr, M. P., H. Stolp, H. G. Trüper, A. Balows, and H. G. Schlegel). pp. 267-273. Springer-Verlag. Berlin. Heidelberg. New York.

- Bishop, O. N. 1971. 'Statistics for Biology'. pp. 56-63. R. Cunningham & Sons Ltd. U.K.
- Bolt, J., and J. Sauer. 1979. Linear Dichroism of Light-Harvesting Bacteriochlorophyll Proteins from *Rhodopseudomonas sphaeroides* in Stretched Polyvinyl Alcohol Films. Biochim. Biophys. Acta **546**: 54-63.
- Bolt, J., J. Sauer, J.A. Shiozawa, and G. Drews. 1981. Linear and Circular Dichroism of Membranes from *Rhodopseudomonas capsulata*. Biochim. Biophys. Acta **635**: 535-541.
- Borisov, A. Yu., R. A. Gadonas, R. V. Danielius, A. S. Piskarskas and A. P. Razjivin. 1982. Minor Component B-905 of Light-Harvesting Antenna in *Rhodospirillum rubrum* Chromatophores and the Mechanism of Singlet-Singlet Annihilation as Studied by Difference Selective Picosecond Spectroscopy. F.E.B.S. Letters. **138**: 25-28.
- Bose, S. K. 1963. Media for Aerobic Growth of Photosynthetic Bacteria. In 'Bacterial Photosynthesis.' (Ed. Gest, H., A. San Pietro, and L. P. Vernon). pp. 501. Yellow Springs. Ohio..
- Breton, J., and A. Vermeglio. 1982. Orientation of Photosynthetic Pigments *in vivo*. In. 'Photosynthesis Volume I: Energy Conversion by Plants and Bacteria'. (Ed. Govindjee). pp. 153-194. Academic Press. New York.
- Breton, J. and E. Navedryk. 1984. Transmembrane Orientation of α -Helices and the Organization of Chlorophyll in Photosynthetic Pigment-Protein Complexes. F.E.B.S. Letters. **176**: 355-359.
- Breton, J., A. Vermeglio, A. Garrigos, and M. Paillotin. 1981. In 'Photosynthesis Volume III: Structure and Molecular Organization of the Photosynthetic Apparatus'. (Ed. Akoyunoglou, G.). Balaban. Int. Sci. Serv. Phil.

- Breton, J., D. L. Farkas, and W. W. Parson. 1985. Organization of the Antenna Bacteriochlorophylls around the Reaction Centers of *Rhodopseudomonas viridis* Investigated by Photoselection Techniques. Biochim. Biophys. Acta **849**: 295-303.
- Brogliè, R. M., C. N. Hunter, P. Delepelaire, R. A. Niederman, N. H. Chua, and R. K. Clayton. 1980. Isolation and Characterization of the Pigment-Protein Complexes of *Rhodopseudomonas sphaeroides* by Lithium Dodecyl Sulphate/Polyacrlamide Gel Electrophoresis. Proc. Natl. Acad. Sci. U.S.A. **77**: 87-91.
- Brunisholz, R. A., P. A. Cuendet, R. Theiler, and H. Zuber. 1981. The Complete Amino Acid Sequence of the Single Light-Harvesting Protein from Chromatophores of *Rhodospirillum rubrum*-G-9⁺. F.E.B.S. Letters. **129**: 150-154.
- Brunisholz, R. A., F. Suter, and H. Zuber. 1984a. The Light-Harvesting Polypeptides of *Rhodospirillum rubrum* I. The Amino Acid Sequence of the Second LH Polypeptide B880- β (B870- β) of *Rs. rubrum* S1 and the Carotenoidless Mutant G-9⁺. Aspects of the Molecular Structure of the Two LH Polypeptides B880- α (B870- α) and B880- β (B870- β) and of the Antenna Complex B880 (B870) from *Rs. rubrum*. Hoppe-Seylers Z. Physiol. Chem. **365**: 675-688.
- Brunisholz, R. A., V. Wiemken, F. Suter, R. Bachofen, and H. Zuber. 1984b. The Light-Harvesting Polypeptides of *Rhodospirillum rubrum* II. Localization of the Amino Acid Terminal Regions of the LH-Polypeptides of B870- α and B870- β and the Reaction Center Subunits L at the Cytoplasmic side of the Photosynthetic Membrane of *Rhodospirillum rubrum* G-9⁺. Hoppe-Seylers Z. Physiol. Chem. **365**: 689-701.

- Brunisholz, R. A., F. Jay, F. Suter, and H. Zuber. 1985. The Light-Harvesting Polypeptides of *Rhodopseudomonas viridis*: The Complete Amino-Acid Sequences of B1015- α , and B1015- β and B1015-Y. Biol. Chem. Hoppe-Seyler. 366: 87-98.
- Brunisholz, R. A., H. Zuber, J. Valentine, J. G. Lindsay, K. J. Woolley, and R.J. Cogdell. 1986. The Membrane Localization of the B890-Complex from *Rhodospirillum rubrum* and the Effect of Carotenoid on the Conformation of its Apoproteins Exposed on the Cytoplasmic Surface. Biochim. Biophys. Acta 849: 295-303.
- Campillo, A. J., R. C. Hyer, T. G. Monger, W. W. Parson and S. L. Shapiro. 1977. Light Collection and Harvesting Processes in Bacterial Photosynthesis Investigated on a Picosecond Time Scale. Proc. Natl. Acad. Sci. U.S.A. 74: 1997-2001.
- Capaldi, R. A. and D. E. Green. 1972. Membrane proteins and Membrane structure. F.E.B.S. Letters. 25: 205-209.
- Chessin, M., R. Livingston, and T. G. Truscott. 1966. Direct Evidence for the Sensitized Formation of a Metastable State of β -Carotene. Trans. Faraday. Soc. 62: 1519-1524.
- Clark, W. G., E. Davidson, and B. L. Marrs. 1984. Variation of Levels of mRNA coding for Antenna and Reaction Center Polypeptides in *Rps. capsulata* in Response to Changes in O_2 Concentration. J. Bacteriol. 157: 945-948.
- Clayton, R.K. 1963. Toward the Isolation of a Photochemical Reaction Centre in *Rhodopseudomonas sphaeroides*. Biochim. Biophys. Acta 75: 312-323.
- *Clayton, R. K. 1966. Spectroscopic Analysis of Bacteriochlorophylls *in vitro* and *in vivo*. Photochem. Photobiol. 5: 669.

- Clayton, R. K. 1967. Photosynthesis: Fluorescence and Photochemistry. J. Theoretical Biol. 14: 173-186.
- Clayton, R. K. 1971. Light and Living Matter; A Guide to the Study of Photobiology. pp. 2-66. McGraw-Hill Book Company. New York.
- Clayton, R. K. 1973. Primary Processes in Bacterial Photosynthesis. Ann. Rev. Biophys. Bioeng. 2: 131-156.
- Clayton, R. K. 1980. 'Photosynthesis: Physical Methods and Chemical Patterns'. pp. 88-110. Cambridge University Press. Cambridge. England.
- Clayton, R. K. and B. J. Clayton. 1972. Relations Between Pigments and Proteins in the Photosynthetic Membranes of Rhodopseudomonas sphaeroides. Biochim. Biophys. Acta 283: 492-504.
- Clayton, R. K. and B. J. Clayton. 1978. Properties of Photochemical Reaction Centers Purified from Rhodopseudomonas gelatinosa. Biochim. Biophys. Acta 501: 470-477.
- Clayton, R. K. and R. Haselkorn. 1972. Protein Components of Bacterial Photosynthetic Membranes. J. Mol. Biol. 68: 97-105.
- Clayton, R. K. and W. R. Sistrom. 1978. 'The Photosynthetic Bacteria'. Plenum Press. New York. London.
- Clayton, R. K., and S. C. Straley. 1972. Photochemical Electron Transport in Photosynthetic Reaction Centers from Rhodopseudomonas sphaeroides. IV. Observations related to the reduced photoproducts. Biophysical J. 12: 1221-1223.

- Clayton, R. K. and H. F. Yau. 1972. Photochemical Electron Transport in Photosynthetic Reaction Centers from *Rhodopseudomonas sphaeroides*.I. Kinetics of the oxidation and reduction of P870 as affected by external factors. Biophysical J. 12: 867-881.
- Clayton, R. K., H. Fleming, and E. Z. Szuts. 1972a. Photochemical Electron Transport in Photosynthetic Reaction Centers from *Rhodopseudomonas sphaeroides*.II. Interaction with external electron donors and acceptors and a reevaluation of some spectroscopic data. Biophysical J. 12: 45-63.
- Clayton, R. K., E. Z. Szuts, and H. Fleming. 1972b. Photochemical Electron Transport in Photosynthetic Reaction Centers from *Rhodopseudomonas sphaeroides*.III. Effects of orthophenanthroline and other chemicals. Biophysical J. 12: 64-79.
- Cogdell, R. J. 1985. Carotenoids in Photosynthesis. Pure and Applied Chemistry. 57: 723-728.
- Cogdell, R. J. and A. R. Crofts. 1978. Analysis of the Pigment Content of an Antenna Pigment-Protein Complex from Three Strains of *Rhodopseudomonas.sphaeroides*. Biochim. Biophys. Acta 502: 409-416.
- Cogdell, R. J. and H. Scheer. 1985. Circular Dichroism of Light-Harvesting Complexes from Purple Photosynthetic Bacteria. Photochem. Photobiol. 42: 669-689.
- Cogdell, R. J. and J. P. Thornber. 1979. The Preparation and Characterization of Different Types of Light-Harvesting Pigment-Protein Complexes from some Purple Bacteria. in; 'Chlorophyll Organization and Energy Transfer in Photosynthesis'. Ciba Foundation Symp. 61 (new series). (Ed. Wolstenholme, G. and D. W. Fitzsimons). pp. 61-79. Elsevier/Excerpta Medica.

- Cogdell, R. J. and J. P. Thornber.** 1980. Light-Harvesting Pigment-Protein Complexes of Purple Photosynthetic Bacteria. F.E.B.S. Letters. **122**: 1-8.
- Cogdell, R. J. and J. Valentine.** 1983. Bacterial Photosynthesis: Yearly Review. Photochem. Photobiol. **38**: 769-772.
- Cogdell, R. J., D. C. Brune, and R. K. Clayton.** 1974. Effects of Extraction and Replacement of Ubiquinone upon the Photochemical activity of Reaction Centers and Chromatophores from *Rhodopseudomonas sphaeroides*. F.E.B.S. Letters. **45**: 344-347.
- Cogdell, R. J., J. G. Lindsay, J. Valentine, and I. Durant.** 1982. A Further Characterization of the B890 Light-Harvesting Pigment-Protein Complex from *Rhodospirillum rubrum* strain S1. F.E.B.S. Letters. **151**: 151-154.
- Cogdell, R. J., I. Durant, J. Valentine, J. G. Lindsay and K. Schmidt.** 1983. The Isolation and Partial Characterization of the Light-Harvesting Pigment-Protein Complement of *Rhodopseudomonas acidophila*. Biochim. Biophys. Acta **772**: 427-435.
- Cogdell, R. J., K. J. Woolley, R. C. Mackenzie, J. G. Lindsay, H. Michel, J. Dobler and W. Zinth.** 1985. Antenna and Reaction Centers of Photosynthetic bacteria. In Springer Series in Chemical Physics **42**. (Ed. Michel-Beyene, M. E.). pp. 85-87. Springer-Verlag. Berlin. Heidelberg. New York. Tokyo.
- Cogdell, R. J., K. J. Woolley, L. A. Ferguson and D. J. Dawkins.** 1987. Progress in Crystallizing Bacterial Antenna Complexes. In 'Workshop-Structure, Function and Formation of Membrane-Bound Complexes in Phototrophic Bacteria'. pp. 11 Freiburg. Fed. Rep. Germany. April, 1987.

- Cohen-Bazire, G., and W. R. Sistrom. 1966. In 'The Chlorophylls' (Ed. Vernon, L. P. and G. R. Seely). pp. 313. Academic Press. New York.
- Cohen-Bazire, G. and R. Y. Stanier. 1958. Inhibition of Carotenoid Synthesis in Photosynthetic Bacteria. Nature. **181**: 250-252.
- Cohen-Bazire, G., W. R. Sistrom, and R. Y. Stanier. 1957. Kinetic Studies of Pigment Synthesis by Non-Sulphur Purple Bacteria. J. Cell. Comp. Physiol. **49**: 25-68.
- Davis, B. J. 1964. Disc Electrophoresis II. Method and Application to Human Serum Proteins. Ann. New York Acad. Sci. **121**: 404-427.
- Davis, D. R. and D. M. Segal. 1971. Protein Crystallization: Micro Techniques Involving Vapour Diffusion. In 'Methods of Enzymology'. (Ed. Jakoby, W. B.) pp. 266-269. Academic Press. New York
- Debus, R. J., G. Feher, and M. Y. Okamura. 1985. LM Complex of Reaction Centers from *Rhodopseudomonas sphaeroides* R-26: Characterization and Reconstitution with the H-Subunit. Biochemistry. **24**: 2488-2500.
- Deisenhofer, J., O. Epp, K. Miki, R. Huber, and H. Michel. 1984. X-ray Structure Analysis of a Membrane Protein Complex. J. Mol. Biol. **180**: 385-398.
- Deisenhofer, J., O. Epp, K. Miki, R. Huber, and H. Michel. 1985. Structure of the Protein Subunits in the Photosynthetic Reaction Centre of *Rhodopseudomonas viridis* at 3 Å Resolution. Nature. **318**: 618-624.
- DeMartini, M. and M. Inouye. 1978. Interaction Between Two Major Proteins of *Escherichia coli*: the Matrix Protein and the Lipoprotein. J. Bacteriol. **133**: 329-335.

- Dickerson, R. E., T. Takano, D. Eisenberg, B. Kallai, L. Samson, A. Cooper and E. Margulies. 1971. Ferricytochrome C. I. General Features of the Horse and Bonito Proteins at 2.8 Å Resolution. J. Biol. Chem. **246**: 1511-1535.
- Dixon, M, and E. C. Webb. 1961. Enzyme Fractionation by Salting-Out: A Theoretical Note. Adv. Protein Chem. **16**: 197-219.
- Drews, G. 1978. Structure and Development of the Membrane System of Photosynthetic Bacteria. In 'Current Topics in Bioenergetics. Volume 8' (Ed. Sanadi, D. R. and L.P. Vernon). pp. 161-207. Academic Press. New York.
- Drews, G. 1985. Structure and Functional Organization of Light-Harvesting Complexes and Photochemical Reaction Centres in Membranes of Photosynthetic Bacteria. Microbiological Reviews. **49**: 59-70.
- Drews, G., R. Feick, A. Schumacher, and N. N. Firsow. 1977. Organization and Formation of the Photosynthetic Apparatus of *Rhodopseudomonas capsulata* and *Rhodopseudomonas palustris*. In 'Proceedings of the Fourth International Congress on Photosynthesis' (Ed. Hall, D. O., J. Coombs, and T. W. Goodwin). pp. 83-93. The Biochemical Society. London.
- Drews, G., J. Peters, and R. Dierstein. 1983. Molecular Organization and Biosynthesis of Protein-Pigment Complexes of *Rhodopseudomonas capsulata*. Ann. Microbio. (Inst. Pasteur). **134B**: 151-158.
- *Duysens, L.M.N. 1952. Transfer of Excitation Energy in Photosynthesis. Thesis. University Of Utrecht. 1-96.
- Duysens, L. N. M., W. J. Huiskamp, J. J. Vos. and J. M. van der Hart. 1956. Reversible Changes in Bacteriochlorophyll in Purple Bacteria upon Illumination. Biochim. Biophys. Acta **19**: 188-190.

- Eimhejellen, K. E., O. Aasmundrud and A. Jenson. 1963. A New Bacterial Chlorophyll. Biochem. Biophys. Res. Commun. **10**: 232-242.
- Eimhjellen, K. E., H. Steensland, and J. Traetteberg. 1967. A. Thiococcus sp. nov. gen., Its Pigments and Internal Membrane System. Archiv. für Mikrobiologie **59**: 82-92.
- Engelhardt, H., W. Baumeister, and W. O. Saxton. 1983. Electron Microscopy of Photosynthetic Membranes Containing Bacteriochlorophyll b. Arch. Microbiol. **135**: 169-175.
- Engelhardt, H., A. Engel, and W. Baumeister. 1986. Stoichiometric Model of the Photosynthetic Unit of Ectothiorhodospira halochloris. Proc. Natl. Acad. Sci. U.S.A. **83**: 8972-8976.
- Fairbanks, G., T. L. Steck, and D. F. H. Wallach. 1971. Electrophoretic Analysis of the Major Erythrocyte Membrane. Biochemistry **10**: 2606-2617.
- Fajer, J., D. C. Brune, M. S. Davis, A. Forman, and L. D. Spaulding. 1975. Primary Charge Separation in Bacterial Photosynthesis: Oxidized Chlorophylls and Reduced Pheophytin. Proc. Natl. Acad. Sci. U.S.A. **72**: 4956-4960.
- Feher, G., and M. Y. Okamura. 1978. Chemical Composition and Properties of Reaction Centers. In 'The Photosynthetic Bacteria' (Ed. Clayton, R. K. and W. R. Sistrom). pp. 349-386. Plenum Press. New York..
- Feher, G., and M. Y. Okamura. 1984. Structure and Function of the Reaction Center from Rhodopseudomonas sphaeroides. in 'Advances in Photosynthesis Research. Volume II'. (Ed. Sybesma, C.). pp. 155-164. Nijhoff/Junk Publishers. The Hague. Boston. Lancaster.

- Feher, G., M. Y. Okamura and J. D. McElroy. 1972. Identification of an Electron Acceptor in Reaction Centers of *Rhodopseudomonas sphaeroides* by EPR Spectroscopy. Biochim. Biophys. Acta **267**: 222-.
- Feher, G., A. J. Hoff, R. A. Isaacson, L. C. Ackerson. 1975. Endor Experiments in Chlorophyll and Bacteriochlorophyll *in vivo* and in the Photosynthetic Unit. Ann. N. Y. Acad. Sci. **244**: 239-259.
- Feick, R., and G. Drews. 1978. Isolation and Characterization of Light-Harvesting Bacteriochlorophyll: Protein Complexes from *Rhodopseudomonas capsulata*. Biochim. Biophys. Acta **501**: 499-513.
- Firsow, N. N., and G. Drews. 1977. Differentiation of the Intracytoplasmic Membrane of *Rhodopseudomonas palustris* by Variations of Oxygen Partial Pressure of Light Intensity. Arch. Microbiol. **115**: 299-306.
- Foote, C. S. 1968. Methods of Photosensitized Oxidation. Science **162**: 963-970.
- *Foote, C. S., and R. W. Denny. 1968. Ann. Chem. Soc. **90**: 6233.
- Fraker, P. J., and S. Kaplan. 1972. Isolation and Characterization of a Bacteriochlorophyll-Containing Protein from *Rhodopseudomonas sphaeroides*. J. Biol. Chem. **247**: 2732-2737.
- Frank, H. A., S. Shahriars, A. Teremi, and J. R. James. 1987. Crystallization and Preliminary X-ray and Optical Spectroscopic Characterization of the Photochemical Reaction Centre from *Rhodobacter sphaeroides* strain 2.4.1. F.E.B.S. Letters (in press).

- Francis, G. A. and W. R. Richards. 1980. Localization of Photosynthetic Membrane Components on *Rhodopseudomonas sphaeroides* by a Radioactive Labelling Procedure. Biochemistry 19: 5104-5111.
- *Füglister, P., R. Rumbeli, F. Suter, and H. Zuber. 1984. Physiol. Chem. 365: 675-
- Fyfe, W. H. M. 1985. The Choice of a Suitable Detergent for the Solubilization and Purification of the Antenna Complexes of Two Purple Non-Sulphur Bacteria. Undergraduate BSc. project, Unpublished.
- Garavito, R. M. and J. P. Rosenbusch. 1980. Three-Dimensional Crystals of an Integral Membrane Protein: An Initial X-Ray Analysis. J. Cell Biol. 86: 327-329.
- Glazer, A. N. 1983. Comparative Biochemistry of Photosynthetic Light-Harvesting Systems. Ann. Rev. Biochem. 52: 127-157.
- Goedheer, J. C. 1973. Fluorescence Polarization and Pigment Orientation in Photosynthetic Bacteria. Biochim. Biophys. Acta 292: 665-676.
- Gogel, G. E., P. S. Parkes, P. A. Loach, R. A. Brunisholz, and H. Zuber. 1983. The Primary Structure of a Light-Harvesting Bacteriochlorophyll-binding Protein of Wild-Type *Rhodospirillum rubrum*. Biochim. Biophys. Acta 746: 32-39.
- Gomez, I., F. F. Del Campo, and J. M. Ramirez. 1982. The Antenna System of *Rhodospirillum rubrum*: Derivative Analysis of the Major Near Infrared Absorption Band of Chromatophores. F.E.B.S. Letters 141: 185-188.
- Griffiths, M., W. R. Sistrom, G. Cohen-Bazire, and R. Y. Stanier. 1955. Function of Carotenoids in Photosynthesis. Nature 176: 1211-1214.

- Hames, B. D. 1981. An Introduction to Polyacrylamide Gel Electrophoresis. In 'Gel Electrophoresis of Proteins: A Practical Approach'. (Ed. Hames, B. D. and D. Rickwood). pp. 1-91. IRL Press. London.
- Hayashi, H., M. Nakano, and S. Morita. 1982a. Comparative Studies of Protein Properties and Bacteriochlorophyll-Protein Complexes from Spectrally Different Types of *Rhodopseudomonas palustris*. J. Biochem. **92**: 1805-1811.
- Hayashi, H., M. Miyao, and S. Morita. 1982b. Absorption and Fluorescence Spectra of Light-Harvesting Bacteriochlorophyll-Protein Complexes from *Rhodopseudomonas palustris* in the Near-Infrared Region. J. Biochem. **91**: 1017-1027.
- Henderson, R. and D. Shotton. 1980. Crystallization of Purple Membrane in Three Dimensions. J. Mol. Biol. **139**: 99-109.
- Helenius, A., and K. Simons. 1975. Solubilization of Membranes by Detergents. Biochim. Biophys. Acta **415**: 29-79.
- Helenius, A., D. R. McCaslin, E. Fries, and C. Tanford. 1979. Properties of Detergents. Methods in Enzymology: Volume **LVI**: 734-749.
- Hipkins, M.F. and N. R. Baker. 1986. Spectroscopy. In 'Photosynthesis-Energy Transduction-A Practical Approach'. (Ed. Hipkins, M. F. and N. R. Baker). pp. 50-101. IRL Press Ltd. Oxford.
- Hunter, C. N., R. van Grondelle, N. G. Holmes, O. T. G. Jones, and R. A. Niederman. 1979. Fluorescence Yield Properties of a Fraction Enriched in Newly Synthesized Bacteriochlorophyll a-Protein Complexes from *Rhodopseudomonas sphaeroides*. Photochem. Photobiol. **30**: 313-316.

- Hunter, C. N., R. A. Niederman, and R. K. Clayton. 1981. Excitation Energy Transfer by Antenna Complexes Isolated from *Rhodopseudomonas sphaeroides* by Lithium Dodecyl Sulphate/Polyacrylamide Gel Electrophoresis. In 'Proceedings of the Fifth International Congress on Photosynthesis' (Ed. Akoyunoglou, G.). pp. 539-545. Balaban Int. Sci. Serv. Phil. P.A.
- Hunter, C. N., J. D. Pennoyer, and R. A. Niederman. 1982. Assembly and Structural Organization of Pigment-Protein Complexes in Membranes of *Rhodopseudomonas sphaeroides*. In 'Proceedings of the Special F.E.B.S. Meeting on Cell Function and Differentiation'. (Ed. Evangelopoulos, E.). Alan R. Liss. Inc. New York.
- Hunter, C. N., H. J. M. Kramer, and R. van Grondelle. 1985. Linear Dichroism and Fluorescence Emission of Antenna Complexes During Photosynthetic Unit Assembly in *Rhodopseudomonas sphaeroides*. Biochim. Biophys. Acta 807: 44-51.
- Imhoff, J. F., H. G. Trüper, and N. Pfennig. 1984. Rearrangement of the Species and Genera of the Phototrophic "Purple Nonsulphur Bacteria". International J. Systematic Bacteriol. 34: 340-343.
- Jay, F., M. Lambillotte, W. Stark, and K. Mühlethaler. 1984. The Preparation and Characterization of Native Photoreceptor Units from the Thylakoids of *Rhodopseudomonas viridis*. The EMBO J. 3: 773-776.
- Kaufman, N., H. Reidl, J. R. Golecki, A. F. Garcia and G. Drews. 1982. Differentiation of the Membrane System in Cells of *Rhodopseudomonas capsulata* after Transition from Chemotrophic to Phototrophic Growth Conditions. Arch. Microbiol. 131: 313-322.

Ke, B., L. P. Vernon, A. Garcia, and E. Ngo. 1968. Coupled Photooxidation of Bacteriochlorophyll P890 and Photoreduction of Ubiquinone in a Photochemically Active Subchromatophore Particle Derived from *Chromatium*. *Biochemistry* 7: 311-325.

Kendall-Tobias, M. W., and M. Seibert. 1982. A Rapid Procedure for the Isolation and Purification of Photosynthetic Reaction Centers from *Rhodopseudomonas sphaeroides* R-26. *Arch. Biochem. Biophys.* 216: 255-258.

Klug, G., R. Liebetanz, and G. Drews. 1986. The Influence of Bacteriochlorophyll Biosynthesis on Formation of Pigment-Binding Proteins and Assembly of Pigment-Protein Complexes in *Rhodopseudomonas capsulata*. *Arch. Microbiol.* 146: 284-291.

Kramer, H. J. M., R. van Grondelle, C. N. Hunter, W. H. J. Westerhuis and J. Ames. 1984a. Pigment Organization of the B800-850 Antenna Complex of *Rhodopseudomonas sphaeroides*. *Biochim. Biophys. Acta* 765: 156-165.

Kramer, H. J. M., J. D. Pennoyer, R. van Grondelle, W. H. J. Westerhuis, R. A. Niederman and J. Ames. 1984b. Low Temperature Optical Properties and Pigment Organization of the B875 Light-Harvesting Bacteriochlorophyll-Protein Complex of the Purple Photosynthetic Bacteria. *Biochim. Biophys. Acta* 767: 335-344.

*Krinsky, N. I. 1968. *Photophysiology* 3: 123-195.

*Krinsky, N. I. 1979. *Pure Applied Chemistry* 51: 649-660.

Laemmli, U. K. 1970. Cleavage of Structural Proteins During the Assembly of the Head of Bacteriophage T4. *Nature* 227: 680-685.

Lascelles, J. 1968. The Bacterial Photosynthetic Apparatus. *Advances in Microbial Physiology* 2: 1-42.

- Lien, S. and H. Gest. 1973. Chlorophyll Synthesis in Photosynthetic Bacteria. J. Bioenergetics 4: 423-434.
- Loach, P. A. 1980. Bacterial Reaction Center and Photoreceptor Complex Preparations. Methods in Enzymology 69: 155-172.
- Mäntele, W., K. Steck, T. Wacker, and W. Welte. 1985. Antennas and Reaction Centers of Photosynthetic Bacteria. in 'Springer Series in Chemical Physics 42' (Ed. Michel-Beyerle, M.E.). pp. 88-94. Spring-Verlag, Berlin. Heidelberg. New York. Tokyo.
- Mäntele, W., A. Becker, T. Wacker, and W. Welte. 1987. Spectroscopic Studies of the Crystallized Reaction Center-B875 Light-Harvesting Complexes of *Rhodopseudomonas palustris*. In 'Workshop, Structure, Function and Formation of Membrane-Bound Complexes in Phototrophic Bacteria. pp. 13. Freiburg. Fed. Rep. Germany.
- Margolis, J. and K. G. Kenrick. 1968. Polyacrylamide Gel Electrophoresis in a Continuous Molecular Sieve Gradient. Analytical Biochem. 25: 347-362.
- Matsuura, K. and K. Shimada. 1986. Cytochromes Functionally Associated to Photochemical Reaction Centers in *Rhodopseudomonas palustris* and *Rhodopseudomonas acidophila*. Biochim. Biophys. Acta 852: 9-18.
- Mauzerall, D. 1972. Light-Induced Fluorescence Changes in *Chlorella* and the Primary Photoreactions for the Production of Oxygen. Proc. Natl. Acad. Sci. U.S.A. 69: 1358-1362.
- McPherson, A. 1976. Crystallization of Proteins from Polyethylene Glycol. J. Biol. Chem. 251: 6300-6303.
- McPherson, A. 1982. 'Preparation and Analysis of Protein Crystals'. J. Wiley & Sons, Inc. U.S.A.

- McPherson, A. and R. Spencer. 1975. Preliminary Structure Analysis of Canavalin from Jack Bean. Arch. Biochem. Biophys. **169**: 650-661.
- Meinhardt, S. W., P. J. Kiley, S. Kaplan, A. R. Crofts and S. Harayama. 1985. Characterization of Light-Harvesting Mutants of *Rhodopseudomonas sphaeroides*. I. Measurement of the Efficiency of Energy Transfer from Light-Harvesting Complexes to the Reaction Center. Arch. Biochem. Biophys. **236**:130-139.
- Mejbaum-Katzenellenbogen, W. and W. Dobryszczycka. 1959. New Method for Quantitative Determination of Serum Proteins Separated by Paper Electrophoresis. Clinica. Chimica. Acta. **4**: 515-522.
- Meyer, R., M. Snozzi, and R. Bachofen. 1981. Freeze-Fracture Studies of Reaction Centres from *Rhodospirillum rubrum* in Chromatophores and Liposome. Arch. Microbiol. **130**: 125-128.
- Michel, H. 1982. Three-Dimensional Crystals of a Membrane Protein Complex.: The Photosynthetic Reaction Centre from *Rhodopseudomonas viridis*. J. Mol. Biol. **158**: 567-572.
- Michel, H. 1983. Crystallization of Membrane Proteins. Trends in Biochemical Science **8**: 56-59.
- Michel, H. and D. Oesterhelt. 1980. Three-Dimensional Crystals of Membrane Proteins: Bacteriorhodopsin. Proc. Natl. Acad. Sci. U.S.A. **77**: 1283-1285.
- Michel, H., K. A. Weyer, H. Gruenberg, and F. Lottspeich. 1985. The 'Heavy' Subunit of the Photosynthetic Reaction Center from *Rhodopseudomonas viridis*: Isolation of the Gene, Nucleotide and Amino-Acid Sequence. EMBO. J. **4**: 1667-1672.

- Michel, H., K. A. Weyer, H. Gruenberg, I. Dunger, D. Oesterhelt and F. Lottspeich. 1986. The 'Light' and 'Heavy' Subunits of the Photosynthetic Reaction Centre from *Rhodopseudomonas viridis*: Isolation of the Genes. Nucleotide and Amino-Acid Sequence. EMBO. J. 5: 1149-1158.
- Miller, K. R. 1979. Structure of a Bacterial Photosynthetic Membrane. Proc. Natl. Acad. Sci. U.S.A. 76: 6415-6419.
- Miller, K. R. 1982. Three-Dimensional Structure of a Photosynthetic Membrane. Nature 300: 53-55.
- Miller, K. R. and J. S. Jacob. 1983. Two-Dimensional Crystals Formed from Photosynthetic Reaction Centers. J. Cell. Biol. 97: 1266-1270.
- Miller, K. R. and J. S. Jacob. 1985. The *Rhodopseudomonas viridis* Photosynthetic Membrane: arrangement *in situ*. Arch. Microbiol. 142: 333-339.
- *Molisch, H. 1907. Die Purpurbakterien nach neuen untersuchungen. Fischer Verlag. Jena: 95.
- Monger, T. G. and W. W. Parson. 1977. Singlet-Triplet Fusion in *Rhodopseudomonas sphaeroides* Chromatophores: A Probe of the Organization of the Photosynthetic Apparatus. Biochim. Biophys. Acta 460: 393-407.
- Monger, T. G., R. J. Cogdell and W. W. Parson. 1976. Triplet States of Bacteriochlorophyll and Carotenoids in Chromatophores of Photosynthetic Bacteria. Biochim. Biophys. Acta 449: 136-153.
- Morrison, L., J. Runquist, and P. Loach. 1977. Ubiquinone and Photochemical Activity in *Rhodospirillum rubrum*. Photochem. Photobiol. 25: 73-84.

- Nabedryk, E, and J. Breton. 1981. Orientation of Intrinsic Proteins in Photosynthetic Membranes. Biochim. Biophys. Acta 635: 515-524.
- Nabedryk, E., D. M. Tiede, P. L. Dutton, and J. Breton. 1982. Conformation and Orientation of the Protein in the Bacterial Photosynthetic Reaction Centre. Biochim. Biophys. Acta 682: 273-280.
- Niederman, R. A., D. E. Mallon, and J. J. Langan. 1976. Membranes of *Rhodopseudomonas sphaeroides*. IV. Assembly of Chromatophores in Low-aeration Cell Suspensions. Biochim. Biophys. Acta 440: 429-447.
- Nishi, N., M. Kataoka, G. Soe, T. Kakuno,, T. Ueki, J. Yamashita and T. Horio. 1979. Disintegration of *Rhodospirillum rubrum* Chromatophore Membrane into Photoreaction Units, Reaction Centres, and Ubiquinone-to Protein with Mixture of Cholate and Deoxycholate. J. Biochem. 86: 1211-1224.
- Norris, J. R., R. A. Uphaus, H. L. Crespi, and J. J. Katz. 1971. Electron Spin Resonance of Chlorophyll and the Origin of Signal I in Photosynthesis. Proc. Natl. Acad. Sci. U.S.A. 68: 625-628.
- Oelze, J. and G. Drews. 1972. Membranes of Photosynthetic Bacteria. Biochim. Biophys. Acta 265: 209-239.
- Oelze, J. and J. R. Golecki. 1975. Properties of Reaction Center Depleted Membranes of *Rhodospirillum rubrum* (Mutant Strain VI). Arch. Microbiol. 102: 59-64.

- Okamura, M. Y., L. A. Steiner and G. Feher. 1974. Characterization of Reaction Centers from Photosynthetic Bacteria. I. Subunit Structure of the Protein Mediating the Primary Photochemistry in *Rhodopseudomonas sphaeroides* R-26. Biochemistry **13**: 1394-1402.
- Okamura, M. Y., G. Feher and N. Nelson. 1982. Reaction Centers In 'Photosynthesis Volume I: Energy Conversion by Plants and Bacteria'. (Ed. Govindjee). pp. 195-272. New York. Academic Press.
- Ornstein, L. 1964. Disc Electrophoresis. Ann. N. Y. Acad. Sci. **121**: 321-349.
- Parker, R. E. 1979. Introductory Statistics for Biology. (Second Edition). Studies in Biology **43**. Arnold. London.
- Parson, W., D. Holten, C. Kirmaier, A. Scherz and Woodbury. 1984. Primary Reactions in Bacterial Reaction Centers in 'Advances in Photosynthesis Research Volume I' (Ed. Sybesma, C.). pp. 187-194. Martinus Nijhoff/Dr. W. Junk Publishers. The Hague/Boston/Lancaster.
- Pearlstein, R. M. and Heminger, R.. 1978. Bacteriochlorophyll Electronic Transition Moment Direction in Bacteriochlorophyll a Protein. Proc. Natl. Acad. Sci. U.S.A. **75**: 4920-4924.
- Peter, J., J. Takemoto and G. Drews. 1983. Spatial Relationships Between the Photochemical Reaction Center and the Light-Harvesting Complexes in the Membrane of *Rhodopseudomonas capsulata*. Biochemistry **22**: 5660-5667.
- Peter, J., W. Welte and G. Drews. 1984. Topographical Relationships of Polypeptides in Photosynthetic Membranes of *Rhodopseudomonas viridis* Investigated by Reversible Chemical Cross-Linking. F.E.B.S. Letters **171**: 267-270.

- Pfennig, N. 1967. Photosynthetic Bacteria. Ann. Rev. Microbiol. 21: 285-324.
- Pfennig, N. 1978. General Pysiology and Ecology of Photosynthetic Bacteria. In 'The Photosynthetic Bacteria' (Ed. Clayton, R. K. and W. R. Sistrom). pp. 3-14. Plenum Press. New York. London.
- Pfennig, N. and H. G. Trüper. 1981. Isolation of Members of the Families Chromatiaceae and Chlorobiaceae. In 'The Prokaryotes-A Handbook of Habitata, Isolation and Identification of Bacteria. Vol. I.' (Ed. Starr, M. P., H. Stolp, H. G. Trüper, A. Balows and H. G. Schlegel). pp. 274-279. Springer-Verlag. Berlin. Heidelberg. New York.
- Picorel, R, G. Bélanger, and G. Gingras. 1983. Antenna Halochrome B880 of *Rhodospirillum rubrum* S1. Pigment, Phospholipid and Polypeptide Composition. Biochemistry 22: 2491-2497.
- Pradel, J., J. Lavergne and I. Moya. 1978. Formation and Development of Photosynthetic Units in Repigmenting *Rhodopseudomonas sphaeroides* Wild-Type and 'Phofil' Mutant-Strain. Biochim. Biophys. Acta 502: 169-182.
- Prince, R. C. and J. P. Thornber. 1977. A Novel Electron Paramagnetic Resonance Signal Associated with the 'Primary' Electron Acceptor in Isolated Photochemical Reaction Centers of *Rhodospirillum rubrum*. F.E.B.S. Letters. 81: 233-237.
- Pucheu, N. L., N. L. Kerber, and A. F. Garcia. 1976. Isolation and Purification of Reaction Center from *Rhodopseudomonas viridis* NHTC 133 by Means of LDAO. Arch. Microbiol. 109: 301-305.

- Radcliffe, C. W., J. D. Pennoyer, R. M. Brogue and R. A. Niederman. 1984. In 'Advances in Photosynthesis Research. Volume II'. (Ed. Sybesma, C.). pp. 215-218. Nijhoff/Junk. The Hague. Boston. Lancaster.
- Raymond, S. 1964. Acrylamide Gel Electrophoresis. Ann. N. Y. Acad. Sci. 121: 350-365.
- Raymond, S. and L. Weintraub. 1959. Acrylamide Gel as a Supporting Medium for Zone Electrophoresis. Science 130: 711.
- Razjivin, A. P., R. V. Danielius, R. A. Gadonas, A. Yu. Borisov and A. S. Piskarkas. 1982. The Study of Excitation Transfer Between Light-Harvesting Antenna and Reaction Center in Chromatophores from Purple Bacterium *Rhodospirillum rubrum* by Selective Picosecond Spectroscopy. F.E.B.S. Letters. 143: 40-44.
- Reed, D. W., and R. K. Clayton. 1968. Isolation of a Reaction Center Fraction from *Rhodopseudomonas sphaeroides*. Biochem. Biophys. res. Comm. 30: 471-775.
- Remson, C. C. 1978. Comparative Subcellular Architecture of Photosynthetic Bacteria. in 'The Photosynthetic Bacteria' (Ed. Clayton, R. K. and W. R. Sistrom). pp. 31-77. Plenum Press. New York. London.
- Reynolds, J. A. and C. Tanford. 1970. The Gross Conformation of Protein-Sodium Dodecyl Sulphate Complexes. J. Biological Chemistry. 245: 5161-5165.
- Rothe, G. M. and Maurer, W. D. 1986. in 'Gel Electrophoresis of Proteins' (Ed. Dunn, M. J.) pp. 37-140. J. Wright. Bristol.

- Rijgersberg, C. P., R. van Grondelle and J. Ames.** 1980. Energy Transfer and Bacteriochlorophyll Fluorescence in Purple Bacteria at Low Temperatures. Biochim. Biophys. Acta **592**: 53-64.
- Sauer, K. and L. A. Austin.** 1978. Bacteriochlorophyll-Protein Complexes from the Light-Harvesting Antenna of Photosynthetic Bacteria. Biochemistry **17**: 2011-2019.
- Schachman, H.K., A.B. Pardee and R.Y. Stanier.** 1952. Studies on the Macromolecular Organization of Microbiol Cells. Arch. Biochem. Biophys. **38**: 245-260.
- Schmidt, K., R. Brunisholz, and H. Zuber.** Unpublished. Cited by Brunisholz, R. (1987). Structural Aspects of the Antenna Polypeptides from *Rhodopseudomonas acidophila* and *Rhodocyclus gelatinosus*. In 'Workshop-Structure, Function and Formation of Membrane-Bound Complexes in Phototrophic Bacteria'. pp. 9. Freiburg. Fed. Rep. Germany.
- Schumacher, A. and G. Drews.** 1978. The Formation of Bacteriochlorophyll-Protein Complexes of the Photosynthetic Apparatus of *Rhodopseudomonas capsulata* During Early Stages of Development. Biochim. Biophys. Acta **501**: 183-194.
- Sebban, P., B. Robert and G. Jolchine.** 1985. Isolation and Spectroscopic Characterization of the B875 Antenna Complex of a Mutant of *Rhodopseudomonas sphaeroides*. Photochem. Photobiol. **42**: 573-578.
- Shapiro, A. L., E. Vinuela, and J. V. Maizel.** 1967. Molecular Weight Estimation of Polypeptide Chains by Electrophoresis in SDS-Polyacrlamide Gel Electrophoresis. Biochem. Biophys. Res. Comm. **28**: 815-820.
- Shepherd, W. D., and S. Kaplan.** 1978. Effect of Heat and 2-Mercaptoethanol on Intracytoplasmic Membrane Polypeptides of *Rhodopseudomonas sphaeroides*. J. Bacteriol. **135**: 656-667.

- Shiozawa, J. A., W. Welte, N. Hodapp, and G. Drews. 1982.** Studies on the Size and Composition of the Isolated Light-Harvesting B800-850 Pigment-Protein Complex of *Rhodopseudomonas capsulata*. Arch. Biochem. Biophys. **213**: 473-485.
- Shuvalov, V. A. and A. A. Asadov. 1979.** Arrangement and Interaction of Pigment Molecules in Reaction Centers of *Rhodopseudomonas viridis*. Biochim. Biophys. Acta **545**: 296-308.
- Skoog, D. A., and D. M. West. 1980.** In 'Principles of Instrumental Analysis. Third Edition'. pp. 148-168. Saunders Golden Sunburst Series.
- Simons, K. and A. Helenius. 1975.** Solubilization of Membrane by Detergents. Biochim. Biophys. Acta **415**: 29-79.
- Singer, S. J. 1974.** The Molecular Order of Membranes. Ann. Rev. Biochem. **43**: 805-833.
- Singer, S. J., and G. L. Nicolson. 1972** The Fluid Mosaic Model of the Structure of Cell Membranes. Science **175**: 720-731.
- Stanier, R.Y. 1970.** In 'Twentieth Symposium of the Society for General Microbiology'. pp. 1. Cambridge University Press. Cited in 'Handbook of Microbiology, Volume 1'. 1973. (Ed. Lechevalier, L.). pp. 17. C.R.C. Press.
- Stanier, R. Y., E. A. Adelberg, and J. L. Ingraham. (Ed.) 1976.** The Photosynthetic Prokaryotes. In 'General Microbiology; Fourth Edition'. pp. 527-563. The MacMillan Press Ltd. London.

Stanier, R. Y., N. Pfennig, and H. G. Trüper. 1981. Introduction to Phototrophic Prokaryotes. In 'The Prokaryotes- A Handbook of Habitats, Isolation and Identification of Bacteria. Vol. I.' (Ed. Starr, M. P., H. Stolp, H. G. Trüper, A. Balows and H. G. Schlegel). pp. 195-211. Springer-Verlag. Berlin. Heidelberg. New York.

Stark, W., W. Kühlbrandt, I. Wildhaber, and K. Mühlethaler. 1984. The Structure of the Photoreceptor Unit of *Rhodopseudomonas viridis*. The EMBO. J. 3: 777-783.

Straley, S. C., W. W. Parson, D. C. Mauzerall and R. K. Clayton. 1973. Pigment-Content and Molar Extinction Coefficients of Photochemical Reaction Centers from *Rhodopseudomonas sphaeroides*. Biochim. Biophys. Acta 305: 597-609.

Sutton, M. R., D. Rosen, G. Feher, and L. A. Steiner. 1982. Amino-Terminal Sequences of the L, M, and H Subunits of Reaction Centers from the Photosynthetic Bacterium *Rhodopseudomonas sphaeroides* R-26. Biochemistry 21: 3842-3849.

Tadros, M. H., F. Suter, G. Drews, and H. Zuber. 1983. The Complete Amino Acid Sequence of the Large Bacteriochlorophyll-Binding Polypeptide from Light-Harvesting Complex II (B800-850) of *Rhodopseudomonas capsulata*. Eur. J. Biochem. 129: 533-536.

Tadros, M. H., F. Suter, H. H. Seydewitz, I. Witt, H. Zuber, and G. Drews. 1984. Isolation and Complete Amino Acid Sequence of the Small Polypeptide from Light-Harvesting Pigment-Protein Complex I (B870) of *Rhodopseudomonas capsulata*. Eur. J. Biochem. 138: 209-212.

- Tadros, M. H., R. Frank, and G. Drews.** 1985. The Complete Amino Acid-Sequence of the Small Bacteriochlorophyll-Binding Polypeptide B800-850 β from Light-Harvesting Complex B800-850 of *Rhodopseudomonas capsulata*. F.E.B.S. Letters **183**: 91-94.
- Tadros, M. H., R. Frank, B. Dörge, N. Gad'on, and G. Drews.** 1987a. Orientation of the B800-850, B875 and Reaction Center Polypeptides on the Cytoplasmic and Periplasmic Surface of *Rhodobacter capsulatus* Membranes. In 'Workshop-Structure, Function and Formation of Membrane-Bound Complexes in Phototrophic Bacteria'. pp. 21. Freiburg. Fed. Rep. Germany.
- Tadros, M. H., R. Frank, G. Drews, and Y. Takemoto.** 1987b. Localization of Reaction Center Subunits and Light-Harvesting Polypeptides of *Rhodobacter sphaeroides*. In 'Workshop-Structure, Function and Formation of Membrane-Bound Complexes in Phototrophic Bacteria'. pp. 22. Freiburg. Fed. Rep. Germany.
- Tadros, M. H., R. Cortese, and G. Drews.** 1987c. The Polypeptides of the Light-Harvesting Complex of *Rhodopseudomonas palustris*: DNA and Amino Acid Sequences. In 'Workshop-Structure, Function and Formation of Membrane-Bound Complexes in Phototrophic Bacteria'. pp. 56. Freiburg. Fed. Rep. Germany.
- Takemoto, J.** 1974. Kinetics of Photosynthetic Membrane Protein Assembly in *Rhodopseudomonas sphaeroides*. Arch. Biochem. Biophys. **163**: 515-520.
- Takemoto, J., J. Peters, and G. Drews.** 1982. Cross-Linking of Photosynthetic Membrane Polypeptides of *Rhodopseudomonas capsulata*. F.E.B.S. Letters. **142**: 227-230.

- Tanaka, K., T. Kakuno, J. Yamashita, and T. Horio. 1983. Chemical Nature of Protein Complex of Photoreaction Unit Including Reaction Centres in Chromatophores of Photosynthetic Bacterium. *Rhodospirillum rubrum* as Detected by Successive Dissociation Method. J. Biochem. **94**: 1815-1826.
- Tanford, C. 1973. 'The Hydrophobic Effect'. J. Wiley. New York. London.
- Tanford, C. 1980. 'The Hydrophobic Effect'. J. Wiley. New York. Chichester.
- Tanford, C., and J. A. Reynolds. 1976. Characterization of Membrane Proteins in Detergent Solutions. Biochim. Biophys. Acta **457**: 133-170.
- Taylor, D. P., S. N. Cohen, W. G. Clark, and B. L. Marrs. 1983. Alignment of Genetic and Restriction Maps of the Photosynthetic Region of the *Rhodopseudomonas capsulata* Chromosome by a Conjunction-Mediated Marker Rescue Technique. J. Bacteriol. **154**: 580-590.
- Theiler, R., and H. Zuber. 1984. The Light-Harvesting Polypeptides of *Rhodopseudomonas sphaeroides* R26.1. II. Conformational Analysis by Attenuated Total Reflection Infrared Spectroscopy and Possible Molecular Structure of the Hydrophobic Domain of the B850 Complex. Hoppe-Seyler's Z. Physiol. Chem. **365**: 721-729.
- Theiler, R., F. Suter, and H. Zuber. 1983. N-Terminal Sequences of Subunits L and M of the Photosynthetic Reaction Centre from *Rhodospirillum rubrum* G-9 \pm . Hoppe-Seylers Z. Physiol. Chem. **364**: 1765-1776.
- Theiler, R., F. Suter, V. Wiemken, and H. Zuber. 1984a. The Light-Harvesting Polypeptides of *Rhodopseudomonas sphaeroides* R-26.1. Hoppe-Seylers Z. Physiol. Chem. **365**: 689-701.

- Theiler, R., F. Suter, H. Zuber and R. J. Cogdell. 1984b. A Comparison of the Primary Structure of the Two B800-850-Apoproteins from Wild-Type *Rhodopseudomonas sphaeroides* strain 2.4.1. and a Carotenoidless Mutant Strain R-26.1. F.E.B.S. Letters. **175**: 231-237.
- Thornber, J. P.. 1970. Photochemical Reactions of Purple Bacteria as Revealed by Studies of Three Spectrally Different Carotenobacteriochlorophyll-Protein Complexes Isolated from *Chromatium* Strain D. Biochemistry **9**: 2688-2697.
- Thornber, J. P., T. L. Trosper, and C. E. Strouse. 1978. Bacteriochlorophyll *in vivo*: Relationship of Spectral Forms to Specific Membrane Components. In 'The Photosynthetic Bacteria' (Ed. Clayton, R. K. and W. R. Sistrom). pp. 133-155. Plenum Press. New York. London.
- Thornber, J. P., R. J. Cogdell, B. K. Pierson, and R. E. B. Seftor. 1983. Pigment-Protein Complexes of Purple Photosynthetic Bacteria: An Overview. J. Cell. Biochem. **23**: 159-169.
- Trüper, H. G., N. N. Pfennig. 1978. Taxonomy of the Rhodospirillales. In 'The Phototrophic Bacteria' (Ed. Clayton, R. K. and W. R. Sistrom). pp. 19-27. Plenum Press. New York. London.
- Ueda, T., Y. Morimoto, M. Sato, T. Kakuno, J. Yamashita, and T. Horio. 1985. Isolation, Characterization, and Comparison of a Ubiquitous Pigment-Protein Complex Consisting of a Reaction Centre and Light-Harvesting Bacteriochlorophyll Proteins Present in Purple Photosynthetic Bacteria. J. Biochem. **98**: 1487-1498.

- Valkirs, G. E., and G. Feher. 1982. Topography of Reaction Centre Subunits in the Membrane of the Photosynthetic Bacterium *Rhodopseudomonas sphaeroides*. J. Cell. Biol. **95**: 179-188.
- Valkūnas, L., A. Razivin, and G. Trinkūnas. 1985. Interaction of the Minor Spectral Form Bacteriochlorophyll with Antenna and the Reaction Centre in the Process of Excitation Energy Transfer in Photosynthesis. Photochem. Photophys. **9**: 139-142.
- van Dorssen, R. J., M. Vos, A. Korenhof, C. N. Hunter, R. van Grondelle, and J. Amesz. 1987. Spectroscopic Properties of Antenna Complexes of *Rhodobacter sphaeroides* in vivo. In 'Workshop-Structure, Function and Formation of Membrane-Bound Complexes in Phototrophic Bacteria'. pp. 26. Freiburg. Fed. Rep. Germany.
- van Grondelle, R. 1985. Excitation Energy Transfer, Trapping and Annihilation in Photosynthetic Systems. Biochim. Biophys. Acta **811**: 147-195.
- van Grondelle, R.. 1987. The Organization of the Light-Harvesting Apparatus of *Rhodobacter sphaeroides* and *Rhodospirillum rubrum*. In 'Workshop-Structure, Function and Formation of Membrane-Bound Complexes in Phototrophic Bacteria'. pp. 27. Freiburg. Fed. Rep. Germany.
- van Grondelle, R., H. J. M. Kramer, and C. P. Rijgersberg. 1982. Energy Transfer in the B800-850 Carotenoid Light-Harvesting Complex of Various Mutants of *Rhodopseudomonas sphaeroides* and *Rhodopseudomonas capsulata*. Biochim. Biophys. Acta **682**: 208-215.
- van Grondelle, R., C. N. Hunter, J. G. C. Bakker, and H. J. M. Kramer. 1983. Size and Structure of Antenna Complexes of Photosynthetic Bacteria as Studied by Singlet-Singlet Quenching of the Bacteriochlorophyll Fluorescence Yield. Biochim. Biophys. Acta **723**: 30-36.

*van Niel, C. B. 1931. Arch. Mikrobiologie 3: 1-113.

van Niel, C. B. 1941. The Bacterial Photosyntheses and their Importance for the General Problem of Photosynthesis. Adv. Enzymol. 1: 263-328.

van Niel, C. B. 1944. The Culture, General Physiology, Morphology and Classification of the Non-Sulphur Purple and Brown Bacteria. Bacterial Rev. 8: 1-118

Vos, M., R. van Grondelle, F. W. van der Kooij, D. van de Poll, J. Amesz, and L. N. M. Duysens. 1986. Singlet-Singlet Annihilation at Low Temperatures in the Antenna of Purple bacteria. Biochim. Biophys. Acta 850: 501-512.

Varga, A. R. and L. A. Staehelin. 1983. Spatial Differentiation in Photosynthetic and Non-Photosynthetic Membranes of Rhodopseudomonas palustris. J. Bacteriol. 154: 1414-1430.

Varga, A. R. and L. A. Staehelin. 1985. Pigment-Protein Complexes from Rhodopseudomonas palustris: Isolation, Characterization, and Reconstitution into Liposomes. J. Bacteriol. 161: 921-927.

Vredenberg, W. J. and J. Amesz. 1967. Absorption Characteristics of Bacteriochlorophyll Types in Purple Bacteria and Efficiency of Energy-Transfer Between Them. In 'Brookhaven Symposia in Biology 19: 49-61.

Vredenberg, W. J. and Duysens, L. N. M. 1963. Transfer of Energy from Bacteriochlorophyll to a reaction center During Bacterial photosynthesis. Nature 197: 355-357.

Wacker, T., N. Gad'on, A. Becker, W. Mäntele, W. Kreutz, G. Drews, and Welte, W. 1986. Crystallization and Spectroscopic Investigation with Polarized Light of the Reaction Center-B875 Light-Harvesting Complex of Rhodopseudomonas palustris. F.E.B.S. Letters 197: 268-273.

- Weber, K., and M. Osborn. 1969. The Reliability of Molecular Weight Determinations by Dodecyl-Sulphate-Polyacrylamide Gel Electrophoresis. J. Biol. Chem. **244**: 4406-4412.
- Welte, W., and W. Kreutz. 1982. Formation, Structure and Composition of a Planar Hexagonal Lattice Composed of Specific Protein-Lipid Complexes in the Thylakoid Membranes of *Rhodopseudomonas viridis*. Biochim. Biophys. Acta **692**: 479-488.
- Welte, W., T. Wacker, M. Leis, W. Kreutz, J. Shiozawa, N. Gad'on, and G. Drews. 1985. Crystallization of the Photosynthetic Light-Harvesting Pigment-Protein Complex B800-850 of *Rhodopseudomonas capsulata*. F.E.B.S. Letters **182**: 260-264.
- Welte, W., T. Wacker, K. Steck, and W. Mäntele. 1987. Studies of Crystallized B800-850 Complexes of *Rhodopseudomonas palustris*: Arrangement of Protein Complexes in the Unit Cell Revealed by X-Ray Diffraction and Microphotometry. In 'Workshop-Structure, Function and Formation of Membrane-Bound Complexes in Phototrophic Bacteria'. pp. 12. Freiburg. Fed. Rep. Germany.
- Werli, E., and O. Kübler. 1980. In 'Electron Microscopy at Molecular Dimensions'. (Ed. Baumeister, W. and W. Vogell). pp. 48-56. Springer-Verlag. Berlin.
- Westerhuis, W. H. J., J. Ames, and R. A. Niederman. 1987. Structural Organization of Photosynthetic Units in Phospholipid-Enriched Membranes of *Rhodobacter sphaeroides* as Determined by Singlet-Singlet Annihilation. In 'Workshop-Structure, Function and Formation of Membrane-Bound Complexes in Phototrophic Bacteria'. pp. 35. Freiburg. Fed. Rep. Germany.

- Wiemken, V., and R. Bachofen. 1982. Probing the Topology of Proteins in the Chromatophore Membrane of *Rhodospirillum rubrum* G-9 \pm with Proteinase K. Biochim. Biophys. Acta **681**: 72-76.
- Williams, J. C., L. A. Steiner, R. C. Ogden, M. I. Simon, and G. Feher. 1983. Primary Structure of the M Subunit of the Reaction Center from *Rhodopseudomonas sphaeroides*. Proc. Natl. Acad. Sci. U.S.A. **80**: 6505-6509.
- Williams, J. C., L. A. Steiner, G. Feher, and M. I. Simon. 1984. Primary Structure of the L-Subunit of the Reaction Center from *Rhodopseudomonas sphaeroides*. Proc. Natl. Acad. Sci. U.S.A. **81** 7303-7307.
- Williams, J. C., L. A. Steiner, and G. Feher. 1986. Proteins **1**: 312-325.
- Wraight, C. A. 1979. The Role of Quinones in Bacterial Photosynthesis: Yearly Review. Photochem. Photobiol. **30**: 767-776.
- Yeates, T. O., H. Korniya, D. C. Rees, J. P. Allen, and G. Feher. 1987. Structure of the Reaction Center from *Rhodobacter sphaeroides* R-26: Membrane-Protein Interactions. Proc. Natl. Acad. Sci. U.S.A. **84**: 6438-6442.
- Youvan, D. C., E. J. Bylina, M. Alberti, H. Begusch, and J. E. Hearst. 1984. Nucleotide and Deduced Polypeptide Sequences of the Photosynthetic Reaction Center. B870-Antenna. and Flanking Polypeptide from *Rhodopseudomonas capsulata*. Cell **37**: 949-957.
- Youvan, D. C., and S. Ismail. 1985. Light-Harvesting II (B800-850 Complex) Structural Genes from *Rhodopseudomonas capsulata*. Proc. Natl. Acad. Sci. U.S.A. **82**: 58-62.

- Zeppezauer, M.** 1971. Formation of Large Crystals. In 'Methods in Enzymology 22 (Ed. Jakoby, W. B.). pp. 253.
- Zhu, Y. S., and J. E. Hearst.** 1986. Regulation of Expression of Genes for Light-Harvesting Antenna Proteins LH-I and LH-II: Reaction Center polypeptides RC-L, RC-M, and RC-H; and Enzymes of Bacteriochlorophyll and Carotenoid Biosynthesis in *Rhodobacter capsulatus* by Light and Oxygen. Proc. Natl. Acad. Sci. U.S.A. 83: 7613-7617.
- Zhu, Y. S., D. Cook, F. Leach, G. Armstrong, M. Alberti, and J. E. Hearst.** 1986. Oxygen-Regulated mRNAs from Light-Harvesting and Reaction Center Complexes and for Bacteriochlorophyll and Carotenoid Biosynthesis in *Rhodobacter capsulatus* During the Shift from Anaerobic to Aerobic Growth. J. Bacteriol. 168: 1180-1188.
- Zinth, W., W. Kaiser, and H. Michel.** 1983. Efficient Photochemical Activity and Strong Dichroism of Single Crystals of Reaction Centers from *Rhodopseudomonas viridis*. Biochim. Biophys. Acta 723: 128-131.
- Zinth, W., M. Sander, J. Dobler, W. Kaiser, and H. Michel.** 1985. Single Crystals from Reaction Centers of *Rhodopseudomonas viridis* Studied by Polarized Light. In 'Springer Series in Chemical Physics 42'. (Ed. Michel-Beyerle, M.). pp. 97-102. Springer Verlag. New York.
- Zuber, H.** 1985. Structure and Function of Light-Harvesting Complexes and Their Polypeptides: Yearly Review. Photochem. Photobiol. 42: 821-844.

(* References which were unavailable).

